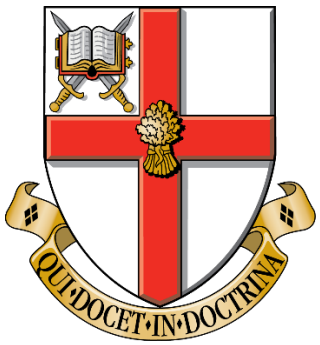

University of Chester

Predicted Structure and Potential Binding of the Nematode Tetraspanin 7 Protein (tsp-7) With Human Tissue Inhibitor Metalloproteinase 1 (TIMP-1): a Possible Role In Parasite- Host Interactions

Thesis submitted in accordance with the requirements

of the University of Chester for the degree of Doctor

of Philosophy by

Brogan Jones

February 2023

Declaration

The material being presented for examination is my own work and has not been submitted for an award of this or another HEI except in minor particulars which are explicitly noted in the body of the thesis. Where research pertaining to the thesis was undertaken collaboratively, the nature and extent of my individual contribution has been made explicit.

Signed:

Date:

Acknowledgements

Firstly, I would like to thank my supervisor Professor Frank Michelangeli, for saving this project and supporting me in every way possible. I would like to thank Dr Laurence Seabra and Dr Jon Power for their input and time. To all the technicians in Medical school and Biological sciences. I would also like to thank Dr Robert Coleman for his continued optimism and Dr James Brown for the laughs!

I would like to take this opportunity to thank Dr Claire Lucas and Professor Elizabeth Mason-Whitehead for supporting me throughout this very long emotional journey. To Dr Michael Randles for answering my 1000 questions. I would also like to thank Dr Navaneethan Palanisamy for continued help in labs.

I would like to thank my mum, for supporting me throughout. I know it's been difficult, but we made it to the end. You don't need to worry about me anymore. To my brother, David, for paying for my Netflix account and all that coffee I bought off his bank card. I appreciate it. And my dad for being a good taxi driver.

To Alex for being the most supportive friend, and for always giving me the best advice which I should take more often, thank you. I would also like to thank Andy for contributing to this thesis, for encouraging and supporting me and for having a major impact on my life.

To Alice, for making my days in lab much better and reminding me to take breaks.

I'd like to thank Dr Chelsea Wood for being my "lab role model," and for listening to my rants. And thank you to all the PhD students and for Professor Eustace Johnson for challenging me and for all the support.

Finally, I'd like to thank my dogs, Caesar, and Harry, for being the best mental support there is.

Abstract

Human parasitic nematodes evade the host immune system through cross communication by unknown mechanisms. The proteins of the parasitic nematodes are still poorly annotated. CD63 is a human tetraspanin and binds to TIMP-1 a metalloproteinase inhibitor, which has recently been found to play an active role in inflammation by acting as a cytokine when bound to CD63. *Caenorhabditis elegans* is a free-living nematode, a model organism for both human and parasitic nematodes. *C. elegans* tetraspanin protein -7 (tsp-7) is an orthologue of human CD63. The model organism used can provide information about potential tetraspanin proteins from parasitic nematodes, which are believed to play a role in the cross communication between parasite and host. The tsp-7 protein sequence from *C. elegans* shares a high percentage similarity, identity, and homology with a variety of human parasitic nematode proteins. Using a number of computer-based programmes including 'Alpha-Fold,' which is currently the most powerful Artificial Intelligence protein structure prediction programme, the structure of the *C. elegans* tsp-7 was determined. From the predicted structure, the tsp-7 protein has one highly likely, membrane exposed tyrosine phosphorylation site, with implications of its potential involvement in signalling pathways and immune responses. Using multiple protein docking databases and programmes, tsp-7 has been shown to theoretically bind to human TIMP-1. Two mutant strains of *C. elegans* were obtained from *Caenorhabditis* Genetics Centre, University of Minnesota, USA, with amino acid deletions within the tsp-7 protein (mutant tm5046 and mutant tm5761). These tsp-7 mutant strains were shown to have an overall longer life span than the wild type *C. elegans* (N2). The mutant tm5761 showed a greater stress response compared to the N2 wild-type, when exposed to various chemical stimuli, however, mutant tm5046 was more similar to wild type *C. elegans*. Under heat stress, mutant tm5761 and wild type N2, were less tolerant to heat compared to the tm5046 mutant. In general, mutant tm5046 was more stable and displayed a reduced stress behavioural response compared to mutant tm5761. A primary polyclonal antibody was produced against the tsp-7 large extracellular loop domain, believed to be the key active site in protein-protein interactions. The expression of tsp-7 in mutant tm5761 was detected at lower concentrations than the wild type and mutant tm5046 in an ELISA assay and it also could not be detected by western blotting. Mutant tm5046 was detected weakly by western blotting. Cos-7 cells transfected with the tsp-7 protein-GFP tagged plasmid were incubated with active human TIMP-1. The tsp-7 tagged cells showed co-localisation with TIMP-1, using immuno-fluorescence microscopy, thus adding to the evidence that tsp-7 could interact with human TIMP-1. Such an interaction may well play a role in parasite-host interactions and its effects on the immune response.

As *C. elegans* tsp-7 shares high similarity with many parasitic nematodes that are known to infect humans, it is a good protein candidate to further explore the potential interactions of parasitic nematodes with humans, in terms of cross communication and interaction with the host immune system.

Table of Contents

List of Figures

List of tables

Abbreviations

AB	Antibody
ACT	Artemisinin Combination Therapy
ADAMs	A Disintegrin and Metalloproteinase
ADCC	Antibody-Dependent Cellular Cytotoxicity
CD	Cluster of Differentiation
CDC	Centre for Disease Control
CDK2	Cyclin Dependent Kinase
CKII	Casein kinase 2
CNS	Central Nervous System
CXCR4	Chemokine Receptor 4
DCs	Dendritic Cells
DEC	Diethylcarbamazine citrate
DNAPK	DNA Dependent Protein Kinase
E2	Envelope Glycoprotein
EC	Extracellular
ECM	Extracellular Matrix
ECP	Eosinophil Cationic Protein

EDN	Eosinophil Derived Neurotoxin
ELISA	Enzyme Linked Immunosorbent Assay
EPO	Eosinophil Peroxidase
ESCRT	Endosomal Sorting Complex Required for Transport
EVs	Extracellular vesicles
FAK	Focal Adhesion Kinase
FcεRI	IgE High Affinity Receptor
GFP	Green Fluorescence Protein
HAART	Highly Active Antiretroviral Therapy
HCV	Hepatitis C Virus
HIV	Human Immunodeficiency Virus
IFNγ	Interferon gamma
IgA	Immunoglobulin A
IgE	Immunoglobulin E
IgG	Immunoglobulin G
IgSF	Immunoglobulin Superfamily
ILs	Interleukins
ILVs	Intraluminal Vesicles

INSR	Insulin Receptor
ITGB	Integrin Beta 1
LAMP	Lysosome-Associated Membrane proteins
LEL	Large Extracellular Loop
LPO	Lactoperoxidase
MBP	Major Basic Proteins
MHC	Major Histocompatibility Complex
MMP	Metalloproteinases
MPO	Myeloid Peroxidase
MSCs	Mesenchymal Stem cells
MVBs	Multivesicular Bodies
NCBI	National Centre for Biotechnology Information
NET	Neutrophil Extracellular Traps
NGAL	Neutrophil Gelatinase Associated Lipocalin
NGM	Nematode Growth Medium
NMR	Nuclear Magnetic Resonance
OLFM-4	Olfactomedin-4
Orai1	Calcium Release-Activated Calcium Modulator 1

p38MAPK	p38 Mitogen Activated Protein Kinase
PAMPs	Pathogen Associated Molecular Patterns
PCR	Polymerase Chain Reaction
PKA	Protein Kinase A
PKC	Protein Kinase C
POP	Persistent Organic Pollutants
PZQ	Praziquantel
Rf	Relative flow
RMSD	Root Mean Square Deviation
RNS	Reactive Nitrogen Species
ROM	Retinal Degeneration slow family
ROS	Reactive Oxygen Species
SCARB2	Scavenger Receptor Class B Member 2
SDCBP	Syndecan Binding Protein
SEL	Small Extracellular Loop
SELP	Selectin-P
SIL	Small Intracellular Loop
SIRPα	Signal Regulatory Protein alpha

STH	Soil Transmitted Helminths
STN	Soil Transmitted Nematodes
Th	T helper cells
TIMP-1	Tissue Inhibitor of Metalloproteinase 1
TLRs	Toll-Like Receptors
TM	Transmembrane
TPO	Thyroid Peroxidase
Treg	Regulatory T Cells
tsp-7	Tetraspanin Protein 7
UNSP	Unspecified
UPK	Uroplakin
WBC	White Blood Cell
WBP	Weibel-Palade Bodies
WHO	World Health Organisation

Chapter 1: Introduction

1.1 Nematodes

Nematode biodiversity spans the Earth reaching the dry valleys in Antarctica and the Namib desert. Nematodes are one the most abundant animals with an estimation of over a million species. Despite this, only around 20,000 have been described, and *Homo sapiens* are host to about 35 parasitic nematodes (Al-Banna & Gardner., 2022).

Nematodes can be parasitic and have the capacity to infect both animal and plant species. The Centre for Disease Control (CDC) and World Health Organisation (WHO), recognise 17 neglected tropical diseases that need further research and monitoring, of these, 4 are caused by nematodes: *Dracunculus medinensis, lymphatic filariasis, Onchocerciasis,* and soil transmitted helminths (STH's). Parasitic nematodes are of global importance medically and a threat to livestock, costing billions of dollars globally. In the UK, the cost of nematodes in livestock is around £42.3 million alone and €1.8 billion across Europe (Charlier *et al*., 2020).

The most sustainable treatment would be better access to healthcare and better hygiene and sanitation, which is currently not feasible, especially in developing countries, therefore most nematode treatment depends on chemotherapy. However, the widespread use of a few drugs against these infections has led to the problematic development of drug resistance (Stear *et al.,* 2023).

Designing, producing, and approving new drugs is laborious and expensive. Although there are better approaches being explored and developed in the drug discovery pipeline, the process is still costly. With funding going elsewhere on other diseases, and new pandemics spreading across the globe it is understandable why nematode infection treatment research will likely remain neglected.

1.1.1 Life cycle

The life cycle of all species of nematode parasites are complex yet similar in that they develop from eggs with three or four larval stages, with a free-living larval stage, developing into an adult stage in the final host (Lu *et al*., 2020). There are some nematode species that can complete their entire life cycle in the final host such as pinworm. Others require an intermediate host, such as *Brugia malayi, Trypanosoma brucei* and *Onchocerca volvulus,* which require both an invertebrate and vertebrate host to complete their life cycle (Castelletto *et al.*, 2020). The intermediate host differs depending on the species (Gang & Hallem., 2016).

Most of the globally important human nematodes complete their life cycle in the definitive host. This is particularly true with the gastrointestinal nematodes, however other nematodes require an intermediate host (Majewska *et al*., 2021) these nematodes usually reside in the tissue or muscles of humans. In some instances, the human becomes an accidental host, when the parasites are ingested from the intermediate host (Stepek *et al*., 2006).

Embryonation occurs within the eggs of nematodes and hatch into their first larval stage (L1). The L1 juvenile stage then moult into another three larval stages (L2, L3 and L4), each time shedding their cuticle and increasing in size. The larval stage then moults into a final adult stage (Figure 1.1.1.1). There are some variations of the life cycle depending on the species (Mkandawire *et al*., 2022). Both female and male nematodes exist within a population, however, depending on the species, the frequency of males differs, and the frequency of hermaphrodite nematodes increases (Van Goor *et al*., 2021). In parasitic nematodes of humans, the larval stage is passed either directly or indirectly back into the final host in which extensive migration occurs at the final location of the nematode, here they develop into adults (Stepek *et al*., 2006).

The nematode eggs act as a barrier, protecting the nematode from external factors and stress stimuli (Mkandawire *et al*., 2022). However, the eggs of the globally important parasitic nematodes, do not hatch within the host. Usually, the human host is infected with a late juvenile stage or the adult nematode (Stepek *et al*., 2006).

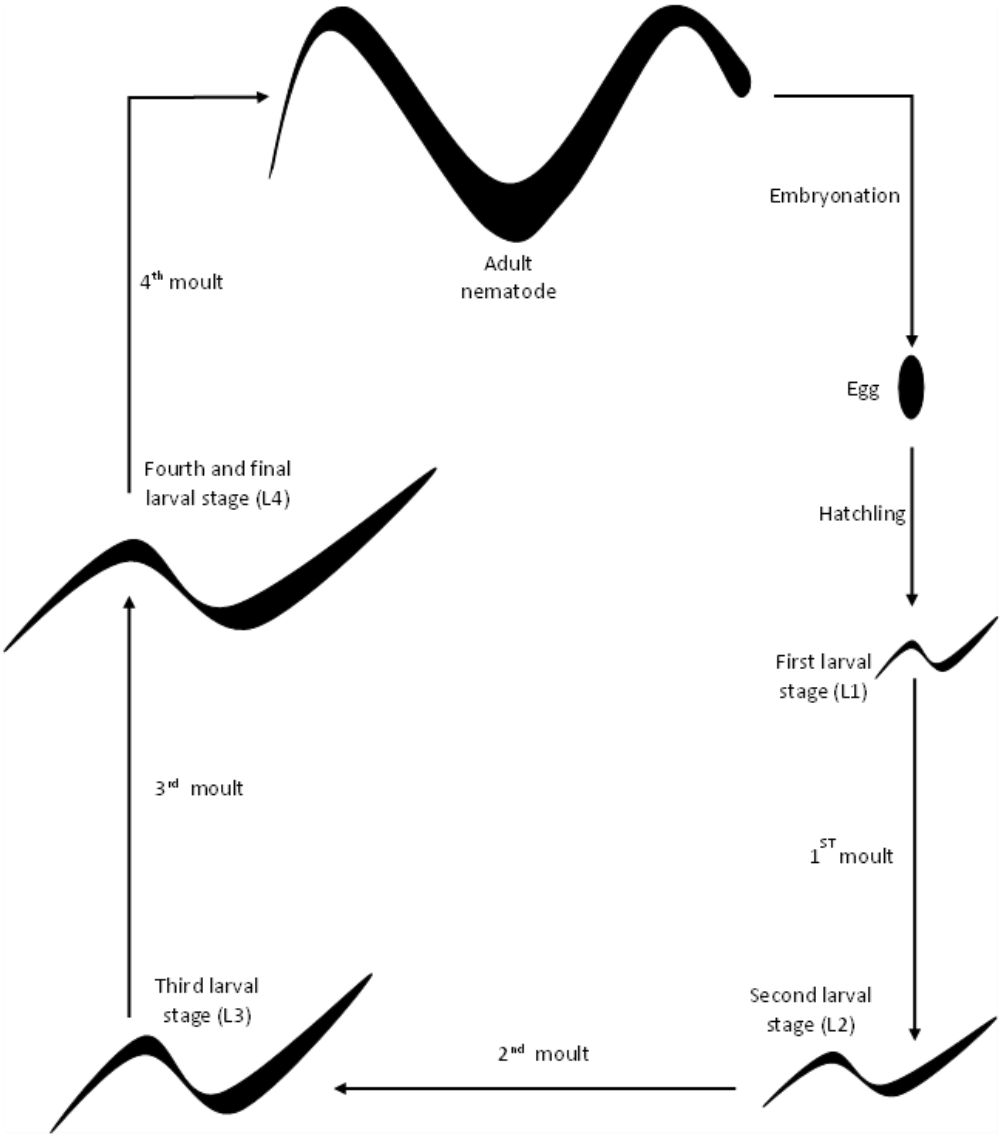

Figure 1.1.1.1. Generic life cycle of most nematode species. The nematodes usually undergo four juvenile developmental stages, before reaching adulthood. The time spent at each developmental stage depends on nematode species.

1.1.2 Symptoms

Generally, with most nematode infections, the host very rarely show symptoms or usually present as mild symptoms such as diarrhoea and nausea. The nematodes are identified when there is significant swelling and inflammation, either within tissue or organs, this is largely due to the number of nematodes within a specific infected site (Stepek *et al*., 2006).

The nematodes ultimately cause blockages due to the heavy load. In the case of filariasis this usually means that the lymph cannot be drained leading to extreme swelling. However, in most cases, at least two thirds of those infected, there are no symptoms of filariasis even if a person is infected with millions of worms (Nag *et al*., 2019).

The issue arises when the nematodes die, triggering an immune response which leads to the formation of granulomas encasing the worms, eventually leading to the inflammation of the lymphatic system. (Taylor *et al*., 2010). When the nematodes are alive, the immune system is highly regulated by the nematodes and thus there are very few, if any, symptoms. Metalloproteinases (MMP's) are involved with cleavage mechanisms of cytokines and chemokines (Bruschi & Pinto., 2013). MMP9 is secreted by neutrophils, and responsible for the regulation of inflammation (Zhang *et al*., 2020). TIMP-1 is an inhibitor of MMP9, dysregulation of the MMP9/TIMP-1 pathway leads to chronic inflammation (Ma *et al*., 2015). This is the case with most helminthic infections, parasitic worms generally tend to only cause symptoms either when the immune response attacks the eggs which have imbedded in muscle and tissue or when the worms are dead or dying. Most infections do not present clinical

pathology. The cause of river blindness is due to the extensive immune response to dead worms in the ocular region of the host (Taylor *et al*., 2010).

Anisakid nematodes are transmitted through ingestion of raw or uncooked fish. Infection of the anisakid nematode may cause anisakiasis which presents as severe abdominal pain and is usually symptomatic, but up to 40% of cases are asymptomatic (Takasaki *et al*., 2020). The nematode infection is often diagnosed as inflammatory bowel disease or another gastrointestinal ailment rather than the anisakiasis infection. Most cases are under-reported for asymptomatic anisakiasis, and the majority of the cases reported are primarily in Japan (Takasaki *et al*., 2020).

1.1.3 Treatment

To date, there are still no vaccines available for the treatment of helminth infections, therefore it is imperative to develop new classes of drugs for their treatment (Furtado *et al*., 2016). Praziquantel (PZQ) is one of the standard drugs used for helminth infections, however, it cannot be used to treat most nematode infections, where other drugs or a combination of multiple drugs are commonly used.

Nematodes can live in tissues, blood and lymph thus making treatment a challenge. For almost all nematodes, Albendazole or Mebendazole is the choice of drug, for strongyloidiasis the treatment must be Ivermectin. For filarial worms, Diethylcarbamazine citrate (DEC) must be used, which kills the adult worms. (Taylor *et al*., 2010 and Adinarayanan *et al*., 2007).

Drug resistance has not been reported for nematode infections in humans but reports from the field suggest that nematodes now have alleles for resistance to the Benzimidazoles, the drugs primarily targeting nematode infections. Soil transmitted nematodes (STNs) such as, *Necatar americanus, Ancylostoma duodenale* and *Ancylostoma ceylanicum* have now been found to contain anthelmintic resistant alleles to the benzimidazole drug class of treatments. And with the extensive use of this class of drugs, the resistant alleles have been reported in greater frequency amongst the STNs (Elfawal *et al*., 2019). Listed in Table 1.1.3.1 are the anthelmintics currently used to treat the different nematode infections.

Table 2.1.3.1. Anthelmintics currently available on the market. Different anthelmintics are used to treat different parasitic infections, the small class of drugs used to treat multiple helminths can lead to drug resistance.

Nematode	**Anthelmintic**
Filarial	Ivermectin
	Diethylcarbamazine
Pinworms	Piperazine
	Mebendazole
	Pyrantel pamoate
Hookworm	Mebendazole
Whipworm	
Ascarids	

Nematode resistance in animals, particularly livestock, is well documented and has been a major issue within veterinary science for decades (Vande Velde *et al*., 2018). The drugs used for veterinary nematode infections are the same drugs used for human infections (Canton *et al*., 2021). Therefore, the likelihood of human nematodes becoming resistant may well be inevitable. However, the studies have found that although some nematodes have resistant alleles, it would seem that, to date, there are no reports of resistant nematodes in the field (Kaminsky *et al*., 2008). This could possibly be due to poor surveillance systems in countries where these infections are endemic (Zajíčková *et al*., 2020). This could also be due to the lack of observational or diagnostic techniques available due to the infections being classified as neglected tropical diseases, and therefore not a priority for drug company investment (Tsai *et al*., 2013).

With increased surveillance, the goal of eradication may soon be accomplished for most pathogenic nematode species. One method being developed is the treatment of livestock in the poorer communities. The goal is the mass-administration of drug treatment. However, numerous studies have flagged major issues, for example the efficacy has not been adequately reported (Mkupasi *et al*., 2013). To date, the most effective prevention method is practising sanitation and hygiene, if these methods were followed, the infection rates of nematodes would dramatically decrease.

1.1.4 Morphology

One of the most common difficulties is identifying the nematode species due to similar morphological features (Bogale *et al*., 2020). The majority of the life cycle stages (apart from the egg) all have the same cylindrical shape and can sometimes be extremely difficult to tell apart between different species (Bredtmann *et al*., 2017). It is the posterior end of the nematode in which identifying the species is made easier, however, to tell the species apart from the tail alone require expertise. Polymerase chain reaction (PCR) techniques allow rapid amplification of specific segments of DNA and will often provide sufficient results to correctly identify the species within ruminants, this is also applicable to human nematode species (Roeber *et al*., 2017). Recently, databases such as WormBase ParaSite and NCBI contain genome entries for most of the human nematodes, including various strains. These databases are constantly updated, providing research with valuable information.

1.1.5 *Caenorhabditis elegans* as a model organism

Caenorhabditis elegans (*C. elegans*) is a free-living nematode and is the standard animal model for developmental biology research, initially used and promoted by Sydney Brenner in the early 1960's (Wu *et al*, 2019). For this reason, *C. elegans* was the first animal to have its genome completely sequenced in 1998 (Hotaling *et al.,* 2021).

C . elegans has a genome size of 100Mb and 20,000 genes identified (Hillier *et al.,* 2005). As well as having a smaller genome size compared to other animals, *C.*

elegans are easily maintained and inexpensive. Worm stocks can be frozen and used for many years. Aside from the convenient storage, one adult hermaphrodite can release up to 150 eggs per day. To grow a strain of *C. elegans*, healthy adult hermaphrodites are required.

According to InVivo Biosystems, the disadvantage of using *C. elegans* as a model organism is the number of neurons within the organism. *C. elegans* have significantly less neurons than other model organisms. Another issue is the gene homology for human diseases, which is very low amongst all the current animal model organisms, the mouse model has homology >90% but *C. elegans* is at 65% (Lai *et al*., 2000). The short and rapid life cycle of *C. elegans* makes them the ideal model organism, however mutant knockouts are usually hard to identify based on phenotype alone (Brenner., 1974).

The life cycle of *C. elegans* is similar to other nematodes, in which the eggs hatch into the L1 larval stage. The larva then moults a further 4 times into the L2, L3, and L4 stage and finally the adult. There are male and hermaphrodite worms in the species. Within the population the males are considered rare, while the hermaphrodites make up the majority of the worms population. Figure 1.1.1.1 shows a general schematic life cycle of nematodes, *C. elegans* also follow this cycle but with an addition of a dauer stage which is an arrested stage in response to stress (Lu *et al*., 2020).

The WormBase database (https://wormbase.org) is a dedicated online platform freely available, containing a plethora of detailed genomic annotations specifically for *C. elegans*, including all the potential mutants available. The database also contains

multiple resources to conduct various experiments with *C. elegans* from simple procedures for maintenance to more complex techniques such as RNAi. The Japanese bio-consortium is also dedicated in providing knockout strains of *C. elegans*, which are available at a low cost.

The similarity between *C. elegans* and parasitic nematodes is what defines this organism as the ideal model for this project. The anthelmintics currently available for treatment of nematode infections are also active against *C. elegans*, making this free-living nematode a good model for parasitic nematodes of humans (Burns et al., 2020). Resistant alleles to the marketed anthelmintics have been identified using *C. elegans* (Rehborg *et al*., 2023). Two thirds of the *C. elegans* genome are homologous to humans, therefore age-related disease studied can be performed using this free-living organism as a model system (Zhang *et al*., 2020). Using *C. elegans* as the model organism for this project, comparisons can be made between host and model to model and parasite.

1.2 Parasites and the Immune system

1.2.1 Various immune cells and their function

Eosinophils are phagocytotic leukocytes from the innate immune system, activated by parasites and allergens (Spencer *et al*., 2009). Eosinophils migrate from the blood into tissues and the immunoglobulins; IgA, IgG and IgE are triggers of eosinophils, causing degranulation, increased survival, and an increase in surface receptors (Tsuda & Miyasato., 1993). Eosinophils contain multiple proteins which specifically

target parasitic nematodes, such as major basic proteins (MBP), eosinophil peroxidase (EPO) and eosinophil cationic protein (ECP) (Enokihara & Koike., 1993).

MBP is a small enzymatic protein and is the main constituent of the eosinophil crystalline core. MBP is involved with the cytotoxicity of helminths (Specht *et al*., 2006). MBP in eosinophils delays maturation of larval nematodes by inducing permeation of nematode membranes (Obata- Ninomiya *et al*., 2020). EPO belongs to the peroxidase family and is more similar to myeloid peroxidase (MPO), a neutrophil granulocyte protein with bactericidal activity, and lactoperoxidase (LPO), an antibacterial agent EPO has been shown to have bactericidal as well as parasiticidal activity (Specht *et al*., 2006). Eosinophils release extracellular DNA traps, which prevent the movement of nematodes, allowing the peroxidase and cytotoxic molecules to disrupt the permeability of the nematode membranes (Ehrens *et al*., 2021). ECP is a cytotoxic ribonuclease, it has been shown to kill helminths by binding to cell surface membranes and altering permeability and ionic equilibrium within the cells. MPO, EPO and ECP work together to immobilise and neutralise parasitic nematodes (Navarro *et al*., 2010).

Neutrophils are phagocytes, similar to eosinophils and are produced in the bone marrow by haematopoiesis. Neutrophils circulate in the blood and tissue for a short time and contain primary, secondary, and tertiary granules. Neutrophils are first to arrive at the site of nematode infections, thus are primarily involved in inflammation and repair (Pesce *et al*., 2008). It is also believed that neutrophils may play a more pivotal role in immunity and disease, by cross-communication with dendritic cells (DC's), by secretion of specific chemokines, inducing chemotaxis of immature DC's to the site of infection (Bennouna *et al*., 2003). Neutrophils activate macrophages

which contains and help kill nematodes, the neutrophils and macrophages surround the parasitic helminths, however this can lead to tissue damage and chronic inflammation (Allen *et al.,* 2015).

Neutrophils account for the majority of white blood cells (WBC) in circulation and are therefore one of the first immune cells to respond to pathogens. If there is a decreased level of neutrophils, microbes become unchecked particularly in the respiratory system, however an increased level could lead to septic shock due to the cytokine storm triggered by the neutrophils, this can be fatal for the host (Lacy., 2006). Neutrophils have the ability to defend against, bacteria, viruses, parasites, and fungi.

The primary or azurophilic granules of neutrophils contain hydrolytic enzymes, particularly elastases, cathepsins, myeloperoxidases (MPO) and defensins (Lacy., 2006 and Sheshachalam *et al*., 2014). Secondary granules, also referred to as specific granules contain; lactoferrin, neutrophil gelatinase associated lipocalin (NGAL), resistin, olfactomedin-4 (OLFM-4) and signal regulatory protein alpha (SIRPα) (Lawrence *et al*., 2018). The tertiary (gelatinase) granules are a sub-population of the peroxidase negative granules (secondary) and contain essentially the same content as well as metalloproteinases (MMP's) (Murav'ev *et al*., 2003). Neutrophils form extracellular traps (NET's) around nematodes, containing the neutrophil granules, macrophages, and eosinophils (Masucci *et al*., 2020).Gelatinases are a class of MMPs, Matrix metalloproteinase 9 (MMP9) is secreted mainly by neutrophils (Rosales., 2018), and have been shown to breakdown the extracellular matrix (ECM) components and activating cytokines and chemokines, promoting a strong inflammatory response (Yabluchanskiy *et al*., 2013 and Heissig *et al*., 2010). In

patients with nematode infections, MMP9 expression increased as well as elevated levels on TIMP-1. Activated macrophages express higher levels of MMP9, which further drives an inflammatory response (Kumari & Kumar., 2023). Basophils are the least abundant granulocyte in circulation, they are very short lived but upon activation can release multiple histamines, chemokines, cytokines, and other mediators promoting the Th2 response (Eberle & Voehringer., 2016). Elevated levels of basophils are an indication of nematode infection and help drive inflammation. Both basophils and mast cells express the IgE high affinity receptor (FcεRI), however basophils also express defined markers which are not expressed in mast cells (Min *et al*., 2012). Nematode galectins and glycoproteins interact with IgE on basophils and mast cells (Donskow-Łysoniewska *et al.*, 2021). It is thought that CD4+ T cells are responsible for the basophil activation, resulting in a Th2 immune response, through production of the IL-4 and IL-13 cytokines (Sokol & Medzhitov., 2010). The Th2 response is primarily responsible for eliciting an immune response against parasitic infections, for example, schistosome eggs have been shown to induce a powerful Th2 response (Schramm *et al*., 2003). However parasitic helminths have been shown to supress basophil activation, and chronic infection of helminths leads to a production of IL-10, which suppresses IL-4 and IL-13 production. It is also believed that other complex mechanisms are involved in the suppression of basophils, how these mechanisms contribute is still unknown (Larson *et al*., 2012). The decrease in basophil activation means that the Th2 immune response is dampened, thus allowing the survival of the helminths within the host.

Mast cells express FcεRI receptors, as well as receptors for IgA and IgG, pathogen associated molecular patterns (PAMP's) and Toll-like receptors (TLR's) (Krystel-

Whittemore *et al*., 2016). Mast cells and basophils are extremely similar in terms of function and are mainly involved by driving the humoral immune response (Voehringer., 2013). Mast cells increase expression of high affinity IgE receptor during nematode infection. IgE bound to the high affinity receptor on mast cells and basophils binds to parasite proteins which then activate immune cells (Caminati *et al*., 2018), releasing cytokines such as IL-4 and IL-13. Both IL-4 and IL-13 induce Th2 differentiation which are part of the cell-mediated immune response. Th2 cells produce more IL-4 in a positive feedback loop, as well as recruiting eosinophils and inducing class switching of B cells to IgE and IgG (Allen & Sutherland., 2014). IgE then binds to the IgE low affinity receptor (FcεRII) expressed on eosinophils (Fitzsimmons *et al*., 2014). The activated eosinophils then undergo degranulation leading to the release of cytotoxic compounds able to kill or immobilise parasitic helminths. Degranulated eosinophils act as an effector cell for antibody-dependent cellular cytotoxicity (ADCC) in response to helminth infections (Mukai *et al*., 2016 and Motran *et al*., 2018). Tissue inhibitor metalloproteinase 1 (TIMP-1), has been shown to activate neutrophils to release NET's, further driving the pro-inflammatory Th1 response. TIMP-1 is expressed and regulated in Th1 cells but not in Th2 cells (Schoeps et al., 2022 and Ding *et al*., 2019). TIMP-1 has been shown to have a key role in the haematopoietic stem cell differentiation (Forte *et al*., 2017). The TIMP-1/MMP9 balance is also crucial for the differentiation of mesenchymal stem cells, inhibition of TIMP-1 in MSCs promotes differentiation to osteogenic lineages (Egea *et al*., 2012). Figure 1.2.1.1 illustrates how the different immune cells interact with helminths and the activation of Th2 and IgE expression.

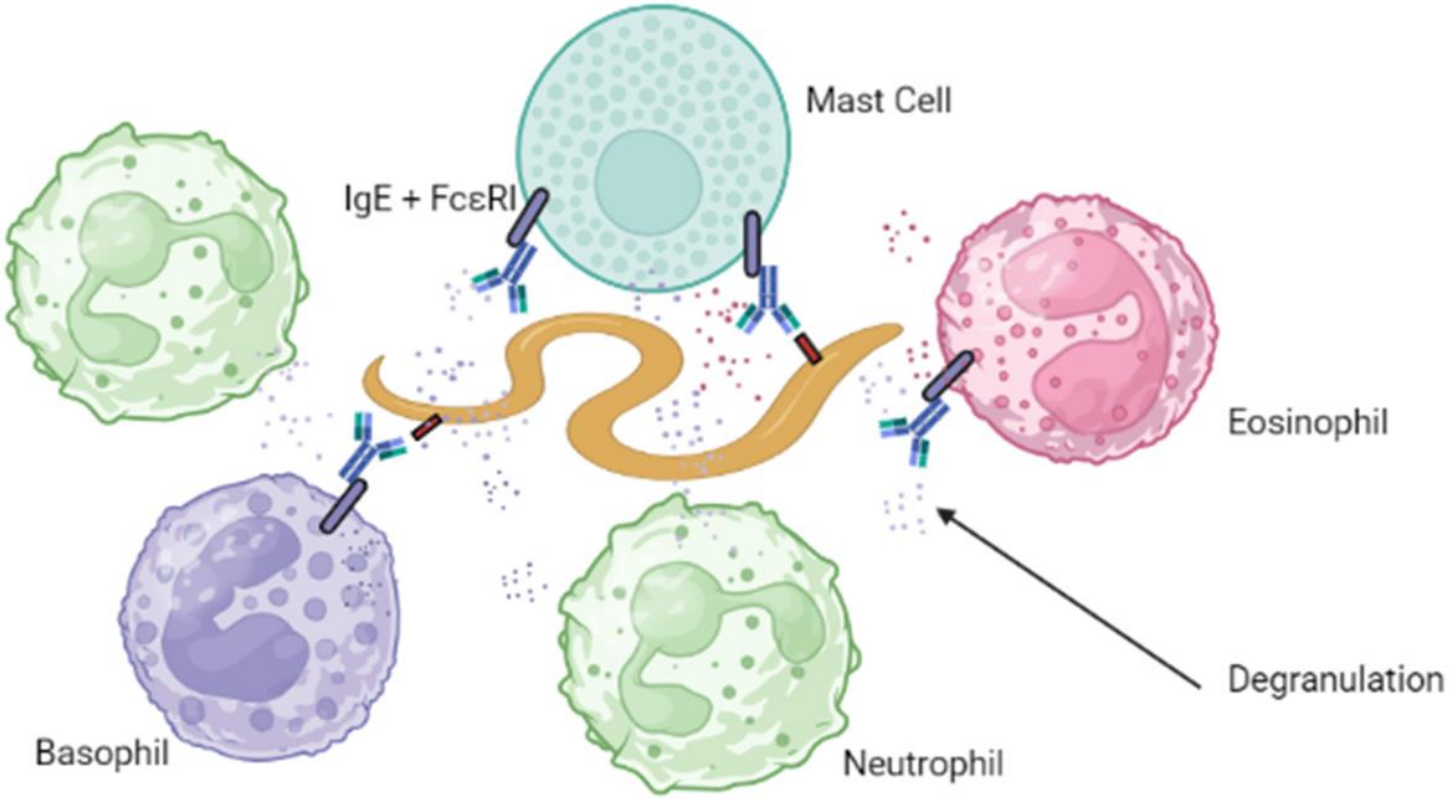

Figure 1.2.1.1 . Immune cells involved with parasitic infection and Th2 response to nematodes. The innate immune cells bind to nematode molecules causing degranulation. The degranulation causes a release of IL's activating the Th2 response. IgE expression increases leading to further degranulation and death of the nematode, through membrane permeability.

1.2.2 Parasite immune evasion methods

Helminths have evolved complex and elaborate immune evasion mechanisms, establishing chronic infection in a favourable environment (Shi *et al*., 2022), by developing sophisticated molecular adaptations to evade immune responses and communicate with the host immune system (Coakley *et al*., 2016). The mechanisms by which the parasites evade the immune system have been extensively studied, from basic strategies of hiding from the immune system to complex class switching between the Th1/Th2 pathway (Schmid-Hempel., 2009). A common immune evasion strategy employed by helminths is mimicry of host molecules, the immune system recognises the helminth as a self-molecule, ensuring parasitical survival. However, overexpression of "self" could also trigger an autoimmune response by the host leading to chronic inflammation and destruction of self-tissue and increasing immunopathology (Sorci *et al*., 2013).

The type of immune evasion technique deployed by the parasite, depends on the species (Chulanetra & Chaicumpa., 2021). For example, protozoan parasites can essentially hide from the immune response (Schmid-Hempel., 2009), toxoplasma parasites can physically hide within the central nervous system (CNS) or the eye (Bhopale., 2003). The reason for this is because the eye as well as the CNS; including the brain, are immune privileged, unleashing a full immune response in these areas can cause more permanent damage, immunity is therefore limited (Zambrano-Villa *et al*., 2002).

1.2.3 Passive immune evasion

Plasmodium species have the ability to protect its surface proteins from the immune system after they become opsonized (Schmid-Hempel., 2009). The mechanism is still unknown, however recent studies suggest the rosette formation could prevent immune clearing of the marked molecules on the plasmodium parasite as well as binding to multiple blood cells which are not marked for clearing (Lee *et al*., 2022).

Another common evasion technique is antigenic variation, both unicellular and multicellular parasites have both demonstrated this ability (Maizels *et al*., 2016). This is achieved either by containing antigenic variation glycoproteins on the surface, as observed in the protozoan Trypanosomes (Silva Pereira *et al*., 2021 and Barry & McCulloch., 2001) or by using host self- antigens such as blood glycoproteins, in which case the parasite is marked as self "mimicry"; observed mainly in helminths, in particular Schistosomes (Sepulveda *et al*., 2010).

The Plasmodium species have yet another method of evasion, entering a quiescent state, essentially remaining in a dormant state within the host. This is particularly challenging when the host is currently being treated with artemisinin- combination therapy (ACT), which under normal circumstances has a very high efficacy and has proved to be the most promising anti-malaria drug (Rathmes *et al*., 2020) However, once the parasite is dormant, ACT will then stop being administered to the patient, and the disease recurs again (Codd *et al*., 2011). This could potentially lead to drug resistant malaria which has emerged increasingly as of 2018, however ACT -resistant malaria had been reported in controlled environments only and not within the field (Tyagi *et al*., 2018 and Afonso *et al*., 2006).

The methods of evasion described above are considered a type of passive evasion, in which there is less complex communication with the host immune system. There is no activation or suppression of particular molecules and is mainly concerned with the parasites ability to hide or become unrecognisable. Despite the fact that these techniques are passive, they are in no way basic and involve elaborate mechanisms, most of which are poorly understood (Chulanetra & Chaicumpa., 2021). The mechanisms outlined here are characteristics of protozoans and Schistosomes. Another type of evasion which is also poorly understood and is considerably more complex is the active interference of the immune system, these are elaborate mechanisms of helminths (Mohd-Shaharuddin *et al*., 2021).

1.2.4 Active immune modulation

Most helminths do not multiply within their final host but produce eggs and larvae often leading to the debilitating diseases and presenting clinical, sometimes fatal, symptoms (Maizels & McSorley., 2016). Parasitic worms are often responsible for severe morbidity but lower mortality rates (Maizels *et al*., 1993). Parasites have developed extremely sophisticated molecular adaptations to evade the host immune responses as well as communicate with the host immune system (Coakley *et al*., 2016 and Schmid-Hempel., 2009). Table 1.2.4.1 shows a summary of the passive and active immune evasion techniques of human parasites.

Table 1.2.4.1. Parasites have evolved different immune evasion techniques. The intracellular parasites usually use passive immune evasion techniques, whereas the helminths tend to use more active immune evasion techniques, directly modulating the host immune response.

<table>
<tr><th>Parasite</th><th>Evasion mechanism</th><th></th></tr>
<tr><td>Protozoans</td><td>Antigenic Variation</td><td rowspan="4">Passive</td></tr>
<tr><td>Schistosomes</td><td>Molecular mimicry</td></tr>
<tr><td rowspan="2">Plasmodium</td><td>Quiescence</td></tr>
<tr><td>Hiding within immune cells or immune privileged sites</td></tr>
<tr><td>Nematodes</td><td rowspan="3">Immune modulation</td><td rowspan="6">Active</td></tr>
<tr><td>Cestodes</td></tr>
<tr><td>Trematodes</td></tr>
<tr><td>Nematodes</td><td>Competitive inhibition</td></tr>
<tr><td rowspan="3">Helminths</td><td>Signalling interference</td></tr>
<tr><td>Secreting Excretory/Secretory products</td></tr>
<tr><td>Extracellular vesicles - Exosomes</td></tr>
</table>

1.2.5 Th1 / Th2 pathways

T helper cells (Th) become activated and divide when presented with antigenic peptides by major histocompatibility complex II (MHC) molecules. MHC II molecules are on the surface of antigen presenting cells. There are two responses (Th1 or Th2) depending on the type of infection and the MHC molecule presenting the antigen to the T-cell receptor (TCR). The strength of the TCR signal determines the production of interleukins (IL) which in turn determines a Th1 or Th2 response. IL-12 drives the Th1 pathway while IL-4 drives a Th2 response, again the production of these Il's is determined by the strength of the TCR and the costimulatory facto CD28 (Dong & Flavell., 2000). Th1 cells respond to intracellular invasive organisms; bacteria, viruses, and protozoans (Miller *et al*., 2009). Whereas Th2 cells respond to helminth infections, causing an increase in various cytokines including multiple interleukins (IL-4, IL-5, IL-6, IL-13, and IL-10), as well as expansion of plasma cells, IgE secretion, and an increase in eosinophils, mast cells and basophils (Anthony *et al*., 2007). Some of the cytokines secreted during the Th2 response can also down regulate inflammation and can counteract the effect of the cytokines produced in the Th1 response. It is ideal to have a perfect balance between Th1/Th2 immune responses, a skewed Th1 response leads to chronic inflammation as well as neuronal damage and autoimmune disease (Vereertbrugghen et al., 2023). However, a skewed Th2 response leads to allergies (Kidd., 2003 and León *et al.*, 2021 and Berger., 2000). Allergies are considered a weighted Th2 imbalance (Cooper., 2009), increased production of IL-3, 4 and 5 lead to increased levels of IgE and B cells, as well as an increase in eosinophils and mucous secretion. A decrease in interferon-gamma has been observed in asthmatics, which is produced in the Th1 pathway

(Krammer *et al*., 2021 and Deo *et al*., 2010). There is a negative correlation between parasitism and allergies (Cooper., 2009), a high worm burden is generally associated with low allergic responses (McSorley *et al*., 2019). However, the exact mechanism between IgE, allergy and parasites are complex and not completely understood, although evidence and data has been significantly improved (Fitzsimmons *et al*., 2014). Previous studies have shown that there is strong evidence suggesting that in the absence of parasites, IgE binds to non-specific glycoproteins leading to hypersensitivity and over-production of eosinophils and mast cells (Prakash *et al*., 2022). When a helminth infects the host, the Th2 response is activated, suppressing the Th1 response. When the parasitic worms shift the immune response and activate the Th1 response, a chronic helminth infection is established (Miller., 2009).

The mechanism in which the intestinal helminths interact and modulate the host immune system still remains unknown, however, research suggests that extracellular vesicles (EV's) may be vital for this interaction (Zakeri *et al*., 2018). Exosomes secreted form helminths contain active biomolecules such as lipids, proteins, and RNA. The quantity of exosomes secreted from parasites differ between life cycle stages. Also, the specific protein cargo is not universal between each species. This implies that the exosomes secreted are specific to each host and are necessary to manipulate the host immune system for survival at different life cycle stages (Drurey & Maizels., 2021).

Th cells, also referred to as CD4+ cells, mature in the thymus, the same way as T-cells, and are vital for acquired immunity. Th cells must be activated into effector cells, this is achieved by two distinct signals. The first signal must come from an antigen bound to major histocompatibility complex (MHC). A second signal, signal 2 must come from costimulatory factors, this aims to amplify the signal. If signal 1 is received but not signal 2 the cell will trigger apoptosis. (Dong & Flavell, 2000 and Alberts *et al*., 2003)

When both signals are received, the Th cells then proliferate and depending on the environment and pathogen, the Th cells will differentiate into either Th1 or Th2 cells (Jankovic & Feng., 2015 and Romagnani., 1991). The importance of Th cells is observed in HIV, in which the virus infects CD4+ cells, hiding from the very cells which are designed to fight pathogens. This also implies that every pathogen has evolved their own elaborate mechanism of avoiding the immune system and in some cases being very successful as is the case with HIV (Clark *et al*., 2023 and Li *et al*., 2023).

The naïve T cell, releases cytokines produced before activation of the Th subset, which then induces transcription factors. Activation of specific transcription factors then decides differentiation of the Th cells into Th1, Th2, Th17 and Treg Cells, also known as suppressor T cells, which regulate and maintain the immune system (Khantakova *et al*., 2022).

The naïve T cells produce interferon gamma (IFNγ) and interleukin 12 (IL-12) cytokines; interleukins are a subset of cytokines (Lighvani *et al*., 2001), which then induce the T-bet transcription factor, leading to proliferation of Th1 cells (Kanhere *et al*., 2012). For Th2 cells, the naïve T cells produce IL-4 and IL-2, inducing the GATA-3 transcription factor (Zhou & Ouyang., 2003). Inflammation is highly regulated by metalloproteinases (MMPs) which are themselves regulated by TIMPs. TIMP-1 has been shown to display pro-inflammatory properties, activating the Th1 response, inducing cytokines promoting inflammation (Schoeps *et al*., 2022)

Cytokines are proteins which are secreted and can act within the endocrine, paracrine, and autocrine systems (Zhang & An., 2007). The BioLegend website (https://www.biolegend.com/) contains interactive pathways which describe each immune network in great detail. There is an entire completed cytokine network illustrating which cells produce which cytokine and what affect this cytokine has within the immune system.

1.2.6 Th1/Th2 imbalance and allergies

Completely removing antigens that would trigger the Th2 response can trigger an auto-immune response, usually referred to as the hygiene hypothesis, and is associated with Western societies and lifestyle. Exposure to helminths is negligible in the UK, any case of helminth infection is considered rare and is usually only found in migrants and those who have travelled. This leads to an imbalance of the Th1/Th2 response, causing a decrease in T-regulatory cells (Romagnani., 2004). Regulatory T cells (Treg) are CD4+ T cells, a type of Th cell, and have a role in suppressing and removing deleterious Th cells (Corthay., 2009). Treg cells are vital for maintaining

immune tolerance and preventing excessive immune responses and autoimmunity (Romano *et al*., 2019). Allergies are considered a weighted Th2 imbalance (Cooper., 2009). Production of IL-3, 4 and 5 lead to increased levels of IgE and B cells, as well as an increase in eosinophils and mucous secretion. A decrease in interferon-gamma has been observed in asthmatics, which is produced in the Th1 pathway (Deo *et al*., 2010).

Basophils, mast cells and eosinophils are vital for protection against parasitic helminths due to NET formation and degranulation, however they are also responsible for allergies. When no parasite proteins are present, IgE binds to foreign proteins, thus inducing the Th2 pathway, in the same way it would for parasitic infections (Galli & Tsai., 2012). In a normal functioning immune response, Treg cells would supress the Th2 pathway by secreting IL-10. This cytokine has an active role in basophil suppression (Larson *et al*., 2012). The connection between IgE, parasitism and allergy has led to the question can parasite proteins protect against allergy?

1.3 Tetraspanin proteins

1.3.1 Tetraspanin structure and domain function

Tetraspanins are a family of integral transmembrane proteins (Figure 1.3.1.1), there are distinctive characteristics of tetraspanin proteins such as: four transmembrane helices (TM1- TM4), with two extracellular regions, (EC1 and EC2), which are also referred to as the small extracellular loop domain (SEL) and a large extracellular loop domain (LEL), and three intracellular regions (Termini *et al*., 2017). They have

short NH2 and COOH cytoplasmic tails. Tetraspanin proteins are small transmembrane proteins with a size of 3-5nm and a molecular wight between 20-37kDa (Min *et al*., 2006), and have been shown to interact with other molecules including other tetraspanin proteins forming a "tetraspanin web", organising proteins into a multimolecular network of membrane domains (Jiang *et al*., 2015). Tetraspanin proteins have a highly conserved transmembrane helices, and a distinctive Cysteine-Cysteine-Glycine (CCG) amino acid motif in the EC2/ LEL domain, this domain is situated between TM3 and TM4 (Kitadokoro *et al*., 2001). The EC2 domain also contains between 2-8 cysteine residues, which are responsible for the disulphide bonds creating the structurally stable protein, these residues are conserved within a three-helix subdomain. The EC2 domain also contains a variable secondary structure, located within the conserved subdomain. Two important post-translational modifications often occur: glycosylation and palmitoylation. N-glycosylation sites are found within the EC2/LEL domain, apart from CD9 which has a N-glycosylation site in the EC1/SEL and CD81 which is non-glycosylated (Charrin *et al*., 2014 and Zimmerman *et al.*, 2016).

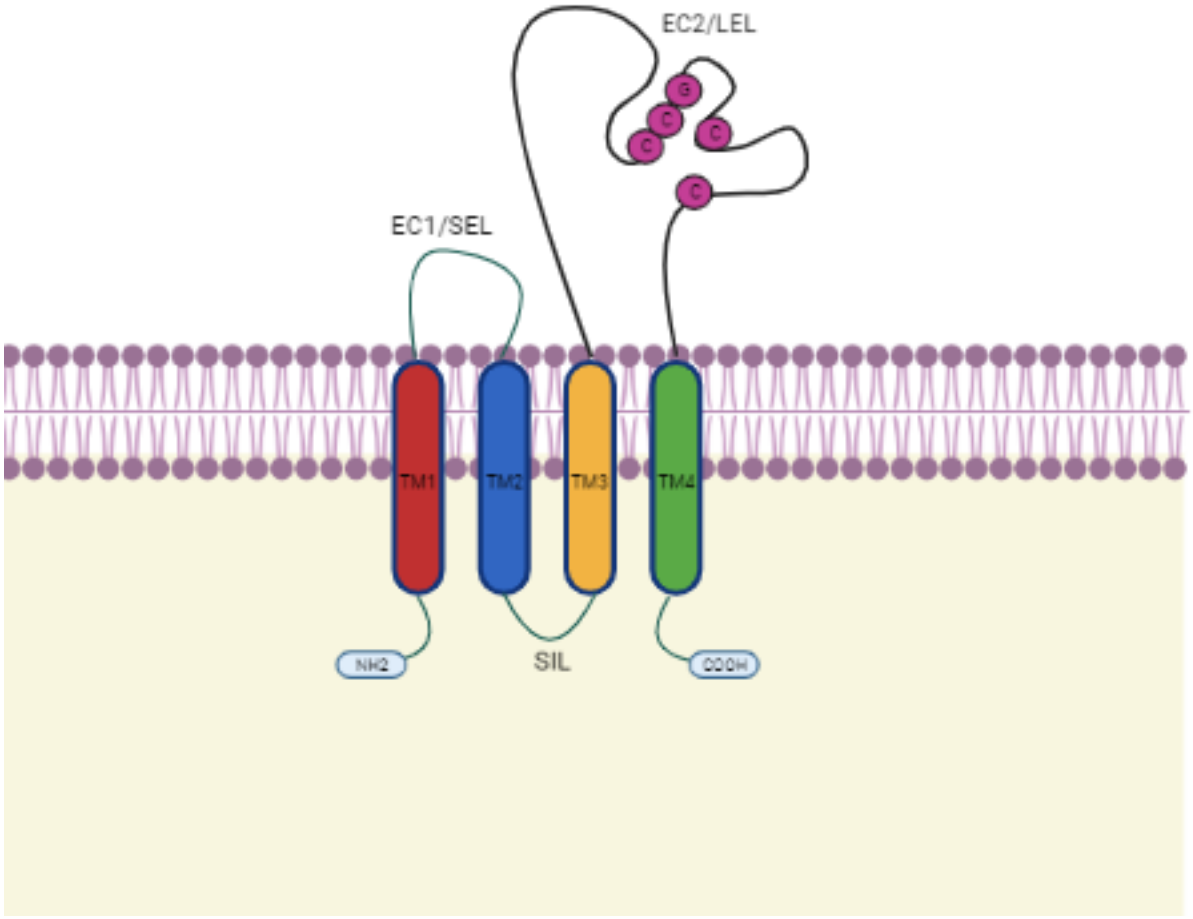

Figure 1.3.1.1. Schematic of CD63 tetraspanin protein. The protein consists of 4 transmembrane helices (TM1-TM4)**.** A small extracellular loop (SEL/EC1), a large extracellular loop (LEL/EC2) and a small intracellular loop (SIL) . Within the LEL are C-C-G and P-X-X-C-C motifs. NH2 = N terminus and COOH = C terminus. Image created with BioRender.com.

All the tetraspanin proteins share the same structure, which includes the 33 human tetraspanin proteins. Cluster of differentiation (CD) is the nomenclature used for proteins or molecules expressed on cell surfaces, which can act as ligands, receptors, or adhesion molecules (Engel *et al*., 2015). A table of the 33 human tetraspanins are listed in Table 1.3.1.1. CD9, CD81 ,CD63 and CD151 are the most abundant tetraspanin proteins , these proteins have been found to bind to multiple molecules. The function of these complexes formed are thought to be responsible for cell-cell communication and are involved with intracellular and extracellular signalling (Kummer *et al*., 2020, Termini et al., 2017, Umeda *et al*., 2020, and Dunlock *et al*., 2020). CD81 is usually involved with disease progression, especially cancer, CD81 binds to IgSF proteins and is heavily involved with pathogenesis (Pileri *et al*., 1998), CD63 binds to syntenin-1 which is responsible for the regulation of endocytosis, it has also been shown to bind to focal adhesion kinase (FAK), which then allows the binding of integrin proteins (Shimada *et al*., 2019). Along with CD9 and CD151, CD63 is also found in metastatic tumours at elevated levels (Dauros-Singorenko *et al*., 2018). CD9, CD81 and CD63 have been found to play a role in migration, cell fusion and protein trafficking (Parthasarathy *et al*., 2009), it has been suggested that CD63 may have a suppressor function in malignancy, when this protein was knocked down there was an increase in invasive malignant cells (Willms *et al*., 2018). Tetraspanin proteins mainly function as scaffolding proteins, binding to multiple proteins and forming the highly complex web, which determines the functional role of integrins, immunoglobulins, growth factor receptors, and signalling molecules (Andreu & Yáñez-Mó., 2014). CD63 binds to TIMP-1 and β1 integrin, activating signal transduction pathways and modulating cellular behaviour (Justo & Jasiulionis., 2021).

Table 1.3.1.1. Human tetraspanin proteins. The table shows the 33 known human tetraspanin proteins as well as the commonly used symbols and alternative names. There are 21 known tetraspanin proteins in *C. elegans*.

Tetraspanin	Symbol	Name
TSPAN-1		
TSPAN-2		
TSPAN-3		
TSPAN-4		
TSPAN-5		
TSPAN-6		
TSPAN-7		
TSPAN-8		
TSPAN-9		
TSPAN-10		
TSPAN-11		
TSPAN-12		
TSPAN-13		
TSPAN-14		
TSPAN-15		
TSPAN-16		
TSPAN-17		
TSPAN-18		
TSPAN-19		
TSPAN-20	UPK1B	Uroplakin 1B
TSPAN-21	UPK1A	Uroplakin 1A
TSPAN-22	PRPH2	Peripherin 2
TSPAN-23	ROM1	Retinal Outer Segment Membrane Protein 1
TSPAN-24	CD151	
TSPAN-25	CD53	
TSPAN-26	CD37	
TSPAN-27	CD82	
TSPAN-28	CD81	
TSPAN-29	CD9	
TSPAN-30	CD63	
TSPAN-31		
TSPAN-32		
TSPAN-33		

In unicellular eukaryotes, tetraspanin proteins regulate the morphology of the membrane and are involved in cell-cell interactions allowing for the evolution of multicellular eukaryotes (Wirth *et al*., 2021). The proteins are split into different groups: the CD family containing CD9, CD81, and CD63, including Tspan31. The uroplakin family, UPK 1A/1B, and the retinal degeneration slow family, ROM (Hu *et al*., 2015).

CD81, CD9 and CD63 are present in nearly all cells and most fluids, they also make up the tetraspanin proteins within the membrane of the exosomes (Kushman *et al*., 2017). Parasites release extracellular vesicles (Coakley *et al*., 2016), as a mixed population of microvesicles, exosomes, apoptotic blebs and shedding microvesicles, depending on their site of origin (Mathivanan *et al*., 2010). The importance of exosomes in cell-cell communication is only just being realised and studies have shown that it is the shuttling of the exosomal cargo that is responsible for novel extracellular communication between cells, and in which gene expression can be altered by the cargo of the exosomes (Colombo *et al*., 2014).

These extracellular vesicles are involved with intracellular communication by transferring the contents of their cargo, this includes proteins, lipids, and nucleic acids.

Tetraspanin proteins are known to play a role in membrane stability as well as adhesion, recently the importance of the tetraspanins is becoming apparent. CD63 plays a crucial role in exosome biogenesis. Exosomes containing CD63 are transported to the plasma membrane where the ILV's are released into the extracellular matrix. According to the entries on UniProt, CD63 is also involved with

cell organisation, specifically protein sorting and migration, as well as cell survival. CD63 binds to tissue inhibitors of metalloproteinase 1 (TIMP-1), these proteins modulate the cell to control the external and internal environment (Murphy., 2011). CD63 is a binding partner of TIMP-1, thus controlling regulation of the cell and its survival (Jung *et al*., 2006). TIMP-1 activates neutrophils to form neutrophil extracellular traps (NETs), this promotes inflammation and disease severity. This activation process of NETs is dependent on CD63 (Schoeps *et al*., 2022)

CD63 has some costimulatory factor for T -cell activation, allowing sustained proliferation of T-cell expansion (Pfistershammer *et al*., 2004). CD63 is part of the MHC-II endocytic compartment and can actively form complexes with MHC-II allowing peptide loading regulation of MHC-II (Petersen *et al*., 2011). Most research on tetraspanin proteins and their function is centred on the interaction between integrins and tetraspanins. The binding of CD63 to alpha-IIb CD9 complex could also contribute to activation and modulation of immune cells such as neutrophils (Israels *et al*., 2001).

The exact function of CD63 has not yet been determined, however from the extensive research to date, it is evident that the CD63 tetraspanin protein is more complex than a scaffolding protein, involved in many regulatory pathways. There is much to be discovered about the tetraspanin family and the interactions they have with each other within the highly complex network that they form. The tetraspanin proteins are also involved with pathogenic disease but is still unclear. However, research has identified the human tetraspanin protein 18 (Tspn18) as a Ca^{2+} regulator in Orai1 signalling, and a knockout of Tspn18 leads to a decrease in Ca^{2+} and

impaired Orai1 signalling causing a deficiency in release of thrombo-inflammatory mediators (Noy *et al*., 2019).

Tetraspanin proteins contain very distinct palmitoylation sites, this process is a post-translational enzymatic modification where palmitic acid is covalently attached to Cysteine residues by a thioester linkage (Sobocińska *et al*., 2018). Palmitoylation is responsible for membrane association but may also play a pivotal role in formation and stability of the tetraspanin web (Yang *et al*., 2002). Palmitoylation is a reversible process and is associated with detergent resistant membrane formation (Resh., 1999 and Andreu & Yáñez-Mó., 2014).

The extracellular domains are the least conserved regions of the tetraspanin proteins and are the regions in which glycosylation can occur (Andreu & Yáñez-Mó., 2014). Glycosylation is a secondary protein process which is complex and tightly regulated, determining the tertiary structure of proteins which directly determines the function of the protein (Stanley & Okajima., 2010). The SEL is highly variable between different tetraspanins, and some can be glycosylated and therefore may not be recognised by antibodies. (Andreu & Yáñez-Mó., 2014). However other studies have shown that the SEL within CD81 is required for the LEL to bind at sufficient levels to hepatitis C virus (HCV); major envelope glycoprotein (E2), where the SEL was absent, the LEL binding was significantly reduced. The role of CD81 and HCV binding function is dependent on the EC2 (LEL) domain (Bailey & Thuru., 2023).. CD81 is also capable of recruiting other viral entry factors entry factors such as CD9 and CD63 to allow virus entry into the cell (Lasswitz *et al*., 2022 and Fénéant *et al*., 2014).

CD81 is the most extensively studied tetraspanin, however the studies investigating the LEL and binding capacity with viral pathogens have not been carried out with a majority of the tetraspanin proteins. The tetraspanin proteins are similar and it is therefore inferred that the structure and sites of other tetraspanin proteins would spatially be similar to CD81 (Lasswitz *et al*., 2022 and Andreu & Yáñez-Mó., 2014).

It is the transmembrane regions of the tetraspanin proteins which are conserved, and any mutation reported in these regions have resulted in disease or degenerations, for example, CD9 is essential for fertilisation, CD9 knockout mice lead to a decrease in female fertility due to egg cell deformation (Jégou *et al*., 2011). Dysfunctional tetraspanin proteins have resulted in retinal disorders due to defects in melanosome formation (Edgar *et al*., 2014 and Andreu & Yáñez-Mó., 2014).

The cytoplasmic region is the most crucial to the function of tetraspanins. In CD63 the cytoplasmic regions contain the motif: Glycine-Tyrosine-Glutamic acid-Valine-Methionine (GYEVM) which is responsible for CD63 sorting into late endosomes (Andreu & Yáñez-Mó., 2014). CD63 is crucial for exosome biogenesis (Figure 1.3.1.2) and is directly involved in the ESCRT-independent sorting of intraluminal vesicles (ILV's) into exosomes (van Niel *et al*., 2011). CD63 also plays a key role in clathrin-coated particles and lysosome-associated membrane proteins (LAMP) and sorting, mutation on the GYEVM sequence influences expression concentration (Rous *et al*., 2002).

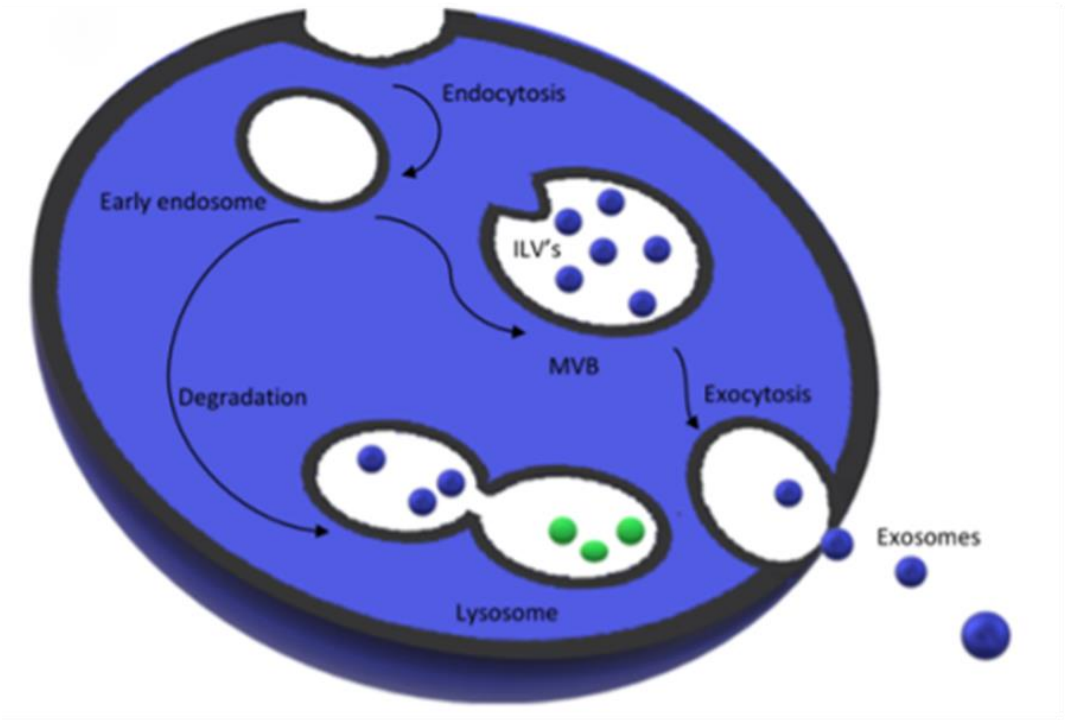

Figure 1.3.1.2. Exosome biogenesis. The plasma membrane invaginates into early endosomes, the early endosomes not tagged with CD63 are marked for degradation. CD63 marked endosomes are recycled in multivesicular bodies (MVBs) and sorted into intraluminal vesicles (ILVs). The MVBs fuse back into the plasma membrane and the ILVs are released during exocytosis as exosomes.

1.3.2 Tetraspanin location

Tetraspanin proteins have been identified in various cells, expressed in nearly all eukaryotic cells (Jiang *et al*., 2015), there are 33 tetraspanin proteins in humans (Kummer *et al*., 2020). Uroplakins are found mainly within the urothelium (Matuszewski *et al*., 2016), and peripherin proteins are restricted to the retina (Tebbe *et al*., 2020). CD37 and CD53 are only found in leukocytes (Dunlock., 2020), but CD9, CD81, CD82, CD63 and CD151 are the most ubiquitous and have a wide distribution within various cells (Kitadokoro *et al*., 2001). Extracellular vesicles are enriched with tetraspanin proteins. CD9, CD81 and CD63 are the most abundant and commonly identified tetraspanins found within the membrane of exosomes.

Current research shows that CD63 could play a pivotal role in activation and degranulation of mast cells (Kraft *et al*., 2013). Basophil activation requires CD63, and anti-CD63 antibodies are currently being considered as therapeutic targets for severe allergic responses (Kraft *et al*., 2005). During basophil activation, levels of CD63 are thought to be increased, CD63 acts as a biomarker for allergies (Erdmann *et al*., 2003). CD63 is not present on the surface of neutrophils until activation, in this sense CD63 acts as an activation marker for allergies and disease and could be a factor in degranulation (Källquist *et al*., 2008).

CD63 is present in a multitude of cells and thus has far greater importance than originally thought, CD63 is critical in trafficking and in the endocytic pathways. CD63 can cross-link with other complexes and activate or influence various immune cells (Pfistershammer *et al*., 2004). It is still unclear if CD63 is involved with disease progression or immune activation as both functions have been observed for CD63.

There is much research needed to identify the connection between exosomes, CD63 and disease, in order to find possible therapeutics or drug targets for these diseases, including autoimmune diseases as well as pathogenic diseases.

1.3.3 Tetraspanins and disease

CD63 interacts with adaptor proteins forming complexes and is linked to clathrin-dependent pathways. CD63 can also be found in Weibel-Palade bodies (WBP's) in abundance (Streetley *et al*., 2019). These granules are found in the lining of blood vessels and the heart and are involved in homeostasis and inflammation. Research suggests that CD63 could be an important co-factor for P-selectin, this protein is involved in the leukocyte activation cascade, as well as binding to other carbohydrates and T- lymphocytes (Doyle *et al*., 2011 and Vischer & Wagner., 1993).

Bacterial membrane vesicles do not contain any tetraspanin proteins, however bacterial cells adhere to human tetraspanin proteins on epithelial cells, particularly CD9, CD63 and CD151. When these tetraspanin proteins where knocked-down, adhesion to epithelial cells was reduced significantly for *Neisseria meningitidis* as well as *staphylococcus species*, *Streptococcu*s and *E. coli* (Andreu & Yáñez-Mó., 2014, Dauros-Singorenko *et al*., 2018, Green *et al*., 2011 and Tippett *et al*., 2013).

Viruses also have the ability to use tetraspanin proteins to their advantage, HIV binds readily to CD63, whereas hepatitis C binds to CD81 (Florin *et al*., 2018 and Farquhar *et al*., 2012). Binding of viral and bacterial pathogens is still poorly understood

especially with regards to their interactions of tetraspanin proteins (Tippett *et al*., 2013). There is still some controversy surrounding CD63 and HIV-1, CD63 has been shown to actively suppress the chemokine CXCR4, a coreceptor for HIV-1 entry into cells (Yoshida *et al*., 2008). CXCR4 is a potential key drug target for HIV and therefore CXCR4 inhibitors in addition to other Highly Active Anti-Retroviral Therapy (HAART), are being developed and used to treat this disease (Grande *et al*., 2019 and Murakami & Yamamoto., 2010). Other studies have shown CD63 proteins can become incorporated into HIV viral particles, although the mechanism and interactions between CD63 and HIV have so far not been elucidated (Fu *et al*., 2015).

CD63 plays a role in infection of some fungal infections, such as *Cryptococcus neoformans*; a fungal disease which can cause meningitis in those who are immunocompromised. CD63 is recruited along with MHC-II and CD82 (Artavanis-Tsakonas *et al*., 2011).

Tetraspanin proteins are currently being investigated as potential candidate leads in the treatment of Schistosomiasis, also known as bilharzia, which is a disease caused by parasitic flatworms called schistosomes. A tetraspanin found within the tegument, which is a cytoplasmic coat separating the parasitic trematode from the host (Winkelmann *et al*., 2022), of *S. mansoni*, (smTSP-2) is being investigated as a potential target vaccine antigen. Mice with recombinant smTSP-2 had a reduction in worm burden (Pinheiro *et al*., 2014). In the parasite *Echinococcus multilocularis*, multiple tetraspanin proteins have been identified in the tegument as well as the larval stages. The efficacy of the tetraspanin vaccine was significant, when administered with Freund's adjuvant, where protection increased, and a strong IgG immune response was induced. Cysts were reduced by 85%, overall, the tetraspanin

vaccine was efficient and provided good immune protection. However, the trial was conducted in mice, and the adjuvant has been found to cause toxicity in humans. The experiment shows that a tetraspanin vaccine is effective and has decent efficacy, however, an adjuvant is needed and finding a suitable one at this time for human administration is proving challenging (Dang *et al*., 2012). *Fasciola hepatica* also contains tetraspanin proteins within the tegument and potentially on the exosomes they release, however the genome entry for *F. hepatica* on the WormBase ParaSite website is still poorly annotated. A bioinformatics approach does suggest that CD63 related gene is incorporated within the genome of *F. hepatica*, but this has yet to be confirmed. A number of potential Tetraspanins have however been identified within the tegument of *F. hepatica*, the sequences were fragmented but did strongly resemble the tetraspanin proteins found within *S. mansoni* (Wilson *et al*., 2011).

1.4 Bioinformatics applied to research

1.4.1 The importance of Bioinformatics

NCBI is arguably the most important biomedical database, containing over 160,000 organism's genome entries. Databases such as WormBase ParaSite (https://parasite.wormbase.org/index.html) can be used for identifying the majority of parasitic organisms. Other databases such as PlasmoDB (https://plasmodb.org/plasmo/app) and TriTrypDB (https://tritrypdb.org/tritrypdb/app), are specific databases for Plasmodium species and Trypanosome species.

Programmes such as Reactome (https://reactome.org/) and BioGRID (https://thebiogrid.org/), are open access tools which are constantly being updated by researchers across the world contributing to the accuracy of the website. Using these programmes, a search for the protein will allow the researcher to identify any interactions or interactors with their target protein. By using a multitude of different network programmes, a complex map of the target protein and its interaction can be established.

Bioinformatics has greater importance in drug discovery. When discovering a drug, it is vital that the molecule or drug does not cause toxicity in the host or have some adverse effect not observed. For example, the thalidomide treatment used in the 1950's-1960's to treat morning sickness in pregnant women, the drug was not tested on the foetus and the side effects of thalidomide caused severe birth defects in babies. Had bioinformatics been established at this time, thalidomide could have been tested through various programmes for its toxicity, and the four stages of breakdown in the body; absorption, distribution, metabolism, and extraction (Audouze & Taboureau., 2022).

1.4.2 Aims and Objectives of the Research Presented

The purpose of this study is to identify similar parasitic proteins to tsp-7, an orthologue to human CD63. TIMP-1/CD63 has been shown to have key roles in inflammation, and cytokine activation. TIMP-1 binding with tsp-7 could suggest that parasitic nematodes use functionally similar proteins to hijack the host immune system by competitively binding with TIMP-1, dampening the immune system, and shifting the immune response in favour of the nematodes in order to establish chronic infection.

A) In this project bioinformatics will be utilised to identify the homologous gene of CD63 in the model organism *Caenorhabditis elegans*. To make alignments between the DNA sequence as well as the protein sequence, creating phylogenetic trees. Specific programmes will be used to identify domains and specific amino acids of potential importance as well as finding the potential interaction of the protein with other proteins or molecules, such as TIMP-1. Potential binding models will be created using multiple docking platforms and compare predicted structures of the protein from generated data against predicted online structures.

The importance of bioinformatics in this project is to lay down the theory and produce the foundation of the project. By identifying what the protein could look like in 3D structure allows research to identify potential protein-protein interactions under normal conditions.

All the programmes used in this project are freely available online and require no service fees. The programmes and platforms are accessible to anyone. The structures designed here are purely theoretical and cannot be validated without proper

laboratory experiments, however through using multiple programmes there is a degree of confidence that the structures are reliable.

Other aims and objectives of the research presented within this PhD Thesis are:

B) The wild type *C. elegans* has been extensively studied in terms of stress response and life span. However, there is no data on stress response behaviour or the life span of mutant *C. elegans* and tetraspanin protein 7 knockouts. Two mutant strains of *C. elegans* with various amino acid deletions will be compared against the wild type *C. elegans*, when exposed to different stimuli. Chemical stimuli will be used to measure three locomotive stress response behaviours (Coiling/ Omega coils, sinusoidal undulation, and reversal frequency). The chemical stimuli used will be: Osmotic stress, exposure to heavy metals (Zn^{2+}), and exposure to environmental pollutants (4-Octylphenol). The mutant strains will be compared to the wild type in terms of average life span under normal conditions and the survival rates between the strains under heat and cold stress (37℃ and 5℃).

C) An antibody will be designed against the LEL of tsp-7, based off the 3D model structures predicted. The antibody will be tested against the wild type and the mutant strain *of C. elegans*. COS-7 cells will be transfected with the full tsp-7 protein tagged with GFP, and incubated with active human TIMP-1 molecule, to establish co-localisation of TIMP-1/tsp-7.

Chapter 2: Methods

2.1.1 Sequence retrieval

The human gene sequence (CD63) encoding CD63 from *H. sapiens,* was obtained from the NCBI website (https://www.ncbi.nlm.nih.gov/). The HomoloGene webpage found on NCBI was used to identify homologues of CD63. Both the amino acid sequence for the protein encoded for by the gene CD63 (*H. sapiens*) and tsp-7 (*C. elegans*) were obtained in FASTA format.

The WormBase ParaSite database (https://parasite.wormbase.org/index.html), was used to identify the protein sequence for *C. elegans* (PRJNA13758).

The genome tab was selected and *C. elegans* was chosen from the nematode list. Tsp-7 was entered into the search bar, gene ID: WBGene00006633. All nucleotide and protein sequences were obtained in FASTA format.

2.1.2 Orthologues, paralogues, and splice variants

The WormBase ParaSite database was used to identify any paralogues, genes that evolved through duplication within the same species and orthologues, genes inherited through speciation. And also, any alternative transcripts (splice variants). The data set retrieved was then filtered to find any nematodes that are parasitic to humans. These are the only species which were included for the following sequence

alignment and phylogenetic trees. All other *Caenorhabditis* species were removed from the search lists.

2.1.3 Blast search of tsp-7

The amino acid sequence for tsp-7 was used in a BLASTP (protein sequence) search on the WormBase website, with the standard recommended parameters against nematode species in the database. The 19 human parasites from the orthologue set were included in the custom search list.

Another BLASTP search was used using the NCBI Blast programme, against all nematode species. Non-redundant protein sequences were chosen as the search set. The protein-protein Blast algorithm was selected as the standard programme.

A second BLASTP search was also conducted, the protein data bank proteins (pdb) was selected as the search set. The parameters were left as recommended by the programme.

2.1.4 Protein sequence alignments

Protein sequences for *C. elegans* tsp-7 protein, were copied to the muscle alignment tool on the EMBL-EBI webpage (https://www.ebi.ac.uk/Tools/msa/muscle/). Output results were converted to Pearson/fasta, and all files downloaded as FASTA files (.fas) format. The sequences could then be opened in multiple programmes for further editing and annotation. The tsp-7 sequence was aligned against the human

equivalent CD63 protein, as well as the other most commonly identified tetraspanin proteins in humans, which are : CD81, CD9, CD53 and CD151.Alignments were also created for tsp-7 and the most closely similar proteins identified from the Blast search. All alignments were then used to compare the percentage similarity and percentage identity at the amino acid level, between *C. elegans* tsp-7 and the human tetraspanin proteins.

2.1.5 Local alignments

Both the human CD63 and *C. elegans* tsp-7 protein sequences were aligned using the lalign programme, the pairwise sequence alignment from the molbio-tools website; (https://www.ebi.ac.uk/Tools/psa/lalign/). Both proteins were aligned against other human tetraspanin proteins identified previously. The proteins used for alignments were: AAC60586.1 CD9 antigen, AAH40693.1 CD53 molecule, AAH13017.1 CD63 molecule, AAH93047.1 CD81 molecule and NP_001034579.1 CD151 antigen from humans and NP_492636.1 Tetraspanin (tsp-7) from *C. elegans*.

2.1.6 Phylogenetic trees

In the MEGA X programme, (https://www.megasoftware.net/), 50% conservation was highlighted in the sequences, across all species aligned. Within the 50% conservation site, marked on the sequence alignments, the CCG motif was identified, (Cysteine – Cysteine – Glycine amino acid sequence). The residue PXXCC (Proline – X – X – Cysteine – Cysteine) was also identified in the sequences and highlighted.

The phylogenetic trees were created using a bootstrap value of 500, applying the maximum likelihood method and JTT matrix-based method (Jones *et al.*, 1992).

Comparisons were made between the human CD63 protein and tsp-7, as well as the other human tetraspanin proteins mentioned above. Also included in the phylogenetic trees are sequences from the 19 identified human parasitic nematodes in chapter 3.2.

2.1.7 3D models

The sequences retrieved from the WormBase ParaSite database and NCBI were used to create a 3D modelling structure of the protein. SWISS MODEL (https://swissmodel.expasy.org/) is an online open server, which is an automated protein homology modelling server. The structures for the predicted 3D tertiary structure of CD63, CD151, CD53 and tsp-7 can be found on the AlphaFold database (https://AlphaFold.ebi.ac.uk/). The theoretical models are created for tsp-7 and CD63, using the AlphaFold monomer V2.0 pipeline, and are recent editions, as of July 2022 and much of the homology and 3D modelling was undertaken prior to these 3D models being available.

On the SWISS-MODEL, website after the sequences had been entered into the target sequence box a template search was conducted. The database searchers for 3D structures already determined and deposited in the PDB database, the template can then be checked for sequence similarity as well as quaternary structure. Three of the similar template structures were selected, models were then based on these templates to create a predicted 3D structure for the tsp-7 protein.

The 3D models were then downloaded from SWISS MODEL as a PDB format. And further manipulated in other freely available programmes.

2.1.8 Chimera X

The files were opened in the UCSF Chimera X programme.

Chimera is a next generation molecular visualisation programme from the Resource of Biocomputing, Visualisation, and Informatics (RBVI).

Using the tools tab, sequence viewer was selected.

In the command line of Chimera, two protein structures were opened simultaneously and morphed to create one protein overlapping the two protein structures. Command = “matchmaker #1 to #2”. The programme was used for the majority of the structure editing.

2.1.9 Domain

The domain for the tsp-7 was found by using information provided in the literature, in which the human tetraspanin CD63 protein is mapped. The information for the tsp-7 protein was therefore based on the paper by Saito *et al*., 2022, identifying domains within the tertiary structure of CD63. These features were then marked up on the tsp-7 model from the AlphaFold database and marked in Chimera X. The information retrieved from mining the literature was corroborated with the sequence provided for tsp-7 in the AlphaFold database.

The NCBI conserved domain search (https://www.ncbi.nlm.nih.gov/Structure/cdd/wrpsb.cgi) and ThreaDom (https://zhanggroup.org/ThreaDom/) was used to also identify the domain within the tsp-7 protein. In the amino acid viewer of Chimera X, the option to highlight various amino acids is available. Using this tool, the entire domain (LEL) can be highlighted.

2.1.10 Residues

NetNglyc1.0 (https://services.healthtech.dtu.dk/service.php?NetNGlyc-1.0) was used to find N- linked glycosylation sites, and Netphos 3.1(https://services.healthtech.dtu.dk/service.php?NetPhos-3.1) server was used to find amino acids subject to potential phosphorylation. All the servers used for identifying key features within the protein sequence can be found on the DTU health Tech website (https://www.healthtech.dtu.dk/english). All features identified were marked using the Chimera X programme.

2.1.11 PyMol

PyMol is a molecular visualisation programme used to compare the protein sequence structure similarity produced from the various models. PyMol uses command lines to interpret the data. The Root Mean Square Deviation is calculated by finding the RMSD of the distance between atoms using the equation:

$$RMSD = SQRT[\{SUM(d_{ii})^2\}/N]$$

d_{ii} = distance between i^{th} atom of structure 1 and i^{th} atom of structure 2

N = number of atoms matched in each structure.

A RMSD value of 2.0Å or less is considered true to the structure.

2.1.12 Protein interaction databases

STRING (https://STRING-db.org/cgi/network?taskId=bS1RxQGPtk3j&sessionId=bbOT2IKzPy5n) is a database of known protein-protein interactions, compiled from literature and experimental data. The CD63 protein from humans was entered into the STRING website to find potential known protein pathways. The tsp-7 protein was also searched for in the STRING database to identify tsp-7 interactions.

Reactome (https://reactome.org/) is another free open-source peer reviewed pathway database containing both Human and *C. elegans* entries. BioGRID (https://thebiogrid.org/) is an online interaction depositary which is freely available.

All three databases were used to collate known interactions and tissue specific sites for both CD63 and tsp-7. The information collected from these databases are either directly from experimental data or have been mined from multiple literature resources.

2.1.13 Binding

Protein-protein docking interactions were created using the HADDOCK, ClusPro and PRODIGY programmes online (https://wenmr.science.uu.nl/haddock2.4/), (https://cluspro.bu.edu/home.php) and (https://bianca.science.uu.nl/prodigy/). For the template binding, the tsp-7 protein produced from AlphaFold was used for the potential interactions against proteins and molecules known to bind to CD63. The proteins used to dock against tsp-7 are taken from the databases used previously.

All of the protein structures were retrieved from the PDB website, UniProt or AlphaFold.

2.2 Husbandry of *Caenorhabditis elegans*

2.2.1 OP50 *E.coli* stock

2.5g LB broth, high salt containing Casein enzyme hydrolysate 10g/l, Yeast extract 5g/l, NaCl 10g/l, pH7.5 (Sigma-Aldrich) was dissolved in 100ml deionized water and autoclaved. Once cooled, an *Escherichia coli* OP50 BactoBead™ (Edvotek) was cut in half and placed into the LB broth. The broth was separated into aliquots of 3 x 5ml T406-2A sterile culture tubes (Simport) and placed in an orbital shaker at 37°C overnight, 125 rev/min (Stuart Scientific).

The following day, when the *E.coli* broth turned cloudy, 500µl of broth was added to 500µl of 50% glycerol stock (final concentration 25% V/V) in a 1.5ml Eppendorf and stored at -80°C.

2.2.2 Nematode growth medium (NGM)

Three strains of *C. elegans* were used throughout the project; Wild Type N2, and two mutant strains derived from the N2 Wild type Bristol strain. Specialised growth medium was formulated for maintenance of the *Caenorhabditis elegans* strains. Both the mutant strains and the wild type were maintained using the same NGM recipe: 3g NaCl, 17g Agar, 2.5g peptone (Sigma Aldrich), and 975ml sterilised water. After the solution had been autoclaved and allowed to cool to 55°C, 1ml 1M $CaCl_2$, 1ml 1M $MgSO_4$ (Sigma Aldrich) was also added. 25ml of a 1M KPO_4 buffer (KH_2PO_4, with NaOH pellets added gradually to pH 6.0) was added. Finally, 1ml of cholesterol

(Sigma Aldrich) was added (stock concentration of 5mg/ml in 100% ethanol, final concentration in media = 5µg).

The medium was poured into standard petri dishes (25ml in 15mm X 100mm) and left to set. The *E.coli* stock solution was removed from -80℃ just before plating, and the top layer was scraped off using a pipette tip and placed into 1ml sterile water. 50µl of diluted *E.coli* OP50 was seeded onto the NGM plate creating an even *E.coli* lawn and incubated at 37℃ overnight.

2.2.3 Obtaining mutant strains and wild type *C. elegans*

Two strains of *C. elegans* with amino acid deletions were obtained from the National BioResource Project Japan (NBRP, collaborators of Caenorhabditis Genetics Centre, Minnesota, USA), which were derived from the original N2 Bristol strain. Allele tm5046 has a deletion of 4 amino acids, while allele tm5761 has a deletion of 69 amino acids within the tsp-7 gene. Figure 2.2.3.1 shows the positions of the deletion in relation to the protein coding transcript of tsp-7. The wild type N2 Bristol strain of *C. elegans* was gifted from Professor Alan Morgan, Liverpool University.

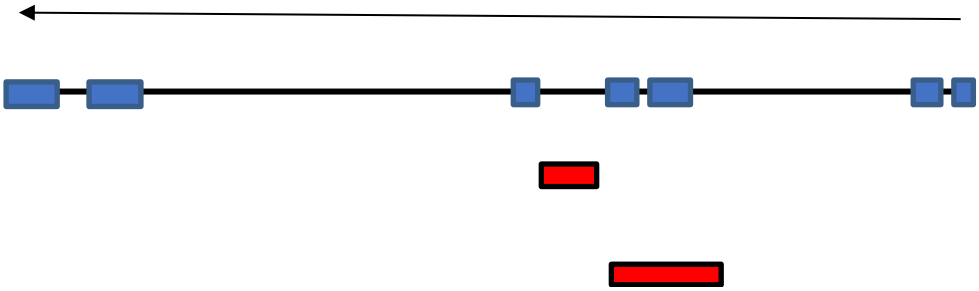

Figure 2.2.3.1. Exon transcript of tsp-7 protein and deletion positions of mutant *C. elegans*. 7 exons coding the tsp7 protein (blue boxes) reading from right to left following the direction of the arrow. The two mutant strains have deletions within the coding sequence of tsp-7 (Red boxes). Tm5046 has deletion of 4 amino acids: TGMV at exon 5. Tm5761 has a deletion of 69 amino acids: RLATPILLLVIGSLCTLLGFLGCCGAIRENYCLTVSFAVLLALLITCEIAAVII GYALHDSFRLGIGNQLQ at exons 3-4.

2.2.4 *C. elegans* transfer

The chunking method was used to transfer both mutant and wild type strains of *C. elegans* onto freshly seeded agar. A chunk of agar containing worms is cut and placed onto the side of the new agar, allowing the worms to crawl out onto the freshly prepared agar. All plates were kept at 10-16°C, and worms were transferred every 3 days to prevent overcrowding. All strains were kept in the same conditions at all times.

2.2.5 Single worm pick

To collect single worms a homemade pick was fashioned (Figure 2.2.5.1). The tip of a small piece of copper wire (5cm) was flattened with the edge of a blade and inserted into ethanol then passed through a flame to burn off excess ethanol. The wire was gently wrapped around a bacterial L-shaped spreader. The copper wire pick can be used to collect 1-10 worms at once. The copper wire was replaced after 5-10 uses due to constant flaming of the copper and replaced with a newly fashioned pick.

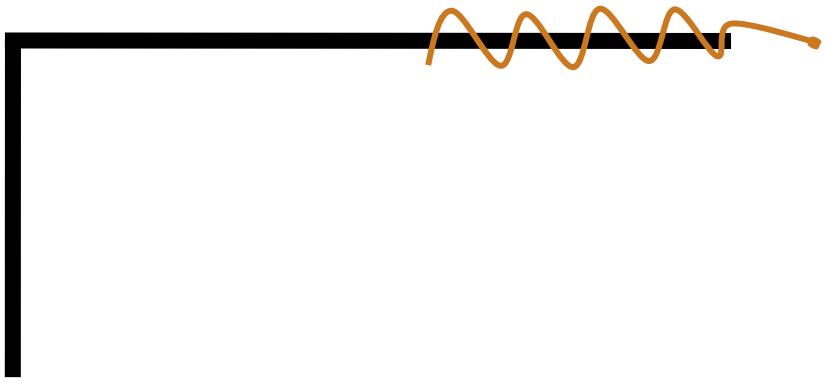

Figure 2.2.5.1. Schematic of the nematode pick. A small piece of copper wire ~5cm, was cut and coiled around a bacterial spreader. Up to 10 worms can be picked at a time using the fashioned nematode pick.

2.2.6 Freezing *C. elegans* stock

Each plate was washed with a 2ml S-buffer (64.5ml 0.05M K_2HPO_4, 435ml 0.05M KH_2PO_4, 2.925g NaCl, pH 6.0) and transferred to a sterile 5ml universal tube. 2ml of sterile 30% glycerol was added to the universal with a final concentration of 15% V/V. The glycerol stock solution was transferred to cryovials and placed in a Styrofoam box and stored at -80℃.

2.2.7 Life-span assays

A synchronous population of *C. elegans* was obtained by single picking 10 adult stage hermaphrodite worms from a semi crowded plate, from each strain and placed onto freshly seeded medium. After 24 hours the eggs were counted, if over 50 eggs had been laid by the adults, they were then removed and placed back into the original population. The eggs were kept at the same temperature and allowed to continue through their life cycle. When the worms reached their adult reproductive stage, they were transferred every day until no more eggs were laid. The worms were subsequently counted daily. A loss of worms due to burrowing, escaping or loss through transfer, were recorded as censored data. Worms that could be considered dead were tapped lightly with the pick; a slight movement was considered as being alive. Any dead worms were removed from the plate and discarded. The assay reached completion when the final worm had died. The assay was carried out in three replicates of ~100 worms per plate unless stated otherwise for each strain. The final worm population was calculated and further analysed using statistical analysis.

2.2.8 Heat shock treatment

Synchronous worm populations were not needed for the heat shock assay. Instead, 10 adult worms were picked and placed into small petri dishes (15.9mm x 90mm). The adults were left at 37℃ for 1 hour, 2 hours and 3 hours respectively, in replicates of two, for each strain, with a total of 60 worms per strain. After 1 hour the first replicates were removed and counted, worms were not removed but allowed to recover at room temperature for 1 hour before being placed back into the cooler. The same process was used after 2 hours and 3 hours. 3 hours is considered lethal. After 24 hours, worms were checked, dead worms were recorded, and the survival percentage calculated.

2.2.9 Cold shock treatment

The cold shock treatment was similar to the heat shock wherein 10 adult worms were picked and placed into smaller petri dishes. The assay was repeated in triplicates for each species and the worms were placed at 5℃ and left for 24 hours. After which the worms were allowed to recover at room temperature. After one hour, the worms observed as dead were recorded. The worms were then placed back into the cooler at which they had been grown and left for another 24 hours. The dead worms were then recorded again, and the survival percentage was recorded.

2.2.10 Osmotic stress

The three strains were subject to osmotic stress on trajectory motion. The normal trajectory motion is the standard locomotion behaviour displayed by *C. elegans*. The "S" shaped undulation, reversing, and omega turns. These trajectory motions can be observed when *C. elegans* are exposed to stress stimuli and measured (Stephens *et al*., 2010). After plates were seeded at 37℃, they were then covered with 100µl 500mM NaCl and 1M NaCl. It has previously been shown that *C. elegans* can adapt and survive exposure of 500mM NaCl after acclimatising to osmotic stress over a 4-week period (Lamitina *et al*., 2004). The plates were then left for 1 hour to dry. 20 adult worms were then placed onto an agar plate containing no *E.coli* and left at room temperature for 60 minutes to acclimatise. The worms were then transferred to the test plate and left at room temperature for another 60 minutes. Locomotion was monitored for 5 worms per replicate plate (representing 25% of the population), for 1 minute each per locomotive behaviour (3 trajectory motions in total). The parameters set out for each locomotive behaviour assessment is as follows:

1) Sinusoidal undulation: the head movement must pass the baseline and the animal must be propelled in a forward motion (Figure 2.2.10a). Head movements but no propulsion is dismissed, and each movement past the baseline is individually counted.
2) Reversal frequency: the animal must move in either the forward or backward direction to be counted as a reversal. Each movement is counted separately (one forward and backwards movement is scored as 2).
3) Coiling frequency: the animals must form a distinct coiling shape (figure 2.2.10b), partial bends are not counted as coiling behaviour.

2.2.10a

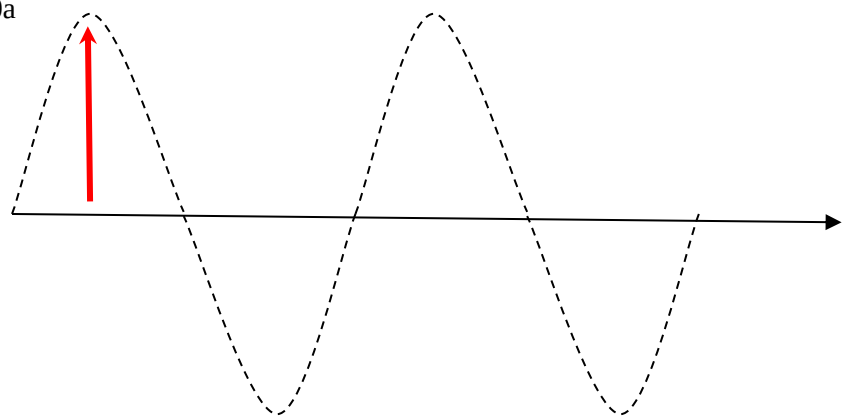

2.2.10b

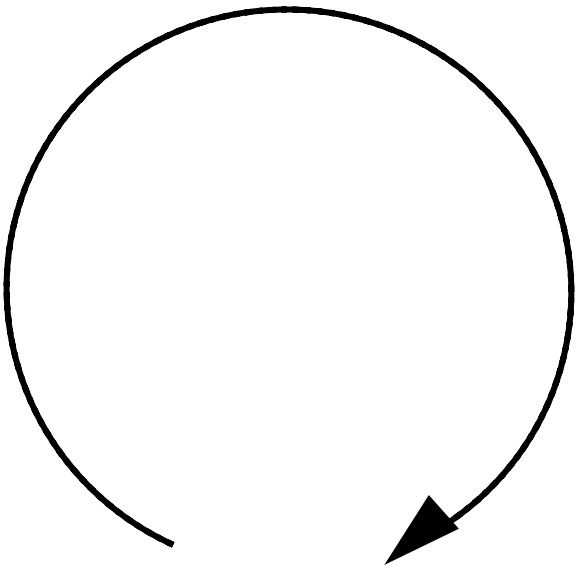

Figure 2.2.10. Schematics showing locomotive stress response behaviour parameters. The Sinusoidal movement (a) set out as a parameter for measuring stress in response to chemical stimuli. Each movement to the left or right (red arrow) past the baseline is counted as one individual turn/movement. All movements must be in the forward direction (black arrow). Worm movements only in the head region that do not pass the baseline are not counted. The coiling behaviour must form a complete circle (b) so that the anterior almost touches the posterior region in order to count as one coil.

2.2.11 Ethanol, 4-Octylphenol and Zinc stress response

Similar to the osmotic stress on locomotion, the same assay was performed using 100µl 100% ethanol (Davies & McIntire., 2004). The same methods were carried out for the assay plates and the same parameters set out above were also followed. Similarly, 100µl of 50mM stock solution of 4-Octylphenol, final concentration 5mM (Weltje *et al*., 2005) and 100µl of 1M and 0.5M Zinc (Park *et al*., 2017) were also used to test locomotive behaviour in response to chemical stimuli.

2.2.13 Liquid Culture

Inoculate LB broth with frozen OP50 stock, by scraping the OP50 *E. coli* stock with a pipette tip and placing in the LB broth then incubate overnight at 37°C. The bacterial culture was then subject to centrifugation at 4,000 rpm for 10 minutes and the supernatant discarded. The bacterial pellet was resuspended in 100µl S-medium (S-Basal, potassium citrate, trace metal solution, 1M $CaCl_2$, 1M $MgSO_4$). S-Basal; 5.85g NaCl, 1g K_2HPO_4, 6g KH_2PO_4, 1ml cholesterol (5mg/ml). Trace metal solution: 0.18g Disodium EDTA, 0.069g $FeSO_4.7H_2O$, 0.02g $MnCl_2.4H_2O$, 0.029g $ZnSO_4.7H_2O$, 0.003g $CuSO_4.5H_20$. 5ml of S-medium was added to 3 plates and the solution transferred to a conical flask. The bacterial pellet was added, and the solutions were left at room temperature in a tabletop incubator at 150rpm for 2-3 days.

2.3 Protein extraction and immunochemistry

2.3.1 *C. elegans* lysis

Standard plates of the three *C. elegans* strains were used, 2ml of M9 buffer were added to each plate (3g KH_2PO_4, 5g NaCl, 1ml 1M $MgSO_4$, 6g Na_2HPO_4, deionized water to 1L, pH 7.02). Autoclaved and stored at 4℃. 1ml of M9 buffer containing the nematodes, was then transferred from the plates to 1.5ml Eppendorf's. The worms were left to settle at the bottom of the tube at room temperature for about 30-60 minutes. The M9 solution was removed from the tubes as much as possible leaving the worms undisturbed. 1ml fresh M9 buffer was added to each tube and subject to centrifugation at 2000rpm for 1 minute. The M9 buffer was removed, and the process repeated another two times. Further washing was required if the solution was not clear.

Worms were left to settle again at the bottom of the tube, in some cases pellets were combined to one tube. The pellets were frozen at -20℃ until further use.

2.3.2 Membrane lysis

The pellets were removed from -20℃ and kept on ice, the pellets were resuspended in 500µl of membrane lysis buffer (5mM HEPES, 0.32M sucrose, ½ protease and phosphatase inhibitor tablet (Pierce, Thermo-Fisher) pH 7.2) and stored at 4℃.

The pellets were then sonicated (Sonic systems, sonic processor p100), the tubes were assembled below the ultrasonic rod, such that the pellets were constantly in contact with the ice to prevent heat damage to the samples. Wattage was increased to 4, samples were sonicated for 30 seconds then immediately submerged in ice for 30 seconds. The process was repeated a total of 3 times for each sample. With a total sonication time of 90 seconds. The pellets were then subject to centrifugation, at 15,000 rpm for 30 minutes at 4℃. The supernatant was removed and 150µl 1-2% SDS was added to the pellets and heated to 95℃ for 15 minutes then left at room temperature for 60 minutes.

2.3.3 Protein estimations

A Bradford assay was used to estimate the protein concentrations of the sample lysates, as well as the A280nm method. A quartz cuvette was used as well as a UV / visible spectrophotometer set to 280nm, and the samples read. The Beer Lambert equation was used to determine the protein estimation of the whole cell lysate. The protein concentration was calculated using the equation : 1.0 Absorbance reading = 1mg/ml of protein.

2.3.4 Antibody development

The protein sequence for the tsp–7 large extracellular loop domain (LEL) was sent to Thermo-Fisher Scientific custom polyclonal antibody service. A 90-day 2x rabbit immunisation protocol was chosen due to optimisation of speed, and serum titre as well as being cost efficient. The protocol includes antigen design, peptide synthesis, Immunisation, Serum collection and purification as well as titre data. The antigen score is based on Thermo- Fisher's proprietary algorithm which considers multiple factors: primary and secondary structure of the sequence, hydrophobicity and hydrophilicity, amino acid charges, isoelectric points, mass, pH mapping, as well as physical and chemical properties. Two New Zealand white rabbits, specific pathogen free were selected. The anti tsp-7 antibodies were conjugated with Keyhole Limpet Hemocyanin (KLH) immunostimulant. Antibodies are guaranteed to reach 1:50 000 minimum titre by indirect ELISA. Antibody: AB3954 final concentration 0.4mg/ml, AB3955 final concentration 0.74mg/ml. Peptide antigen OBS-169-193 concentration of 5mg/ml was also provided. The peptide antigen sequence: EGCARENAPLFEPGCIHSVEQWVLK. The location of this sequence with regards to the LEL of tsp-7 protein structure can be found in chapter 5, Figure 5.3.1.

2.3.5 Antibody stocks

Antibodies were stored at 4°C unopened for two weeks, 6x 500µl aliquots of AB3955 and AB3954 were stored at -80°C, 4x 500µl aliquots were added to 50% glycerol (25% V/V 1ml) and also stored at -80°C. 6x 500µl aliquots of AB3955 were

stored at -20℃, and 2x with 50% glycerol (25% V/V). 2x aliquots of 100µl were also stored at -20℃ as the working stock antibodies. For AB3954 8x 200µl were stored at -20℃ and 2x 500µl with 50% glycerol were also stored at -20℃. When the 100µl or 200µl samples were removed from the freezer, the remaining solution was further stored in smaller aliquots of 20µl to avoid repeated freeze-thawing of the antibody, to minimise degradation.

2.3.6 Dot blot

A dot blot assay was carried out for the peptide developed, as a positive control. The peptide was diluted 10-fold serial dilution with a starting concentration of 5mg/ml, the dilutions were as follows; 1:10, 1:100, 1:1 000, 1:10 000, 1:100 000. A thin strip of nitrocellulose membrane was cut and marked in pencil. The peptide was diluted in a carbonate coating buffer (3.03g Na_2CO_3, 6g $NaHCO_3$, distilled water to 1L). 2µl of samples were loaded onto the membrane at a final concentration of 1000ng, 100ng, 10ng, 1ng and 0.1ng, respectively. A second strip was cut and marked the same way with the same dilutions from the same samples. At the end of each strip, 2µl of each lysate was added (50µg N2, 36µg tm5046 and 28µg tm5761). The membranes were left to dry at room temperature. Once dried the membranes were blocked with a 5% blocking buffer (100ml TBST, 5g Dried milk powder). The blots were left in the blocking buffer for one hour at room temperature. Blocking buffer was poured off and the membrane was incubated with primary antibody. Primary antibody (AB3955) was diluted in blocking buffer with a final concentration of 740ng/ml (1:1000 dilution, recommended by Thermo Fisher Scientific). The membranes were

left in a container and covered in aluminium foil and left at 5°C overnight. The membranes were washed three times for 5 minutes with TBST (100ml TBS, 900ml dH_2O, 0.5ml Tween-20). Membranes were incubated with an anti-rabbit IgG (HRP) secondary antibody (ProteinTech) in blocking buffer (1:1000), for one hour at room temperature. The membranes were washed again, once for 15 minutes in TBST, then twice for 5 minutes also in TBST, then once in TBS for 5 minutes. The first membrane strip was then covered in 2ml (TMB) and left for 1-5 minutes. If blue blots appeared, then the second membrane was covered in 2ml ECL chemiluminescence detection solution (Thermo-Fisher). The membrane was left for 5 minutes then visualised on the BioRad Chemidoc detection system. The membrane was scanned using the Chemidoc XRS scanner. All images were exported as image files and the Image J software was used to further analyse the images.

A second dot blot protocol was designed to optimise binding of primary antibody to the wild-type (N2) and two mutant strains (tm5046 and tm5761). Again, 2µl of lysate sample (50µg N2, 36µg tm5046 and 28µg tm5761) was added to a nitrocellulose membrane and left to dry, no blocking buffer was added, but the primary antibody was immediately added undiluted to the dried lysate sample. Again, these were left to dry at room temperature, the secondary antibody was added (1:100 dilution) and left to air dry. The ECL was added and visualised as described above.

2.3.7 Enzyme-linked immunosorbent assay (ELISA)

ELISA assays were used to compare titre standard between the two designed antibodies and the antigen peptide. An indirect checkerboard titration was carried out as well as a standard titre. The designed peptide was dissolved in 1ml sterile distilled H_2O (5mg/ml) and immediately aliquoted into 5x 200µl and stored at -20°C. For the standard ELISA titrations for both antibodies against the peptide, the standard concentration of 10ug/ml (20µl peptide/ 9.8ml carbonate coating buffer). 100µl of the 10ug/ml peptide was added to 8 wells of a 96 well titre plate and repeated in triplicate. The lid was placed back on to the plate and kept at 5°C overnight. The solution was tipped out and washed with 200µl per well of TBST. After the final wash, 200µl of 5% blocking buffer was added to each well and left at room temperature for 2 hours with the lid on. The blocking buffer was removed, and the wells washed 3 times with 100µl TBST again. The primary antibody was diluted in 5% blocking buffer at a logarithmic dilution as follows: 1:10, 1:30, 1:100, 1:300, 1:1 000, 1:3 000, 1:10 000, 1:30 000. The final concentration of each antibody is as follows: AB3954; 40000ng, 13300ng, 4000ng, 1330ng, 400ng, 133ng, 40ng, 13.3ng. AB3955; 74000ng, 24600ng, 7400ng, 2460ng, 740ng, 246ng, 74ng, 24.6ng.

2.3.8 Western blot

The concentration of protein in the lysates, previously determined using the Bradford assay, were used for the western blots. 5µl of 2x Laemmli sample containing β mercaptoethanol were added to the lysates. The samples were vortexed briefly and placed in a heat block for 5 minutes at 95°C. A mini-protean TGX 12% precast gel (BioRad; 4561043) was used, a pre-stained protein marker, 10-180kDa (ProteinTech, PL00001) was used and 8µl was loaded into the appropriate well. 25µl of sample were loaded into the wells (final concentration of 35µg/25µl). The power supply was set to 120 volts and the samples in the gel were electrophoresed for about 45-60 min. Once switched off, the cassette was then prised open and the gel removed and left in transfer buffer (BioRad) for 10 minutes, while the PVDF membrane was activated in methanol. The membrane and gel were assembled in the blotting system following the manufacturer's instructions and run on a BioRad Turbo Trans blotter, for 10 minutes to transfer the protein bands onto the membrane. The membrane was incubated in blocking buffer at room temperature for 1 hour, with constant agitation. The membrane was then washed in TBST for 10 minutes and incubated in anti-tsp-7 primary antibody 1:1000 (Thermo-Fisher scientific) and left at 4°C for 24 hours. The membrane was washed in TBST 5x 10 minutes each wash. The secondary antibody (Anti-Rabbit HRP, ProteinTech) was diluted in blocking buffer at a concentration of 1:1000. The membrane was incubated with the secondary antibody at room temperature for 30-45 minutes, with agitation. The membrane was washed again three times for 5 minutes in TBST, and chemiluminescence substrate was prepared (Pierce ECL substrate). The membrane was covered in equal volumes of luminol enhancer and peroxide buffer (5ml). The membrane was left at room temperature for

5 minutes, excess solution was removed, and the membrane was transferred to the Chemidoc XRS detection system (BioRad).

2.3.9 Immunohistochemistry

A square of agar from one plate of N2 worms was cut and placed into a cassette, paraffin wax was poured onto the cassette slowly to embed the agar. The wax cassette was placed onto ice and left to completely solidify. After cooling, the cassette was placed on a pre-cooled microtome. The thinly sliced section was then placed into water to remove creases in the section, then placed onto a slide. The slide was heated at 37°C for roughly 30 minutes. The slide was placed into xylene for 10 minutes and then immediately transferred to industrial methylated spirit (IMS) for 10 minutes. The slide was washed in dH_2O for 10 minutes and stained with Toluidine blue. The slide was then placed back into dH_2O, IMS and then xylene for 10 minutes each. The sample was covered with a coverslip and left to set. The slide was visualised using a microscope.

5ml of M9 buffer was added to one plate of N2 worms, the worms were centrifuged at 5,000xg for 5 minutes and placed on ice to allow worms to settle. The supernatant was aspirated slowly so as not to disturb the pellet. The pellet was resuspended in 100µl 100% ethanol, to fixate the worms. A double volume of xylene was added to the worm suspension (200µl). A cassette was half filled with paraffin wax and 50µl of the worm suspension containing xylene was added to the middle of the solidified paraffin wax. More paraffin was added to the worm suspension to seal the sample within the cassette. The process was then repeated same as above.

2.4 Molecular biology and cell expression

2.4.1 LB Agar and broth

20g of LB agar and 12.5g LB broth (Miller) were dissolved in 500ml dH_2O. Once cooled ~55℃, 0.5ml of a 100mg/ml stock ampicillin antibiotic was added to a final concentration of 100µg/ml. Stock ampicillin was sterile filtered through a 0.22µm polyethersulfone syringe filter unit (Millex-GP) and stored at -20℃. The agar was set in a standard petri dish (15mm X 100mm) and inverted, sealed, and stored at 4℃. 2x LB broth solutions were made without adding agar, one contained the same final concentration of ampicillin, the other contained no ampicillin. LB broth was stored at 4℃.

2.4.2 Transformation of DH5α

Three different tagged pcDNA3.1 plasmids containing the tsp-7 (Genscript) were subject to centrifugation for 1 minute at 6,000xg. Plasmid 1 = FLAG tag, plasmid 2 = GFP tag and plasmid 3 = HIS tag. 100µl dH_2O was added to each 10µg of lyophilised plasmid DNA. The plasmids were transferred to aliquots of 10µl and stored at -20℃. Competent DH5α subcloning efficiency *E.coli* cells (Thermo-Fisher) were thawed on ice, then gently mixed using a pipette. 10µl of each plasmid was added to 50µl of competent cells and incubated on ice for 40 minutes. Cells were subject to heat shock for 30 seconds at 42℃ then removed and immediately placed back onto the ice for 2 minutes. 950µl of pre-warmed LB broth containing no

ampicillin was added to the competent cells and incubated at 37℃ for 1 hour (with agitation at 225rpm). 6 X LB/ampicillin plates were pre-warmed, 50µl of competent cells from each plasmid were spread on 3 plates and 100µl on the remaining 3 plates. Plates were incubated at 37℃ overnight. The plates were screened for single colonies. 0.25ml of ampicillin was added to 250ml LB broth (final concentration 100µg/ml). 3ml of LB/ampicillin was added to 15 culture tubes, 5 single colonies were picked from either 50µl or 100µl plate (depending on single colony formation) and placed into the culture tubes. The tubes were incubated at 37℃ overnight, 200rpm (Sciquip incushake maxi).

2.4.3 Transformed DH5α Stock

Culture tubes that had turned turbid where then removed and 3ml of a 50% glycerol stock solution were added to the culture tubes (final concentration of 25% (V/V) glycerol). The optical density at 600nm (OD600nm) was measured and the cultures tubes were stored at -80℃.

2.4.4 Plasmid purification

DNA was purified using the Qiagen mini and maxi prep kit. The mini prep kit was used to purify the DNA from all 15 single colonies. LyseBlue reagent was added to buffer P1 prior to purification at a ratio of 1:1000 following the manufacturer's instructions. After the final step in which 70% ethanol is added to the DNA pellet

and centrifuged at 15,000xg for 10 minutes, the supernatant was removed and the pellet was resuspended in 1ml 10mM Tris-Cl, pH 8.5. The eluted DNA was stored at -20°C.

A culture tube containing stock transformed DH5α containing GFP tag was removed and immediately placed on ice. 200µl of the thawed stock solution was placed in 250ml of pre-warmed LB broth containing ampicillin and incubated overnight at 37°C with agitation in an orbital shaker at 200rpm. The DNA was purified using the same Qiagen protocol and stored in the same Tris-Cl buffer.

The DNA concentration was measured using the 260/280 ratio with a reading >1.7 equalling a pure DNA sample. A reading of 1 O.D at 260nm = 50µg/ml of dsDNA in the sample.

2.4.5 Agarose gels

To make 50X TAE for agarose, 100ml 0.5M EDTA was added to 700ml dH_2O, 242g Tris was dissolved in the solution and 57.1ml 100% acetic acid was added, dH_2O was added to a final volume of 1L (final concentration; 50mM EDTA, 2M Tris, 1M acetic acid). To make a 100ml 0.5M stock of EDTA, 18.61g Na-EDTA was added to 80ml dH_2O. NaOH pellets were added slowly with constant stirring for a final pH 8.0. dH_2O was added to 100ml and the solution was sterilised using a standard autoclave. 1L of 1X TAE running buffer was made using 20ml of the 50x TAE and 980ml dH_2O (final concentration in gel; 1mM EDTA, 40mM Tris, 20mM Acetic acid). All solutions were stored at 4°C.

All DNA samples were run on 1% agarose gel: 1g Agar in 100ml dH_2O and heated for 1 minute until the agar had completely dissolved. The solution was left to cool, then 2ml 50X TAE was added and 10µl GelRed. The agarose was immediately poured into the gel tray.

3µl of DNA ladder (New England Biolabs) was diluted in 12µl dH_2O and 3µl 6X loading dye. 2µl of loading dye was added to 5µl of each of the DNA samples. Agarose gels were run at 120 volts for 45 minutes. Agarose gels were visualised using either the Chemidoc system (BioRad) or using a UV transilluminator.

2.4.6 Primer design

All primers were designed in SnapGene. The primers were designed from the tsp-7 sequence insert in the FLAG tagged vector. Both forward and reverse primers were designed so that only the domain can be amplified for restriction. Nucleotides were added to the sequence as a slight overhang with restriction sites incorporated. Primers are as follows:

Forward primer:

Tsp7_Exd_BamHI_FP 5' aaaggatccATGGTACGATATCACGAGAGTCGAGG 3'

Reverse primer:

Tsp7_Exd_HindIII_RP 5' tttaagcttgAATTCCGCCGACCATTGCTCC 3'

Small letters = restriction site and additional nucleotides

Restriction sites were checked through the New England Biolab programme and the appropriate sequence containing the domain was used. The restriction enzymes chosen, cuts the domain. Bam-HI and Hind-III were chosen.

2.4.7 PCR

The primers were centrifuged briefly and dissolved in 191µl and 217µl dH_2O for the forward and reverse primer, respectively. 0.5µl of the forward and reverse primer were used for the PCR as well as 2µl of FLAG tagged tsp-7 vector from Genscript, 22µl of H_2O and 25µl of 2X Phusion Flash High fidelity master mix (Thermo-Fisher). The PCR protocol is as follows: Preheat to 105℃, Initial denaturation 1 minute at 98℃, Denaturation for 10 seconds at 98℃. Annealing for 15 seconds at 60℃ and extension for 1 minute at 72℃, repeated for 30 cycles. Final extension for 1 minute at 72℃.

The PCR protocol was optimised, wherein a gradient temperature was used to find optimal annealing, from 55℃ – 65.1℃. Again, the PCR protocol was further optimised by using the purified GFP tagged tsp 7 plasmid and increasing the gradient from 60.8℃ to 69.3℃, with the optimum between 66.6℃- 69.3℃. The PCR product was run on a standard 1% agarose gel.

2.4.8 Restriction digestion of pET-21a vector and PCR product

A 40µl reaction containing 3µl of pET21a plasmid, 4µl of 10X CutSmart and 1µl each of BamHI-HF and Hind-III restriction enzymes were incubated for 1 hour at 37℃. 1µl of alkaline phosphatase was added and the reaction incubated for a further 60 minutes at 37℃.

45µl of PCR product was pooled and 250µl of PB buffer was added and mixed for 30 seconds. The solution was transferred to a spin column and subject to centrifugation for 2 minutes at 13,000 rpm. The flow-through was discarded and 750µl of PE buffer was added to the column and subject to centrifugation as above. 34µl of ddH_2O at 50℃ was added and incubated for 1 minute at room temperature and then subject to centrifugation. The purified PCR product was then added to 4µl of 10X CutSmart and 1µl of each primer and incubated at 37℃ for 2 hours.

Both reactions were run on 1% agarose and visualised using a UV transilluminator, the bands were cut for both the pET21a vector and PCR product and placed into separate Eppendorf's and stored at 4℃ for future use.

2.4.9 Gel and PCR clean-up

Both pET21a vector and PCR product were purified using QIAquick PCR & Gel clean up kit. Briefly, 900µl of buffer QG was added to each gel band and incubated at 50℃ for 10 minutes and vortexed every 2 minutes until the gel had completely

dissolved. The samples were added to a spin column and collection tube and subject to centrifugation for 1 min at 16,000rpm. 750µl PE buffer was added to each column (and centrifuged for 1min/16,000rpm). Centrifugation was repeated to remove residue. Columns were transferred to 1.5ml Eppendorf and 50µl EB buffer was added with a final centrifugation spin (1min/16,000rpm).

2.4.10 Ligation

The DNA concentration of purified PCR and plasmid product were measured using a nanodrop spectrophotometer. The purified PCR product was then inserted into the purified pET21a vector via ligation. 3µl of the digested PCR product was added to 5µl of digested plasmid, 1µl each of 10X ligase buffer and T7 ligase (New England Biolabs) were added to the mix and the ligation mixture was left at room temperature for 1 hour and then stored at 4℃.

2.4.11 Transformation of DH5α using pET21a vector

The ligation mixture was then used to transform DH5a competent *E.coli* cells following the same procedure outlined above. 3 single colonies were picked and placed into LB broth at 37℃ (235 rpm) overnight. The following day the 3 colonies were subject to plasmid purification (Qiagen mini prep, see section 2.4.4) and again subject to PCR to confirm plasmid and domain insertion.

2.4.12 Expression of tsp-7 domain in BL21 competent cells

Competent BL21 (DE3) *E.coli* cells were transformed using the purified pET21a vector. The protocol of transforming BL21 (Thermo-Fisher) is the same as above for transformation with DH5α cells. An empty pET21a vector (with no tsp-7 insert) was also used as a control in the transformation. Three colonies of the BL21 containing pET21a tsp-7 insert were picked and placed in 4ml of LB. One colony from the control plate was picked and also placed into 4ml of LB. The cell cultures were incubated at 37℃ overnight (225 rpm). The following day the OD600nm was measured for each sample. 4ml of fresh LB was inoculated to achieve an OD600nm = 0.1. The cells were placed back in the incubator and measured every 30 minutes until the 0D600nm = 0.5. 20µl of 200mM IPTG was added to each culture tube (final concentration of 1mM) and grown at 37℃ for 3 hours (225 rpm). 200µl of the culture was centrifuged and the supernatant discarded, the pellet was resuspended in 10µl 2X Laemmli buffer and incubated at 95℃ for 15 minutes. The cell cultures were run on an SDS-PAGE gel and stained with Page-blue.

2.4.13 Cell culture

COS-7 cells were obtained from Chester medical school. The stock cells were thawed and placed into prewarmed DMEM-F12 GlutaMAX media containing 50ml FBS (10%), 5ml nonessential amino acids (1X concentration) and 5ml Penicillin-Streptomycin (1% concentration) (Thermo-Fisher). The cells were placed in a T-25

flask and left for 3 days at 37℃. All cell culture procedures were carried out in a sterile laminar vertical flow hood (Class II cabinet) under aseptic conditions.

After 3 days the cells were observed under a microscope (Zeiss), if confluency was <70% the cells were washed, and fresh media added. Those with >70% confluency were set up for cell passage.

2.4.14 Cell passage

Cells that had more than 70% confluency were split. The media was removed from the flask, removing all dead cells. The flask was then washed with 10ml PBS (Thermo-Fisher). The PBS was removed and 3ml of Trypsin-EDTA (Thermo-Fisher) was added to each flask. The flask was immediately placed back into the 37℃ incubator for 3 minutes. After three minutes the flask was observed under the microscope to check for cells becoming fully detached. Once 90% of the cells were in suspension, 7ml of media containing 10% FBS was added to the flask to stop trypsin damaging the cells. The suspension was subject to centrifugation at 1000xg for 5 minutes at 4℃. The supernatant was discarded, and the pellet resuspended in 15ml fresh media.

5ml of the media was added to a clean, sterile T-75 flask and 10ml of media added on top for a 1:3 dilution. The cells were placed back in the incubator at 37℃, 5% CO_2 and the media checked daily for cell viability (see 2.4.16).

2.4.15 Stock cell lines

When enough cells had reached confluency, cells were stored at -80°C. Cells were treated the same as they would when passaged, however, once the pellet remains, 3ml of freezing solution is added (9ml DMEM-F12 with 1ml DMSO (10% concentration). The cells were transferred to 1.5ml cryovials and placed in a 'Mr Frosty' Freezing Container (Thermo- Fisher), slowly reducing the temperature at a rate of 1°C/min and stored at -80°C in the short term.

2.4.16 Viable cell count

To assess cell viability, a small sample of 50-100µl of cells are taken from the media and resuspended in fresh media. 20µl of this sample was mixed with 20µl of 0.4% trypan blue (Thermo- Fisher). 20µl of the solution was inserted into a countess chamber slide. The cells were counted automatically in a countess automated cell counter (Life Technologies).

2.4.17 Transfection of COS-7 cells

Cells were prepared 24 hours prior to transfection. Cells were counted using the same method as above and seeded in a 24 well plate. 5.16 x 10^5/ml of viable cells were counted (total cell count = 2.58 x 10^6). 5 x 10^4/ml of cells is the recommended number of adherent cells to seed prior to transfection. 20 wells (1ml/well) were seeded, 1.97ml of the original cell suspension in 20ml of growth medium. The plate

was placed back into the incubator. The following day, 2.5µl of the purified GFP tagged DNA (see section 2.4.7) final concentration of 0.5µg, was added to 2ml of serum free media and aliquoted into each well (100µl/well).

2µl of TurboFect transfection reagent (Thermo- Fisher) is the recommended volume, however a plate was set up with conditions in which the reagent was added in a volume ranging between 1-2.8µl in duplication. Once the optimal volume for transfection reagent was determined a second plate was set up in the exact same way using the two best optimal volumes (2.6 and 2.8µl) of transfection reagent. The 24 well plate as placed back in the incubator and left for 24-48 hours. Cells were viewed under fluorescence microscopy to determine the percentage of cells that were expressing the GFP tagged tsp-7 and therefore appeared to emit green fluorescence.

$$Transfection\ efficiency = \frac{Number\ of\ fluorescent\ cells}{Total\ number\ of\ cells} \times 100$$

2.4.18 TIMP-1 protein interaction with tsp-7

5µl of active TIMP-1 molecule (Abcam) was added to each well containing 100µl media. (stock concentration, 100µg/ml; final concentration of TIMP-1 in each well – 5ng). The test plate was left at room temperature to allow for efficient binding for 1-2 hours.

The primary conjugated antibody, Anti-TIMP-1 Antibody (G-6) Alexa Fluor® 647 (Santa Cruz Biotechnology) was then added 20µl per well (1:50 dilution). The test plate was left again at room temperature for 1 hour. Then visualised using fluorescence microscopy.

2.4.19 Fluorescence microscopy

Before TIMP-1 was added to the test plate, cells were observed under the EVOS FL Auto imaging system (life technologies) then washed and 950µl of fresh media with serum added then observed again. After the primary antibody was added to the wells the plate was the observed again under the phase filter to identify normal cell growth and viability, the GFP filter for successful transfection of the GFP-tagged tsp-7 and RFP filter to observe Anti-TIMP-1/ TIMP-1 binding to GFP tagged cells. Wells containing no GFP but TIMP-1/Anti-TIMP-1 acted as a control (N=8).

2.5 Statistical analysis

An open-source programme was used to generate the Kaplan Meier survival curve analysis, OASIS 2, (Han *et al*., 2016. The null hypothesis was determined as no significance between survival of the wild type N2 strain and both the mutant strains. The log-rank test was the preferred statistical analysis over the Mann-Whitney U test and the F-test. Statistical analysis was performed in both SPSS. Statistical analysis for the *C. elegans* stress assays were conducted in SPSS, using a univariate ANOVA and Independent t-test analysis. Image J was used to visualise cellular images, and plugins such as JACoPs and colocalization finder, were used to predict Pearsons correlation coefficient and produce scatter plots.

Chapter 3: A Structural Biology Study of tsp-7 Tetraspanin-7 Protein in *Caenorhabditis elegans* and its Potential Binding with TIMP-1, Using a Bioinformatics Approach

3.1 Introduction

There are 33 tetraspanin proteins in humans (Reppert & Lang., 2022) and 21 tetraspanin proteins in *C. elegans* (Liu *et al*., 2022). Some of these tetraspanin proteins share substantial homology. Parasitic nematodes of humans also share homologous proteins with *C. elegans* (Hahnel *et al*., 2020).

Tetraspanin proteins are integral membrane proteins, located within the plasma membrane of most cells. These proteins are scaffold proteins, able to interact with other tetraspanin proteins and molecules such as TIMP-1, Orai1 and Integrins forming a highly complex tetraspanin web (Noy *et al*., 2019, Yeung *et al*., 2018 and Kummer *et al*., 2020).

It is believed that parasitic nematodes make use of their own tetraspanin proteins within the human host to aid in their parasitism. These nematode tetraspanin proteins are believed to retain similar functions as those in humans, and thus allow parasites to alter the host immune response by dampening down the Th1/Th2 pathway

(Moreau & Chauvin., 2010). The parasites ability to elude the host immune system still remains a mystery and no vaccine has yet proved efficient in combating helminth infections. Recently, there has been an increase in the role of tetraspanin proteins and their link with other molecules and cross-communication. Other tetraspanin proteins identified in parasites are being considered as drug target candidates, such as smTSP-2 in *Schistosoma mansoni* (Pinheiro *et al.*, 2014) which is currently in phase II of clinical trials.

There is no 3D structure available on the Protein DataBase (PDB) from experimental studies of CD63 protein from humans or tsp-7 from *C. elegans*. Therefore, template models must be used to build the backbone of a theoretical 3D structure.

The aims of this bioinformatic study are:

1. Identify the protein similarity between CD63 tetraspanin from humans and the homologue, tsp-7 from *C. elegans*. Both tetraspanin proteins will be modelled to potentially identify similarities between the human and nematode structures.

2. A 3D model of the tsp-7 tetraspanin protein will be created, using known structures of other tetraspanin proteins (CD81, CD9, CD53) as templates. The models created using the freely accessible programmes will be compared against the tsp-7 and CD63 structure predicted by AlphaFold (a highly advanced AI predictive protein structure programme utilizing the computing power of DeepMind) (Jumper *et al*., 2021). RMSD values will be calculated to assess the protein similarity in terms of atom arrangement. (NB.- The structures predicted by AlphaFold were only made available towards the end of this study, once other template approaches as described here were undertaken).

3. The 3D models will then be used to theoretically analyse the properties of the predicted large extracellular loop domain (LEL) of the tsp-7 protein from *C. elegans*, where it is believed that binding to other protein partners occurs. Theoretical analysis of the properties of the small extracellular loop (SEL) and the four transmembrane helices (TM1-TM4) will also be undertaken.

4. Data mining the literature to identify pathways, networks, and molecular interactions and using this information, predict the binding model of tsp-7 from *C. elegans* and TIMP-1 from *Homo sapiens.*

3.2 Tsp-7 homologue of CD63

Within the list of putative homologues on the NCBI database, *C. elegans* has an entry for the gene tsp-7 (Figure 3.2.1a). The gene tsp-7 encodes the protein NP_492636.1. The protein will be referred to as tsp-7 throughout the study. It is located on Chromosome: I and has seven exons with no splice variants (one transcript). The nucleotide sequence contains 699 base pairs, and the protein contains 232 amino acids with a molecular weight of ~25.2 kDa. The protein sequences for CD63 and tsp-7 are shown in Figure 3.2.1b.

The tsp-7 gene is an orthologue of the CD63 gene, that is, the tsp-7 coding the NP_492636.1 protein should, theoretically retain the same function as CD63. There are 19 paralogues and 115 orthologues to the tsp-7 protein. Within the orthologue set, 19 of the species are parasitic nematodes of humans (Table 3.2.1)

3.2.1a.

3.2.1b.

>NP_001254627.1 CD63 antigen isoform A [Homo sapiens]
MAVEGGMKCVKFLLYVLLLAFCACAVGLIAVGVGAQLVLSQTIIQGATPGSLLPVVIIAVGVFLFLVAFVGCCGACKENYCLMITF
AIFLSLIMLVEVAAAIAGYVFRDKVMSEFNNNFRQQMENYPKNNHTASILDRMQADFKCCGAANYTDWEKIPSMSKNRVPDSCCN
VTVGCGINFNEKAIHKEGCVEKIGGWLRKNVLVVAAAALGIAFVEVLGIVFACCLVKSIRSGYEVM

>NP_492636.1 Tetraspanin [Caenorhabditis elegans]
MVEGGVTIVKYLLFLANLVLWVGGLSLIIVGSILQLKFDNVLDILGDERLATPILLLVIGSLCTLLGFLG
CCGAIRENYCLTVSFAVLLALLITCEIAAVIIGYALHDSFRLGIGNQLQTGMVRYHESRGVESAWDKTHQLFECCGVTNSSDWLTFT
TIPDSCCIEEIEGCARENAPLFEPGCIHSVEQWVLKNGAMVGGICAVLAAIQLVGVCFACCLSKSILKDFHDFYY

Figure 3.2.1. Schematic of homologous genes from the NCBI database and sequences. The tsp-7 gene from *Caenorhabditis elegans* is a putative homologue of CD63 from *H. sapiens*. The data is inferred from the CD63 protein sequence from humans. The schematic (a) shows the large extracellular loop domain (red bar) characteristic of tetraspanins. (b) Protein sequence of CD63 and tsp-7. The protein sequence of CD63 and tsp-7 were obtained from the NCBI database provided with the schematics from the HomoloGene database and aligned for sequence similarity and a sequence identity. The percentage sequence similarity between human CD63 and *C. elegans* tsp-7 is 67.2% and the percentage identity between the two proteins is 33.2%.

Table 3.2.1. The list of the 19 parasitic nematodes of humans. These parasites contain a protein similar to tsp-7 from a single common ancestor. The original list contained 115 orthologues, only the parasitic nematodes were pulled from the list.

Ancylostoma ceylanicum
Ancylostoma duodenale
Angiostrongylus cantonensis
Angiostrongylus costaricensis
Anisakis simplex
Ascaris lumbricoides
Ascaris suum
Brugia malayi
Brugia timori
Dracunculus medinensis
Enterobius vermicularis
Loa loa
Necator americanus
Onchocerca volvulus
Strongyloides stercoralis
Thelazia callipaeda
Toxocara canis
Trichuris trichiura
Wuchereria bancrofti

3.3 BLASTN and BLASTP searches of tsp-7 against parasitic nematode proteins and human tetraspanin proteins

These searches are used to identify proteins with sequence similarities. An E-value of 1E-50 is considered significant, and values between 0.01 and 1E-50 are likely due to homology (Pearson., 2013). E-values are the "expected" number of hits that are due to chance, E-values can be interpreted as the significance threshold. The tsp-7 protein sequence (232 amino acids) was used in a protein BLAST to search for similarities between the 19 previously identified human parasites (Table 3.3.1). The most significant alignments are between *Angiostrongylus cantonensis* (PRJEB493) with an E-value of 7E-39, 150 amino acid length (81.4% identity), *Angiostrongylus cantonensis* (PRJNA350391) E-value: 1.2E-24, 73 amino acids (86.3% identity), *Ancylostoma ceylanicum* (PRJNA231479) E-value: 2.9E-105 232 amino acids (72% identity) and, *Ancylostoma duodenale* (PRJNA72581), E-value: 3.5E-32, 100 amino acids (76% identity). These sequence alignments between the parasites in table 3.2.1 are not due to random chance and may have a protein(s) homologous to *C. elegans* tsp-7. Homology may be inferred between tsp-7 and parasitic nematodes, however the percentage ID and the length of amino acids covered in the alignment must also be taken into consideration.

The DNA alignments, obtained from a BlastN search of tsp-7 against the 19 parasites was not significant (data not shown). The total DNA length of tsp-7 is 950bp, this is the complete coding sequence. The high E-values and low sequence length would suggest that the similarity between DNA sequences is not significant.

Table 3.3.1 BlastP search of tsp-7 protein against the 19 parasitic nematodes on WormBase ParaSite. The length of tsp-7 is 232 amino acids. The table of results show there are similarities between tsp-7 protein sequence and the protein sequences of parasitic nematodes.

Genome	Length	E-Val	%ID
Ancylostoma ceylanicum (PRJNA231479)	232	2.90E-105	72.0
Ancylostoma ceylanicum (PRJNA72583)	180	1.20E-69	67.8
Ancylostoma duodenale (PRJNA72581)	100	3.50E-32	76.0
Angiostrongylus cantonensis (PRJEB493)	93	2.60E-40	65.6
Angiostrongylus cantonensis (PRJEB493)	102	7.00E-39	81.4
Angiostrongylus cantonensis (PRJNA350391)	150	3.00E-59	58.0
Angiostrongylus cantonensis (PRJNA350391)	73	1.20E-24	86.3
Angiostrongylus costaricensis (PRJEB494)	135	2.70E-45	64.4
Anisakis simplex (PRJEB496)	82	1.70E-26	57.3
Ascaris lumbricoides (PRJEB4950)	77	3.40E-27	55.8
Ascaris lumbricoides (PRJEB4950)	82	9.00E-27	57.3
Ascaris suum (PRJNA62057)	77	3.40E-27	55.8
Ascaris suum (PRJNA62057)	82	9.00E-27	57.3
Ascaris suum (PRJNA62057)	77	3.40E-27	55.8
Ascaris suum (PRJNA62057)	82	9.00E-27	57.3
Ascaris suum (PRJNA80881)	77	3.40E-27	55.8
Ascaris suum (PRJNA80881)	82	9.00E-27	57.3
Brugia malayi (PRJNA10729)	77	3.30E-26	53.2

Brugia malayi (PRJNA10729)	82	6.40E-25	54.9
Brugia timori (PRJEB4663)	82	6.40E-25	54.9
Dracunculus medinensis (PRJEB500)	81	3.30E-25	55.6
Enterobius vermicularis (PRJEB503)	73	3.40E-27	54.8
Loa loa (PRJNA246086)	82	4.60E-25	54.9
Loa loa (PRJNA37757)	82	4.60E-25	54.9
Necator americanus (PRJNA72135)	137	4.20E-60	64.2
Onchocerca volvulus (PRJEB513)	80	2.40E-24	55.0
Onchocerca volvulus (PRJEB513)	73	1.70E-23	50.7
Strongyloides stercoralis (PRJEB528)	153	2.10E-55	62.1
Thelazia callipaeda (PRJEB1205)	73	6.50E-27	57.5
Thelazia callipaeda (PRJEB1205)	80	4.50E-23	52.5
Toxocara canis (PRJEB533)	82	9.00E-27	57.3
Toxocara canis (PRJNA248777)	75	1.70E-27	60.0
Toxocara canis (PRJNA248777)	82	9.00E-27	57.3
Wuchereria bancrofti (PRJEB536)	82	6.40E-25	54.9
Wuchereria bancrofti (PRJNA275548)	77	1.20E-25	51.9
Wuchereria bancrofti (PRJNA275548)	82	6.40E-25	54.9

The tsp-7 protein sequence was aligned against all proteins in the protein data bank (Table 3.3.2). Three tetraspanin proteins were identified: a synthetic construct of CD53, CD81 crystal structure, CD81 partial structure (chain B only) and CD9 crystal structure. The CD53, CD81 and CD9 protein are from *H. sapiens*. The percentage identity of CD9, CD53 and CD81 is about the same (average 26.99%). The percentage similarity and identity for CD63 and tsp-7 is 67.2% and 33.2% respectively.

The E-values show that the similarity between tsp-7 and synthetic CD53, CD81 and CD9 are statistically significant (E<0.01). The CD53 is a synthetic construct, as with tsp-7, there is no crystal structure available for either the CD53 construct or CD63 from humans and no structure for tsp-7 from *C. elegans*.

Using only the tsp-7 domain in a protein Blast search on NCBI against proteins deposited in the pdb, only the CD53 synthetic construct was a hit, showing a percentage identity = 31.57%, and statistically significant of (6E-07, E<0.01).

Table 3.3.2. 3D structures from the PDB database. The protein data bank (pdb) only contains protein structures for very few tetraspanin proteins. CD53, CD9 and CD81 protein structures have been resolved using NMR or X-ray crystallography . The comparison between *C. elegans* tsp-7 tetraspanin and human tetraspanin proteins is limited. There is no determined structure of CD63 from humans currently available (at the time of this analysis). The E-values are statistically significant (P<0.001). The difference between percentage identity between all of the pdb structures and tsp-7 is small, the identity percentage ranges from 26%-28%. (PDB ID: CD81 – 5TCX, CD9 – 6K4J, CD53 – 6WVG).

Description	Per. Ident	Query Cover	E value
human CD53 (synthetic)	25.91	94%	3E-19
Crystal structure of tetraspanin CD81	26.69	95%	1E-13
Chain B, CD81 antigen	27.68	90%	2E-14
Crystal Structure of the CD9	27.66	74%	8E-11

To further investigate the similarities of the large extracellular (LEL) domain of tsp-7 from *C. elegans* with those of other parasitic nematodes, a sequence alignment protein blast search against the 19 species of parasitic nematodes was undertaken (Table 3.3.3). The tsp-7 LEL domain contains ~90 - 96 amino acids. The table is a limited list, as any sequence length below 31 was removed (ie 30% alignment length cut-off point). The full table has been included as supplementary 1 (S1). The results in table 3.3.3 are statistically significant, however, *A. ceylanicum, A. cantonensis, A. costaricensis and N. americanus* are the most significant ($P<0.001$).

The percentage identity of the 19 parasites and the tsp-7 LEL domain is less than 60%. The highest percentage identity is 57.9% from *Strongyloides stercorali*, however, the alignment length of the sequence contains 38 amino acids. This covers about 40 - 42% of the tsp-7 sequence. The alignment between *S. stercorali* and *C. elegans*, is therefore statistically significant ($P<0.001$). On the other hand, *Ancylostoma duodenale* has a sequence coverage length of 31 amino acids within the LEL domain (~32 - 36%), and a bit score of 79 ($P<0.05$). Given the low bit score and query cover, it is difficult to determine if the alignment between *A. duodenale* and *C. elegans* is truly significant, however, it cannot be ruled out.

Table 3.3.3 BlastP search of the tsp-7 LEL domain (90 - 96 amino acids) against the 19 parasitic nematode species identified previously using WormBase Parasite. The database contains multiple genome entries for some nematode species, the different genome entries were included in this table. For example, *Ancylostoma ceylanicum* has two entries (PRJNA231489-HY135 and PRJNA72583), both entries have returned the same data in the results table, indicating that the gene hit is the same protein for both entries. When data is to be further analysed, the latest genome entries are selected.

Genome	Gene hit	Length	Scor	E-Val	%ID
Ancylostoma ceylanicum (PRJNA231479 - HY135)	Acey_s0048.g1617	89	278	2.00E-30	55.1
Ancylostoma ceylanicum (PRJNA72583)	maker-ANCCEYDFT_Contig2	89	278	2.00E-30	55.1
Ancylostoma duodenale (PRJNA72581 - Baltimore)	ANCDUO_06578	31	79	0.0086	45.2
Angiostrongylus cantonensis (PRJEB493 - Republic of China)	ACAC_0000791201	57	178	1.50E-16	54.4
Angiostrongylus cantonensis (PRJNA350391 - Guangzhou)	Angca_006845	89	26	1.30E-28	51.7
Angiostrongylus costaricensis (PRJEB494 - Costa Rica)	ACOC_0001145701	77	226	3.30E-23	50.6
Anisakis simplex (PRJEB496)	ASIM_0000011101	48	122	9.10E-09	43.8
Ascaris lumbricoides (PRJEB4950 - Republic of Ecuador)	ALUE_0000372101	48	124	4.80E-09	43.8
Ascaris suum (PRJNA62057 - AG01)	AgR014X_g218	48	124	4.80E-09	43.8
Ascaris suum (PRJNA80881 - A. suum Australian isolate)	GS_08423	48	124	4.80E-09	43.8
Brugia malayi (PRJNA10729 - FR3)	Bma-tsp-7	48	122	9.10E-09	43.8

Brugia timori (PRJEB4663 - Flores	BTMF_0001344401	48	122	9.10E-09	43.8
Dracunculus medinensis (PRJEB500)	DME_0000411801	47	117	4.50E-08	42.6
Enterobius vermicularis (PRJEB503 - Spain/Canary Islands)	EVEC_0000282001	37	99	1.40E-05	43.2
Loa loa (PRJNA246086 - CAT)	EN70_7500	48	123	6.60E-09	43.8
Loa loa (PRJNA37757 - L. loa Cameroon isolate)	LOAG_07930	48	123	6.60E-09	43.8
Necator americanus (PRJNA72135 - N. americanus Hunan isolate)	NAME_07735	89	275	5.10E-30	55.1
Onchocerca volvulus (PRJEB513 - O. volvulus Cameroon isolate)	Ovo-tsp-7	40	119	2.40E-08	50
Strongyloides stercoralis (PRJEB528 - PV0001)	SSTP_0000622900	38	127	1.80E-09	57.9
Thelazia callipaeda (PRJEB1205 - Switzerland/Ticino)	TCLT_0000226701	46	108	8.00E-07	39.1
Toxocara canis (PRJEB533 - Brazil/Ecuador)	TCNE_0000595201	48	124	4.80E-09	43.8
Toxocara canis (PRJNA248777 - PN_DK_2014)	Cd63	48	124	4.80E-09	43.8
Wuchereria bancrofti (PRJEB536)	WBA_0000290501	48	122	9.10E-09	43.8
Wuchereria bancrofti (PRJNA275548 - pt0022)	maker-PairedContig_262-snap-	48	122	9.10E-09	43.8

The complete tsp-7 protein sequence was used in a BlastP search, against the 19 parasitic nematodes, the top 20 hits based off the highest E-value are listed in Table 3.3.4. *A. ceylanicum*, *N. americanus*, *A. cantonensis* and *A. costaricensis* are statistically significant (P<0.001). However, all the 19 species returned a substantially significant result, the full table can be found in supplementary data 2 (S2).

The data collected from the BlastP searches suggest that the tetraspanin tsp-7 protein from *C. elegans* is orthologous to the parasitic nematode proteins. Most of the tetraspanin proteins within parasitic nematodes are theoretical or putative, generally inferred in the other species. This is particularly true when searching databases such as NCBI and WormBase ParaSite.

The results from the BlastP search from NCBI and WormBase ParaSite yield similar results. The same four nematode species mentioned above are, in general, the most statistically significant, and appear the best matched against tsp-7 from *C. elegans*.

Table 3.3.4 BlastP search of tsp-7 tetraspanin protein from *C. elegans* against the 19 previously identified parasitic nematodes. The table shows the top 20 hits, the full table can be found in the supplementary data (S2). The nematodes: *A. ceylanicum*, *A. cantonensis*, *A. costaricensis* and *N, americanus* are the most highly significant results (P< 0.001).

Scientific Name	Max Score	Query Cover	E value	Per. ident	Acc. Len	Accession
Ancylostoma duodenale	148	43%	8.00E-45	76	117	KIH54038.1
Ancylostoma ceylanicum	344	100%	1.00E-120	71.98	232	EYC12107.1
Angiostrongylus cantonensis	300	90%	2.00E-103	69.01	213	KAE9415431.1
Ancylostoma ceylanicum	251	78%	3.00E-84	66.67	204	EPB72344.1
Angiostrongylus costaricensis	247	78%	3.00E-83	65.03	176	VDM63043.1
Toxocara canis	243	90%	5.00E-81	61.61	209	KHN76951.1
Necator americanus	254	79%	3.00E-85	60.09	215	XP_013301032.1
Brugia malayi	286	100%	8.00E-98	59.48	229	XP_042936187.1
Loa loa	291	100%	1.00E-99	59.05	229	XP_003143510.1
Toxocara canis	170	70%	1.00E-52	58.54	190	VDM37215.1
Dracunculus medinensis	229	90%	3.00E-75	58.33	217	VDN58028.1
Brugia timori	259	91%	1.00E-86	58.22	243	VDO39099.1
Wuchereria bancrofti	255	90%	9.00E-86	57.82	215	EJW84669.1
Thelazia callipaeda	244	90%	2.00E-81	57.82	214	VDM98125.1
Anisakis simplex	169	75%	1.00E-51	56.32	222	VDK17292.1
Enterobius vermicularis	234	92%	2.00E-77	52.75	226	VDD87385.1
Trichuris trichiura	167	81%	1.00E-50	41.46	251	CDW55483.1
Ancylostoma ceylanicum	89.4	76%	1.00E-20	27.27	230	EPB69423.1
Ancylostoma ceylanicum	101	96%	1.00E-24	26.74	299	EYC09299.1
Angiostrongylus costaricensis	100	96%	1.00E-24	26.15	280	VDM59075.1

3.4 Sequence alignments between tsp-7, parasitic nematodes and human tetraspanin proteins.

The top hit protein sequences from each parasitic nematode species, identified from table 3.3.4, were aligned against tsp-7 as well as CD63, CD9, CD53 and CD151. Figure 3.4.1 shows a section of the alignments, the CCG (Cysteine – Cysteine – Glycine) residue is a key characteristic of the tetraspanin protein family and is located within the LEL domain.

This motif is present in all the sequences apart from KIH54038.1 *A. duodenale*, the protein does not contain the PXXCC motif within the LEL. These two distinctive motifs are identifiers of tetraspanin proteins. This suggests that KIH54038.1 may not be a true tetraspanin protein but shares some similarity. However, CD81 from *H. sapiens* does not contain the PXXCC motif, despite this, CD81 is classified as a tetraspanin protein (Becic *et al*., 2022 and Berditchevski & Odintsova., 2006)

Of the 33 tetraspanin proteins identified in humans, approximately 50% contain the PXXCC motif, also within the LEL (Becic *et al*., 2022), therefore any sequence that does not contain the PXXCC motif may still retain similar functionality as a tetraspanin. The criteria would therefore depend on the Cysteine residues. All tetraspanin proteins contain several conserved Cysteine residues (Jankovičová *et al.*, 2020). The complete sequence alignment can be found in supplementary data 3 (S3).

The human tetraspanin proteins; CD63, CD9, CD81, CD53 and CD151, were compared against the tsp-7 protein using a local alignment search (Table 3.4.1). The

large extracellular loop domain of tsp-7 was compared against the LEL of the human tetraspanin proteins, this table can be found in supplementary data 4 (S4).

Overall, the tsp-7 protein is more similar to the proteins from the parasitic nematodes than the human tetraspanin proteins. This, however, does not mean that the parasitic proteins do not function in a similar way to human tetraspanin proteins. Tetraspanins are relatively conserved throughout all multicellular organisms (Boavida *et al*., 2013).

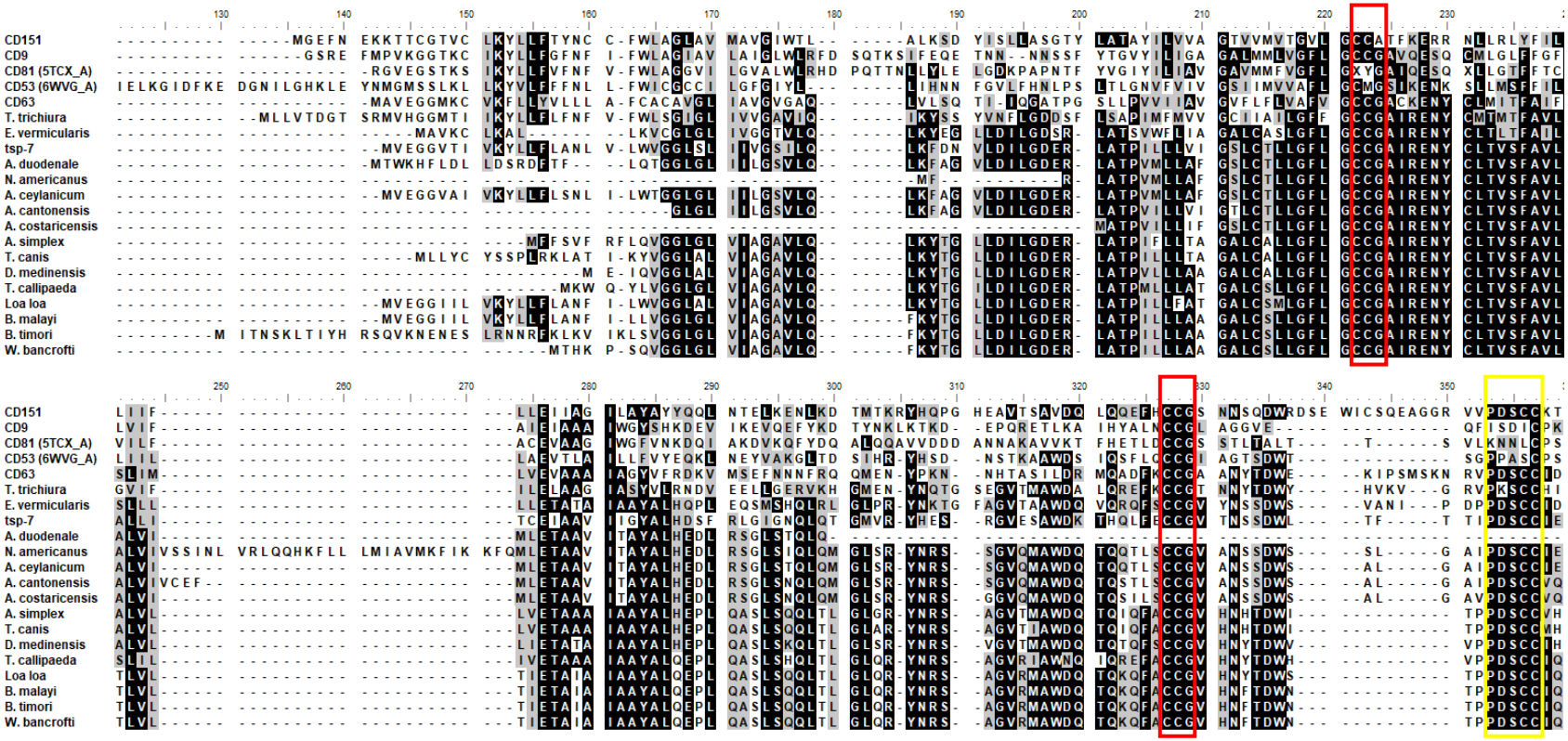

Figure 3.4.1 A sequence alignment, using the accession numbers from table 3.3.4. The C-C-G motifs within the large extracellular domain are highlighted in red. The PXXCC motif, also in the large extracellular domain, is highlighted yellow. The intensity of shading represents the level of conservation. Amino acids highlighted in black are the most conserved, those highlighted white are the least conserved. Those amino acids in grey have similar physicochemical properties but are not identical.

Table 3.4.1 Sequence alignment between tsp-7 from *C. elegans* and tetraspanin proteins from *H. sapiens*. A local alignment search was used to find the percentage identity between tsp-7 and tetraspanin proteins. Tsp-7 is more similar to parasite proteins than the tetraspanin proteins from humans.

	Tetraspanin	Percentage Identity
Tsp-7	CD63	33.2
	CD151	32.1
	CD81 (5TCX)	27
	CD53 (6WVG)	26.2
	CD9 (6K4J)	26

3.5 Phylogenetic tree comparing parasitic nematode proteins, tsp-7 tetraspanin protein from *C. elegans* and multiple tetraspanin proteins from *H. sapiens*

The proteins from the alignment (Figure 3.4.1) were used to create a maximum likelihood phylogenetic tree, Figure 3.5.1. The parasitic nematodes are classed based on the clade they belong to (I – V). *C. elegans* belongs to clade V, the parasitic nematodes in this clade *are A. ceylanicum, A. cantonensis, A. costaricensis, A. duodenale, N. americanus*. The phylogenetic tree shows that the parasitic nematodes in the same clade are more closely related.

C. elegans tsp-7 protein is more genetically similar to *A. cantonensis* (hypothetical protein Angca_006845, partial, KAE9415431.1) and *A. costaricensis* (unnamed protein product, VDM63043.1). *C. elegans* is also more closely related to the clade III parasites than clade I. There is only one parasite belonging to clade I from the list of 19 parasitic nematodes identified, *T. trichiura*.

The parasites not aligned on the phylogenetic tree are *Ascaris lumbricoides, Ascaris suum, Onchocerca volvulus* and *Strongyloides stercoralis*. Therefore, it is likely that the model organism *C. elegans* is more evolutionary dissimilar to the Ascaris species. The list can be narrowed down to 14 parasitic species in which there may be a protein orthologous to tsp-7 tetraspanin protein.

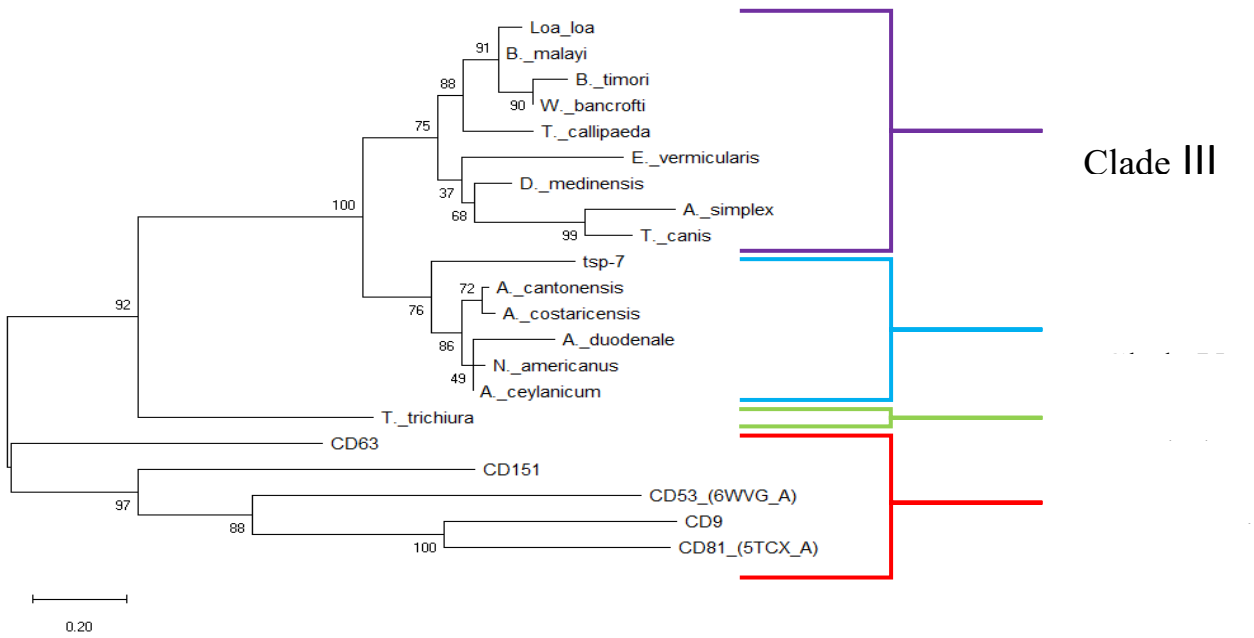

Figure 3.5.1. Phylogenetic tree of tsp-7, human tetraspanins and potential parasitic nematode tetraspanins. The evolutionary history was inferred by using the Maximum Likelihood method and JTT matrix-based model (Jones D.T., *et al*, 1992). The tree with the highest log likelihood (-2955.30) is shown. The percentage of trees in which the associated taxa clustered together is shown next to the branches. Initial tree(s) for the heuristic search were obtained by applying the Neighbour-Joining method to a matrix of pairwise distances estimated using a JTT model. The tree is drawn to scale, with branch lengths measured in the number of substitutions per site. This analysis involved 7 amino acid sequences. All positions with less than 100% site coverage were eliminated, i.e., fewer than 0% alignment gaps, missing data, and ambiguous bases were allowed at any position (partial deletion option). There was a total of 203 positions in the final dataset. Evolutionary analyses were conducted in MEGA X (Kumar., *et al*, 2018).

3.6 Theoretical 3D protein structure of tsp-7 from *C. elegans* using human tetraspanin protein structures as a backbone template

There is no 3D structure for the human CD63 tetraspanin protein or the *C. elegans* tsp-7 tetraspanin protein, available on the PDB database. There are structures available for human CD81, CD9 and CD53. These tetraspanin structures were used as a template to create a theoretical model of tsp-7 from *C. elegans* using the SWISS-Model programme (see chapter 2.1.17) (Figure 3.6.1). Figure 3.6.1 A is the theoretical structure of tsp-7 using human CD81 as a template, the structure appears to be in the closed conformation. An open and closed conformation describes the tetraspanin proteins large extracellular domain and small extracellular domain, either unbound "open" or bound "closed" (Yang *et al*., 2020). Figure 3.6.2 shows a schematic diagram of the open/closed conformations of tetraspanin proteins. Open and closed conformations directly affect the stability of tetraspanin proteins, depending on the tetraspanin protein either the open conformation provides more stability or the closed conformation. The open conformation determines the binding capacity and partners of the tetraspanins. Generally, the EC2 domain (LEL), is less stable in an open conformation and will become stabilised when bound to a partner. In CD53 the EC1 and EC2 domain (SEL and LEL) are required for immune trafficking but a mutation in the EC1 domain hinders immune cell promotion and glycosylation (Yang et al., 2020). CD81 in an open conformation is extended at the LEL, rather than tilting inwards toward the centre of the structure. Figure 3.6.1 B shows the theoretical structure of tsp-7 using the tetraspanin CD9 as a template and

Figure 3.6.1 C shows the human tetraspanin CD53 as a template. All three structures have similar almost identical transmembrane helices, which are the most conserved regions of the tetraspanin proteins. The LEL and to some extent, the SEL, are the least conserved. The variable regions are responsible for the binding capacity of the tetraspanin proteins, dictating the location and function of the transmembrane proteins. Within the LEL, there are conserved residues mentioned in 3.5 (C-C-G motif and P-X-X-C-C motif).

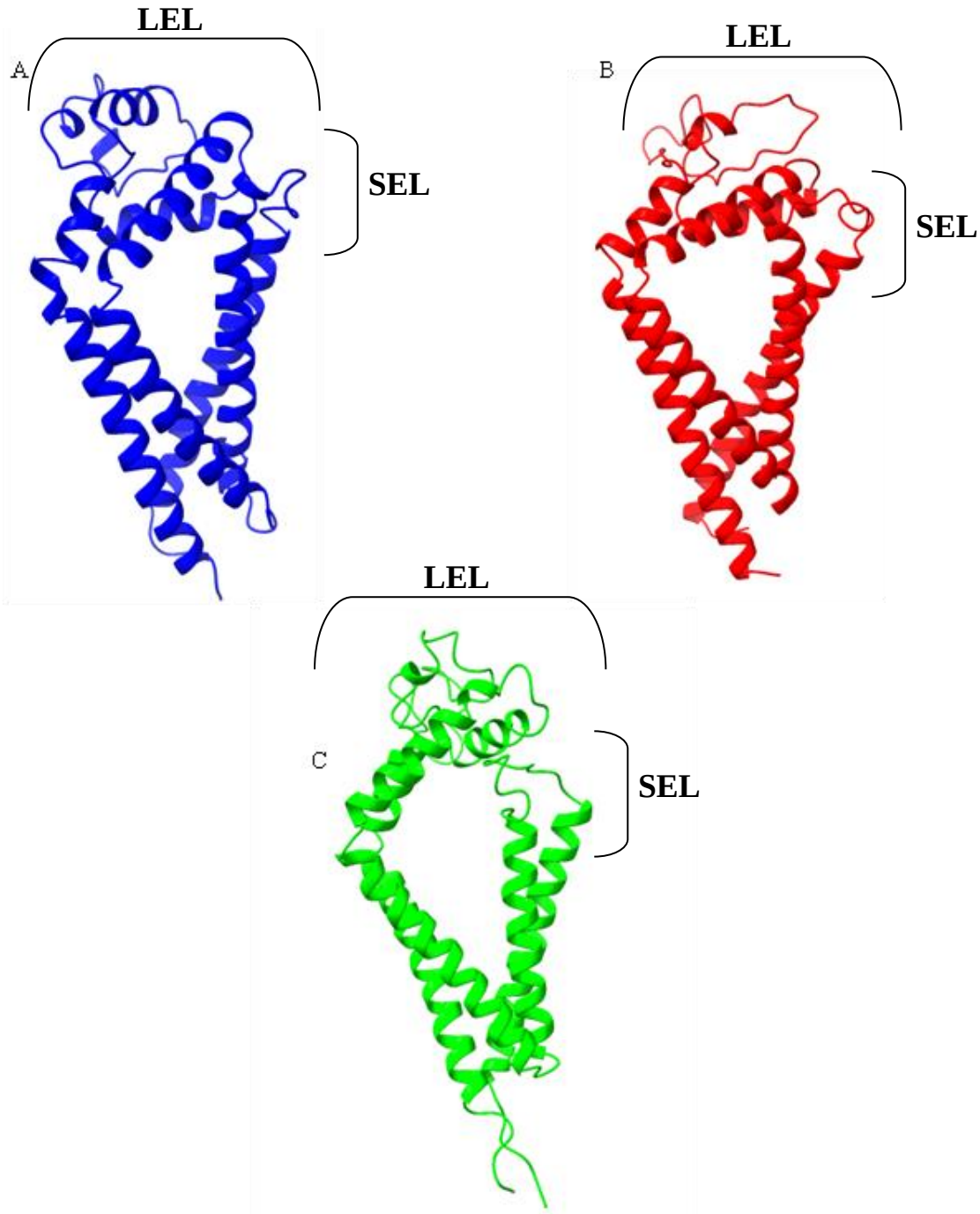

Figure 3.6.1 Theoretical 3D structures of tsp-7 using three different human tetraspanin proteins as a template. A) the structure of tsp-7 using CD81 as the template. B) CD9 as a template and C) CD53 as a template. All three human tetraspanin protein structures have been experimentally determined using X – Ray Diffraction and can be found on the PDB database. All the models were created using SWISS-MODEL, Chimera X and PyMol.

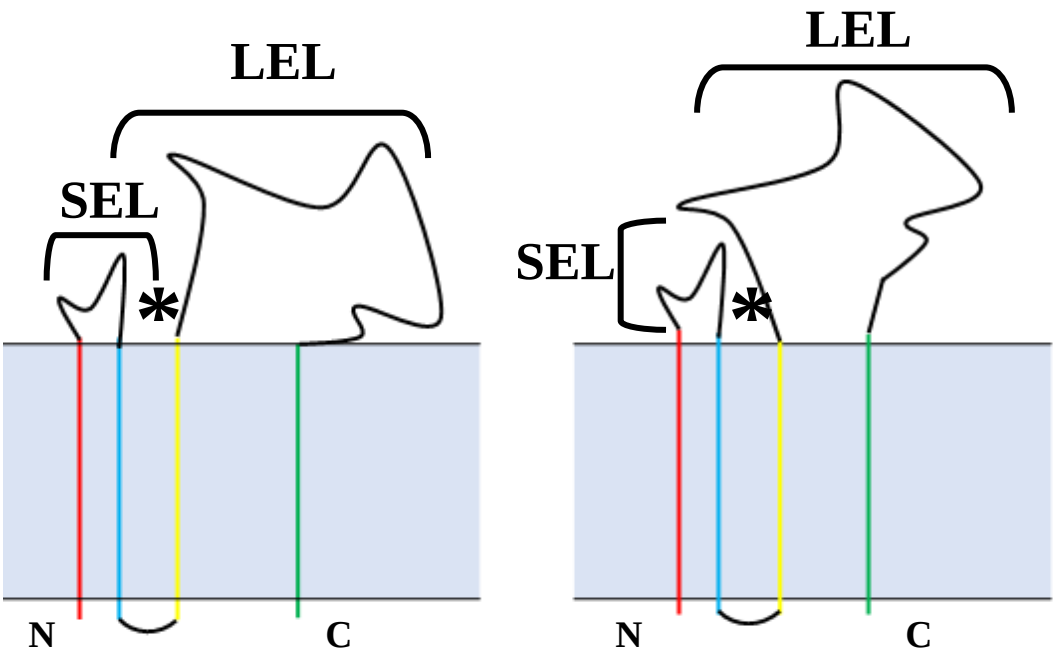

Figure 3.6.2. Schematic showing the open and closed conformation of tetraspanin proteins. The left shows the "open" conformation, TM1- red, TM2- blue, TM3- yellow and TM4- green. SEL = small extracellular loop, LEL = large extracellular loop. The image to the right shows the "closed" conformation. * = the binding pocket between the SEL and the LEL.

A theoretical structure of tsp-7 from *C. elegans* and CD63 from *H. sapiens* (figure 3.6.3) was released on the AlphaFold database in 2022, after the bulk of this study had been previously undertaken (see chapter 2.1.7). Figure 3.6.3 also shows the C-C-G and P-X-X-C-C motif commonly found within the majority of tetraspanin proteins (Becic *et al.*, 2022). The structures were compared against the theoretical tsp-7 structures from Figure 3.6.1. Table 3.6.1 shows the comparison between the AlphaFold models (CD63, CD81, CD53, CD9 from humans and tsp-7 *from C. elegans*) and the theoretical models produced from SWISS-MODEL and Chimera X (see chapter 2.1.7), using the tetraspanin templates. The root mean square deviation (RMSD) values were calculated (chapter 2.1.12). The RMSD is a measurement of the average distance between two atoms of superimposed protein structures. The lower the RMSD value the more likely two proteins are homologous (Cohen & Sternberg., 1980). From Table 3.6.1, the 3D structure of CD63 and tsp-7 are the most similar protein structures in terms of atom arrangement and tertiary structure. The RMSD value is 3.371Å. The CD53 template was the closest structure to tsp-7 when compared against both AlphaFold CD63 and tsp-7 structures. The RMSD value between CD53 modelled from SWISS-MODEL, and CD63 from AlphaFold is 5.243Å and between the same CD53 protein structure and tsp-7 from AlphaFold is 5.665Å. The difference between CD53 (SWISS-MODEL) and CD63 (AlphaFold) is 0.5nm, and 0.6nm for CD53 (SWISS-MODEL) and CD63 (AlphaFold).

In general, the RMSD values are significant in terms of atom arrangement and conformation, the highest RMSD value calculated (between AlphaFold tsp-7 and tsp-7 using CD9 template), is 10.040Å, which is equal to 1nm. The merged tsp-7 model from SWISS-MODEL and tsp-7 from AlphaFold can be found in supplementary 5 (S5).

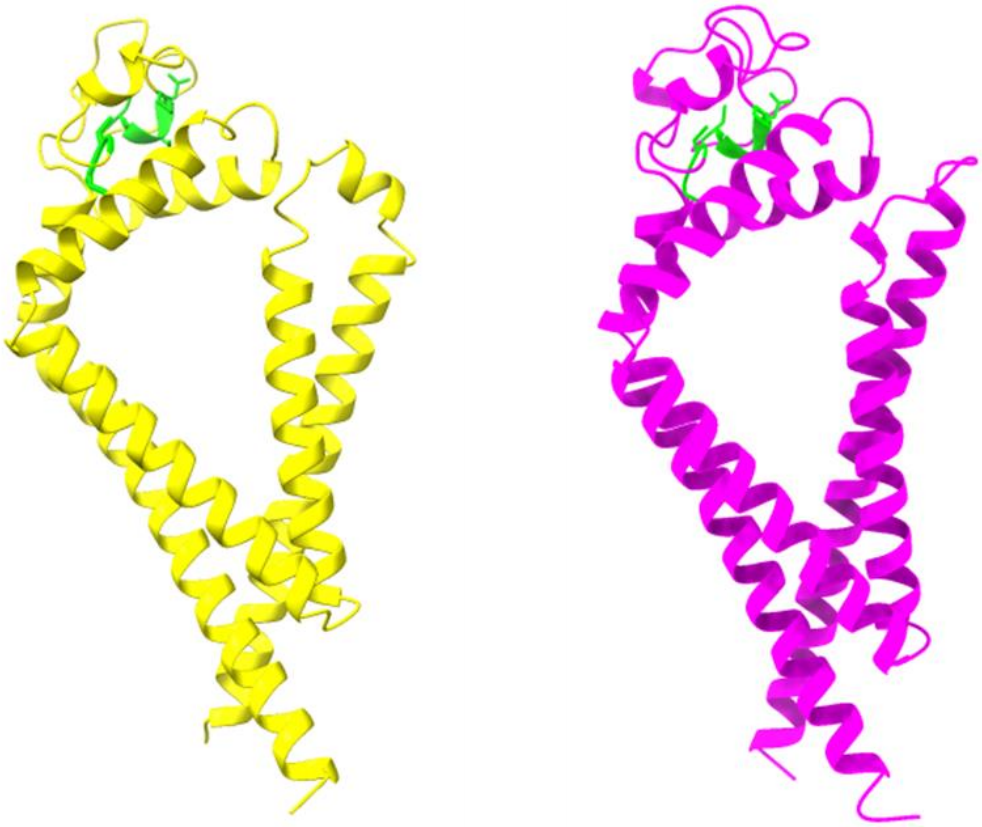

Figure 3.6.3. 3D models of tsp-7 and CD63 deposited in AlphaFold database. Predicted theoretical structures of tsp-7 (yellow) and CD63 (purple) released by AlphaFold. The C-C-G and P-X-X-C-C- motifs within the LEL are highlighted in green. Developed by DeepMind and EMBL European Bioinformatics institute. The AI system used is highly accurate, utilising the latest state of the art technology. The tsp-7 protein and CD63 tetraspanin protein were deposited into the database in June 2022.

Table 3.6.1. Root- mean square deviation for protein comparisons. PyMol was used to calculate the RMSD. Protein structures from AlphaFold – tsp-7, CD63, CD81, CD9 and CD53. Protein structures from SWISS-MODEL/ Chimera X – tsp-7 (CD81 template), tsp-7 (CD9 template) and tsp-7 (CD53 template). 1Å= 0.1nm. RMSD values are the average deviation between two atoms of the protein. The closer the structures are the lower the RMSD. AF= AlphaFold, SM= SWISS MODEL. Tsp = Tetraspanin.

Molecule 1		Molecule 2			Pruned		Total	
Model	Tsp	Model	Tsp	Align score	Atom	Value	Atom	Value
AF	TSP-7	AF	CD63	598.8	122	1.22Å	229	3.371Å
AF	CD53	AF	TSP-7	505.8	107	0.986Å	215	4.373Å
AF	CD63	SM	TSP-7 (CD53)	547.7	110	1.010Å	223	5.243Å
AF	TSP-7	SM	TSP-7 (CD53)	1107.3	99	0.987Å	226	5.665Å
AF	CD63	SM	TSP-7 (CD81)	500.3	93	1.126Å	216	7.416Å
AF	CD63	SM	TSP-7 (CD9)	588.8	119	0.996Å	226	8.111Å
AF	TSP-7	AF	CD9	435.1	100	0.856Å	218	8.584Å
AF	TSP-7	AF	CD81	432.4	63	0.788Å	222	8.805Å
AF	TSP-7	SM	TSP-7 (CD81)	1037.4	61	0.981Å	221	8.839Å
AF	TSP-7	AF	CD151	516.8	83	1.034Å	228	8.876Å
AF	TSP-7	SM	TSP-7 (CD9)	1135.5	87	0.761Å	226	10.040Å
AF	CD53	SM	TSP-7 (CD53)	485.1	190	0.342Å	211	1.939Å
AF	CD81	SM	TSP-7 (CD81)	388	145	0.710Å	210	3.998Å
AF	CD9	SM	TSP-7 (CD9)	445.4	194	0.407Å	215	3.516Å

The 3D protein structure of tsp-7 from AlphaFold was used to determine the amino acid sequence of the four transmembrane helices (TM1-TM4), the SEL and LEL domain. Figure 3.6.4 shows key characteristics of the tetraspanin proteins highlighted. Transmembrane helices 1 = 34 amino acids (VEGGVTIVKYLLFLANLVLWVGGLSLIIVGSILQ), transmembrane helices 2 = 25 amino acids (ATPILLLVIGSLCTLLGFLGCCGAI), transmembrane helices 3 = 26 amino acids (YCLTVSFAVLLALLITCEIAAVIIGY), transmembrane helices 4 = 36 amino acids (GAMVGGICAVLAAIQLVGVCFACCLSKSILKDFHDFY). The small extracellular loop (SEL) is estimated to be about 14 amino acids long (DNVLDI), but most importantly the large extracellular domain (LEL) is estimated to be around 90 -96 amino acids long (ALHDSFRLGIGNQLQTGMVRYHESRGVESAWDKTHQLFECCGVTNSSDWL TFTTIPDSCCIEEIEGCARENAPLFEPGCIHSVEQWVLKN). Figure 3.6.5b shows the same structure, displayed as a Corey-Pauling -Koltun (CPK) space-filling model, where the closed formation structure is more obvious and the binding pocket more visible.

Initially the transmembrane helices and domain lengths were calculated based off the model produced from SWISS-model and Chimera X. The transmembrane helices were estimated to be around 23 for TM1, 20 for TM2, 26 for TM3 and 25 for TM4. The SEL was estimated to be 14 amino acids and 96 for the LEL. Once using the tsp-7 structure from AlphaFold, the amino acids were calculated again against the more accurate structure. The amino acid sequence predicted here for each transmembrane helices and the two extracellular domains are purely theoretical. Experimental determination using X- ray diffraction, NMR or Electron microscopy would truly identify the structure and conformation of tsp-7 and CD63.

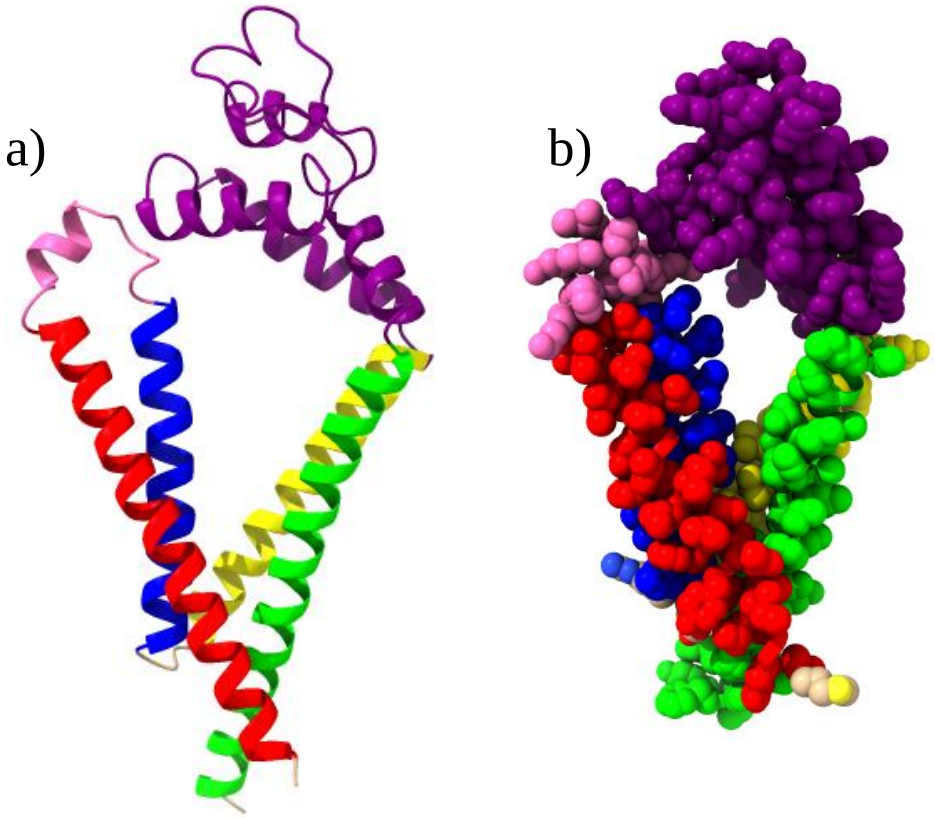

Figure 3.6.4. Theoretical prediction of key tsp-7 tetraspanin features. A) the tsp-7 protein from AlphaFold was used to predict the amino acids for each of the four transmembrane helices (TM1-TM4), as well as the amino acid sequence for the SEL and LEL domains. TM1 (red) is estimated to be around 34 aa's, TM2 (blue), is estimated to be 25 aa's long, TM3 (yellow) is 26 aa's and TM4 (green) is 36 amino acids. The SEL, is highlighted in pink and is around 14 amino acids in length and the LEL, in purple, is 90 amino acids. B) the CPK model shows the space filling structure, the tsp-7 protein occupies a closed formation structure, the binding pocket is more visible.

3.7 Identification of potential N- glycosylation and phosphorylation sites within the tsp-7 protein

A potential N – glycosylation site was identified, using the NetNGlyc - 1.0 programme (chapter 2.1.10), at position 149, within the LEL domain. N-linked glycosylation is important for many biological roles, one such role is the distinction between self and non -self (Alves *et al*., 2022). Parasites have the ability to evade the immune system by presenting themselves as self within the host immune system (chapter 1.2.1).

The predicted LEL domain amino acid sequence mentioned previously is: ALHDSFRLGIGNQLQTGMVRYHESRGVESAWDKTHQLFECCGVT**N**SSDWL TFTTIPDSCCIEEIEGCARENAPLFEPGCIHSVEQWVLKN. The sequence underlined is the position which is likely to be glycosylated. Glycosylation sites can be determined experimentally by western blotting, but to identify the specific site of glycosylation, first the protein is digested by proteases then separated using chromatography. The fragments are treated with PNGase F, an amidase which cleaves N-linked oligosaccharides from the glycoprotein. The products are then further analysed either by fluorescent labelling, Mass spectrometry or liquid chromatography.

The potential sites for phosphorylation for threonine are: 52, 64, 82, 120, 155, and 157 and for serine: 26, 32, 61, 84, 133, 150, 151, and 162, and for tyrosine: 231. Figure 3.7.1 shows the N – glycosylation site on the tsp-7 3D model from AlphaFold and Figure 3.7.2 shows the phosphorylation sites for threonine, serine, and tyrosine. The likelihood of the phosphorylation sites occurring within the protein are listed in Table 3.7.1. Phosphorylation sites can be determined experimentally by high

resolution Mass spectrometry. Tyrosine phosphorylation is important for signal transduction and the regulation of enzymatic activity. Protein Tyrosine kinases (PTK's) are involved with pro-inflammatory responses. The PTK Insulin receptor (InsR) is expressed on immune cells and may be required for pro-inflammation and may drive the NET formation of neutrophils during nematode infection (Makhijani *et al*., 2023).

The NXXD site of glycosylation is present in all but one parasitic nematode, *A. duodenale*. The NXDD sequence is not present in CD81, CD9 or CD53, it is however present in CD151 and more importantly CD63. This further supports the theory that the parasitic nematode species listed in Figure 3.4.1, are potentially orthologues of CD63.

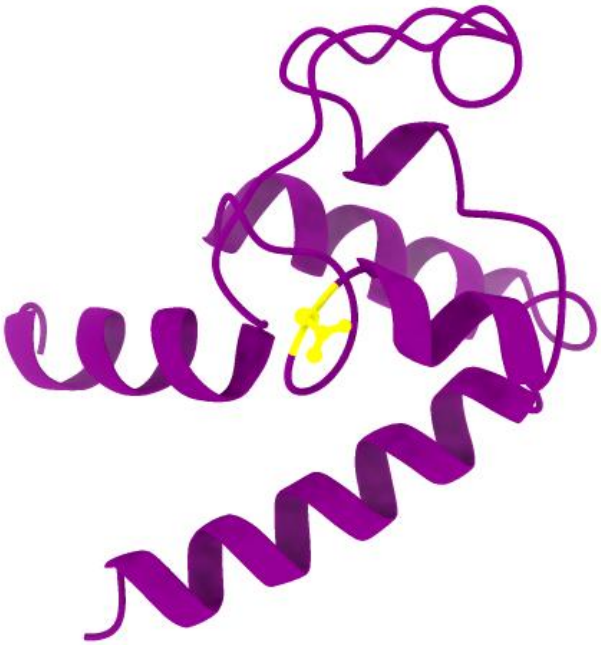

Figure 3.7.1 Theoretical LEL domain prediction of tsp-7 and N-glycosylation sites. The LEL domain (shown in purple) contains one site involved with N – glycosylation (yellow) at position 149. The sequence NXXD, is also present in the protein sequences of the majority of parasitic nematode proteins mentioned in section 3.4. The NXXD motif does not present in the parasitic nematode *A. duodenale* or the human tetraspanin proteins; CD81, CD9 or CD53.

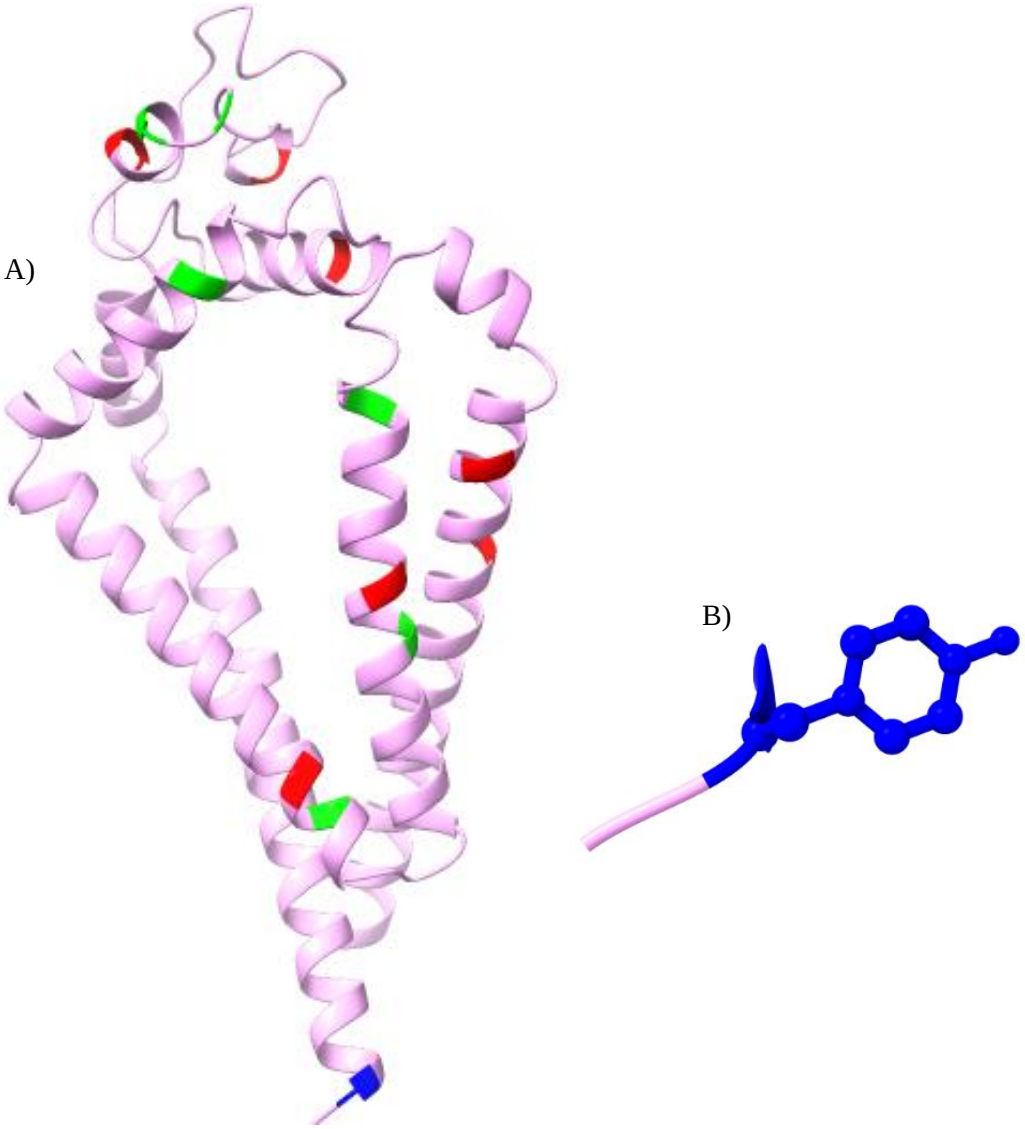

Figure 3.7.2. The theoretical tsp-7 3D structure from AlphaFold. A) Serine phosphorylation sites are in red, threonine phosphorylation sites are marked in green, and the tyrosine phosphorylation site is in blue. To the right (B) is the atoms of the tyrosine amino acid.

Table 3.7.1. Phosphorylation sites of Threonine, Serine, and Tyrosine. The phosphorylation sites predicted, suggest that the likelihood of the Threonine and Serine sites would not be phosphorylated. The most likely site of phosphorylation is the Tyrosine site at position 231. INSR = insulin receptor. X= Unlikely, O = likely. The programmes NetGly 1.0 was used to predict N-linked glycosylation sites, NetPhos was used to predict phosphorylation sites.

	Phosphorylation site	Location	Kinase	Likelihood
Threonine	52	Membrane	p38MAPK	X
			PKA	
			unsp	
	64	Membrane	PKC	X
	82	Membrane	PKC	X
			cdc2	
	120	Extracellular	PKC	X
	155	Extracellular	PKC	X
	157	Extracellular	PKC	X
Serine	26	Membrane	PKA	X
	32	Membrane	PKC	X
	61	Membrane	PKA	X
			DNAPK	X
	84	Membrane	PKA	X
	133	Extracellular	unsp	X
	150	Extracellular	PKA	X
	151	Extracellular	PKA	X
	162	Extracellular	unsp	X
			CKII	X
Tyrosine	231	Intracellular	INSR	O

3.8 Protein interactors and interaction of tsp-7 and CD63 utilising the STRING database

The STRING database for CD63 shows that the tetraspanin protein may likely interact with mainly membrane glycoproteins and molecules such as LAMP-1, LAMP-2, SELP and SCARB2. The interaction between CD63 and SDCBP is vital for exosome biogenesis as well as protein trafficking of the tetraspanins, and more importantly, immunomodulation. LAMP-1 and LAMP-2 are involved with lysosome biogenesis and autophagy (Huynh *et al*., 2007).

CD63 has been shown to interact with TIMP-1, this interaction has been proven experimentally (Justo & Jasiulionis., 2021). TIMP-1 interacts with almost all of the metalloproteinases (Brew and Nagase., 2010). The TIMP-1/CD63/ITGB (integrin) interaction has been documented and is critical for cancer (Justo & Jasiulionis., 2021). Figure 3.8.1 shows these interactions between CD63 and TIMP-1. IL-6 is an interactor of TIMP-1, however recent research suggests there are multiple interleukins that bind to TIMP-1, and it is now only just being realised, the importance of TIMP-1 as a cytokine and the function TIMP-1 has within the immune system (Schoeps *et al.,* 2022). Figure 3.8.2 shows TIMP-1 and its interactions with various ILs, as well as growth factors.

It is theorised in this project, that tsp-7 functions in a similar capacity as CD63, therefore TIMP-1 from humans could bind to tsp-7 from *C. elegans*. If tsp-7 protein is an orthologue to parasitic nematode proteins, then these parasite proteins may utilise this interaction with TIMP-1 thus modulating and downregulating host immune responses.

The proteins tsp-7 interacts with, are retrieved form data mining rather than proven experimentally. The data is inferred from proven experiments from humans with similar proteins. In Chapter 5 we explore the possible interactions of *C. elegans* tsp-7 with human TIMP-1 using cell expression and immune localisation. Calnexin 1 (cnx1) is an integral Ca^{2+} N-glycosylated protein and required to elicit appropriate stress responses (Lee *et al*., 2005). Tumour suppressor gene 101induces stress response and Ca^{2+} leakage from the endoplasmic reticulum (ER) (Kaul *et al.*, 2020). The tetraspanin proteins such as tsp-14, tsp-3 and tsp-2 currently have unknown function and are determined through datamining only.

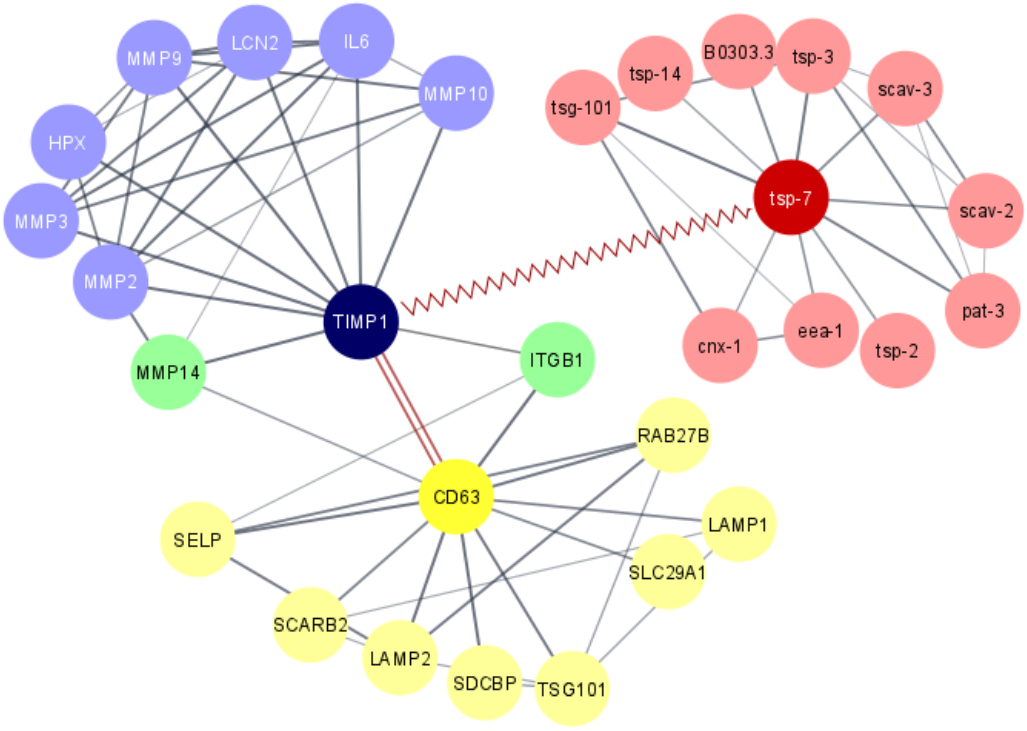

Figure 3.8.1. Interactions of CD63, TIMP-1 and tsp-7 using STRING. The STRING database shows the interactors of CD63 (yellow), TIMP-1 (blue) and tsp-7 (red). TIMP-1 and CD63 have been shown to interact through various experimental studies. This interaction is shown by the parallel red lines, joining the two databases. The red zigzag line is the theoretical interaction between TIMP-1 and tsp-7. The majority of the protein interactions with tsp-7 are inferred, there is no experimental data to confirm these interactions. The image was produced in Cytoscape.

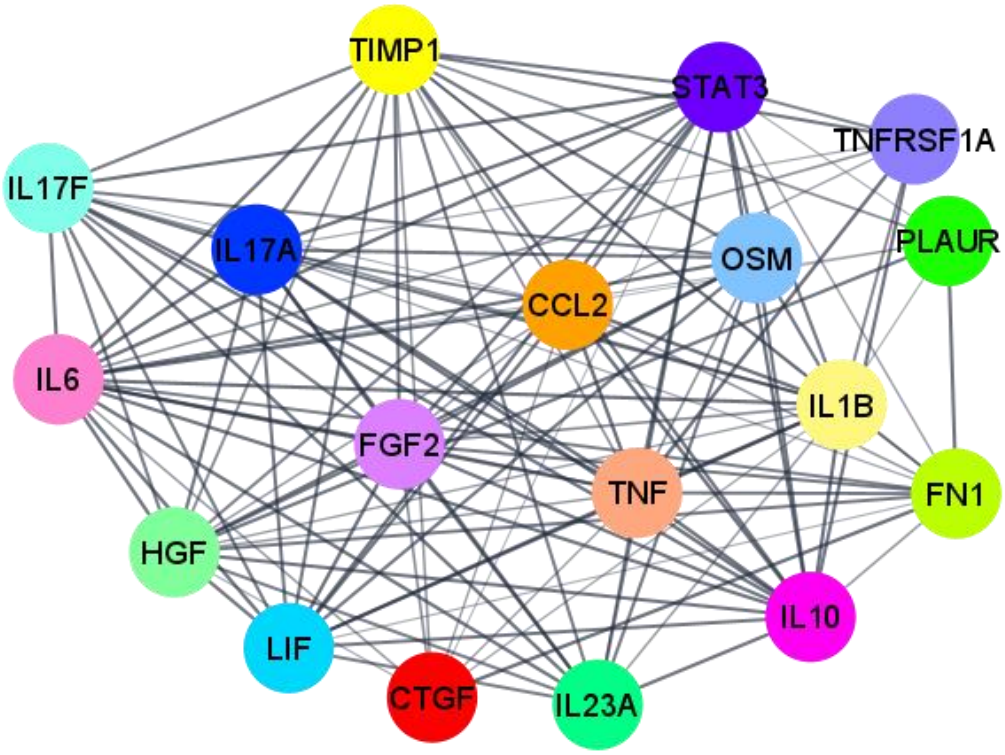

Figure 3.8.2. TIMP-1 network using STRING. TIMP-1 molecule has an important role within the immune system and has been shown to act as a cytokine. The STRING database for TIMP-1 shows various interactions with a variety of interleukins (IL's), and growth factors. It is clear that TIMP-1 has effects on multiple signal transduction pathways. The image is limited to 17 interactors of TIMP-1 for simplicity. The STRING database was altered in Cytoscape.

3.9 Predicting the potential binding of active human TIMP-1 molecule with tsp-7 tetraspanin from *C. elegans*

TIMP-1 has been proven to bind and interact with CD63 (Justo & Jasiulionis., 2021) however, until recently the full extent of this interaction was poorly understood. The TIMP-1/CD63 interaction was thought to play a role in extracellular membrane turnover and repair (Jung., *et al* 2006), as well as aiding CD63 in protein trafficking and migration. However, new studies suggest that TIMP-1 acts as a cytokine like molecule (Schoeps *et al*., 2022). TIMP-1 can act as a pro-inflammatory molecule and anti-inflammatory, depending on the binding partners and cells involved (Arpino *et al*., 2015).

Parasites hijack the host immune system and dampen down the pro-inflammation response (Moreau & Chauvin, 2010). This allows the parasites to live undetected within various organs and tissue within the host. The exact mechanism is unknown. Utilising the latest research of TIMP-1 acting as a cytokine, it could be hypothesised that parasite tetraspanin proteins, with similar function to CD63, hijack this interaction and either act as 'competitive' binding partners of TIMP-1 reducing its interaction with human CD63, or through pathways not yet known, directly affecting the immune system and preventing the appropriate immune response, and perhaps switch to a Th1 response. Eosinophils, and basophils initiate the Th2 pathway (Spencer & Weller., 2010 and Sokol & Medzhitov., 2010), which leads to the activation of IL-4 (Choi & Reiser., 1998) and an increase in IgE (Steinke & Borish., 2001). The increase in IgE leads to mast cell degranulation (Galli & Tsai., 2012). The Th2 pathway is usually associated with an anti-inflammatory response (Berger.,

2000), but IgE is the main immunoglobulin responsible for protection against helminths. However, there is a strong imbalance shifting towards the Th2 pathway, parasitic nematodes interact and modulate the immune response shifting the Th2 pathway in favour of a balanced Th1/Th2 response, this may be achieved through modulation of regulatory T (Treg) cells (Chulanetra & Chaicumpa., 2021) . This balance is associated with intracellular pathogens with an immune response directed away from the nematodes. The Th1 pathway is pro-inflammatory and in most cases, chronic helminth infections are synonymous with chronic inflammation, although nematodes induce IL-10 in excess to counteract the pro-inflammatory response (Iyer & Cheng., 2012).

The *C. elegans* tsp-7 proteins, acts as a model for this theory. Theoretically tsp-7 may have similar functionality to parasitic nematode proteins, tsp-7 is also an orthologue to human CD63. Therefore, TIMP-1 molecule could bind and interact with tsp-7.

Figure 3.9.1 shows CD63 bound to TIMP-1. The C-terminus of TIMP-1 interacts with the LEL of CD63. The RMSD value of CD63 and TIMP-1 is 1.6 +/- 1.2Å. The energy between the van der Waals forces, electrostatic energy and desolvation energy are also calculated, although the measurements are arbitrary (table 3.9.1). The tsp-7 protein and TIMP-1 molecule has an RMSD value of 1.2+/-1.2Å. The binding models are calculated using the HADDOCK programme and the ClusPro programme as well as the PRODIGY programme (see chapter 2.1.13). There is very little difference between the Z-score of CD63/TIMP-1 and tsp-7/TIMP-1, -2 and -1.9 respectively. The Z- score calculates the number of standard deviations a cluster is from the average. The structures shown are from the top clusters only, as they are

more likely to be accurate than structures from lower clusters. The models from ClusPro, are more unreliable than the models produced using HADDOCK. Figure 3.9.2 shows CD63/TIMP-1 and tsp-7/TIMP-1. These models show TIMP-1 interacting with CD63 and tsp-7, wholly or partly, within the transmembrane region which are highly unlikely to occur (Figure 3.9.2). The top cluster structure for tsp-7/TIMP-1 and CD63/TIMP-1 generated in HADDOCK, were then used in the PRODIGY programme to calculate the binding affinity (ΔG) and the dissociation constant (Kd) at 37°C. The results are shown in Table 3.9.1 with the top HADDOCK cluster results.

The experimental studies have determined it is the C terminus of TIMP-1 interacting with the LEL of CD63 (Justo & Jasiulionis., 2021), none of the models from ClusPro demonstrated this. Therefore, the models for tsp-7 cannot be inferred from this modelling programme. HADDOCK has been shown to predict models more successfully than ClusPro (25% compared to 6.2%) (Ambrosetti *et al*., 2020).

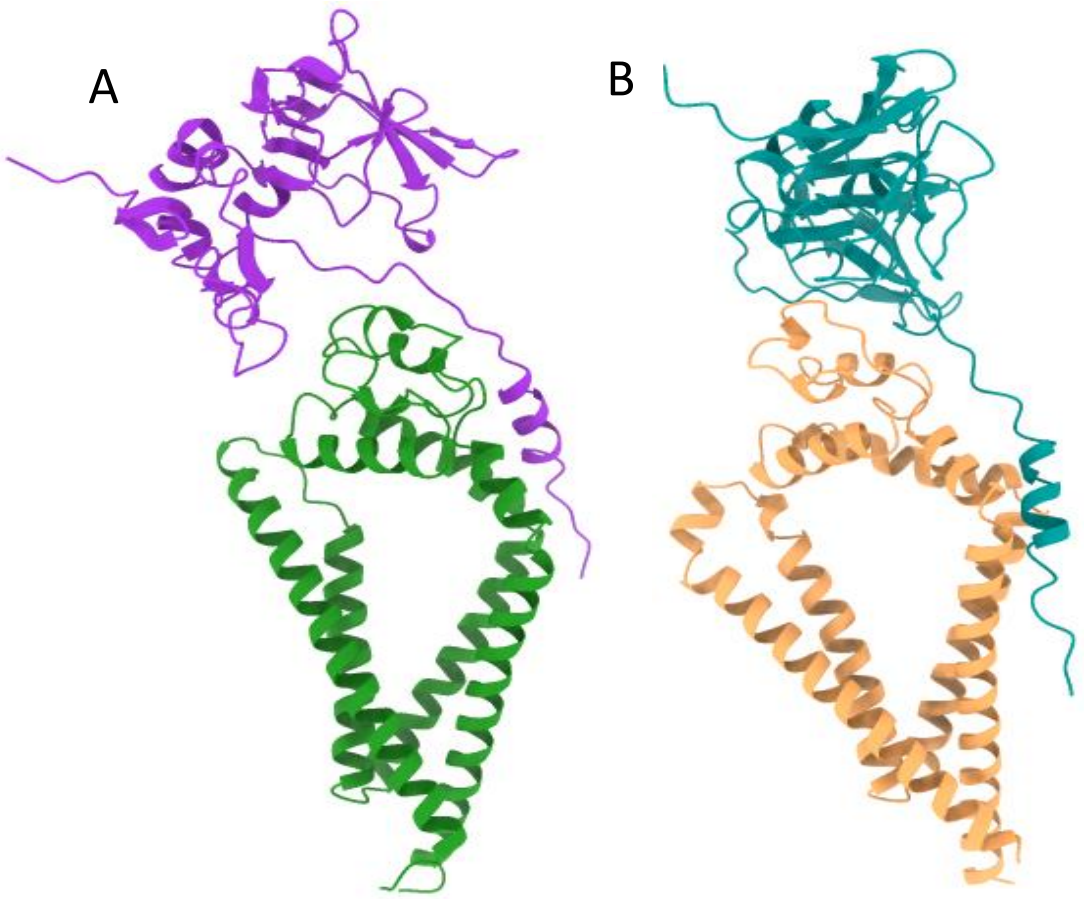

Figure 3.9.1. Potential binding models of CD63/TIMP-1 and tsp-7/TIMP-1 using HADDOCK. A) CD63 and TIMP-1 interaction using the HADDOCK docking programme. The C- terminus of TIMP-1 (purple) is bound to the LEL of the CD63 tetraspanin protein (green). The interaction between CD63/TIMP-1 has been well documented. B) theoretical interaction of tsp-7 from *C. elegans* (beige) and TIMP-1 (blue). The TIMP-1 C-terminus is also bound to the LEL of the tsp-7 protein, however part of the C-terminus extends down the transmembrane helices, however, the LEL domain appears to be imbedded along the C-terminus of TIMP-1. TIMP-1 binds in a 1:1 stoichiometry ratio.

Table 3.9.1. RMSD values and energy scores are shown for the CD63/TIMP-1 interaction and tsp-7/TIMP-1 interaction. Negative results indicate that the interaction is likely to occur under normal conditions. CD63/TIMP-1 is an already established binding partner and is used in this table to compare the RMSD and energy values for the theoretical interaction of *C. elegans* tsp-7 and human TIMP-1. The binding affinity and dissociation constant for CD63/TIMP-1 and tsp-7/TIMP-1 from PRODIGY, is displayed at the end of the table.

CD63 + TIMP-1		**tsp-7 + TIMP-1**	
HADDOCK score	-35.9 +/- 8.3	HADDOCK score	-14.4 +/- 14.2
Cluster size	34	Cluster size	8
RMSD from the overall lowest-energy structure	1.6 +/- 1.2Å	RMSD from the overall lowest-energy structure	1.2 +/- 1.2Å
Van der Waals energy	-59.4 +/- 14.2	Van der Waals energy	-59.9 +/- 9.1
Electrostatic energy	-320.8 +/- 27.9	Electrostatic energy	-181.2 +/- 17.2
Desolvation energy	-2.4 +/- 1.3	Desolvation energy	-32.0 +/- 3.1
Restraints violation energy	900.1 +/- 58.4	Restraints violation energy	1136.9 +/- 100.8
Buried Surface Area	2338.6 +/- 187.5	Buried Surface Area	2516.5 +/- 149.2
Z-Score	-2	Z-Score	-1.9
Binding affinity	-10.3 Kcal mol^{-1}	Binding affinity (ΔG)	-11.1 Kcal mol^{-1}
Dissociation constant (Kd)	5.1E-08	Dissociation constant (Kd)	1.50E-08M

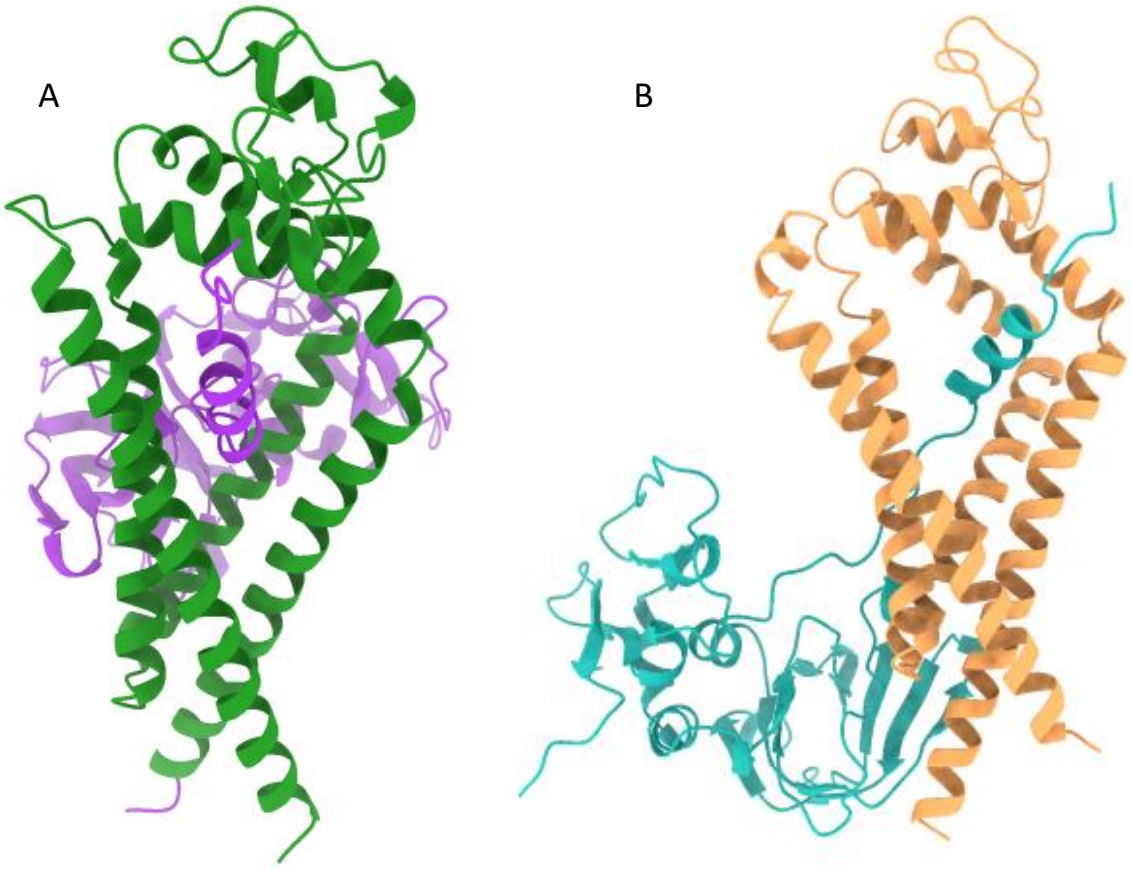

Figure 3.9.2. Binding models of CD63/TIMP-1 and tsp-7/TIMP-1 prediction using ClusPro, A) shows TIMP-1 (purple) and CD63 (green). The C – terminus of TIMP-1 passes through the middle of the transmembrane protein. The rest of the TIMP-1 protein is to the side of the tetraspanin. The entire LEL domain of the CD63 protein is unbound and completely exposed. B) shows tsp-7 (beige) and human TIMP-1 (blue), the binding model is similar to A, where the C – terminus of TIMP-1 binds through the 4 transmembrane helices. The rest of the TIMP-1 molecule is next to the transmembrane helices of tsp-7. The structure is improbable as the position of TIMP-1 binding to tsp-7 would be within the membrane.

3.10 Discussion

The nematode species are classified into five different clades (I, II, II, IV, V). There are no parasitic clade II nematodes. *C. elegans* belongs to clade V, also belonging to this clade are *A. ceylanicum, A. cantonensis, A. costaricensis*, *N. americanus* and *A. duodenale*. With the exception of *A. duodenale*, the other parasitic nematodes were the most similar in terms of amino acid sequence. It could be suggested that the proteins listed in section 3.3.4 for each of the parasites mentioned, retain the same function as tsp-7. Tsp-7 is thought to be a potential orthologue to human CD63. A hypothesis could be that the parasitic nematodes are also functionally and structurally similar to the human tetraspanin CD63 and may utilise the interactions within the host in place of CD63, therefore dampening the immune system, promoting anti-inflammatory responses, and establishing a chronic infection in a highly controlled environment.

The 14 parasites identified in section 3.4 and 3.5, suggest that the proteins may function as tetraspanins. Searching the NCBI database shows that only 5 of the proteins from table 3.3.4 are annotated as tetraspanins: EPB72344.1[Ancylostoma ceylanicum], XP_013301032.1 [Necator americanus], EJW84669.1 [Wuchereria bancrofti]. The other two parasite proteins are identified as CD63 antigens: KHN76951.1 [Toxocara canis] and CDW55483.1 [Trichuris trichiura].

The remaining parasitic nematodes from Table 3.3.4 are annotated as hypothetical or unknown proteins. These proteins may be tetraspanin proteins, or CD63-like tetraspanin proteins. More bioinformatic studies would be necessary to compare each parasitic protein to each other, not just in terms of identity and similarity to tsp-7

from *C. elegans* but between each parasitic clade. A proteomic study could utilise a primary polyclonal antibody raised against the tsp-7 protein and assess the cross-reactivity with each of the species. This however would require obtaining parasitic nematodes, which can be quite challenging, depending on facilities available, licenses to work with human pathogenic nematodes and the cultivation of such nematodes in a lab setting. Parasites are notoriously difficult to maintain within the lab (Ahmed., 2014).

The majority of the phosphorylation sites predicted are unlikely to be true as most of the positions are within the membrane. However, the Tyrosine phosphorylation site is a likely target for kinase signalling pathways. Protein tyrosine kinases induce pro-inflammatory cytokines (Nag & Chaudhary., 2009). Glycosylation of proteins is important inflammation and immune activation responses (Wolfert & Boons., 2013). Glycosylation sites and phosphorylation sites of parasitic nematode proteins may be involved with the interaction of parasite-host communication and immune modulation.

Using the models produced from the different programmes (Chimera X, SWISS-MODEL, PyMol) and AlphaFold, the LEL can be inferred from these 3D structures. The LEL domain must contain the CCG motif as well as the PXXCC motif. When the domain sequence has been determined theoretically, an antibody can be raised to a synthetic peptide within the LEL domain of tsp-7. This antibody can then be used to prove the domain sequence to be somewhat accurate, as most of the tsp-7 interactions occur within the LEL. Obtaining mutant strains with amino acid deletions of the tsp-7 protein, may mean that the protein is non-functional and

therefore may result in no binding of the primary polyclonal antibody. On the other hand, any deletion may have no impact on the LEL domain of tsp-7.

In theory TIMP-1 can bind under normal conditions to tsp-7, implementing this theory in a practical setting, by maintaining a mammalian cell culture and transfecting the cell with a plasmid containing the tsp-7 protein with a fluorescence tag for identification. The cells could then be incubated with TIMP-1 from a human source. This could further support the theory that if TIMP-1 can interact with tsp-7, then TIMP-1 could also bind to parasitic nematode tetraspanins.

The results in this chapter lay the foundation for future experiments, by identifying previously unknown parasite proteins as possible tetraspanins in terms of function. It also suggests that these same proteins interact with molecules from the human host, altering and manipulating the host immune response allowing the nematodes to thrive in a conditioned environment and establishing chronic infection.

Chapter 4: Comparing survival rate and stress response between wild type *C. elegans* and mutant strains

4.1 Introduction

The National BioResource Project in Japan (NBRP) is dedicated to providing deletion mutants of *C. elegans* (N2 Bristol strain). For this project two mutant strains were obtained from NBRP. Stress responses in *C. elegans* have been well documented (Croll., 1977 and Broekmans *et al.*, 2016). Life span assays can be used to measure the aging process, using this model organism. *C. elegans* and various knockout strains, are favoured due to the nematodes simple and short life span (Zhang *et al*., 2020). Assessing nematodes under oxidative stress is a common assay to determine factors of longevity (Hwang *et al*., 2014). Temperature dependent assays, heat stress and cold stress, are used to measure changes in physiological behaviour. Both heat and cold stress can be used to determine the effects of temperature on protein homeostasis (Jovic *et al*., and Robinson & Powell., 2016). *C. elegans* can be used as a model organism to assess the damage from UV-radiation (Ozawa *et al*., 2022), and are key organisms in the field of ionizing-radiation biology (Sakashita *et al*., 2010).

Common assays also include osmotic stress (Rodriguez *et al*., 2013), heavy metal exposure (Patsuhov *et al*., 2017), pollutant exposure (Queirós *et al*., 2019) and alcohol tolerance (Lee *et al*., 2009).

There is currently no data on stress induced factors and the physiological behaviour of the two mutant *C. elegans* strains: tm5046 and tm5761. The deletion of amino acids varies between the two mutants (see chapter 2.2.3). Mutant tm5046 has a 4 amino acid deletion within the LEL of the tsp-7 protein, mutant tm5761 has a much bigger deletion of 69 amino acids, resulting in the loss of transmembrane helices 2, 3 and the SIL. Figure 4.1.1. shows the 3D structure with the amino acid deletions highlighted. In this study, *C. elegans* (wild type and both mutant strains) will be exposed to osmotic stress, as this is a common stress response assay. The nematodes will also be exposed to high concentrations of Zn^{2+}, to assess response to heavy metals found within soil. 4-Octylephenol is a persistent organic pollutant (POP), found within the environment and will also be used as a stress inducer. Ethanol is not fatal to *C. elegans* but severely limits the locomotive behaviour of the nematodes (Albrecht *et al*., 2022). Immunological studies of *C. elegans* usually require FUDr (5-fluoro-2'-deoxyuridine), which prevents egg laying by sterilisation. Immune assays require the same life span measurement as well as populations of L4 and adult nematodes. Again, the timescale and the use of an expensive anticancer drug limited the ability of stress responses behaviours which could be measured. *C. elegans* can be exposed to bacterial, fungal, and intracellular parasitic pathogens. The pathogens used in immune assays include *Pseudomonas aeruginosa* (Kirienko *et al*., 2014, salmonella species (Park *et al*., 2017), *Candida neoformans*, *Candida albicans* (Alspaugh., 2015). The pathogens used to measure immune response are pathogenic to humans and therefore could not be used in this experiment. The intracellular parasites *Nematocida parisii*, is specific to *C. elegans*. Unlike the other pathogens, this intracellular pathogen is classified as a Biosafety level 1 pathogen. However, the cost of obtaining one vial of protists cost upwards of £500. A large quantity would be

needed for this experiment. Another issue would be to determine if the *C. elegans* are displaying avoidance behaviour or innate immunity (Reddy *et al*., 2009 and Park *et al*., 2017). Any studies concerning pathogens would be considered for future experiments, to emphasise the difference between wild type and mutant knockout tsp-7 *C. elegans.*

The effects of ethanol and induced stress in mutant tm5046 and tm5761 is unknown. Finally, the nematodes will be exposed to heat stress over a period of three hours at 37℃, acute heat stress in *C. elegans* is exhibited at 35℃ (Lithgow *et al*., 1994). All three strains will be exposed to cold stress of 5℃.

Assessment of *C. elegans* stress response behaviour is not only measured by locomotive behaviours but also life span assays. The assays would be carried out similar to the overall life span assay in this project. However, the timescale would be much shorter when exposed to some stresses such as U.V or ROS (Park *et al*., 2017). Due to timescale and the manual counting of worms by one observer, viability assays could not be performed to assess stress response. Therefore, the experiments are limited to observable locomotive behaviours.

In wild type *C. elegans* the average life span is typically between 18 and 21 days under normal culture conditions, standard NGM (see chapter 2.2.2.), and a temperature range between 16-25℃ is the standard range of maintenance (Zhang *et al.*, 2020). There is no experimental data for mutant 5046 or mutant 5761. In this study the null hypothesis for each assay is as follows:

1) There is no significant difference between the life span of wild type N2, and the two mutant strains.

2) There is no significant difference between the concentration of NaCl, $ZnSO_4 \cdot 7H_2O$, 4-Octylphenol and absolute ethanol on the locomotive stress responses of *C. elegans*.
3) There is no significant difference between the strain and stress response, in the presence of the compounds listed.
4) Temperature has no effect on stress response in either strain of *C. elegans*.

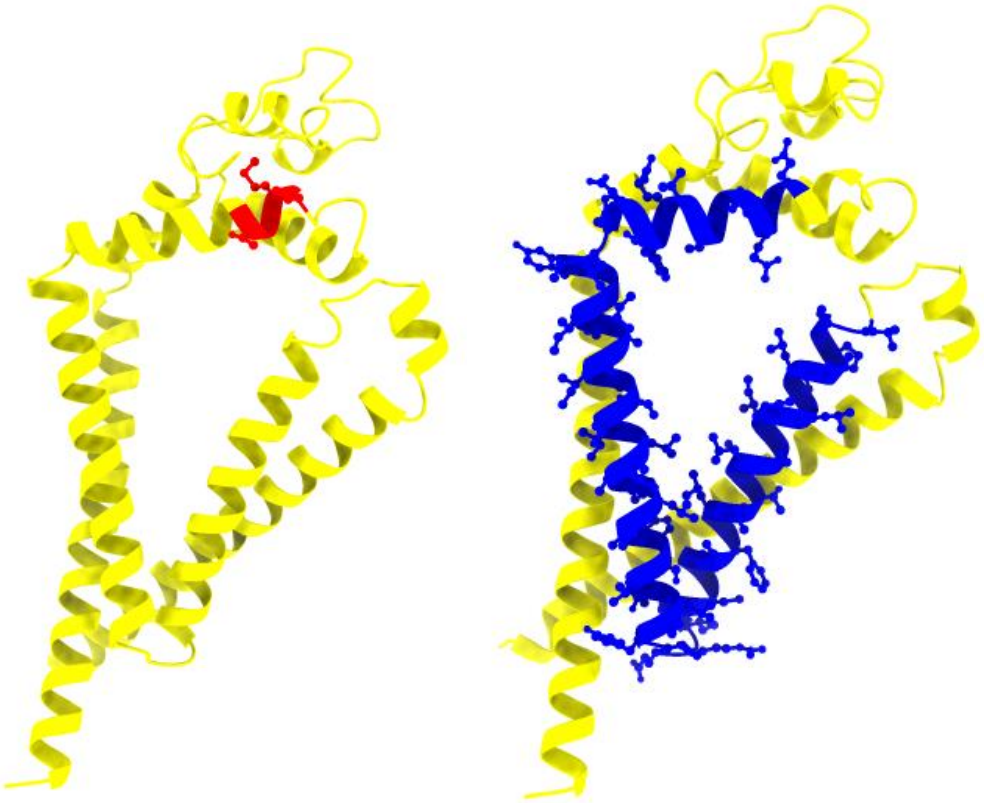

Figure 4.1.1. The amino acid deletion of mutant tm5046 and mutant tm5761.

Mutant tm5046 has a 4 amino acid deletion (red) at the beginning of the LEL, whereas mutant tm5761 has an amino acid deletion of 69 (blue), deleting two transmembrane helices (TM2 and TM3) as well as the small intracellular loop.

Aims of this study:

1. To assess the difference in survival rate between the wild type N2 and the two deletion mutant strains of *C. elegans*. The wild type N2 will act as a control, as there are multiple studies indicating the average life span of Wild type.
2. Compare difference in stress responses (The number of coils per minute, the sinusoidal frequency and the number of reversals performed per minute). The parameters for these assays are set out in chapter 2.2.10. The temperature and chemical stimuli used are:
    A) Heat stress- *C. elegans* are maintained in standard conditions of 14 - 17℃, the nematodes will therefore be exposed to an increase in temperature of 37℃ over a period of three hours.
    B) Cold stress- The nematodes will be exposed to temperatures as low as 5℃ over a period of three hours.
    C) NaCl- The NGM agar contains NaCl at a concentration of 0.05M, the nematodes will be assayed under normal conditions to act as a control to draw comparisons against. The NaCl concentrations used for this assay will be 0.75M and 2M.
    D) Zinc- As the compound $ZnSO_4 \bullet 7H_2O$. The NGM agar does not contain zinc, but the compound is used in trace amounts (~0.001M) whilst maintaining *C. elegans* in a liquid suspension.
    E) Phenol: 4-Octylphenol will be used at a concentration of 5mM. No phenol is present in NGM or liquid culture media.
    F) Ethanol: *C. elegans* will be exposed to100µl absolute ethanol.

4.2 Survival rates of wild type N2 Bristol strain and deletion mutant strains; tm5046 and tm5761

The null hypothesis states, there is no significant difference between the survival rate of the wild type strain of *C. elegans* and the two mutant strains (tm5046 and tm5761). A Kaplan-Meier curve was used to determine the survival rate of each of the strains (Figure 4.2.1). The survival rate measures the full life span from the first hatchling through to the day of death of each nematode (see chapter 2.2.7 and 2.2.12). The log-rank test was used for statistical testing between samples. Based on the log-rank test (Table 4.2.1), the null hypothesis is rejected. There is a significant difference between the survival rate of N2 wild type and tm5046 ($P<0.05$) and tm5761 ($P<0.05$).There is no significance between the two mutant strains tm5046 and tm5761 ($P>0.05$). The Fishers- exact test was used to compare the survival rate at specific time points (Table 4.2.2). There is significant difference between the survival of all three strains at 25% mortality. $P<0.05$ between N2 and tm5761 at 25% mortality, however $P<0.01$ between N2 and tm5046 and between the two mutant strains. At 50% mortality, there is no significance between N2 and tm5761 ($P>0.05$) but there is a significant difference between N2 and tm5046 and between the two mutant strains ($P<0.05$). At 75% mortality, there is no significance between N2 and tm5761 or between tm5046 and tm5761 ($P>0.05$), there is a significance between N2 and tm5046. There is no significance between any of the strains at 90% mortality. The standard errors calculated are within the data point range and were not included on the Kaplan Meier curve.

The general life span for N2 wild type *C. elegans* is between 18-20 days (Zhang *et al*., 2020). Overall, the average life span for wild type *C. elegans* in this study was 20.08 days, the life span of the wild type N2 strain matches what would be expected of N2 *C. elegans*. The average life span of the mutant tm5046 is 25.3 days and has the overall longest lifespan, tm5761 has an average life span of 23.34 days. In general, the mutant strains survive longer than the wild type strain (Table 4.2.3). All standard errors range from 0.08 to 0.00 and are not shown on the survival curves.

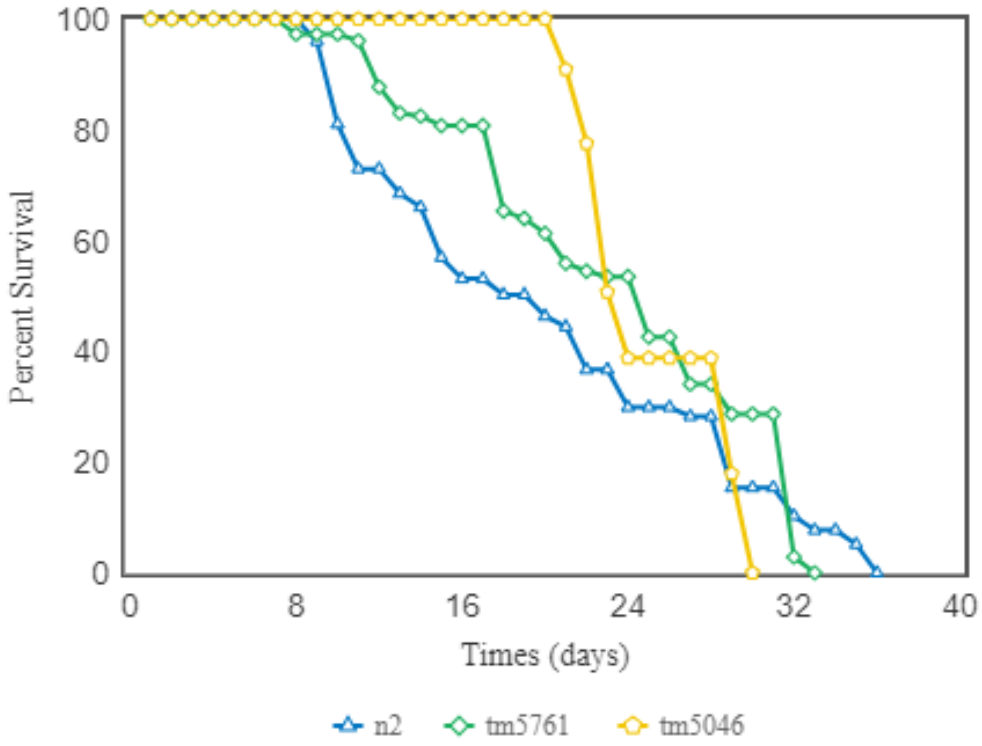

Figure 4.2.1 Kaplan Meier curve showing the life span of wild type N2 *C. elegans* and the two mutant strains (tm5046) and (tm5761). The curve is calculated as the percentage survival of nematodes at different time points. Overall, N2 has a mean life span of ~18-22 days. The mutant strain tm5046 has a mean life span of ~24-27 days. And the mutant tm5761 = ~22-25 days. For N2 N= 230, tm5046 N= 95, tm5761 N=300.

Table 4.2.1. Log rank analysis of life span of *C. elegans*. Log-Rank test used to analyse the overall survival rate of the three strains of *C. elegans*. The comparison between the mutant strains is not significant (P>0.05).

Condition	Chi squared	P-value
N2 v.s. TM5761	12.75	0.0004
N2 v.s. TM5046	9.26	0.0023
TM5761 v.s. TM5046	0.52	0.4694

Table 4.2.2. Fishers-exact analysis of *C. elegans* life span. Fishers- exact test is used to compare survival functions at different time points, from 25% mortality to 90% mortality.

Condition	P-value at 25%	P-value at 50%	P-value at 75%	P-value at 90%
N2 v.s. TM5761	0.01	0.07	0.07	0.17
N2 v.s. TM5046	0.0000014	1e-11	0.01	0.16
TM5761 v.s. TM5046	0.000048	8.5e-7	0.19	0.71

Table 4.2.3. Overall life span between N2 and two mutant *C elegans* strains. The mean and median lifespan of the nematodes overall, and the age at various mortality rates (as percentages). The mutant tm5046 has less subjects due to contamination of test plates. And therefore, a significant number of *C. elegans* could not be recovered.

Name	No. of subjects	Days	S.E.	95% C.I.	25%	50%	75%	90%	100%	95% Median C.I.
N2	230	20.08	0.81	18.49 - 21.67	11.00	20.00	29.00	33.00	36.00	15.0 - 21.0
tm5761	300	23.34	0.59	22.18 - 24.49	18.00	25.00	32.00	32.00	33.00	21.0 - 26.0
tm5046	95	25.31	0.57	24.19 - 26.43	23.00	24.00	29.00	30.00	30.00	23.0 - 28.0

4.3 Stress response assay of *C. elegans* against increased concentrations of NaCl

The standard concentration of sodium chloride is 0.05M within normal nematode growth medium. The concentration of sodium chloride was increased, to assess the stress response to higher salt and osmotic conditions, between the three strains. Figure 4.3.1 shows that at the standard concentration there is no difference in the number of coils per min observed (see chapter 2.2.10), between wild type N2 and both tsp-7 mutant strains. Statistical analysis was conducted using an independent T-test in SPSS. The mutant tm5761 was more sensitive to salt / osmotic stress compared to the wild type and mutant tm5046. The mutant tm5046 displayed a similar stress response to the wild type. There is no significant difference between the wild type and mutant tm5046 and osmotic stress response.

Table 4.3.1 shows a univariate ANOVA statistical analysis test, comparing the difference between the concentrations and between the species. There is a significance between the strain and coiling response ($P<0.05$) and between concentration and coiling response ($P<0.05$). The post-hoc LSD test (Fishers Least Significant difference test) shows a statistical difference overall between strains; N2 and tm5761 ($P<0.001$), and tm5761 and tm5046 ($P<0.001$). There is no statistical difference between N2 and tm5046 ($P>0.05$).

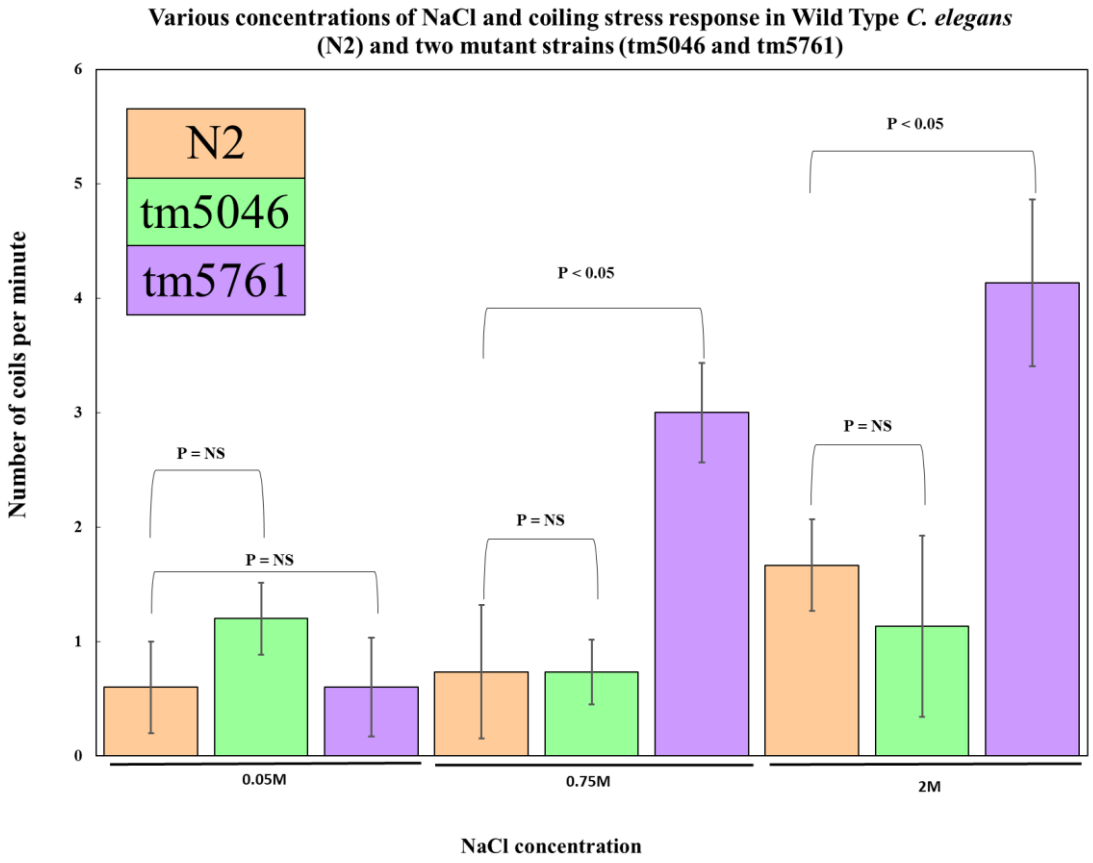

Figure 4.3.1. Coiling frequency and osmotic stress. The graph was produced in Origin and Excel and shows the three different strains (N2= pink, tm5046= green and tm5761= purple), and the number of coils per minute under normal conditions (0.05M NaCl) at increased concentrations (0.75M and 2M). Mutant tm5761 displayed the highest coiling frequency across the concentrations. Mutant tm5046 was more similar to the wild type (N2). At 0.05M N= 5 animals per strains, at 0.75M N= 15 animals for wild type (N2) and mutant tm5046, N = 13 animals for mutant tm5761. At 2M N= 15 animals per strain. Error bars represent the standard error of the mean. P= NS – not significant. Independent T test was conducted in SPSS.

Table 4.3.1. Two -way ANOVA analysis for coiling and osmotic stress. A univariate ANOVA statistical analysis and a Post-hoc LSD test was carried out in SPSS, for the number of coils between each species, across different concentrations of sodium chloride. *Significance at P=0.05 level. The data draws comparison across species and across different concentrations being the fixed variables, the dependent variable is the number of coils per minute. For 0.05M NaCl, N=5 animals per strain, for 0.75M and 2M, N=15 animals for N2 and tm5046. N= 13 animals for tm5761.

Strain		Mean Difference	Std. Error	Sig.
N2	Tm5046	0.14	0.45	0.75
	Tm5761	-2.04*	0.46	<.001
Tm5046	N2	-0.14	0.45	0.75
	Tm5761	-2.18*	0.46	<.001
Tm5761	N2	2.04*	0.46	<.001
	Tm5046	2.18*	0.46	<.001
Concentration		Mean Difference	Std. Error	Sig.
.05M	.75M	-0.62	0.57	0.28
	2.00M	-1.51*	0.57	0.009
.75M	.05M	0.62	0.57	0.28
	2.00M	-.89*	0.41	0.03
2.00M	.05M	1.51*	0.57	0.009
	.75M	.89*	0.41	0.03

Another behavioural assay that can be measured as a sign of stress is the sinusoidal movement of *C. elegans* (see chapter 2.2.10). The sinusoidal movement per minute was counted for each strain (N=5) under normal salt conditions, (0.05M NaCl). The same movement was counted for the nematodes exposed to higher concentrations of NaCl (Figure 4.3.2). An independent T – test analysis showed that there is a significant difference between mutant tm5046 and the wild type at 0.75M NaCl ($P<0.001$) however at 2M $P = 0.05$ between wild type N2 and mutant tm5046 and may not be overly significant.

The two-way ANOVA (Table 4.3.2) shows that there is a significance between the strains and sinusoidal frequency ($P<0.001$) and between the concentration and sinusoidal frequency ($P<0.05$) overall. The Post-hoc Least significant difference analysis shows there is a difference in sinusoidal frequency between the wild type N2 and the mutant tm5046 ($P<0.05$), there is also a significant difference between the two mutant strains tm5046 and tm5761 ($P< 0.05$). In summary, the tm5046 strain appears to be sensitive in its response to high levels of NaCl by exhibiting less frequent sinusoidal movements compared to the wild-type.

The sinusoidal undulation or “crawling” behaviour may be a poor measurement for the osmotic stress response. The test plates were seeded with *E.coli* food source and may have affected the general forward movement of the nematodes. For example, the nematodes generally crawl using the sinusoidal undulation to search for food (Iliff & Xu., 2020), if the plates were covered with a bacterial lawn, the nematodes would not need to actively search for a food source.

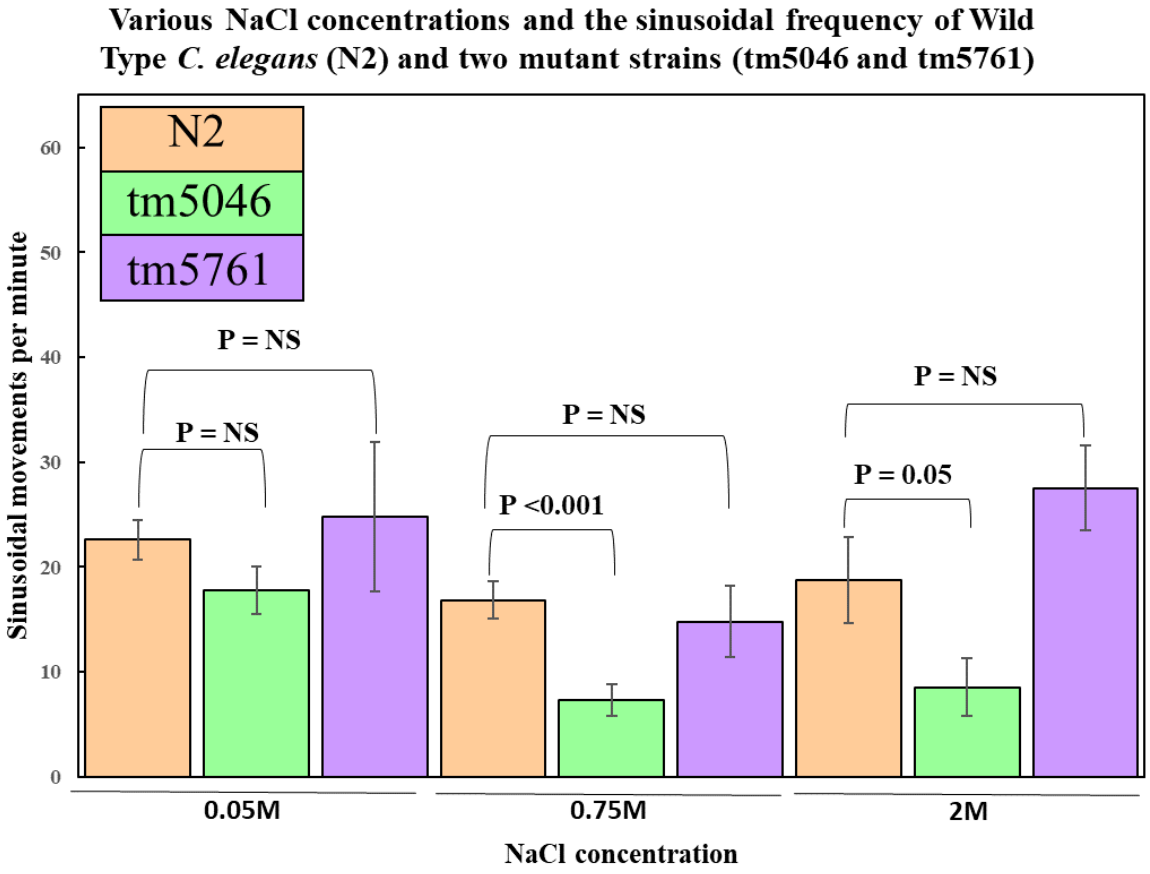

Figure 4.3.2. Sinusoidal frequency and osmotic stress. The sinusoidal frequency of N2 (pink), mutant tm5046 (green) and mutant tm5761 (purple) when exposed to different concentrations of NaCl (0.75M and 2M). The standard concentration for maintaining *C. elegans* is 0.05M. At the standard concentration N= 5 animals per strain, at 0.75M and 2M N= 15 animals for N2 and tm5046. N= 13 animals for tm5761. Error bars represent standard error of the mean. Independent T -test was conducted in SPSS. The graph was produced in Origin and Excel. P= NS – not significant.

Table 4.3.2. Two-way ANOVA analysis on sinusoidal frequency and osmotic stress. A univariate ANOVA statistical analysis and a Post-hoc LSD test was performed in SPSS on the sinusoidal frequency as the dependent variable and the strain and concentration as fixed variables. The analysis compares between samples. * = statistical significance at the P= 0.05 value.

Strain		Mean Difference	Std. Error	Sig.
N2	Tm5046	9.17*	2.79	0.001
	Tm5761	-3.61	2.83	0.206
Tm5046	N2	-9.17*	2.79	0.001
	Tm5761	-12.78*	2.83	0
Tm5761	N2	3.61	2.83	0.206
	Tm5046	12.78*	2.83	0
Concentration		Mean Difference	Std. Error	Sig.
.05M	.75M	8.85*	3.50	0.013
	2.00M	3.47	3.48	0.321
.75M	.05M	-8.85*	3.50	0.013
	2.00M	-5.38*	2.49	0.033
2.00M	.05M	-3.47	3.48	0.321
	.75M	5.38*	2.49	0.033

The final observational parameter measured in response to osmotic / salt stress was the number of reverse movements per minute (reversals), the method of determining the parameters for this measurement can be found in chapter 2.2.10. Under the standard conditions, the number of reversals for N2, tm5046 and tm5761 are similar (Figure 4.3.3) with a mean frequency of; 2.4/min, 3.2/min, and 2.6/min, respectively.

The independent T- test analysis showed that, like the coiling assay, the mutant tm5761 is more sensitive to osmotic stress than the wild type N2 and the mutant tm5046. There was no difference between the wild type and mutant tm5046. The mutant strain (tm5046) appears to be the most tolerant of the two mutant strains, with osmotic stress in terms of reversal frequency.

A univariate ANOVA statistical analysis was performed in SPSS. There is an overall significance between strain and reversals ($P<0.05$) and between the concentration and number of reversals per min ($P<0.05$). Table 4.3.3 shows the post-hoc LSD analysis with a significance between wild type N2 and mutant 5761 and between both mutants tm5046 and tm5761 ($p<0.001$). There is no significant difference in the overall number of reversals per minute between wild type N2 and mutant tm5046 ($P>0.05$). The mutant strain tm5761 displayed an increase in stress behaviour compared to both N2 and tm5046. The mutant tm5046 remained relatively stable across all concentrations of NaCl and showed a similar stress response to wild type N2. Independent T-test for NaCl and stress response behaviour can be found in supplementary data 6 (S6).

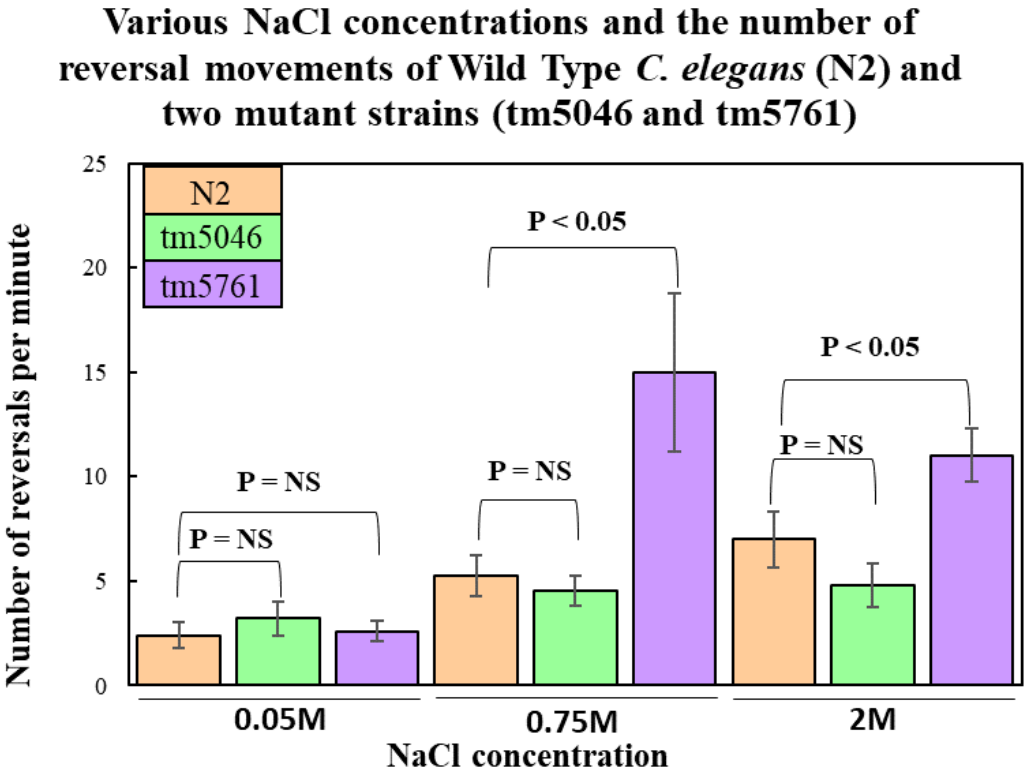

Figure 4.3.3. Reversal frequency and osmotic stress. The graph was produced in Origin and the standard concentration of NaCl is 0.05M which was increased to 0.75M and 2M. The number of reversals per minute was measured against the concentration of NaCl. N=5 at 0.05M, N= 15 at both 0.75M and 2M (N2 and tm5046). N= 13 animals for tm5761. Error bars are displayed as standard error of the mean. An independent T-test assay was conducted in SPSS. P= NS – not significant.

Table 4.3.3. Two-way ANOVA analysis of Reversal frequency and osmotic stress. A univariate ANOVA and a Post-hoc LSD test was performed in SPSS, the statistical analysis compares the number of reversals between strains and between the different concentrations. * = statistical significance at the P= 0.05 level.

Strain		Mean Difference	Std. Error	Sig.
N2	Tm5046	1.14	1.46	0.437
	Tm5761	-5.70*	1.49	<.001
Tm5046	N2	-1.14	1.46	0.437
	Tm5761	-6.85*	1.49	<.001
Tm5761	N2	5.70*	1.49	<.001
	Tm5046	6.85*	1.49	<.001
Concentration		Mean Difference	Std. Error	Std. Error
0.05M	0.75M	-5.22*	1.84	0.006
	2M	-4.88*	1.83	0.009
0.75M	0.05M	5.22*	1.84	0.006
	2M	0.35	1.31	0.787
2M	0.05M	4.87*	1.83	0.009
	0.75M	-0.35	1.31	0.787

4.4 Stress response assay of *C. elegans* and Zinc Sulphate Heptahydrate ($ZnSO_4•7H_2O$)

$ZnSO_4•7H_2O$ is used to grow and maintain *C. elegans* within a liquid culture, (see chapter 2.2.13). The final concentration used in this assay was 1mM. There is no $ZnSO_4•7H_2O$ used in the maintenance of *C. elegans* in nematode agar growth medium. The control in this assay is labelled 0.00M and the stress responses under normal conditions is the same as 4.3 above. In order to assess the effects of the heavy metal Zn^{2+} at very high concentrations that may mimic highly polluted environments that nematodes may be exposed to, the wild type and mutant strains of the *C. elegans* were cultured in 0.5M and 1M $ZnSO_4•7H_2O$.

The independent T- test (Figure 4.4.1) shows that there was a significant difference between the number of coils /min in Wild type (N2) and the mutant tm5761 at 0.5M ($P < 0.05$). There was no significant difference between wild type and mutant tm5046 at 0.5M or 1M. There was also no significant difference between the coiling frequency in wild type and mutant tm5761 at 1M. From 0.5M to 1M, all three strains showed a slight difference in coiling frequency. However, it should be noted that the average number of coils/min only varies between 1-2 coils across all strains and all Zn^{2+} concentrations, which indicates that coiling frequency shows a relatively mild stress response when it comes to Zn^{2+} exposure. The univariate ANOVA analysis (Table 4.4.1) shows that there is no overall significance between strains or between concentrations. Overall, the addition of $ZnSO_4•7H_2O$ at 1M did not have a significant effect on the frequency of coils/min displayed by either strain.

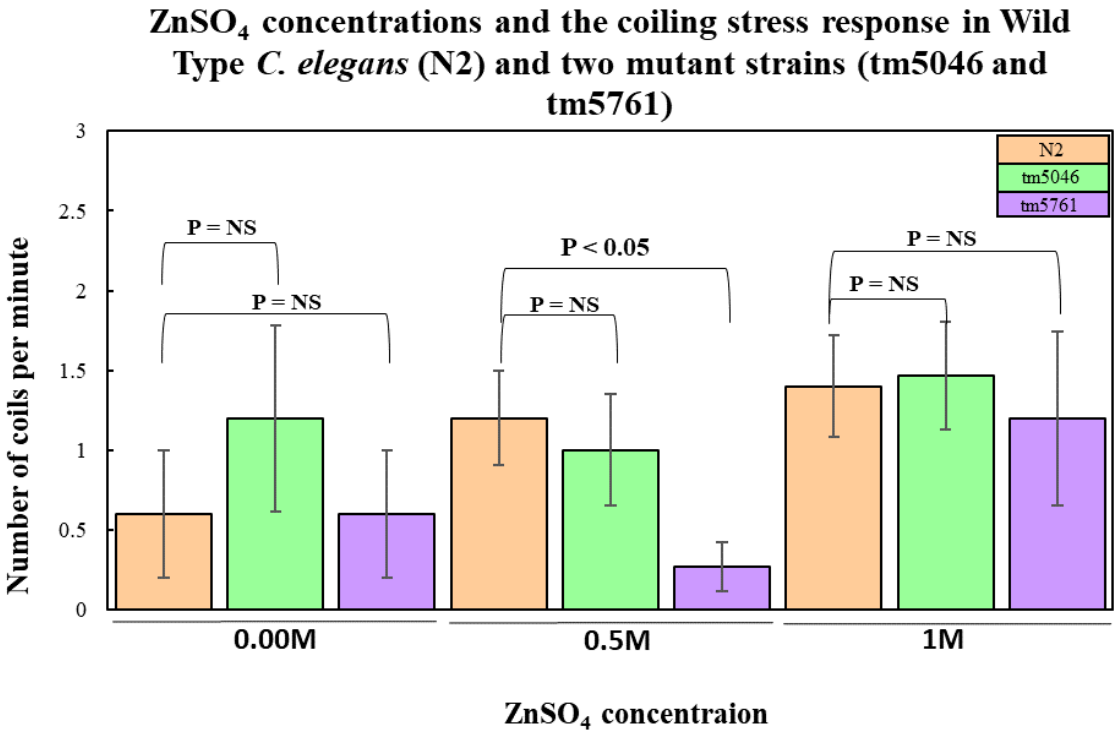

Figure 4.4.1. Coiling frequency and Zn^{2+} exposure. The graph was produced in Origin and Excel. The graph shows the number of coils under standard conditions (0.00M) compared to the addition of Zinc at 0.5M and 1M. N= 5 for each strain at 0M, N= 14 at 0.5M (tm5046), N= 15 at 0.5M (tm5761) and (N2), N= 15 at 1M for all three strains. Error bars represent the standard error of the mean. Independent t-test was conducted in SPSS. P= NS – not significant.

Table 4.4.1. Two-way ANOVA analysis and heavy metal exposure. A univariate ANOVA test was performed in SPSS. A Post-hoc LSD test was also conducted in SPSS (not significant). The coiling response is the dependent variable, and the strain and concentration are the fixed independent variables. The table shows no difference between groups (strains and concentration) and the frequency of coiling in response to stress.

Source	Type III Sum of squares	df	Mean square	F test	Sig.
Concentration	7.42	2	3.71	2.12	0.13
Strain	4.04	2	2.02	1.16	0.32
Concentration / Strain	3.18	4	0.79	0.45	0.77

The sinusoidal movement frequency between wild type and mutant tm5761 at 1M was statistically significant ($P < 0.05$). At 1M Zn^{2+}, the sinusoidal frequency increased in all species compared to their response in 0.5M Zn^{2+}, but this appeared to be less exaggerated in mutant tm5761 (Figure 4.4.2). Overall, the mean sinusoidal frequencies for wild type and mutant strains tm5046 in 1M Zn^{2+} is relatively similar to the observed frequency under standard conditions, ranging from 20-25 sinusoidal movements.

The univariate ANOVA statistical analysis (Table 4.4.2) shows a significance between wild type N2 and mutant tm5761 ($P<0.05$), overall, between groups. There is no significance between wild type N2 and tm5046, or between the two mutant strains tm5046 and tm5761 ($P>0.05$). There is an overall significant difference between the concentrations of $Zn^{2+,}$ 0M to 0.5M, 0M to 1M and 0.5M to 1M ($P<0.05$) and the overall sinusoidal frequency from all three strains.

In summary, with respect to Zn^{2}+ and the frequency of sinusoidal movements, all three strains responded similarly within groups (independent t- test), but there is an overall significance between groups at different concentrations (univariate ANOVA).

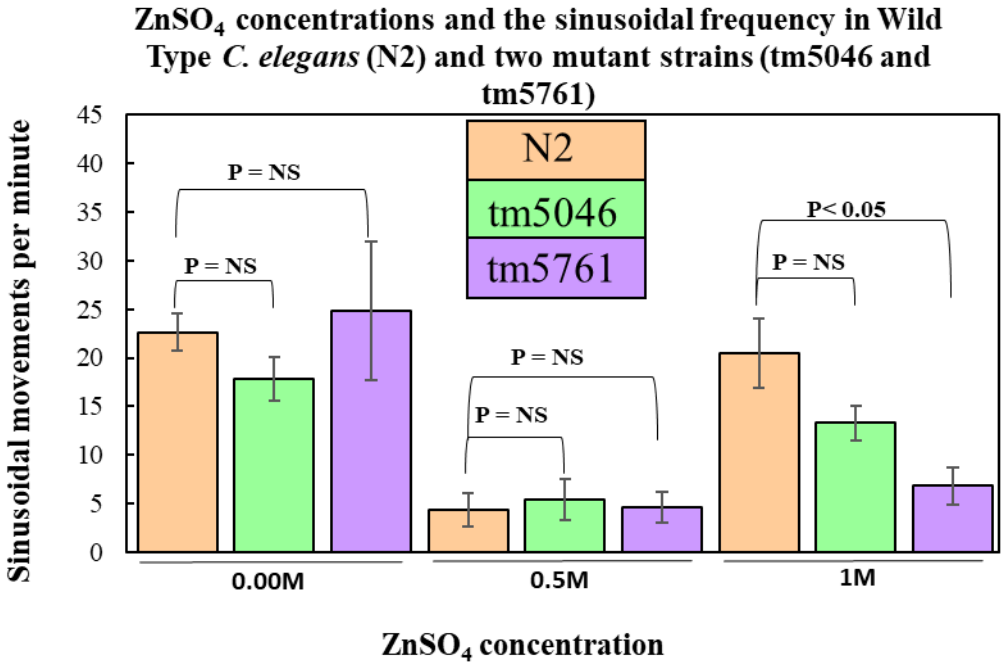

Figure 4.4.2 Sinusoidal frequency and Zn^{2+} exposure. The graph, produced in Origin and excel, shows the sinusoidal frequency movements under standard conditions for each strain and with the addition of 0.5M and 1M $ZnSO_4 \bullet 7H_2O$. N= 5 for each strain at 0M, N= 14 at 0.5M (tm5046), N= 15 at 0.5M (tm5761) and (N2), N= 15 at 1M for all three strains. In general, the mean number of sinusoidal movements decreases with the addition of 0.5M but increases with an addition of 1M, from 0.5M. At 0.5M, all three strains have similar sinusoidal frequency. Error bars represent the standard error of the mean. P= NS – not significant. Independent T-test was conducted in SPSS.

Table 4.4.2. Two-way ANOVA analysis of sinusoidal frequency and heavy metal exposure. The table shows the statistical analysis of the data, using a univariate ANOVA analysis and a Post-hoc LSD test (SPSS). The data shows there is a significance between N2 and tm5761, but no significance between N2 and tm5046 and no significance between tm5046 and tm5761. There is statistical significance between all three concentrations. *= significance at the P= 0.05 level.

Species		Mean Difference	Std. Error	Sig.
N2	Tm5046	3.12	2.11	0.143
	Tm5761	5.40*	2.10	0.012
Tm5046	N2	-3.12	2.11	0.143
	Tm5761	2.28	2.11	0.284
Tm5761	N2	-5.40*	2.10	0.012
	Tm5046	-2.28	2.11	0.284
Concentration		Mean Difference	Std. Error	Std. Error
0M	0.5M	16.96*	2.62	0
	1M	8.24*	2.62	0.002
0.5M	0M	-16.96*	2.62	0
	1M	-8.72*	1.86	0
1M	0M	-8.24*	2.62	0.002
	0.5M	8.72*	1.86	0

The final assay using $ZnSO_4 \bullet 7H_2O$, compared the number of reversal movements per minute of each strain, in response to an increase in zinc ion concentration. The independent t-test suggests that there is no difference between the number of reversals/min displayed by each strain with the addition of 0.5M Zn^{2+} or 1M Zn^{2+} (Figure 4.4.3).

The univariate ANOVA statistical analysis (Table 4.4.3) shows there was a significance between concentration and reversal frequency ($P<0.001$) but no significance between the strain and reversal frequency ($P>0.05$). A post-hoc analysis was performed for the concentrations and reversal frequency. There was a significance between the number of reversals between 0.00M (standard) and at 1M ($P<0.05$) and a significance between 0.5M and 1M. There was no significance between the standard (0.0M) and 0.5M concentration ($P>0.05$). Overall, this reversal movement assay shows the mutant and wild type strains respond similarly to this stressor.

An independent T-test for each strain across the different concentrations, for all three observable parameters can be found in supplementary data 7 (S7).

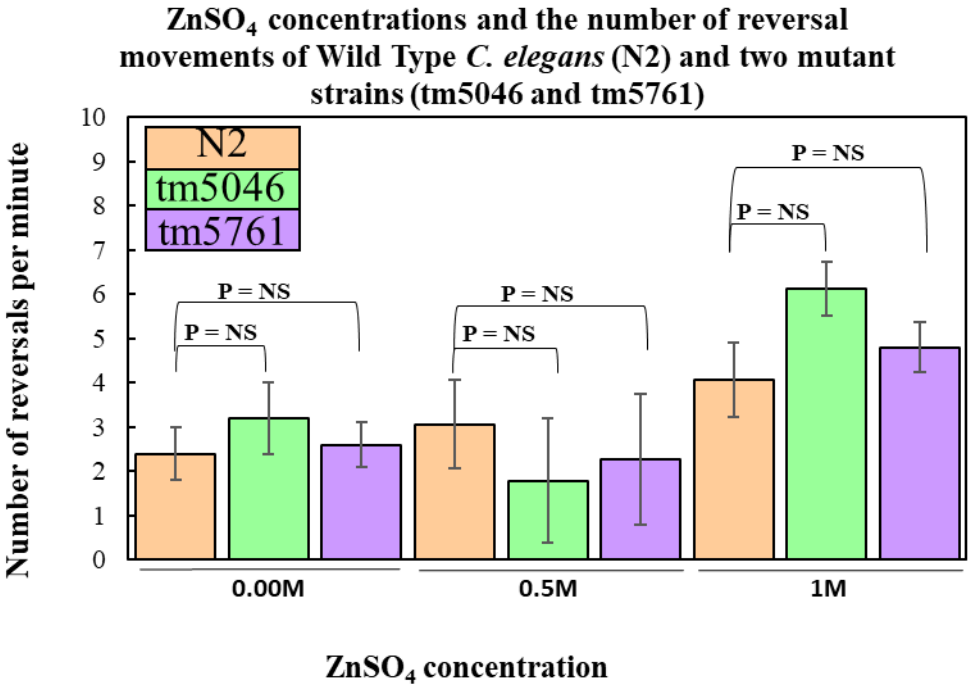

Figure 4.4.3. Reversal frequency and Zn^{2+} exposure. The graph was produced in Origin and Excel. There is no significance in reversal frequency and concentration of Zn^{2+} within groups. N= 5 for each strain at 0M, N= 14 at 0.5M (tm5046), N= 15 at 0.5M (tm5761) and (N2), N= 15 at 1M for all three strains. Error bars represent standard error of the mean. P= NS – not significant. Independent T-test was conducted in SPSS.

Table 4.4.3. Two -way ANOVA analysis of reversal frequency and heavy metal exposure. The Univariate ANOVA statistical analysis and Post-hoc LSD test shows that there is no significance between the strains and the reversal frequency. There is a significant difference between the concentration of Zinc and the reversal frequency, between 0M (standard) and 1M and between 0.5M and 1M ($P<0.05$). *= significance at the P= 0.05 level.

Source	Type III SoS	df	Mean Square	F test	Sig.
Concentration	165.49	2	82.75	9.18	0.000
Strain	4.60	2	2.30	0.26	0.775
Concentration /Strain	41.66	4	10.42	1.16	0.336

Concentration		Mean Difference	Std. Error	Sig.
0M	0.5M	0.35	0.90	0.7
	1M	-2.27*	0.90	0.013
0.5M	0M	-0.35	0.90	0.7
	1M	-2.61*	0.64	0
1M	0M	2.27*	0.90	0.013
	0.5M	2.61*	0.64	0

4.5 Stress response assay of *C. elegans* and 4-Octylphenol

4-Octylphenols are pollutants that disrupts endocrine functions, often used in detergents, pesticides, and fuel (Olaniyan *et al.*, 2020). 4-Octylphenol was dissolved in absolute ethanol and the concentration of 4-Octylphenol in the final assay was 5mM.

The graph below (Figure 4.5.1) shows the number of coils/min made by the *C. elegans* strains under standard conditions, and the number of coils/min recorded for each strain when exposed to 5mM 4-Octylphenol. The graph shows that there was an increase overall in the number of coils per minute observed when exposed to 4-Octylphenol. The independent t-test showed that there is no significance in the coiling response with the addition of 5mM 4-Octylphenol. The univariate ANOVA (Table 4.5.1) suggest there is no significance between groups (coiling and strain $P > 0.05$, and between coiling and concentration $P > 0.05$).

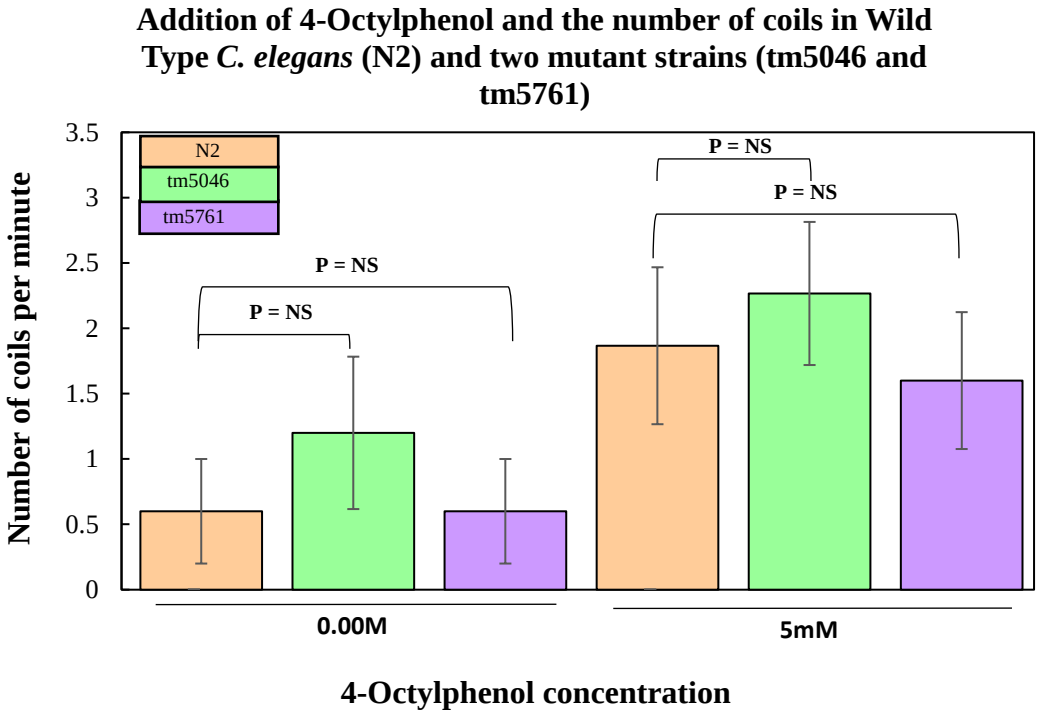

Figure 4.5.1 Coiling frequency and 4-Octylpehnol exposure. The graph was produced in origin and Excel. 5mM addition of 4-Octylphenol was selected as the maximum concentration with less than 50% fatality rate of the nematodes. N= 5 at 0.00M for each strain, N=15 animals at 5mM for each strain. Error bars represent the standard error of the mean. P= NS – not significant. Independent T-test was conducted in SPSS.

Table 4.5.1. Two-way ANOVA analysis of coiling response and 4-Octlyphenol. The two-way ANOVA suggests there is no significance between groups and the effect on coiling. (P>0.05), no further analysis was required for this data set. Post-hoc LSD test was not significant.

Source	Type III SoS	df	Mean Square	F test	Sig.
Concentration	13.89	1	13.89	3.58	0.064
Strain	3.34	2	1.67	0.43	0.652
Concentration / Strain	0.14	2	0.07	0.02	0.982

The sinusoidal frequency with addition of 5mM 4-Octylphenol was significant between wild type (N2) and mutant tm5761 ($P < 0.001$) (Figure 4.5.2). However, There was no significance between wild type (N2) and mutant tm5046 ($P > 0.05$).

For this data set, the standard deviation and standard error of the mean are relatively high. This suggests that the data is more spread out about the mean. It could also indicate that the results are not completely representative of the population.

The univariate ANOVA analysis (Table 4.5.2) demonstrates that there is a statistical significance between the sinusoidal frequency and the different strains ($P<0.05$). The difference between sinusoidal frequency between groups and the addition of 4-Octylphenol is not significant. This univariate ANOVA tests between all of the sinusoidal frequency combined in the standard group against the combined frequency with the addition of 5mM. The combined mean of sinusoidal frequency for all three strains under standard conditions is 65.2, with the addition of 5mM 4-Octylphenol the average is 76.7. The difference between the two groups is ~11 sinusoidal movements.

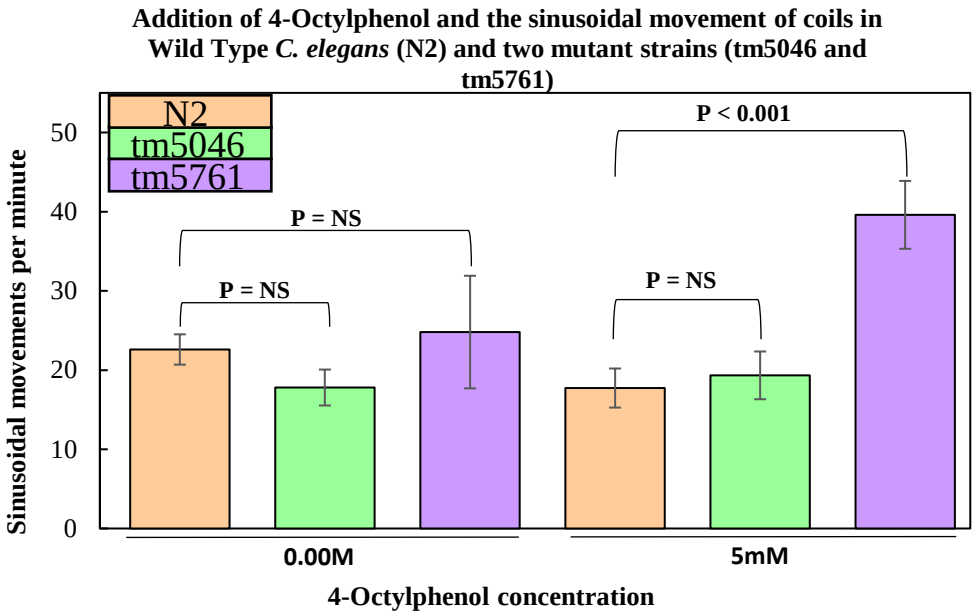

Figure 4.5.2 Sinusoidal frequency and 4-Octylpehnol exposure. The graph shows an increase in sinusoidal frequency with an addition of 5mM phenol. The graph was produced in Origin and Excel. N= 5 at 0.00M for each strain, N=15 animals at 5mM for each strain. Error bars represent standard error of the mean. P= NS – not significant. Independent T-test was conducted in SPSS.

Table 4.5.2. Two-way ANOVA analysis of sinusoidal frequency and 4-Octylphenol exposure. The two-way ANOVA (univariate test) and a Post-hoc LSD test, produced in SPSS, shows a significance between strain and sinusoidal frequency. There is no significance between concentration and sinusoidal frequency. *= significance at the P= 0.05 level.

Source	Type III SoS	df	Mean square	F-test	Sig.
Concentration	164.36	1	164.36	1.08	0.304
Strain	1666.14	2	833.07	5.46	0.007
Concentration / Strain	754.68	2	377.34	2.48	0.094

Strain		Mean Difference	Std. Error	Sig.
N2	Tm5046	0.00	3.90	1.000
	Tm5761	-16.95*	3.90	0.000
Tm5046	N2	0.00	3.90	1.000
	Tm5761	-16.95*	3.90	0.000
Tm5761	N2	16.95*	3.90	0.000
	Tm5046	16.95*	3.90	0.000

The final measurement recorded was the number of reversals per minute under standard conditions and with the addition of 4-Octylphenol. There is no significant difference between the number of reversals / min and the strains with the addition of 4-Octylphenol. The number of reversals/ min was similar between the three strains under standard conditions and were similar with the addition of 4-Octylphenol (Figure 4.5.3).

The univariate ANOVA (Table 4.5.3) shows that there is no significance between the strain and the number of reversals under standard conditions (0mM), and no significance between the concentration of 4-Octylphenol and reversals/min ($P>0.05$). No further Post-hoc analysis were carried out on this data set.

An independent T-test for each strain with the addition of 4-Octylphenol for each of the three parameters can be found in supplementary 8 (S8).

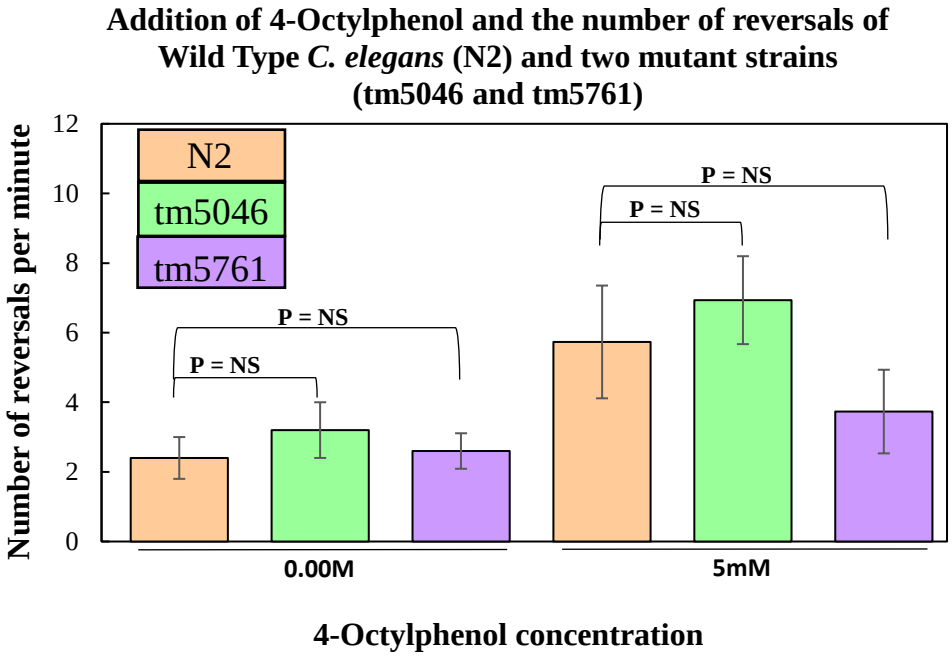

Figure 4.5.3. Reversal frequency and 4-Octylphenol exposure. The graph demonstrates a clear increase in the number of reversals recorded for each species. However, the increase for mutant tm5761 is smaller than the increase for wild type N2 and mutant tm5046. N= 5 at 0.00M for each strain, N=15 animals at 5mM for each strain. P= NS – not significant. Independent T – test was conducted in SPSS.

Table 4.5.3. Two-way ANOVA analysis of reversal frequency and 4-Octylphenol exposure. The two-way univariate ANOVA analysis shows that there is no significance between either independent variable (strain and addition of phenol) and the number of reversals displayed. Post-hoc LSD test was not significant.

Source	Type III SoS	df	Mean square	F-test	Sig.
Concentration	84.05	1	84.05	3.74	0.058
Strain	27.10	2	13.55	0.60	0.551
Concentration / Strain	14.70	2	7.35	0.33	0.723

4.6 Stress response assay of *C. elegans* with the addition of 100% ethanol

The maintenance of *C. elegans* requires cholesterol added in 100% ethanol. There are multiple studies confirming that *C. elegans* can survive ethanol and over time becomes tolerant to high concentrations. Ethanol has an effect on the motor-neuronal system of *C. elegans* as well as locomotion (Albrecht *et al*., 2022*)*. In this study 100µl of absolute ethanol (~92% concentration) was used to cover the agar (see chapter 2.2.11). The concentration of ethanol is small when added to the nematode growth medium, therefore the standard assay is recorded as 0%, with no addition of ethanol.

Figure 4.6.1 shows that there is no significant difference in coiling stress response with the addition of ethanol ($P > 0.05$).

The two-way univariate ANOVA statistical analysis (Table 4.6.1) shows that there is no significance between the strain and coiling frequency or between the addition of ethanol and coiling frequency ($P > 0.05$).

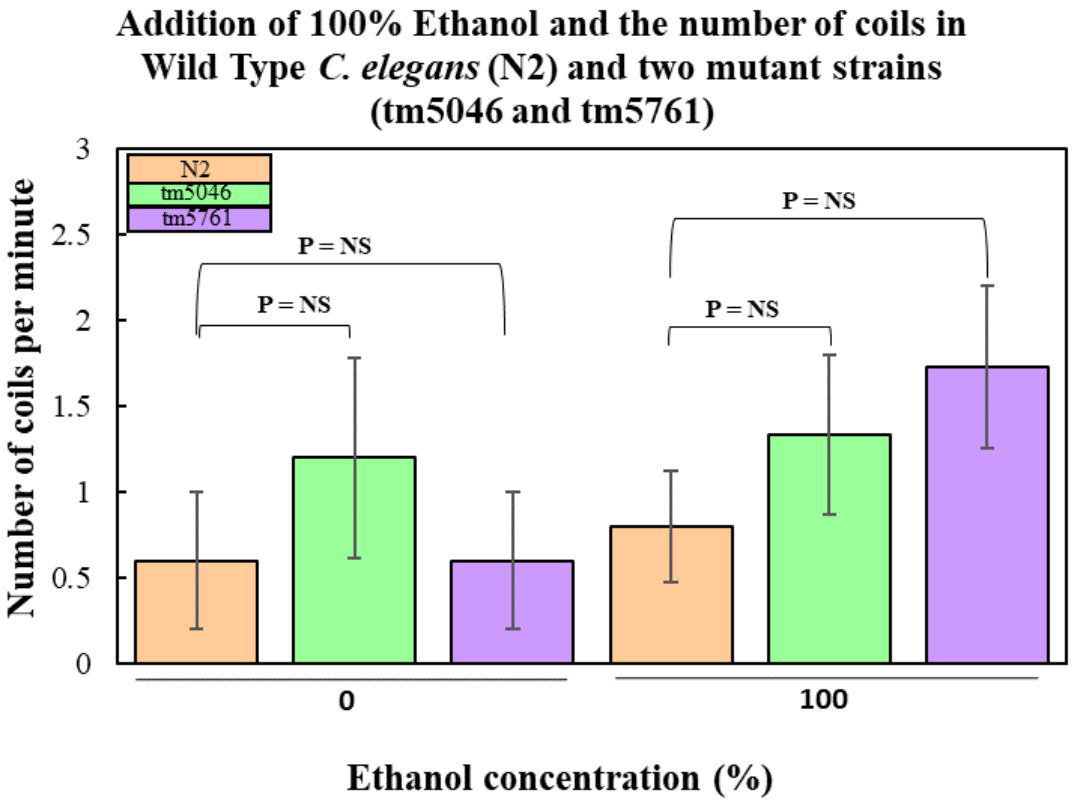

Figure 4.6.1. Coiling frequency and ethanol exposure. The graph shows a slight increase in coiling response with an addition of 100% ethanol. The graph was produced in Origin and Excel. N= 5 at 0% ethanol for each strain, N=15 animals at 100% ethanol for each strain. Error bars represent the standard error of the mean. P= NS – not significant. Independent T- test was conducted in SPSS.

Table 4.6.1. Two-way ANOVA analysis of coiling response and the addition of Ethanol.

The univariate ANOVA tests between groups and suggests that there is no significance between the strain and number of coils (P = 0.564), and no significance between the number of coils and the addition of ethanol (P = 0.291). The Post-hoc LSD test was not significant. The null hypothesis is accepted.

Source	Type III SoS	df	Mean square	F-test	Sig.
Concentration	2.69	1	2.69	1.14	0.291
Strain	2.74	2	1.37	0.58	0.564
Concentration / Strain	2.34	2	1.17	0.50	0.612

The mean number of sinusoidal movements per minute increases across all three strains, with the addition of 100% ethanol (Figure 4.6.2). Under standard conditions, there is little difference between the sinusoidal frequencies between the wild type N2 and the mutant tm5046. The independent t-test demonstrates that there is no significance between the sinusoidal frequency and the addition of ethanol across each strain.

The univariate ANOVA (table 4.6.2) shows that there is a significance between the variables, concentration, and sinusoidal frequency ($P<0.05$) but overall, there is no significance between the strain and sinusoidal frequency ($P>0.05$).

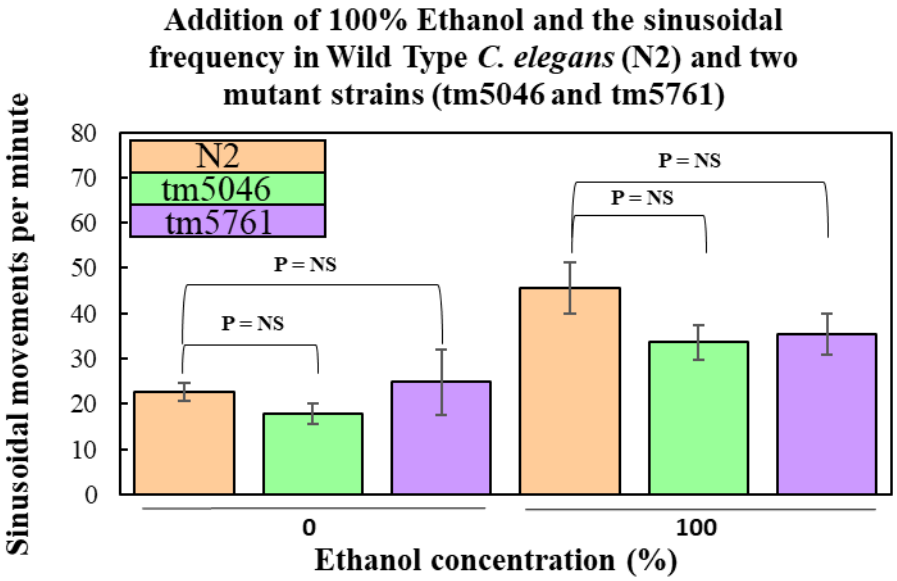

Figure 4.6.2. **Sinusoidal frequency and ethanol exposure** The graph shows the sinusoidal frequency of each (N2, tm5046, tm5761) under standard conditions and with the addition of 100% ethanol. N= 5 at 0% ethanol for each strain, N=15 animals at 100% ethanol for each strain. Error bars represent the standard error of the mean. P= NS – not significant. Independent T-test was conducted in SPSS.

Table 4.6.2. Two-way ANOVA analysis of sinusoidal frequency and the addition of Ethanol. The two-way ANOVA was performed in SPSS, the analysis shows that there is a significant difference between the sinusoidal frequency and the addition of ethanol ($P<0.05$). No post-hoc analysis was needed. Post-hoc LSD test was not significant.

Source	Type III SoS	df	Mean square	F-test	Sig.
Concentration	3042.22	1	3042.22	10.61	0.002
Strain	529.48	2	264.74	0.92	0.403
Concentration / Strain	293.74	2	146.87	0.51	0.602

The final assay using this chemical stimulus, was to measure the number of reversals per minute displayed by each strain and against the addition of ethanol. Figure 4.6.3 suggests there is no significance in reversals between wild type and both the mutant strains when exposed to ethanol.

The biggest increase in reversal frequency is displayed by the mutant tm5761, from a mean frequency of 2.6/min to 5.2/min. The mutant tm5046, showed the smallest increase but overall, this was not significantly different than the wild type or mutant tm5761.

The univariate ANOVA (table 4.6.3) showed that there is no significance between all three strains and the reversal frequency, or between the concentration and reversal frequency ($P>0.05$). The null hypothesis was therefore accepted for this data set. An independent T-test for each strain with the addition of ethanol for each parameter can be found in supplementary data 9 (S9).

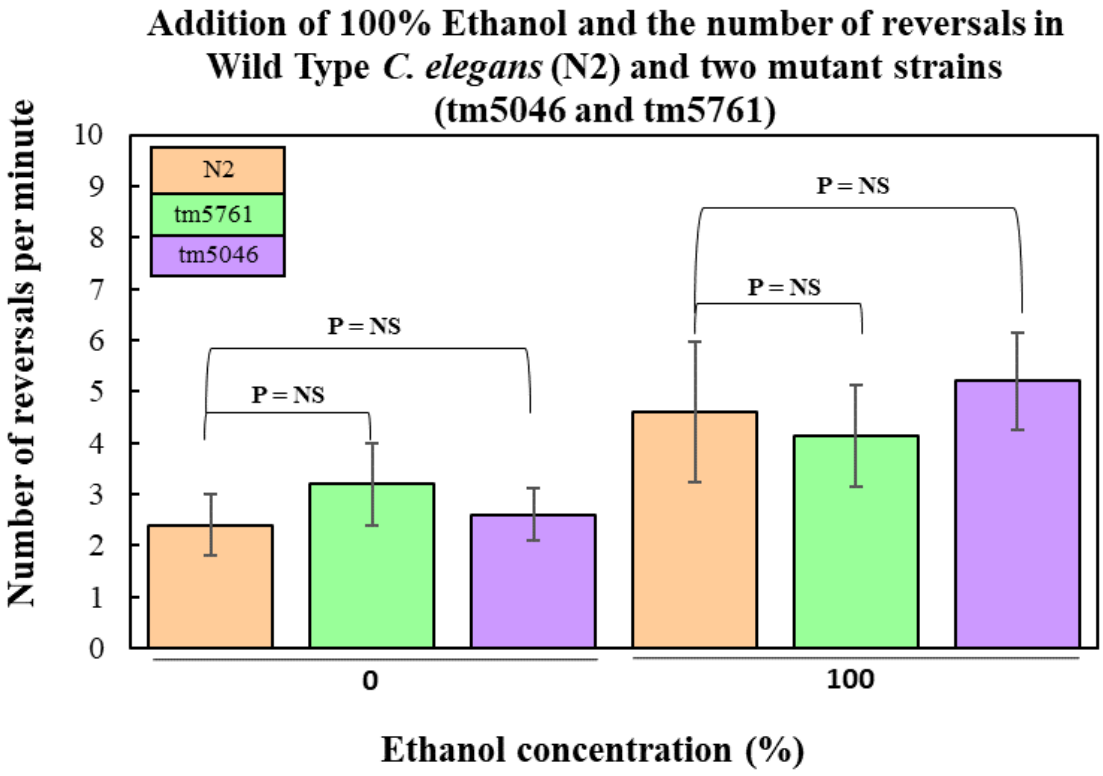

Figure 4.6.3. Reversal frequency and ethanol exposure The graph, produced in Origin and Excel, shows a trend in the number of reversals per minute across all three strains. There is overlap between the standard and with the addition of 100% ethanol. N= 5 at 0% ethanol for each strain, N=15 animals at 100% ethanol for each strain. Error bars represent the standard error of the mean. P= NS – not significant. Independent T-test was conducted in SPSS.

Table 4.6.3. Two-way ANOVA analysis of reversal frequency and the addition of Ethanol. The two-way ANOVA statistical analysis shows that there is no significance between the strain and the reversal frequency and no significance between the addition of ethanol and the reversal frequency. Post-hoc LSD test was not significant.

Source	Type III SoS	df	Mean square	F-test	Sig.
Concentration	41.09	1	41.09	2.72	0.105
Strain	1.21	2	0.61	0.04	0.961
Concentration * Strain	5.68	2	2.84	0.19	0.829

4.7 The effects of temperature on the survival of wild type *C. elegans* and two mutant strains

The final physiological assay was designed to measure the effects of temperature on the survival of *C. elegans*. The first study tested the survival of nematodes exposed to an elevated temperature of 37℃. Under normal conditions, *C. elegans* are grown at 15-18℃ and for these experiments, the temperature was increased to 37℃ (see chapter 2.2.8). Heat stress at 37℃ may cause membrane instability as *C. elegans* have an optimal temperature of around 15-20℃. This however would not be the case for parasitic nematodes as the host temperature is 37℃ and therefore membrane stability of parasites would not be affected.

Figure 4.7.1 shows the bar graph of the survival rate of the three strains over a period of three hours at 37℃. The independent t-test showed that there was a significant difference in survival rate between the wild type N2 and the mutant tm5046 after 2 hours at 37℃ ($P < 0.05$), there was also a significance between these two strains after 3 hours at 37℃ ($P < 0.05$).

Figure 4.7.2 shows that after 24 hours at 5℃, all of the *C. elegans* strains were quite tolerant of the low temperature. The wild type N2 had a survival rate of 80%, and for both the mutant strains, the survival rate was 100%. There is no significant difference in survival rate between the wild type and both mutant strains after 24 hours at 5℃ ($P > 0.05$).

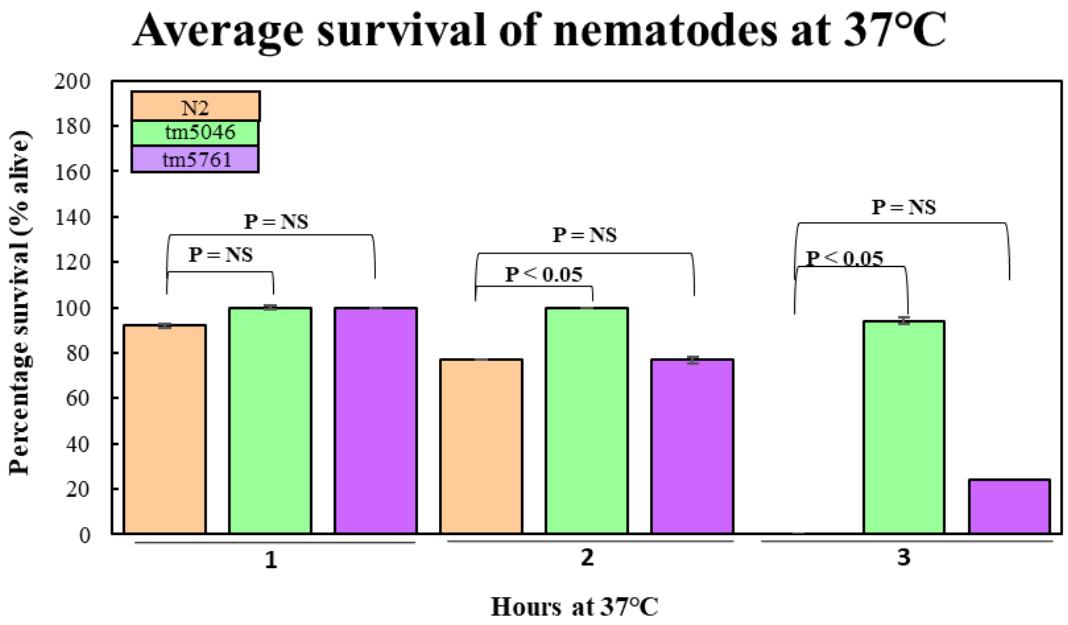

Figure 4.7.1 Survival rates and heat exposure. The graph shows the survival rate of the three strains at 37°C, over a period of three hours. N=10 per strain at each hour, with two replicates each. Overall N= 60 animals per strain. Error bars represent the standard deviation (SD). P= NS – not significant.

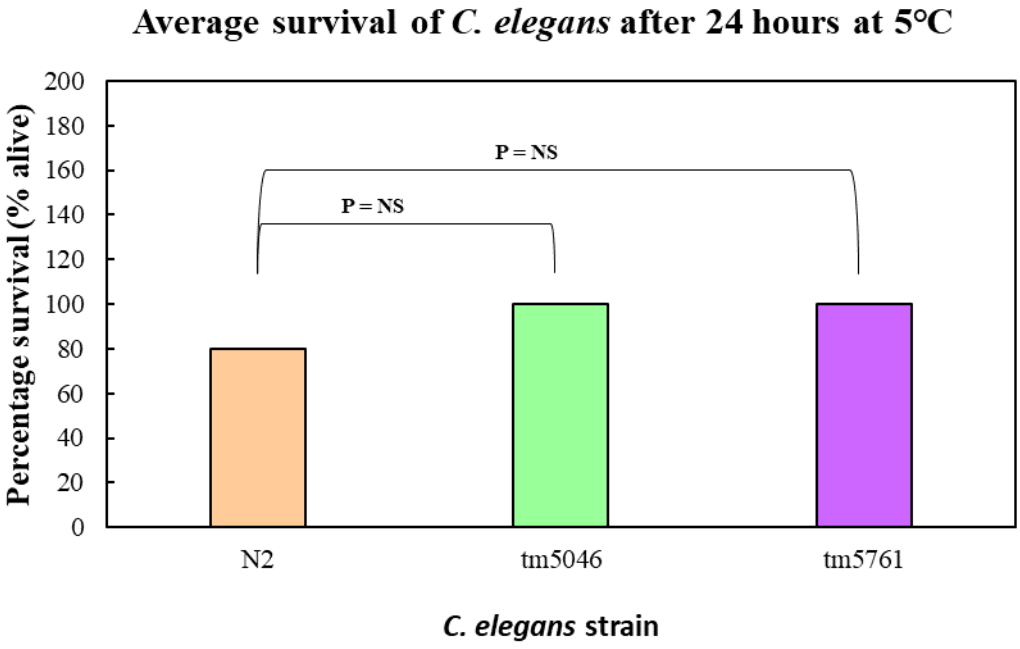

Figure 4.7.2. Survival rates and cold exposure The graph shows the survival rate of the three strains of *C. elegans* at 24 hours at 5°C. N=10 per with two replicates each. Overall N= 20 animals per strain. P= NS – not significant.

4.8 Discussion

The locomotion of *C elegans* is a good observable behavioural response to stress stimuli (Croll., 1974). The reversals of nematodes can be induced in response to stress stimuli avoidance. The *C. elegans* use the omega turn (coiling) as a stress response mechanism when avoiding harm or searching for food (Broekmans *et al.*, 2016).

In this study, animals were placed on seeded plates. Although the presence of food may cause a bias, in this study it was deemed necessary. No concentration gradient was used to measure locomotion, instead the agar was covered with a specific concentration of a compound, the animals would not be able to avoid the chemical stimuli, low concentrations of compounds that are not fatal to *C. elegans* were used. Therefore, if the food source was removed and the animals could survive the concentration of solution on agar they may show more of a stress response in search for food and thus the response behaviour may not be due to chemotaxis.

In general, the overall life expectancy of the mutant strains was greater than that of the wild type, evidenced in the Kaplan Meier curves. This is particularly true for the early stage of life cycle development. At the later adult stages, the mean survival was not significant. The null hypothesis stated in section 4.1, is rejected. There is a significant difference between the life span of the mutant strains compared to the

wild type (N2). Stress can be an inducer of autophagy, CD63 is vital for regulating endosomal activity and autophagy (Hurwitz *et al*., 2018). *C. elegans* upregulates autophagy under stress as a survival mechanism (Chen *et al*., 2017), however autophagy has been shown to promote cell death (Das *et al*., 2012). The mutant strain

tm5761 with a 69 amino acid deletion, may express a non-functioning tsp-7 protein. This could suggest unregulated autophagy leading to cell death and could explain why this mutant strain was less resistant to the various types of stress. On the other hand, autophagy is crucial for longer life span within *C. elegans*, both mutant strains did have a longer life span than the wild type (N2). Perhaps autophagy was elevated with the mutant strains, thus the longer life span, but much more exaggerated in mutant tm5761. Further studies into survival and stress assays with regards to tsp-7 and autophagy are required to understand the potential mechanism.

In humans, CD63 is present on the membranes of intraluminal vesicles (ILV's), these ILV's are then exported to the plasma membrane and released as exosomes (see figure 1.3.1.2). ILV's with no CD63 biomarker are usually signalled for degradation, usually via autophagy. It is thought that CD63, plays an important role in shuttling between the endosomal pathway or autophagic pathway (Hurwitz *et al.*, 2018). CD63 is a known interactor of mTORC1, an inhibitor of autophagy (Deleyto-Seldas & Efeyan., 2021). CD63 negatively regulates mTORC1, the more CD63 expressed the more mTORC1 is active, decreasing autophagy (Chang., 2020). Studies with knockout CD63 mice showed a decrease in mTORC1 on EV's and increased levels of LC3-II, leading to an increase in basal levels of autophagy which is associated with increased longevity and life span (Hurwitz *et al.*, 2018). Therefore, this may also be part of the explanation for *C. elegans*, tsp-7 knockout nematodes having an increased life span (Bubier *et al*., 2019). Wild type (N2) *C. elegans* tsp-7 protein may negatively regulate mTORC1-like proteins, shuttling between EV release and autophagy. Mutant tm5761, with the largest amino acid deletion had increased longevity (22 -25 days). When the mutant was exposed to various stress

stimuli, this further increased basal levels of autophagy. With no functioning tsp-7 proteins, autophagy becomes uncontrollable. Extreme autophagy leads to vacuoles within the cells due to complete depletion of nutrients, this eventually leads to cell death. This could explain the low tolerance of mutant tm5761 when exposed to stress, compared to the wild type or the mutant tm5046. To test this theory, it would be beneficial to identify the normal expression levels of tsp-7 at the different life cycle stages. It would also be interesting to compare the exosome protein makers released from both the wild type and the mutants strains. Another experiment to test autophagy levels in cells is an immunoblot analysis of LC3-I to LC3-II conversion. LC3-II correlates with the number of phagosomes formed and therefore activated autophagy. Another more accurate experiment would be assessing puncta formation using confocal microscopy in which LC3 is tagged with florescent protein such as GFP (Yamamoto-Imoto *et al*., 2022 and Singh & Bhaskar., 2019). Figure 4.8.1a shows theoretical tsp-7 mTORC1 interaction in wild type under and Figure 4.8.1b shows increased autophagy in mutant *C. elegans.*

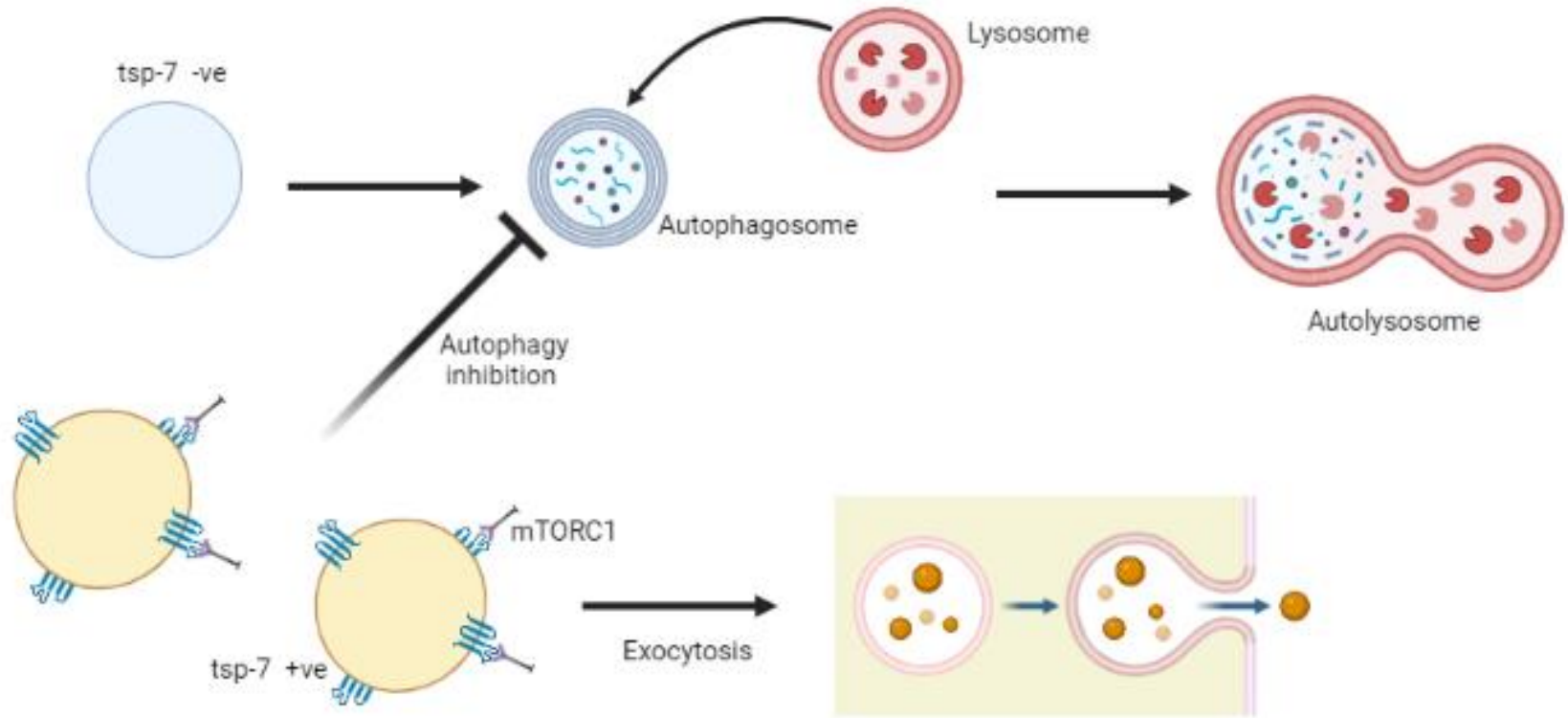

Figure 4.8.1a. Potential autophagy mechanism involving tsp-7 in wild type *C .elegans*. Under normal conditions, the shuttling between exocytosis may be regulated by tsp-7. The vesicles tagged with tsp-7 bind to and activate mTORC1. This inhibits the vesicles containing tsp-7 from being degraded through autophagy and are instead released as exosomes or other extracellular vesicles. Images created with BioRender.com.

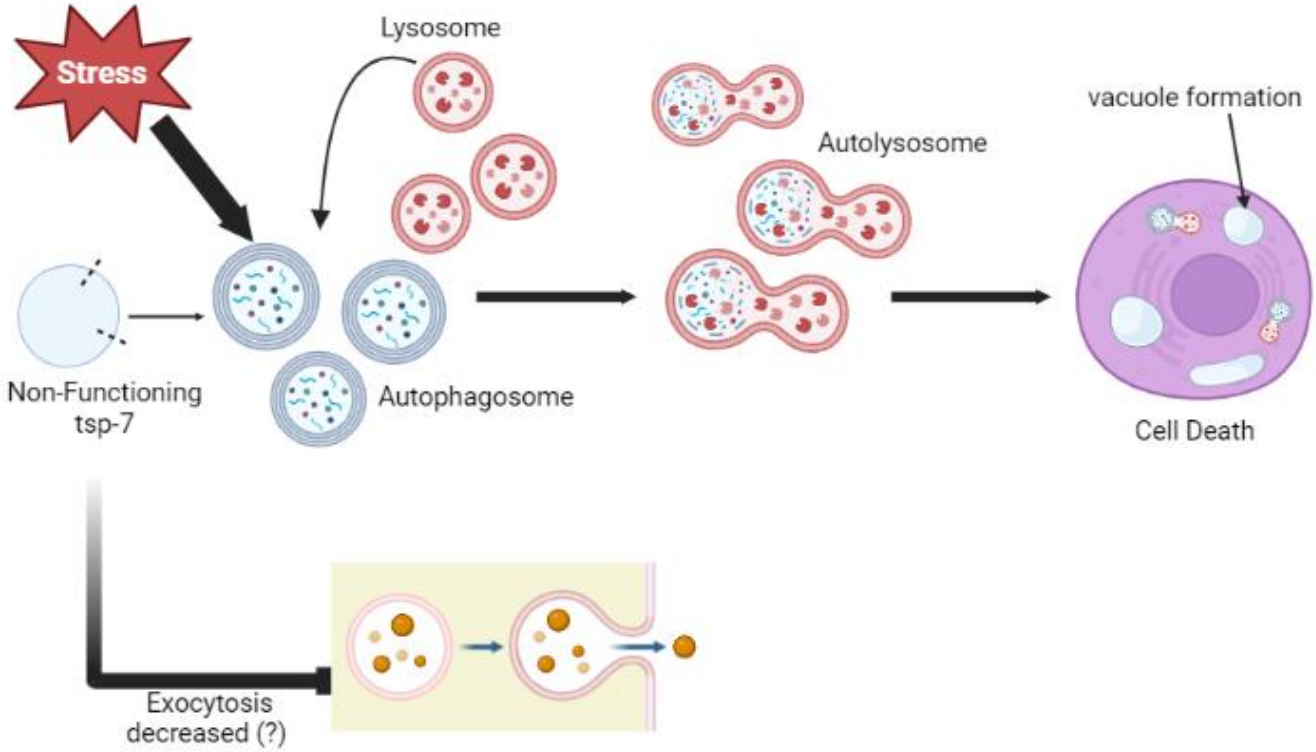

Figure 4.8.1b. A possible theoretical mechanism for increased autophagy in mutant *C. elegans*. Stress response and longevity observed in mutant *C. elegans*. Non-functioning tsp-7 may not regulate the shuttling of vesicles, leading to a decrease in m TORC1. This drives an increase in autophagy, contributing to longer life span. However, the addition of stress further drives autophagy with no inhibition. The autophagic pathway becomes out of control leading to large vacuoles and depletion of cellular contents eventually causing cell death. Exocytosis may be decreased which would be observable through exosome quantification. Images created with BioRender.com.

The chemotaxis assays show that either the strain, or concentration or both, can have a significant effect on the stress response behaviour displayed by the *C. elegans*. In the sodium chloride / osmotic stress assays, there was a significant difference between the wild type and mutant tm5761 in terms of coiling and reversal frequencies. In the zinc (Zn^{2+}) assay, the concentration has a statistically significant effect on the sinusoidal frequency and the reversal frequency between wild type N2 and mutant tm5761. But there is no statistical significance on the coiling response.

In the 4-Octylphenol assay the addition of the compound seemed to have a significant difference between wild type N2 and mutant tm5761 with respect to sinusoidal frequency. There was no significant difference between the wild type and mutant tm5046 across any of the observable stress responses. Finally, for the ethanol assay, the addition of absolute ethanol had no significance between any of the strains and the stress response. The fact that the stress movement responses to organic compounds are similar between the Wild type and the tsp-7 mutant strains of *c. elegans,* probably indicates that either tsp-7 does not play a significant in the response that would normally be elicited, or that the stress responses that is caused by exposure to high levels of these organic chemicals does not cause a change in these movement- based stress parameters. It would be of interest to see if other physiological responses such as growth rates and life span might be affected by long term exposure to organic chemicals and also whether tsp-7 might play a role.

The temperature-based assays did show a significant difference between wild type N2 and mutant tm5046. But it was not significant between N2 and tm5761. Under the conditions used in these undertaken here, heat exposure at 37°C proved completely fatal to the wild type N2 worms after exposure for 3 hours and to an

almost similar level with the tm5761 strain. Heat had less of an effect on the mutant tm5046. The cold assay was not significant for any of the strains. Both mutant strains had a survival rate of 100%, the survival rate of N2 was around 80%. Heat stress causing membrane stability affect conformation of membrane proteins, perhaps the heat stress causes severe conformational change in the fully functioning tsp-7 protein in wild type *C. elegans* thus leading to high mortality rates. The mutant strains may be non-functioning or expressed at low levels and therefore any conformational change to these proteins is negligible in terms of heat stress and protein function. It remains unclear as to why a small deletion mutation (i.e., 4 amino acids) in tsp-7 of the tm5046 *C. elegans* strain should confer resistance to death by higher-than-normal temperatures, although again autophagy is known to be affected by high temperatures (Kumsta *et al*., 2017). Therefore, more experiments to explore this interesting observation would need to be undertaken.

Sodium Chloride appeared to have the most effect in terms of stress response, Zn^{2+} did not. Zinc heptahydrate is a heavy metal compound, in excess can cause acute toxicity, when used in feeds for additional nutrition, animals can become nauseous, and develop gastrointestinal and abdominal pian (Zeng *et al.*, 2018). This is not the case for nematodes, however, the assay only focused on the observable movements of the nematodes. These movements were recorded by one observer, manually. The effect that the zinc ion has on the neurotransmitters and the biochemistry is unknown and was not assessed. This would be a further study to continue the chemical stimuli on stress. It is also unclear if Zn^{2+} had any effect on growth rate, or egg laying rate as this was not measured.

4-Octylphenol is normally used in the production of detergents and industrial cleansers. The phenols are lethal at certain doses and studies have shown in detail the effects of phenols on *C. elegans* and various strains (De la Parra-Guerra & Olivero-Verbel., 2020). The concentration of the phenol in this study was still fatal for the nematodes. In which case the movements would be severely limited. An observation of this assay was that at the 5mM concentration, a portion of the worms were dying during the recording. The study must be conducted with a series of lower concentrations of 4-Octylphenol to present a more accurate description of this compound on the stress responses of *C. elegans* and the two mutant strains used. Any future experiments would explore this further.

In the ethanol assay, the alcohol, appeared to have very little effect on the nematodes, although studies suggest that over time, *C. elegans* can become tolerant of very high concentrations of ethanol (Lee *et al.*, 2009).

Overall, this study begins to look at the potential effect of certain compounds and physical conditions on the locomotive stress response of the *C. elegans*. A more definitive study would investigate in greater detail, the effects on the growth rate, egg laying rate, and a variety of biochemistry and genetic effects. Preferably, the strains should all be synchronised to allow assessment of same-aged worms, in this study that was not possible, this could have impacted the observational measurements as nematodes nearing end of life generally move less or at a decreased rate than the more juvenile nematodes (Newell-Stamper *et al*., 2018). While there are improvements needed for this study, the findings can provide preliminary data to further analyse the stress response of the wild type and the mutant strains. The physiological and biochemical stress responses can be measured with greater

accuracy, and for a more robust set or parameters and concentration gradients. This would allow a better understanding of the implication of stress response and the role tsp-7 could have in the stress response mechanisms. Tm5046 was more resistant and tolerant of the various stress stimuli, this mutant strain also had a longer life span than the wild type and the mutant tm5761. The mutant tm5761 was the least tolerant across all assays and tsp-7 could not be detected by western blot using the custom-made antibody (see chapter 5.4). This mutant strain has a deletion of 69 amino acids, deleting a large portion of the structure, possibly leading to little or no expression. The connection between tsp-7 and stress response mechanism has not yet been determined in the literature and this study begins to determine, if any, what role the tsp-7 tetraspanin protein could have.

Chapter 5 Immunochemical and Expression studies of tsp-7 from *C. elegans*

5.1 Introduction

Tsp-7 is a homologue of the human tetraspanin protein CD63. These integral transmembrane proteins are found within the membrane of most endothelial cells (Kummer *et al*., 2020). The large extracellular loop containing the protein domain, interacts with molecules such as tissue inhibitor metalloproteinases and other tetraspanin proteins, forming a highly complex tetraspanin network (Müller *et al.,* 2022). Within humans, CD63 is involved with cell adhesion, protein trafficking, migration, and suppressor function. CD63 binds to TIMP-1, a metalloproteinase inhibitor (Jung *et al.,* 2006). The TIMP-1/CD63 complex promotes a cytokine like function, inducing inflammatory responses (Kobuch *et al*., 2015). Neutrophil extracellular trap formation (NETs), which are saturated with bioactive molecules that drive the inflammation, was dependent on TIMP-1 binding to its CD63 receptor (Schoeps *et al*., 2021).

TIMP-1 is a natural inhibitor of matrix metalloproteinases (MMP's), these proteins are responsible for extracellular matrix turnover (Justo & Jasiulionis., 2021). TIMP-1 is expressed by various cells and tissues (Egea *et al.,* 2012) and induced by cytokines and growth factors such as, IL-6 and IL-1 (Justo & Jasiulionis., 2021 and Reis., 2013). TIMP-1 also inhibits a Disintegrin and metalloproteinases (ADAM's),

evidence has shown that tetraspanin proteins associate with ADAM's (Müller *et al.*, 2022), forming a network of tetraspanins, MMP's and ADAM's. This network is responsible for various cell functions, such as growth, migration, apoptosis, and protein trafficking (Edwards *et al.*, 2008). There are four native TIMP molecules in humans, there are also TIMP molecules expressed *in C. elegans* (Costa *et al.*, 2022) and parasitic helminths of humans, such as nematodes and trematodes (Cantacessi *et al.*, 2013).

The aims of the expression studies are:

1. To bind the polyclonal anti-tsp-7 antibody produced by Thermo- Fisher, to tsp-7 extracted from three *C. elegans* strains: Wild-type N2 (Bristol strain), mutant 5046 and mutant 5761 (National BioResource project, Japan). This would be achieved by immunoassays such as western blotting and ELISA's. The purpose of this study is to determine if an antibody can be produced for a tetraspanin protein within a nematode species. Tetraspanin proteins are notoriously challenging for antibody production (Noy *et al.*, 2019), to date there is no antibody commercially available for tsp-7 in *C. elegans.*

2. To express the tsp-7 domain from within the large extracellular loop, in a pET21a vector. Specific primers will be designed to the large extracellular loop domain only and will have a His-tag at the C-terminal end. This will be inserted into a pET21a vector for high level expression in *E. coli*. The successful expression of the domain would allow for specific binding and pulldown assays in the future.

3. Assess potential binding capacity based on theoretical bioinformatic studies (see chapter 3.9), between tsp-7 derived from *C. elegans* and human TIMP-1 using fluorescence labelling and fluorescence microscopy. Such an interaction of human TIMP molecules reacting with nematode tetraspanins would provide some evidence to support the theory that parasitic tetraspanins cross-talk with host molecules to influence the immune system and establish chronic infection (Coakley *et al.*, 2016).

5.2 Sample preparation of tsp-7 from *C. elegans* for immunochemical studies

The wild type N2 Bristol strain *C. elegans* were used in a preliminary experiment to identify the most efficient means of tissue lysis via mechanical and chemical methods. Four pellets (see chapter 2.3.1) were thawed on ice and subject to either sonication and RIPA or sonication and Triton buffer or heat and RIPA or heat and Triton buffer. RIPA buffer (Sigma Aldrich) consists of 50 mM NaCl, 1.0% IGEPAL® CA-630, 0.5% sodium deoxycholate, 0.1% SDS, 50 mM Tris, pH 8.0. Triton buffer contains: 50mM Tris, 150mM NaCl, 1% Triton, 1X protease and phosphatase inhibitor mini tablet (Pierce, Thermo- Fisher). The pellet was suspended in either RIPA or Triton buffer and placed in a heat block at 95℃ for 10 minutes, or sonication (see chapter 2.3.2). The results from these comparisons are listed below (Table 5.2.1). Addition of Triton to either heat or sonication had no significant difference in yield (0 -2.4mg/ml with heat and 0 -2.5mg/ml with sonication).

Sonication and the addition of RIPA buffer yielded a slightly higher protein concentration of up to 3.6mg/ml.

To assess the success of lysis after sonication, the nematodes were viewed under a microscope to look for potential "ghosting" of the outer-cuticle (Figure 5.2.1). Ghosting is when the cuticle becomes transparent, suggesting that the nematode contents have been forcefully expelled into the surrounding solution. RIPA buffer was then substituted for another lysis buffer, known to yield high concentrations of membrane protein. This buffer was composed of 5mM HEPES, 0.32M sucrose, ½ protease and phosphatase inhibitor tablet (see chapter 2.3.2). This membrane lysis buffer was then used throughout the project in replace of both the RIPA and Triton buffer. Concentrations varied between the three different strains: Wild type N2, mutant 5046 and mutant 5761 (Table 5.2.2). In general, the pellets contained higher protein concentrations than the supernatant as was expected. Supernatants were retained, which were believed to contain intact and disrupted internal cells and cellular contents of *C. elegans* and used for further biochemical and immunological assays.

Table 5.2.1 Mechanical and chemical lysis had varying levels of success on concentration yield. The addition of triton as a detergent for membrane proteins was less effective than RIPA. Sonication also proved to yield the greater concentration of protein from wild type N2 *C. elegans* strain. Sonication and RIPA was the most successful combination.

Whole Lysate Concentration Estimations		
Mechanical Lysis	Chemical Lysis	Concentration Yield
Heat	RIPA	2.2 - 2.4 mg/ml
Heat	Triton	0 - 2.5 mg/ml
Sonication	RIPA	3.0 - 3.6 mg/ml
Sonication	Triton	0 - 2.4 mg/ml

Figure 5.2.1. Successful mechanical lysis of *C. elegans* shows "ghosting" of the cuticle. Sonication at 4 Watts fragments the nematode cuticle of *C. elegans* (red arrow). The black arrow shows the complete ghosting of a nematode, with a transparent cuticle, and the contents

Table 5.2.2. Protein concentrations between the pellet and supernatant for all three nematode strains; N2 (wild type Bristol strain), mutant 5046, mutant 5761. Sonication and membrane lysis buffer was used to extract membrane protein from the nematodes. Overall, the protein concentration within the pellets is greater than the concentration within the supernatant for all three strains.

Whole Lysate Concentration Estimations		
Strain	Sample	Concentration Yield
N2	Pellet	7.8 - 25.4 mg/ml
N2	Supernatant	3.1 - 6.6 mg/ml
TM5046	Pellet	6.6 - 18.3 mg/ml
TM5046	Supernatant	6.3 - 6.7 mg/mg
TM5761	Pellet	7.4 - 14.3 mg/ml
TM5761	Supernatant	4.8 - 10.4 mg/ml

5.3 Antibody concentration detection using ELISA's

Antibodies to tetraspanin proteins have been notably difficult to raise and use in earlier studies (Noy *et al.*, 2019). In this study, a bioinformatics approach was employed to try to design antibodies to *C. elegans* tsp-7, which targeted the predicted extracellular domain, with the best probability of being highly immunogenic.

The antibody obtained from Thermo- Fisher Scientific, was provided at two different concentrations from the two rabbits, rabbit 1 (AB-54, 0.4mg/ml) and rabbit 2 (AB-55, 0.74mg/ml), used to raise antibodies against the peptide sequence within the extracellular domain (see chapter 2.3.4). Figure 5.3.1 below, shows theoretically, where the antibody would recognise the peptide on the protein structure as well as the amino acid sequence of the peptide (EGCARENAPLFEPGCIHSVEQWVLK).

Direct ELISA assays were performed to determine the level of cross reactivity between the antigenic peptide used and the anti tsp-7 peptide antibody present in the purified serum samples obtained from Thermo- Fisher.

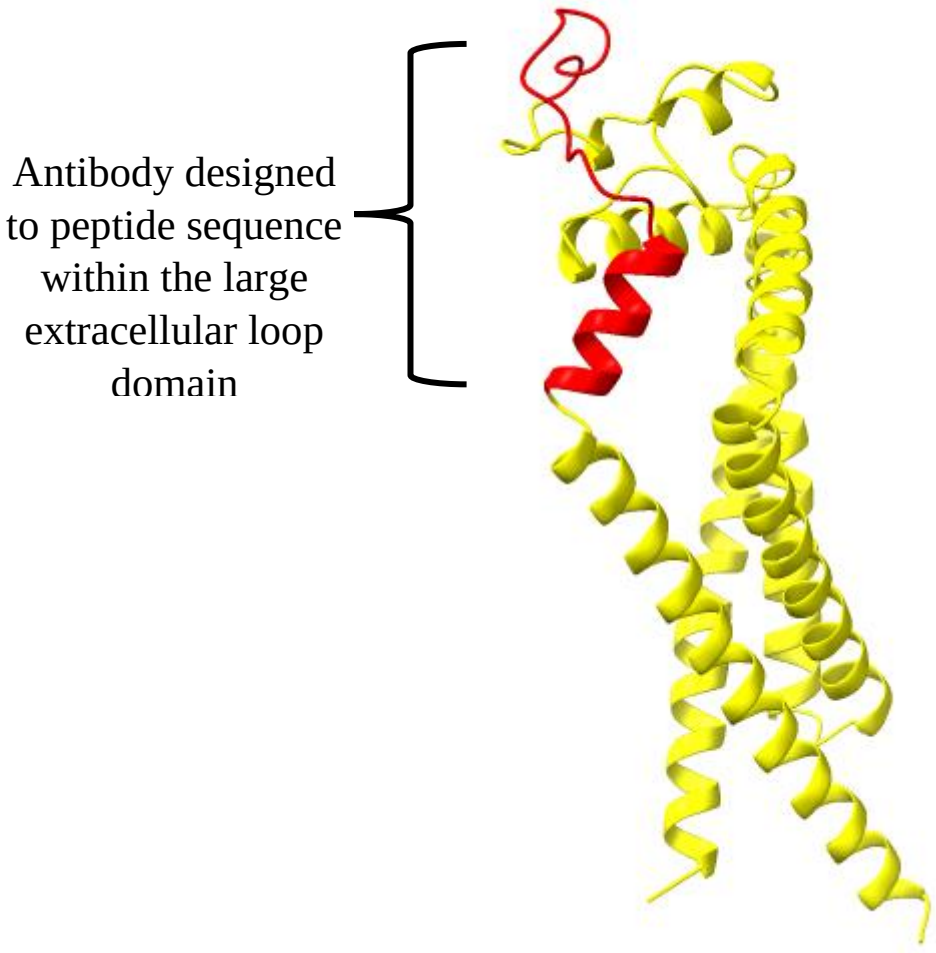

Figure 5.3.1. Anti-tsp-7 antibody designed against the LEL epitope. Antibody raised against the peptide located in the large extracellular loop domain (shown in red) of the tsp-7 protein. Protein model downloaded from the AlphaFold database and edited in Chimera X. Peptide sequence: EGCARENAPLFEPGCIHSVEQWVLK,

Direct ELISA assays were performed to determine the level of cross reactivity between the antigenic peptide used and the anti-tsp-7 peptide antibody present in the purified samples obtained from Thermo- Fisher. The standard curves for the antibody against the peptide are shown in Figure 5.3.2. Both antibodies were compared using the peptide at the same concentration in each of the wells with a 100µl final volume in each well (10µg/ml per well). The antibodies showed similar absorbance levels and followed similar trends.

Two separate ELISA's were set up to determine the optical density readings of the different concentrations of antibody against various concentrations of peptide. A checkboard titration ELISA was used to assess two variables at once and in this study it was used to test antibody concentration against peptide antigen concentration. This type of ELISA allows for optimisation, it also enables the concentration of tsp-7 from all three *C. elegans* strains to be determined. Two checkboard titrations were designed for both the 0.74mg/ml and 0.4mg/ml antibodies (Figure 5.3.3 and 5.3.4). The antibody could detect the peptide at concentrations as low as 0.3ng/ml albeit with an extremely low absorbance. Overall, the higher concentrated antibody (0.74mg/ml) performed better at binding across a dilution of peptide concentrations as the absorbance readings were higher. For rabbit 1 (AB-54), there is a significant difference for the peptide diluted to 1:10 (1µg/ml) against the anti tsp-7 antibody at a concentration of 1330ng/ml.

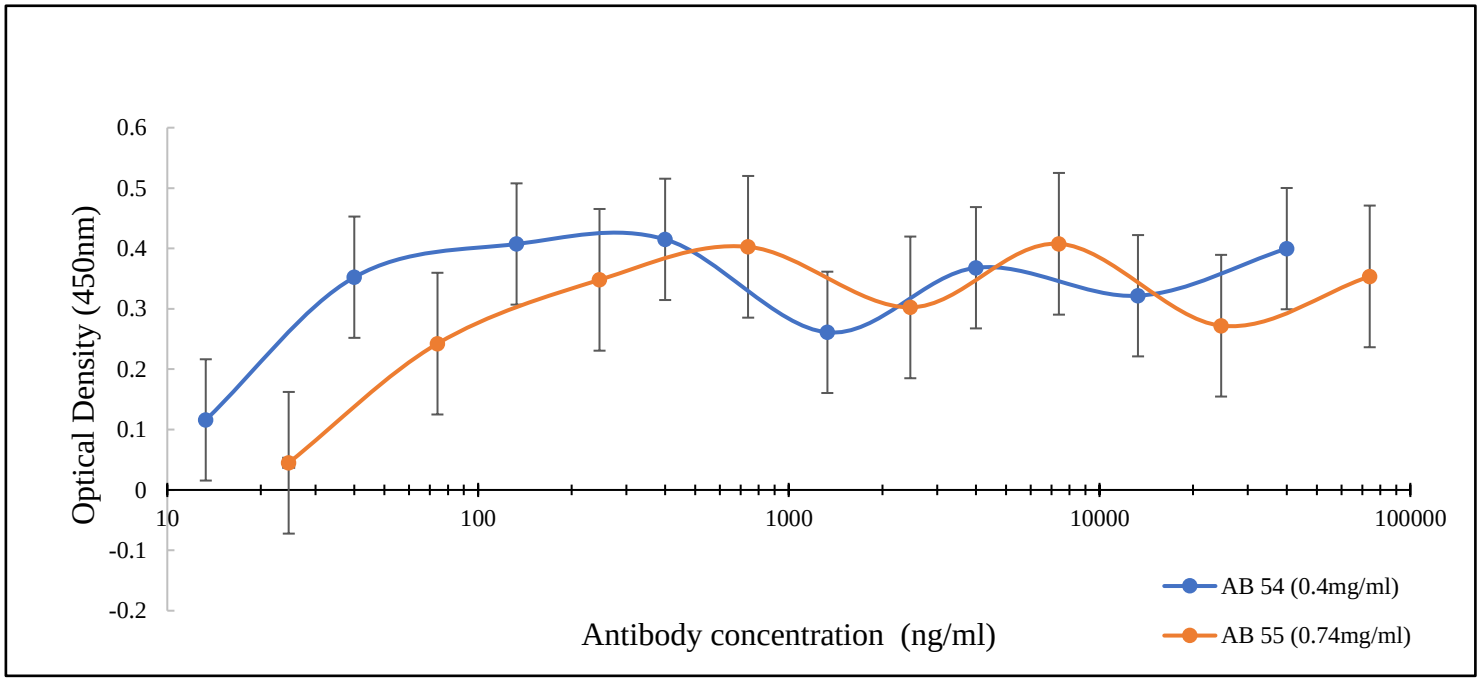

Figure 5.3.2. Standard ELISA curves for both concentrations of primary anti tsp-7 antibody from two different rabbits against the synthetic tsp-7 peptide. Peptide concentration remained consistent (10µg/ml) and was designed synthetically and provided by Thermo Fisher Scientific. The blue curve represents data from rabbit 1 (AB -54) with a concentration of 0.4mg/ml and the orange curve represents rabbit 2 (AB-55) the more concentrated antibody, 0.74mg/ml. Error bars represent the standard deviation (SD). N=3.

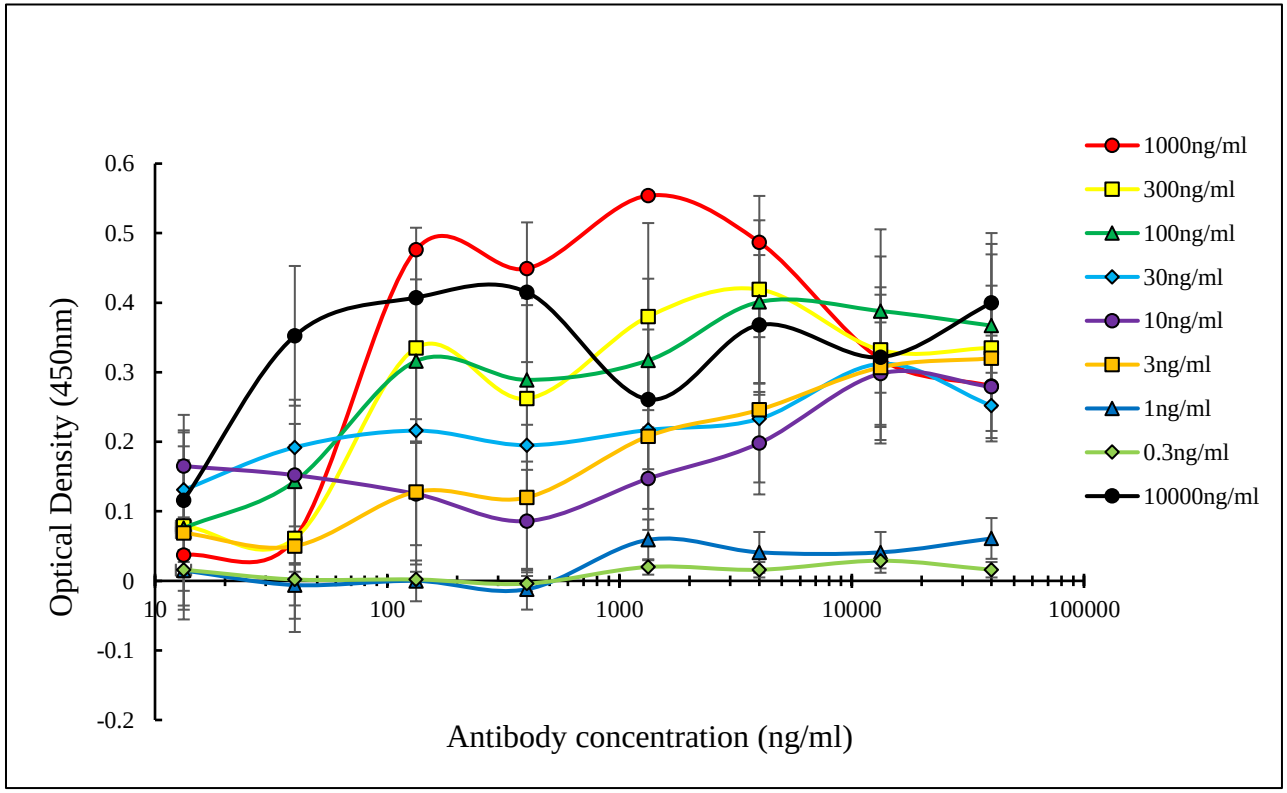

Figure 5.3.3. ELISA checkboard titration for rabbit 1 (Ab 54) provided at a concentration of 0.4mg/ml against various tsp-7 antigen peptide concentrations. Antibody was diluted from 1:10 to 1:30 000. Each line on the graph represents the peptide a different concentrations. The starting concentration of the peptide antigen is 10µg/ml, this was then also diluted 1:10 to 1:30000. Error bars are shown as standard deviations (SD). N=3.

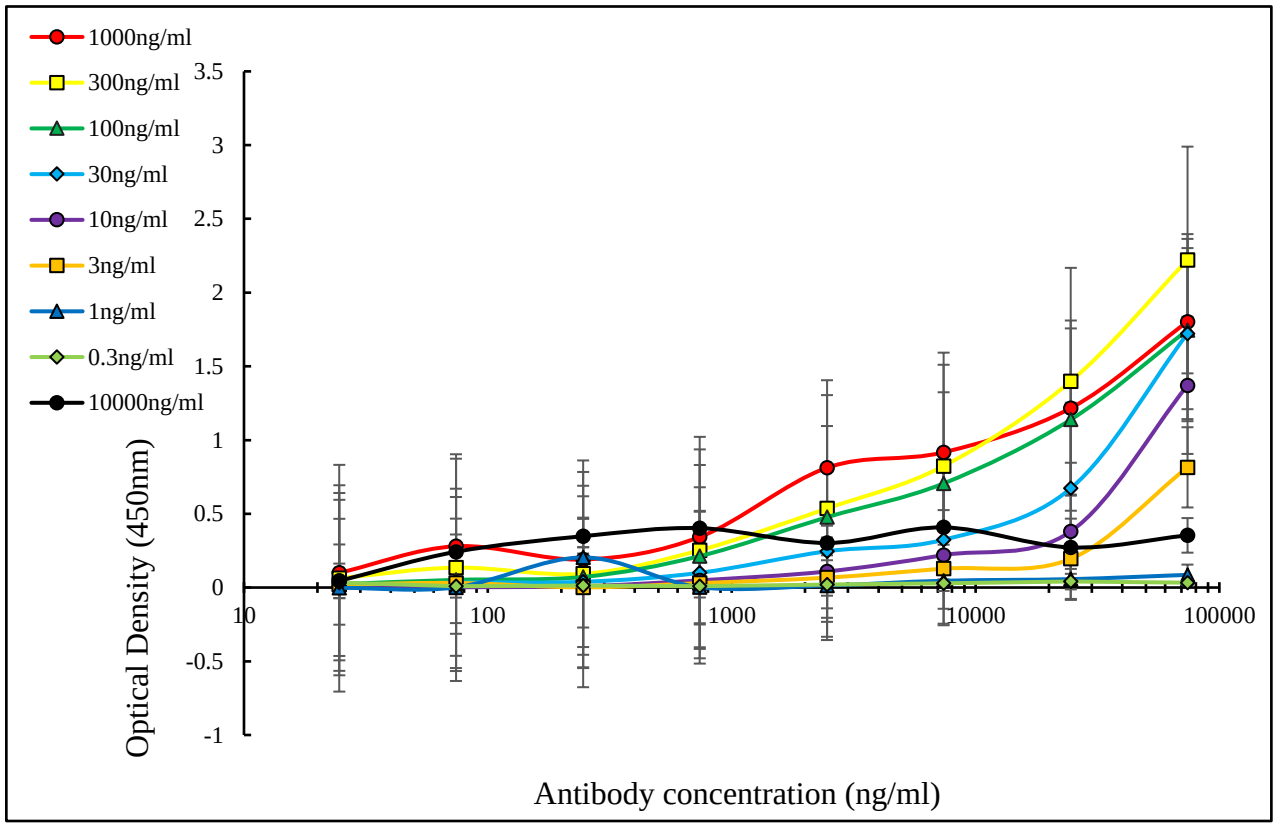

Figure 5.3.4. ELISA checkboard titration for rabbit 2 (Ab 55) provided at a concentration of 0.74mg/ml against various tsp-7 antigen peptide concentrations. The Antibody was diluted from 1:10 to 1:30 000. Each line on the graph represents the peptide a different concentrations. The starting concentration of the peptide antigen is 10µg/ml, this was then also diluted 1:10 to 1:30 000. Error bars are shown as standard deviations (SD). N=3.

Rabbit 2 (Ab 55) at a concentration of 740ng/ml (1:1000) was used throughout the project for the immunochemical studies. This was the dilution recommended by Thermo- Fisher. Using the trends from both antibodies at 1:1000 against the various peptide antigen concentrations, a calibration curve was used to determine the concentration of tsp-7 from lysate samples from all three strains of *C. elegans* (Figure 5.3.5), although the confidence in these values is low, the curves provide a rough estimate of tsp-7 concentration. The lysates have concentrations between 40-325ng/ml, based off the standard curves produced for both antibodies and peptide dilutions. All of the lysates have tsp-7 in relatively low abundance but sufficient to be detected. There is no difference is concentration between the tsp-7 in pellets from both TM5046 and TM5761 mutant strains. Wild type N2 pellet contained a higher tsp-7 concentration than the mutant strains. Overall, the supernatant from the mutant 5046 had the highest concentration of tsp-7 protein within the sample.

At this concentration (1:1000), the anti tsp-7 antibody from rabbit 2 (Ab 55) with concentration of 0.74mg/ml is better at detecting tsp-7 from the three strains of *C. elegans.*

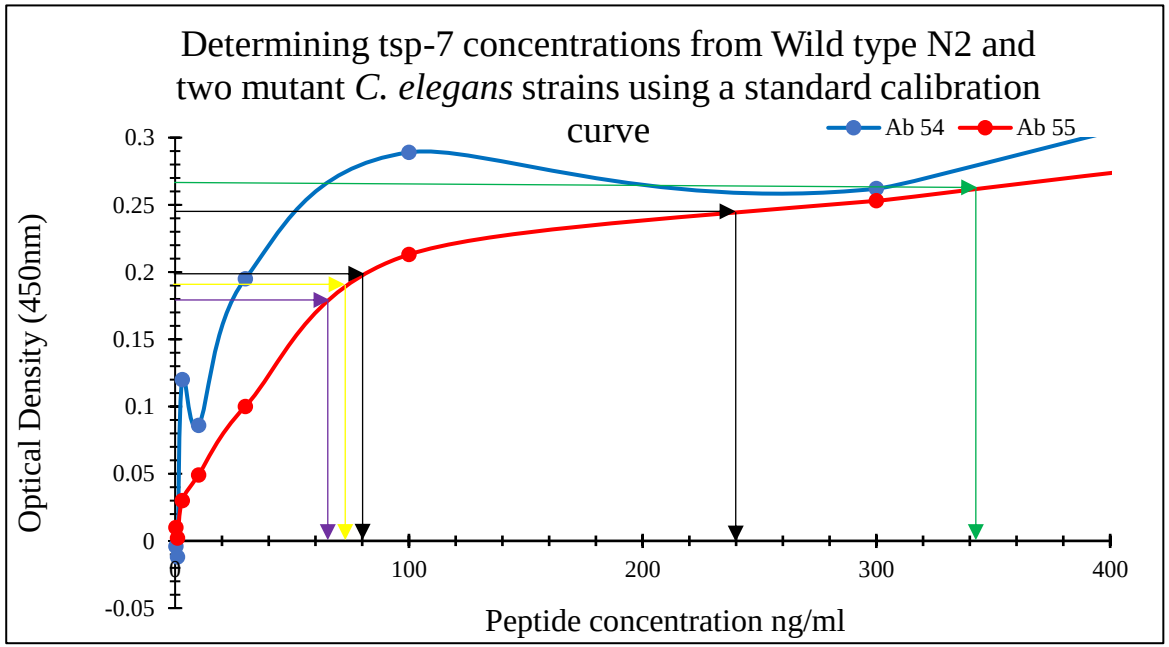

Figure 5.3.5. The two-anti tsp-7 antibodies from both rabbits were used as a calibration curve against the different concentrations of peptide antigen. From the curves, the concentration of tsp-7 from the wild type N2 and two mutant *C. elegans* strains can be determined. The antibody from rabbit 2 (Ab 55) was used against the tsp-7 protein from all of the strains. The wild type strain had a higher concentration of tsp-7 in the pellet (black lines) than the two mutant strains (purple arrow). N2 pellet = ~90ng/ml, TM5046 + TM5761 pellet = ~62-65ng/ml. The mutant strain TM5046 contained the highest concentration overall from the supernatant lysate sample, TM5046 supernatant = ~342-344ng/ml (green line). Wild type N2 supernatant = ~240ng/ml. Mutant TM5761 supernatant = ~72-75ng/ml (yellow arrow). Concentrations are rough estimates.

5.4 tsp-7 protein detection using western blotting and dot blots

Immunochemical staining using the antibodies to determine their usefulness in detecting Tsp-7 form a range of biological samples was then undertaken. A dot protocol was optimised in which 2µl of undiluted primary anti tsp-7 antibody from rabbit 2 (Ab 55, 0.74mg/ml) was placed onto the samples from all three strains, bound to a nitrocellulose membrane. Various concentrations of primary anti-tsp-7 antibody were used for the dot blots but did not yield any results (see chapter 2.3.6.) Figure 5.4.1 shows the lysates from all three strains of *C. elegans*. The dots for each strain (different lanes) are replicates, using the same lysate sample. The blots are clearly visible for the wild type N2 strain; possible faint blots can be seen for the mutant strain tm5046, although this is debatable. It is very difficult to see any blots for the mutant tm5761, although there is potentially some very weak binding of the anti tsp-7 antibody (0.7mg/ml) to native tsp-7 from this mutant strain. It is unclear from the dot blots for tm5761 if there is a weak signal or if the dots are artefacts. It is likely, that the antibody could not detect the tsp-7 proteins in either mutant strain. But this would need to be confirmed with more dot blot studies. Total protein normalisation was attempted used using Page-blue staining, the stained SDS gel can be found in supplementary data S10.

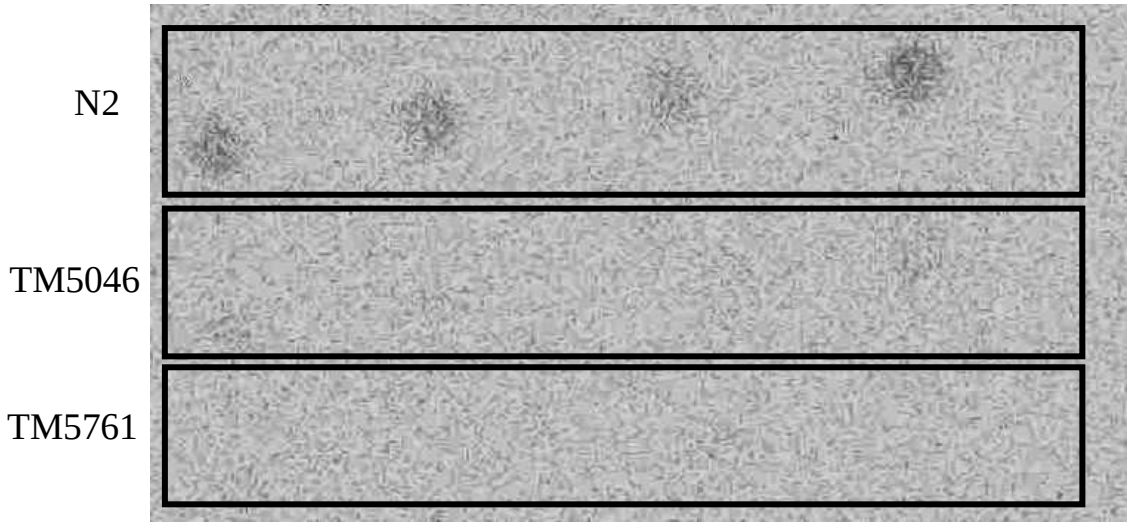

Figure 5.4.1. The dot blots for all three strains of *C. elegans*; Wild type N2, mutant TM5046 and mutant TM5761. For each strain, four samples were taken from a single pellet lysate. For N2, the samples are from the pellet, and for both mutant strains the samples are from the supernatant, as these contained the highest total protein concentration. (N=8).

The western blot below (Figure 5.4.2) shows a band at the correct size for the tsp-7 (~27kDa) protein from the N2 wild type lysate (N=1). The Rf value was calculated for the tsp-7 protein band using a standard curve (Figure 5.4.3) and the molecular weight of the tsp-7 protein band was estimated to be 27.45kDa. The mutant lysate TM5046 could only be detected slightly by western blotting but was not clear enough to be definitive. The mutant 5761 could not be detected after multiple attempts. The anti tsp-7 antibody was used at a concentration of 1:1000 (rabbit 2, Ab 55-0.74mg/ml), however the band for the wild type N2 could only be detected when the antibody was used at a concentration as high as 1:100. This concentration was also used for the mutant lysates.

The mutant TM5046 has a partial deletion of four amino acids, expressed at the beginning of the large extracellular loop domain (see Figure 2.1). The mutant TM5761 has a deletion of 69 amino acids, this results in a loss of part of the small extracellular loop, both membrane helices TM2 and TM3 as well as part of the large extracellular domain. A large portion of the tsp-7 protein would not be expressed in this mutant strain. This could possibly affect the epitopes for the antigenic sequence in which the antibody was raised.

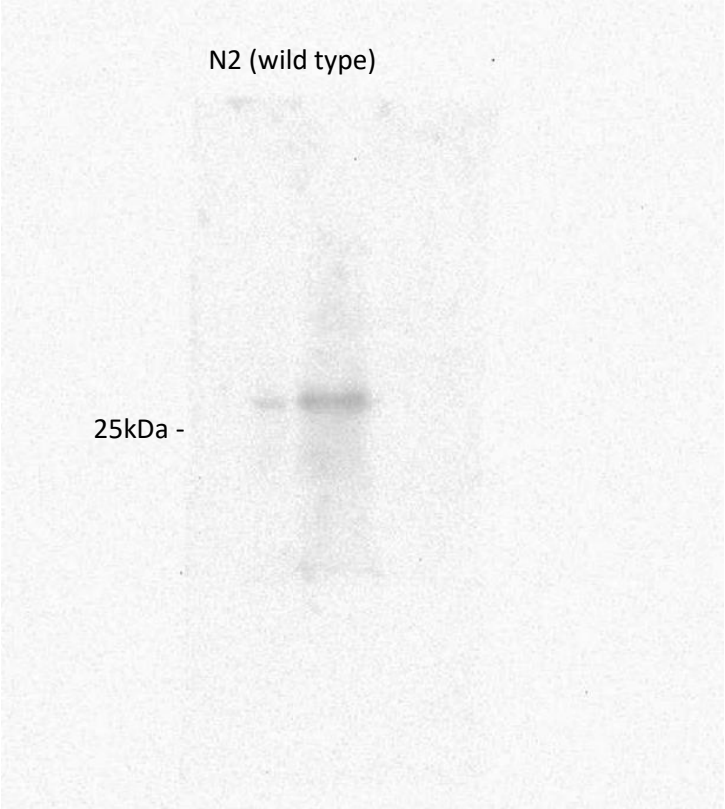

Figure 5.4.2. Western blot of tsp-7. The blot shows a band at the predicted size of 27kDa. The band is present for tsp-7 protein from the wild type N2 *C. elegans* strain.

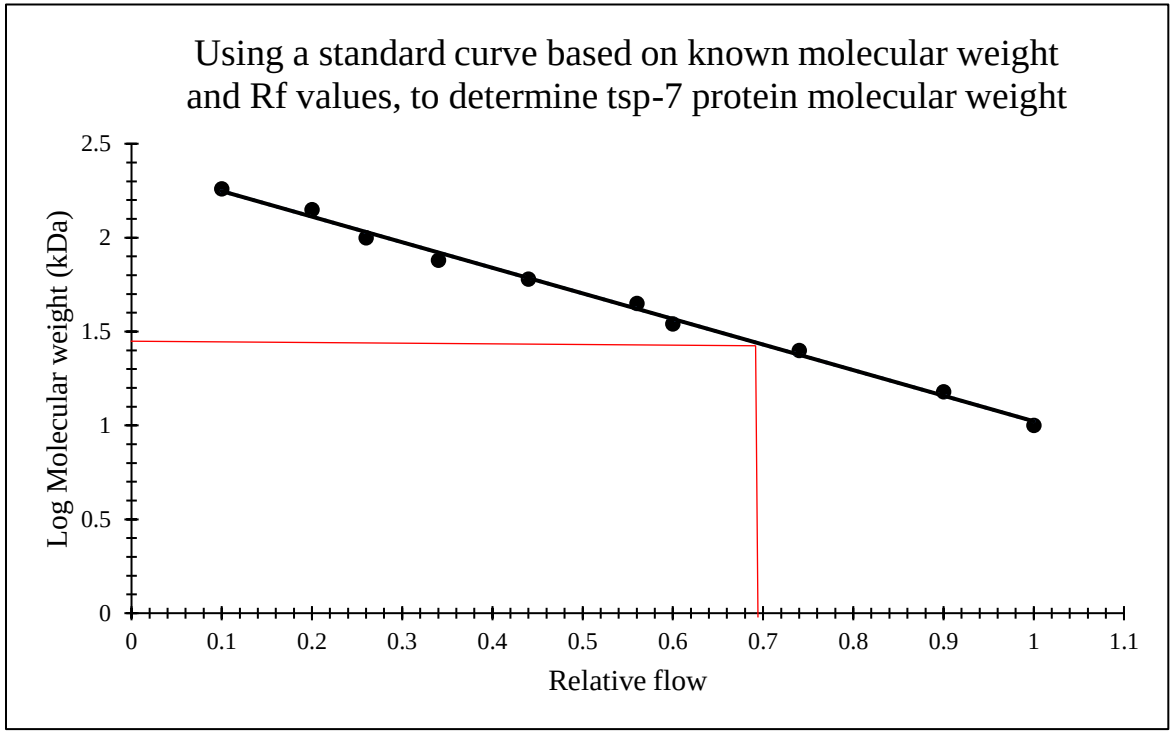

Figure 5.4.3. Calculation of the Rf value for tsp-7 using western blotting. The Relative flow values for the tsp-7 protein band was calculated and the molecular weight was determined from a standard curve from the molecular weight of the known protein marker. Using the curve, the tsp-7 protein molecular weight is estimated to be ~27.45kDa.

5.5 Transformation of tsp-7 – GFP tagged plasmid into DH5α

The GFP tagged plasmid (Figure 5.5.1) containing the full tsp-7 sequence insert (Genscript, Accession number: NM_060235.2, Clone ID: Oca335434), was successfully transformed into DH5α cells. Once the plasmid was extracted and purified from the bacteria, the purified tsp-7-GFP plasmid was run on an agarose and shown to be the correct plasmid size of 6.8kb (Figure 5.5.2). The DNA concentration was determined using the 260/280 ratio with an O.D reading of 0.8, (1.0 OD = 50ug/ml). The total concentration of plasmid DNA obtained after transformation and purification = 0.4mg/ml.

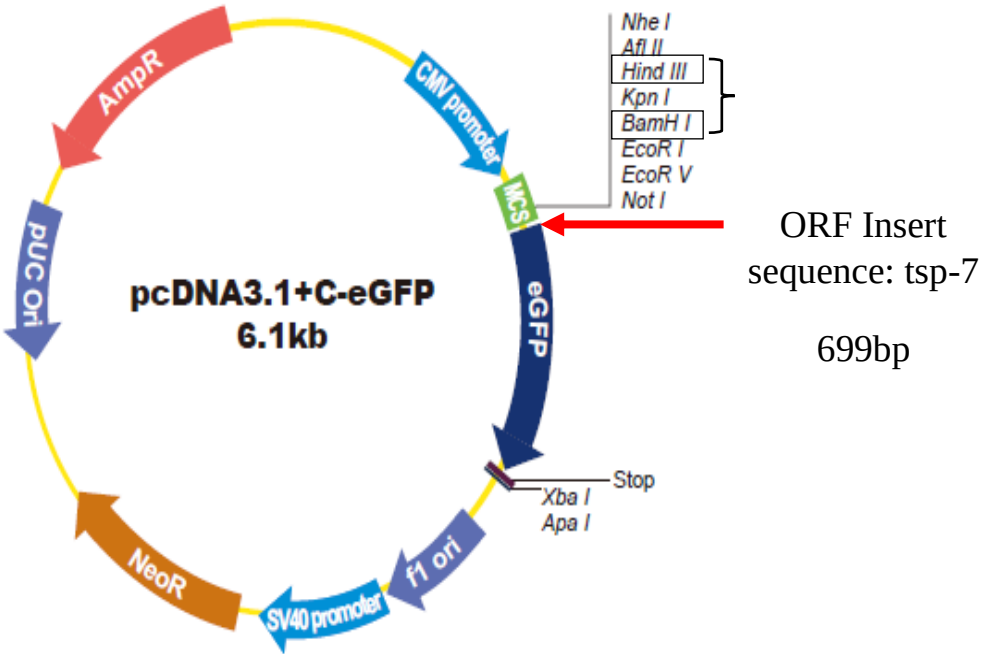

Figure 5.5.1. Plasmid from Genscript containing the full tsp-7 sequence insert, within the multiple cloning site (MCS). The restriction enzymes chosen using the SnapGene tool were, HindIII and BamHI. The tsp-7 sequence was copied to the New England BioLab restriction enzyme tool, to determine the site of restriction. The domain product length is expected to be 240 base pairs.

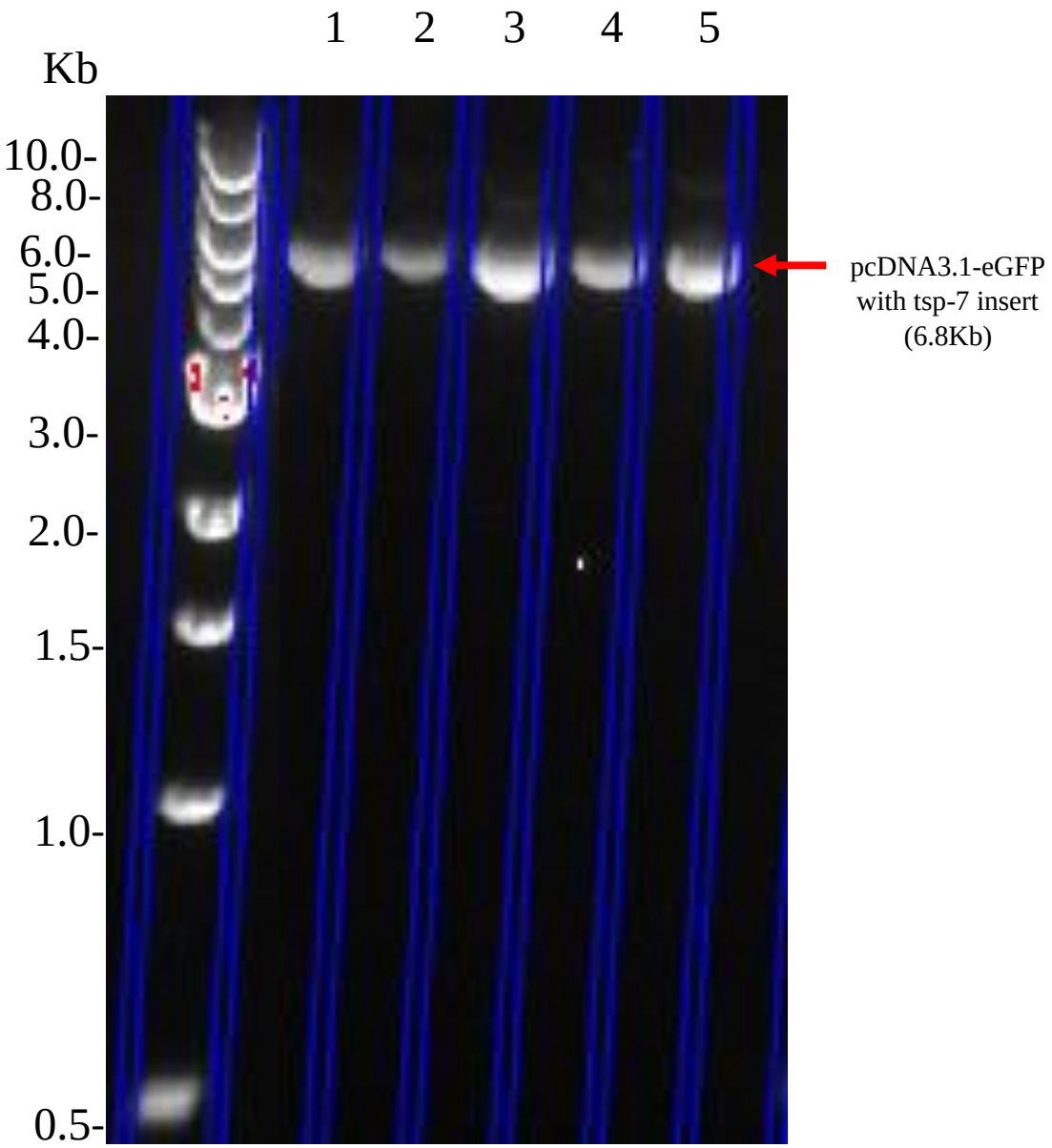

Figure 5.5.2. The tsp7 -GFP tagged plasmid insertion into DH5α competent *E.coli* via transformation. The extracted and purified plasmid was run on a 1% agarose gel. 5 colonies were chosen, all bands are at the correct size for the plasmid containing the full tsp-7 insert.

5.6 Transformation of DH5α and BL21 containing the tsp-7 domain only within the pET-21a vector

After deciding to use the purified GFP tag from previous experiments (0.4mg/ml) and a temperature gradient increase from 60℃-70℃. The results showed successful PCR amplification of the tsp-7 domain (Figure 5.6.1). Bands from lane 6-10 show greater concentration of DNA at higher annealing temperatures.

The DH5α and pET21a vector was digested using specific restriction enzymes, BamHI -HF and HindIII-HF (see chapter 2.4.8), BamHI cuts at recognition sites: G/GATCC, and HindIII cuts at recognition sites: G/GATCC. The product was extracted from the agarose gel and purified. The empty pET21a vector size is roughly 6Kb about the same size as the pcDNA3.1-GFP tagged plasmid. The domain was inserted into the pET21a vector via ligation as described in chapter 2.4.10. The ligation mixture was inserted into DH5α, 4 colonies were selected and run on an agarose gel. If time had allowed, the plasmid containing the tsp-7 domain would be an efficient tool for pull down assays, in which the binding of tsp-7 and TIMP-1 may be confirmed. The tsp-7 tagged plasmid acts as the bait protein, in this experiment the tagged tsp-7 / TIMP-1 binding complex would further confirm that TIMP-1 is binding to tsp-7 and not a CD63 like protein which may be expressed in mammalian cells.

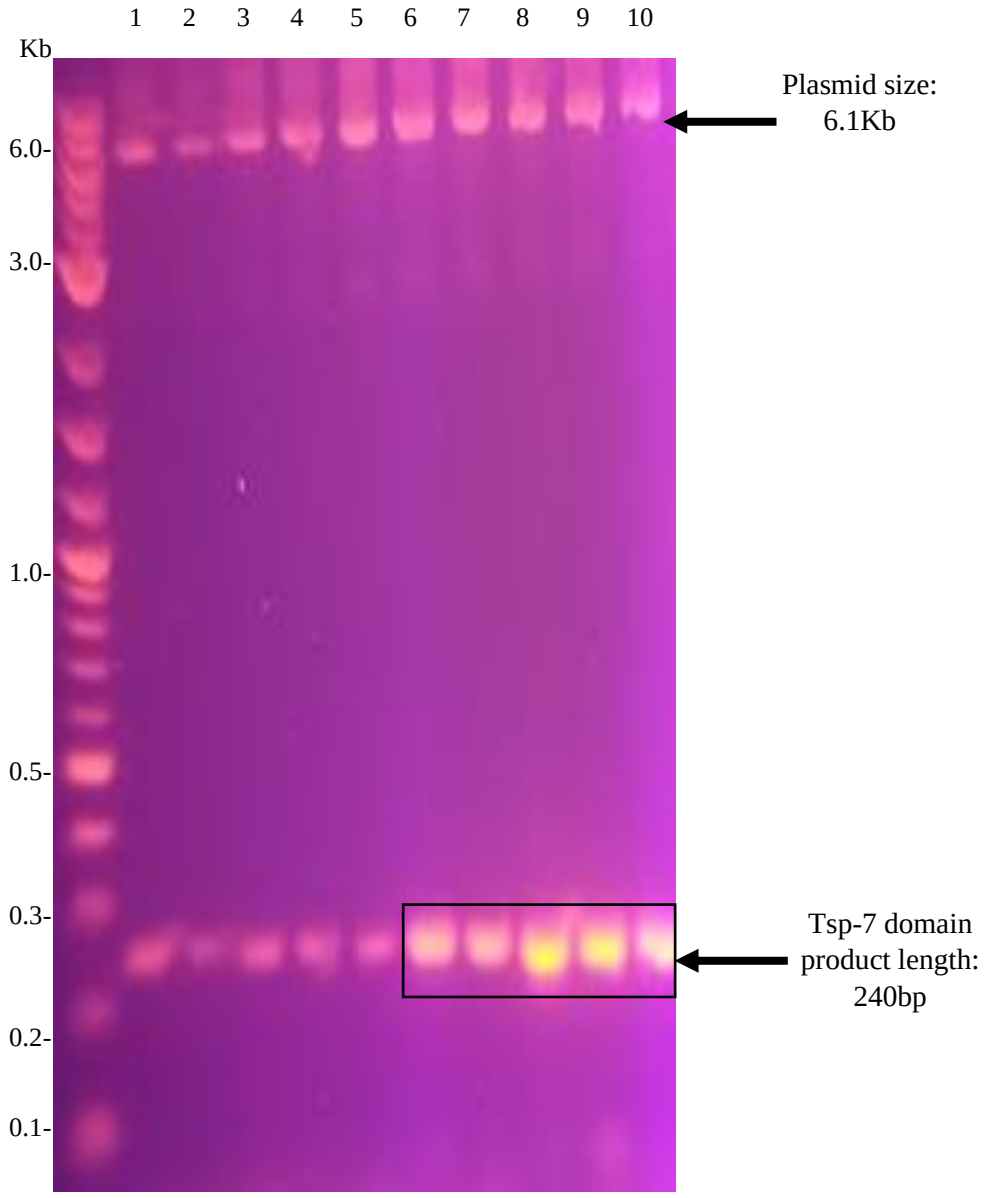

Figure 5.6.1. Temperature gradient PCR. The five bands highlighted within the black box are the most prominent. The temperature increases from 60℃ to 70℃ was the most optimal and these were samples chosen for digestion as they were more likely to contain the highest DNA concentration.

5.7 Transfection of COS-7 cells with GFP-tagged tsp-7 plasmid

Figure 5.7.1 below shows the healthy COS-7 cells grown in supplemented media (see 2.3.24). The cells were counted for viability, 5.16 X 10^5/ml of viable cells were counted and determined to be approximately 92% viability, before being seeded within the wells of a 24-well plate, at a density of 5 X 10^4/ml (1ml per well = 50000 cells seeded in each well).

Cells were seeded in serum (FBS) enriched media for 24 hours before transfection to allow complete adhesion of cells to the wells. The cells were transfected (see 2.3.28) and viewed after 24- and 48-hours using fluorescence microscopy in order to observe whether the cells were expressing the GFP-tagged-tsp-7 protein.

Figure 5.7.2 shows a COS-7 cells transfected with pcDNA3.1 and tsp-7-GFP plasmid. As can be visualised from the images, there is no fluorescence within the nucleus of the cells, however, there was substantial green GFP fluorescence throughout the body of the cell as well as up to the membrane. Overall transfection efficiency was estimated to be around 20-25%. The image of the cells, shown with multiple nuclei, is taken from a visual field of many fluorescent cells.

The bright-field phase contrast images of the COS-7 cells and those that have taken up the plasmid are shown in Figure 5.7.3. The images of the cells in the same field of view i.e., phase contrast and green fluorescence, were merged to show the efficacy of transfection (~25%). Cells were also seeded but no transfection reagent or plasmid was added to these cells as a control for both transfection and TIMP-1 binding. Cells

were also seeded in serum-free media, however the COS-7 cells appeared smaller than those in serum enriched media.

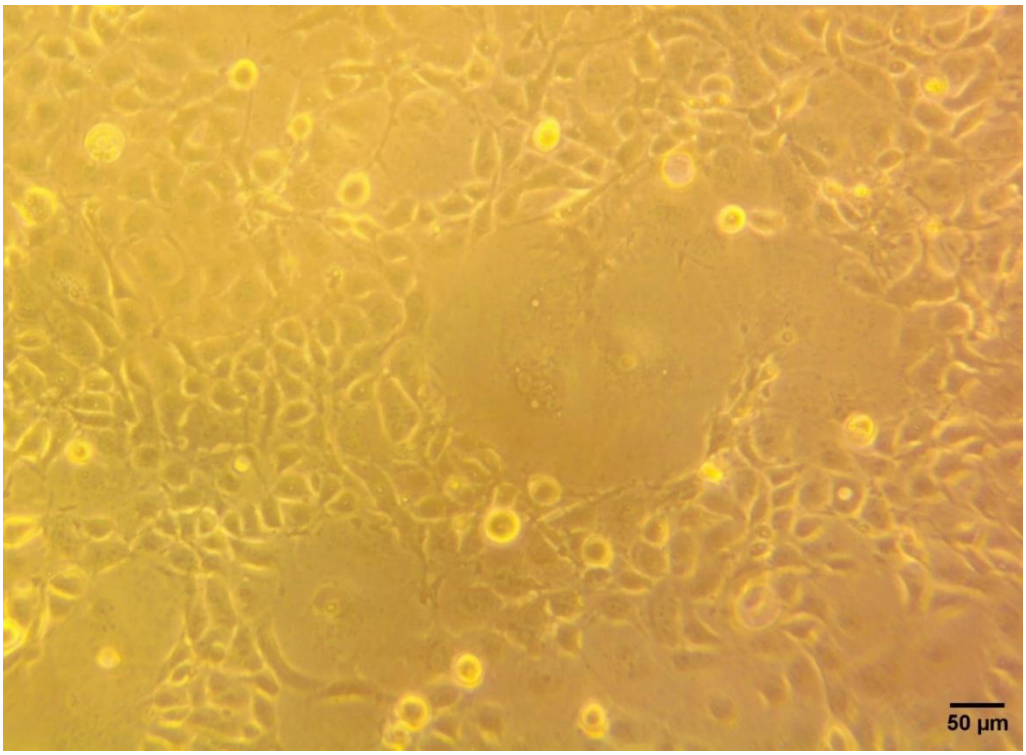

Figure 5.7.1. Healthy COS-7 cells, with an estimation of 92% viability. Cells were seeded at density of 5 X 10^4/ml in a 24 well plate (1ml per well) and incubated for 24 hours at 37°C (5% CO_2), before transfection. Cells were scanned with a 10X objective.

Nucleus of multiple COS-7 cells adhered to the surface of the well.

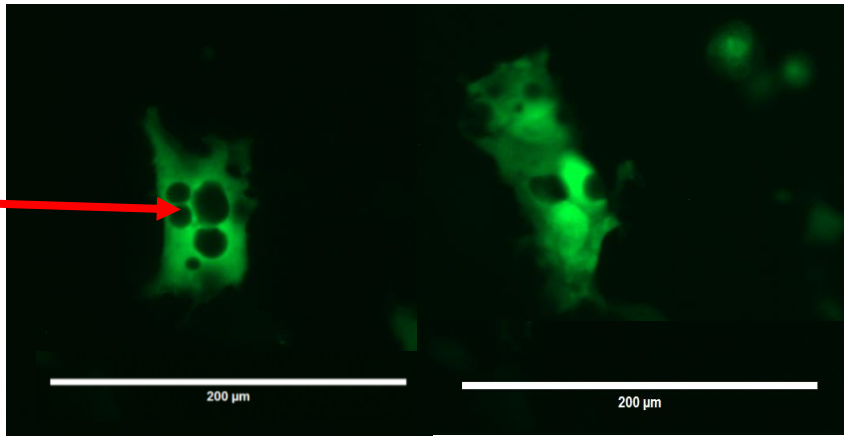

Figure 5.7.2. Transfection of COS-7 cells with GFP tagged tsp-7 protein. The image shows multiple cells, with the nucleus containing no green fluorescence protein. Tetraspanin proteins are not expressed within the nucleus, the image confirms the expression of the tsp-7 -GFP tagged plasmid. The entire body of the cells are fluorescent, this is consistent with the tsp-7 protein being expressed in cellular compartments such as exosomes as well as the membrane of cells.

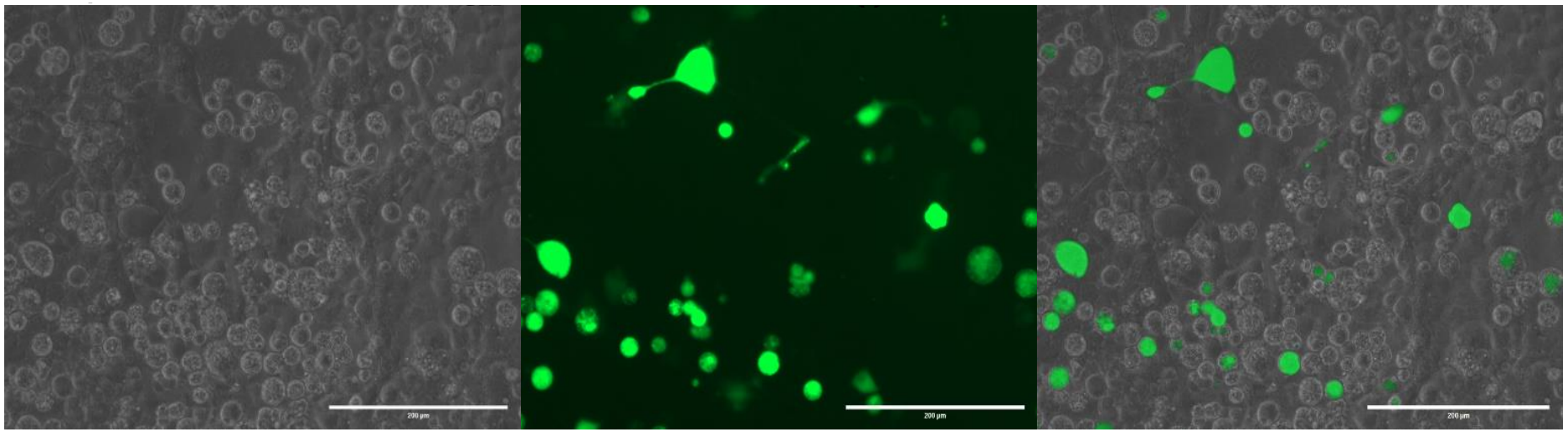

Figure 5.7.3. Successful transfection of COS-7 with 25% efficiency. From left to right, the phase image of the COS-7 cells after transfection. The cells are viable and have adhered to the well. The cells that fluoresce green are the cells that have successfully incorporated and expressed the tsp-7-GFP tagged plasmid. The transfection efficiency was calculated at 20-25%. The image of the fluorescent cells was merged with the phase image of the same cells, Transfection efficiency = Number of cells transfected / Number of cell in the sample (X100).

5.8 Binding of TIMP-1 to tsp-7

The cells that had successfully taken up the plasmid and were expressing the tsp-7-GFP protein were then exposed to 0.5ng of human TIMP-1 active molecule. TIMP-1 is known to bind to human CD63 (Jung *et al.*, 2006). To remove the potential of TIMP-1 binding to the CD63 equivalent from the mammalian COS-7 cells, TIMP-1 was also added to the cells seeded which had not been transfected with the tsp-7-GFP plasmid. *Chlorocebus aethiops* which the COS-7 cells originate do not have any entries for CD63 or equivalent, however close relatives of this species do contain CD63 like proteins. The cells which had not been transfected acted as a control, therefore demonstrating that TIMP-1 is only binding to the transfected tsp-7-GFP tagged protein, and not a CD63 like protein from *C. aethiops.*

The 24 well plate was visualised using fluorescence microscopy, the contrast of the red fluorescence protein against the GFP protein showed that there is binding of the TIMP-1 protein to the tsp-7 protein from *C. elegans* (Figure 5.8.1). The red fluorescence protein can be visualised within the cells, rather than on the plasma membrane, which is what would be expected for the tetraspanin protein. This could suggest that the concentration of tsp-7 is greater within the cells than the membrane. This may be due to the biogenesis of exosomes, formed within the cell (Gurung *et al*., 2021).

The cells form lipid rafts throughout the entire plasma membrane, these rafts contain a plethora of molecules; GPI- anchored proteins, palmitoylated proteins as well as, cholesterol, sphingomyelin, and glycosphingolipids. These lipid rafts are the centre of cell regulation, communication, and signalling (Simons & Toomre., 2000 and

Ouweneel *et al*., 2020). Tetraspanins have a specific cholesterol binding pocket, therefore, the lipid rafts are enriched with cholesterol and tetraspanin proteins. The COS-7 cells would also contain these lipid rafts throughout the membrane. The fluorescence microscopy excites the cell equally which could explain the patches or spots seen within the cells. The cells had not been permeabilized therefore no TIMP-1 could cross the membrane and cannot be fluorescing within the cell. To further prove that the TIMP-1 is binding to these lipid rafts across the membrane, confocal microscopy would allow specific co-localization visualisation.

The difference in red fluorescence intensity varies within the cells (Figure 5.8.1). There are areas in which the tsp-7 and TIMP-1 are more concentrated, although there is binding of TIMP-1 to tsp-7, TIMP-1 did not bind to all the cells which fluoresced green. This could suggest that TIMP-1 binds weakly to tsp-7. TIMP-1 is concentrated within the cell; however, TIMP-1 may bind at the plasma membrane as well as within the cell, but this would require further studies to confirm the binding capacity of TIMP-1 and tsp-7 within the membrane. The Pearson's correlation coefficient was calculated for single cells using the JACoP application in ImageJ, r = 0.12 for Figure 5.8.1a and r = 0.862 for Figure 5.8.1b. This suggests that there is co-localization of TIMP-1 and tsp-7, especially in Figure 5.8.1b, as a r value of 1 represents almost perfect co-localisation (Bolte & Cordelières., 2006). Scatter plots produced in ImageJ using the JACoP and Colocalization finder plugin, can be found for both Figure 5.8.1a and 5.8.1b in supplementary data set 11 (S11). About 25% of the transfected cells shows some binding with TIMP-1 with a Pearson's correlation coefficient of r = 0.64 (Figure 5.8.2). Figure 5.8.3, the control study, cells which had not been transfected with tsp-GFP tagged plasmid, did not show strong TIMP-1 –tsp-7 binding. This could suggest that the CD63 equivalent from the COS-7 cells is less

identical to human CD63 than tsp-7 from *C. elegans.* However, there is a few red dots which can be seen within a few of the cells. It is unclear from this image if these are artefacts or if TIMP-1 is binding to a potential CD63-like protein within the membrane of the COS-7 cells.

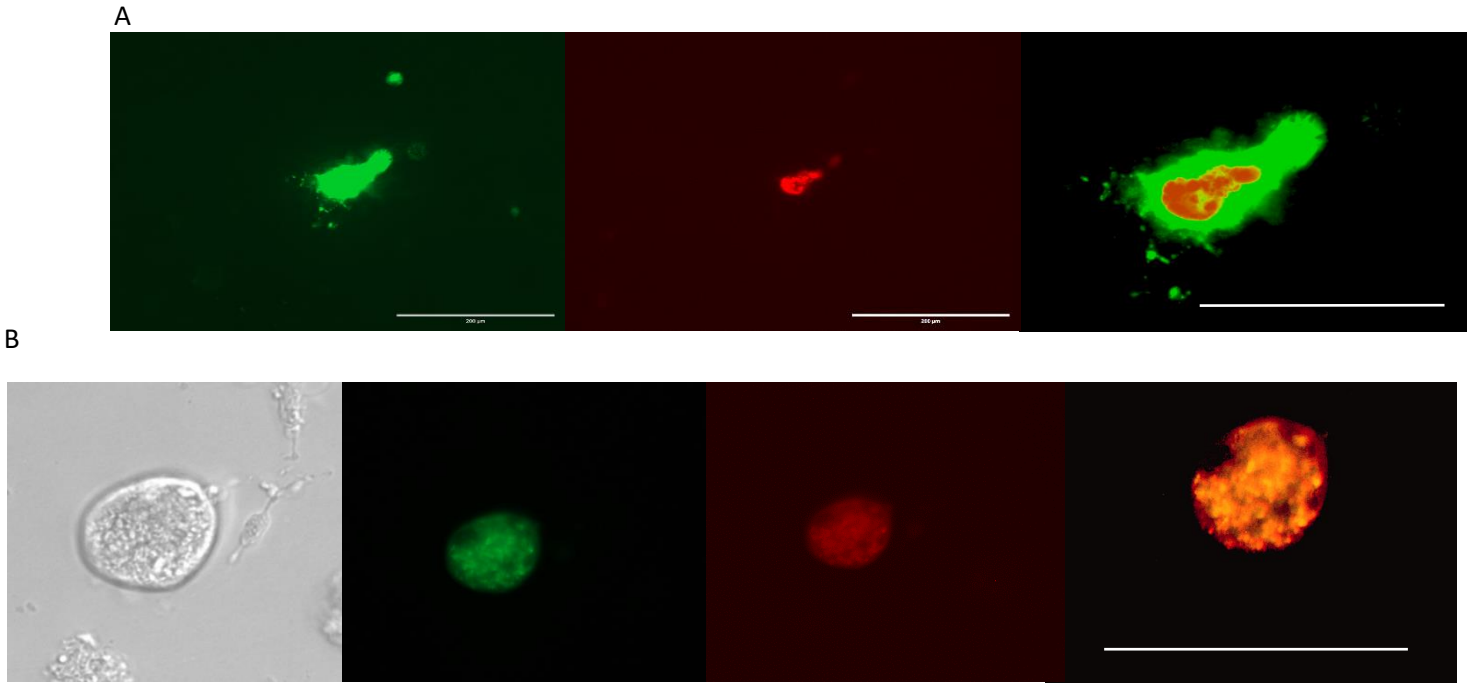

Figure 5.8.1. Co-localisation of TIMP-1 and tsp-7. A) The left image shows a fluorescent cell after successful transfection with the tsp-7-GFP tagged plasmid. The image on the right shows specific areas fluorescing red, due to the binding of TIMP-1 and its primary conjugated anti-TIMP-1 Alexa-fluor 647 antibody. B) From left to right, a phase image of a COS-7 cell. The middle image shows a cell which has taken up the GFP tagged plasmid and the right image shows TIMP-1 fluorescence. Images were taken at 40X and 100X objective.

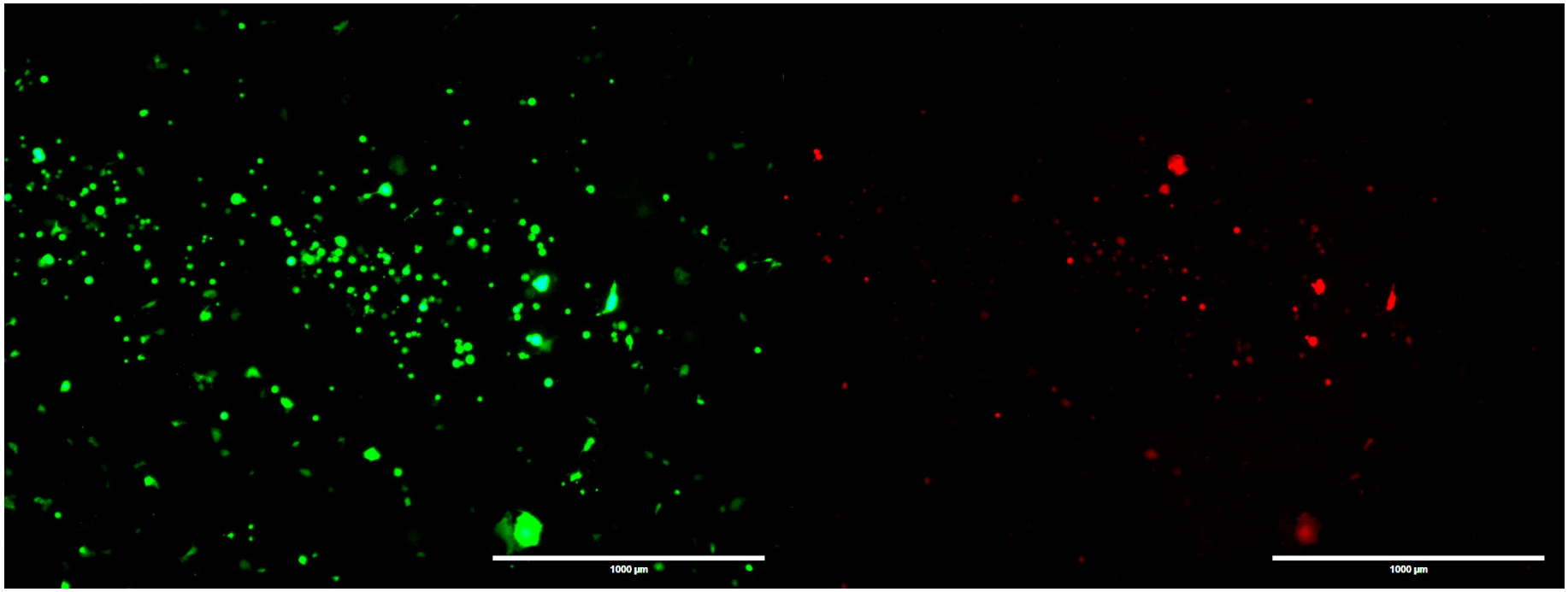

Figure 5.8.2. Colocalization of multiple COS-7 cells with TIMP-1 and tsp-7. Roughly 25% of the COS-7 cells show colocalization, the Pearson's correlation coefficient r= 0.64. The image is more representative of the cells observed. Cells were observed at 10X objective.

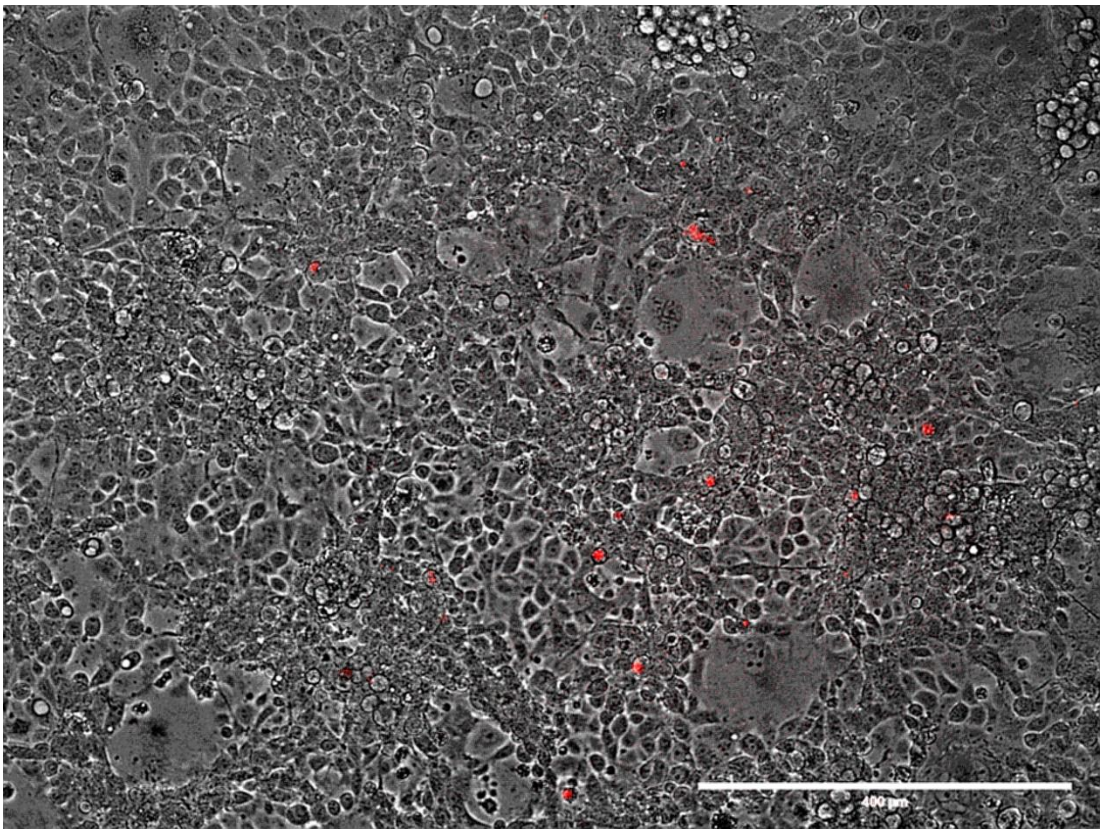

Figure 5.8.3. Transfection and binding of TIMP-1 control cells. The image shows cells that had not been transfected with GFP-tagged plasmid, acting as a control. The image shows healthy COS-7 cells under phase contrast. The COS-7 cells were incubated with TIMP-1. The image was merged with the phase contrast cells. The red dots may be artefacts or may be TIMP-1 binding to a CD63-like protein within the plasma membrane of COS-7 cells.

5.9 Discussion

An obstacle to overcome in this project was obtaining pure lysates of tsp-7 membrane protein. The samples contained whole cell lysates, this could mean that the true concentration of tsp-7 was very low and would have required extensive steps to achieve a high yield to be detected with the primary antibody. One method to achieve a high membrane protein yield is using commercialised membrane extraction kits (Muinao *et al.*, 2018).

It is unknown at what stage in the life cycle the *C. elegans* were, at the time of lysis. It is possible tsp-7 is only expressed at the adult stages, making the juvenile and larval stages redundant. It could also be that tsp-7 is only expressed at low levels at the membrane within *C. elegans*. The immunohistochemistry did not yield any results; however, this was understandable as the method described in the *C. elegans* worm-book, is much more complex. To gain access to the tsp-7 the nematode cuticle must be cracked, this defeats the object of using the method of paraffin wax and a microtome when it would be impossible to slice the nematodes due to their size of 1mm. The *C. elegans* worm-book (http://www.wormbook.org/) reports that there are two, somewhat successful, methods of extracting and visualising proteins, one of these methods is the use of western blots. The second method is cyto-immunochemistry, but this method depends on the location of the protein. Most of the methods require trial and error with various fixation methods and freeze-crack protocols. Due to time and cost being a major limiting factor this was not possible to achieve.

Without proper visual analysis, it is uncertain what the domain structure of tsp-7 looks like in its native state. The protein can also change conformation depending on the molecules binding to the protein. For example, a closed or open domain conformation (Yang *et al.*, 2020). Nuclear Magnetic Resonance (NMR) would be used to determine the structure of tsp-7 and in particular the domain. NMR requires pure, highly concentrated protein samples (Kozak *et al.*, 2016), achieving high yields of tsp-7 was a major challenge in this project.

Despite the relatively low yield of tsp-7 from all three *C. elegans* strains (Wild-type N2, mutant tm5046 and mutant tm5761), tsp-7 was still detected in the ELISA assays. However, the tsp-7 protein could not be detected in the western blot for both mutant strains using these antibodies. The tsp-7 protein could be detected in wild type; however, optimisation of the antibody meant the concentration was increased to 1.48μg/ml (1:500) after initially using a 740ng/ml concentration (1:1000). In one experiment, 2ml of purified primary antibody (0.74mg/ml) was used for a western blot, again this yielded no visible bands. Due to time, and cost of primary antibody, the volumes used were limited. It would be useful to attempt to optimise the primary antibody with higher concentrations with 1:500 being the lowest concentration, as well using densitometry methods to calculate and compare tsp-7 protein abundance between the wild type and mutant *C. elegans* strains.

Controls were used in order to assess the efficiency of the western blot method. Known lysate samples from humans could be detected using a western blot following the same method, used for the *C. elegans* tsp-7 lysates, such as GAPDH within HEK and HRT cancer cell protein lysates (supplementary S12). When alpha tubulin and beta actin antibodies, species specific to *C. elegans*, were used as a control, these

proteins could not be detected. This would suggest that the protein extraction method is inefficient, or the volume of nematodes used in the study was too low. This could be improved by large scale cultivation of *C. elegans*, this method however, requires the use of a bioreactor (Heshof *et al.*, 2019), which was not feasible for this project.

An issue in expressing the domain could be due a mutation in the epitope of the mutant nematodes. The mutant strain tm5761 contains a deletion of 69 amino acids , completely removing two of the four transmembrane helices as well as deleting the small extracellular loop and a portion of the large extracellular loop which contains the antigen domain. It may be possible that the protein is non-functional and therefore not expressed as much as the wild type or the mutant tm5046.

The images of the cells fluorescing green (due to the tsp-7- GFP tagged plasmid) and red (anti- TIMP-1 antibody binding to TIMP-1), are promising in that there is evidence to suggest that the human molecule TIMP-1 can bind to tsp-7 orthologue from *C. elegans*. If this is the case then it may also be plausible that TIMP-1 can bind to tsp-7 orthologues in parasitic nematodes of humans. This would support the theory that parasitic nematodes use their own tetraspanin proteins to interact and bind with host molecules thus dampening down the immune system and establishing a chronic infection. *C. elegans* is more genetically similar to some human parasitic nematodes and is still the best model for anthelmintic drug development (Hahnel *et al.*, 2020), but also shares similarities with humans, about two thirds of the *C. elegans* genome shares homologues with human disease related genes (Zhang *et al.*, 2020). The model system used here, COS-7 mammalian cells and nematode protein is useful in predicting the potential likelihood that parasitic nematodes also express tsp-7 like proteins within the membrane and possibly exosomes. The system also supports the

theory that tsp-7 may be an orthologue of CD63 by being expressed within a mammalian cell. Using this model system is more appropriate a GFP-tagged tsp-7 *C. elegans* cannot be achieved without freeze cracking procedures, as well as the inability to incubate *C. elegans* in TIMP-1. To visualise co-localisation would require the excretory/secretory products (ESP) including microvesicles. *C. elegans* cannot survive at 37℃ as shown in chapter 4, TIMP-1 binding to parasitic proteins would occur at 37℃ due to the environment of the human host. In this sense using mammalian cells with GFP tagged nematode proteins is a more reliable system.

Interestingly, the tsp-7 -GFP tagged plasmid fluoresces within the cell and potentially the membrane. This suggests that, like CD63, tsp-7 could also be expressed on the membrane of exosomes. As exosome are constantly formed within the cell, the tsp-7 may be internalised into intraluminal vesicles (Colombo *et al.*, 2014). Unfortunately, exosome studies could not be carried out for this project due to lack of sufficient equipment, the gold standard of exosome retrieval is ultracentrifugation of speeds reaching 120,000xg as well as some form of particle tracking either nano tracking analysis, dynamic light scattering or atomic force microscopy (Bagrov *et al*., 2021).

Overall, there is evidence of antibody binding to tsp-7, however, developing antibodies to membrane proteins, particularly tetraspanins is extremely difficult and there are commercially very few antibodies available for tetraspanins, this is still currently a major problem within the field (Tomlinson *et al.*, 2017). If parasitic nematodes do utilise a similar protein to CD63, in order to establish infection, it would not be cost efficient to develop antibodies. The domain is generally variable; however, research has shown that there is within the variable domain human

tetraspanin 15, a conserved region involved with binding of ADAM10 (Lipper *et al.*, 2022). There are motifs that define a tetraspanin but not enough similarity in the domain to produce an antibody to target a group of nematodes. Perhaps it is possible to repurpose a drug to target the tetraspanin proteins within nematodes to stop the protein functioning effectively. What effect this would have on infection is unknown and would require extensive, research. The two mutant strains cultivated in this project could be used in following experiments, comparing drugs between these strains and the wild type N2 strain. The ability of parasites able to easily infect, avoid and alter the host immune system remains elusive, to date no vaccines been successfully produced to treat helminth infections (Perera & Ndao., 2021). The tsp-7 tetraspanin protein in the mutant strains had an effect on longevity of the *C. elegans*. A deletion in the amino acid sequence of parasitic proteins may have a similar unwanted effect. However, the mutant tm5761 showed less tolerance to induced stress, therefore deletion of a substantial section of the tsp-7 protein, along with nematode anthelmintics may have a greater efficacy on worm fatality. An antibody to the LEL domain could be developed for the parasitic nematodes, as the tsp-7 protein could be detected by the polyclonal anti tsp-7 primary antibody, within the wild type (N2). This suggests a potential for specific clade nematode antibodies against CD63/tsp-7 like- proteins.

Chapter 6: General Discussion

Parasitic nematode associated diseases still remain largely neglected, due to low levels of funding compared to funding given to other parasitic diseases. However, some efforts have been made to identify possible drug candidates to treat such pathological nematode associated diseases. One of the most promising drug target candidates being developed so far is smTSP-2, a tetraspanin protein found in *Schistosoma mansoni* (Pinheiro *et al.*, 2014). The genome databases for nematode parasites still remain poorly annotated, and with only three drug classes being developed so far, it is becoming a concern due to rising incidences of drug resistance.

It is understood that parasite infections can affect the immunological response of the host by modulating the Th1/Th2 pathways , and more recently, research has found that parasite-derived vesicles (exosomes) may play a significant role in parasite-host-communication and the immunological switch from Th1 to Th2 response (Wu *et al*., 2019 and Coakley *et al.*, 2016).

Matrix metalloproteinases (MMPs) have a far greater effect on the immune system than previously thought, especially in the cytokines and chemokines involved (Bruschi & Pinto., 2013). Some tissue inhibitors of MMPs (TIMPs) and particularly TIMP-1 is known to bind to CD63, and β1 Integrin, forming a complex which has the capacity to activate signal transduction pathways, modulating cellular and immunological behaviour (Justo & Jasiulionis., 2021).

In recent scientific reports it has been shown that TIMP-1 has cytokine-like functions, particularly as a pro-inflammatory response factor (Schoeps *et al*, 2022).

TIMP-1 and MMPs affect hematopoietic stem cells (HSCs), by controlling biochemical signals, and altering factors that determine the fate of HSCs (Saw *et al.*, 2019). An immune response to helminth infection relies on the proliferation of basophils, neutrophils, mast cells, hematopoietic stem cells and progenitor cells (Inclan-Rico & Siracusa., 2019).

In this study, tsp-7 protein, which is an orthologue to human CD63, that is present in *C. elegans* was investigated As no 3D structures are available for either human CD63 or tsp-7 from *C. elegans*, one of the major objectives of this research was to theoretically predict a 3D protein structure of tsp-7 using a variety of commonly used bioinformatics programmes. Furthermore, shortly after the completion of the initial 3D modelling studies undertaken here, it was fortuitous that the DeepMind AI computer had developed the 'AlphaFold' programme for predicting protein structure and that they had also released a predicted 3D model structure for both human CD63 and *C. elegans* tsp-7. A comparison between the tsp-7 3D structure originally predicted by more conventional structure prediction programmes and that predicted by AlphaFold was indeed very close between the two models. One suggestion for future experiments would be to try to successfully determine the actual structure of tsp-7 and CD63. As it is still difficult to generate X-ray crystal structures of membrane proteins, an NMR approach may prove more successful as tsp-7 has a sufficiently low molecular weight for this approach to be viable. However, like with X-ray crystallography, the NMR approach requires pure concentrated samples of the protein. One of the aims of this project was to begin to develop approaches in order to express and purify the tsp-7 membrane protein or its domains at high concentrations.

A study to further analyse the parasitic proteins, identified in chapter 3, with similarity to tsp-7 could also be used to create theoretical 3D models of these proteins. Most of the proteins identified as potential CD63-like tetraspanins in this study are either putative or theoretical. The parasitic nematode proteins could also be docked with TIMP-1. A working hypothesis from the results in this study could be that tsp-7 from nematodes, either expressed on its surface or secreted via exosomes, can compete for secreted TIMP-1 from the host. This could possibly lead to a mechanism of parasitic survival within the host, since by competing for TIMP-1 this would decrease its availability to act as a cytokine and thus prevent or reduce any further downstream pro-inflammatory responses. Figure 6.1 illustrates how this might occur.

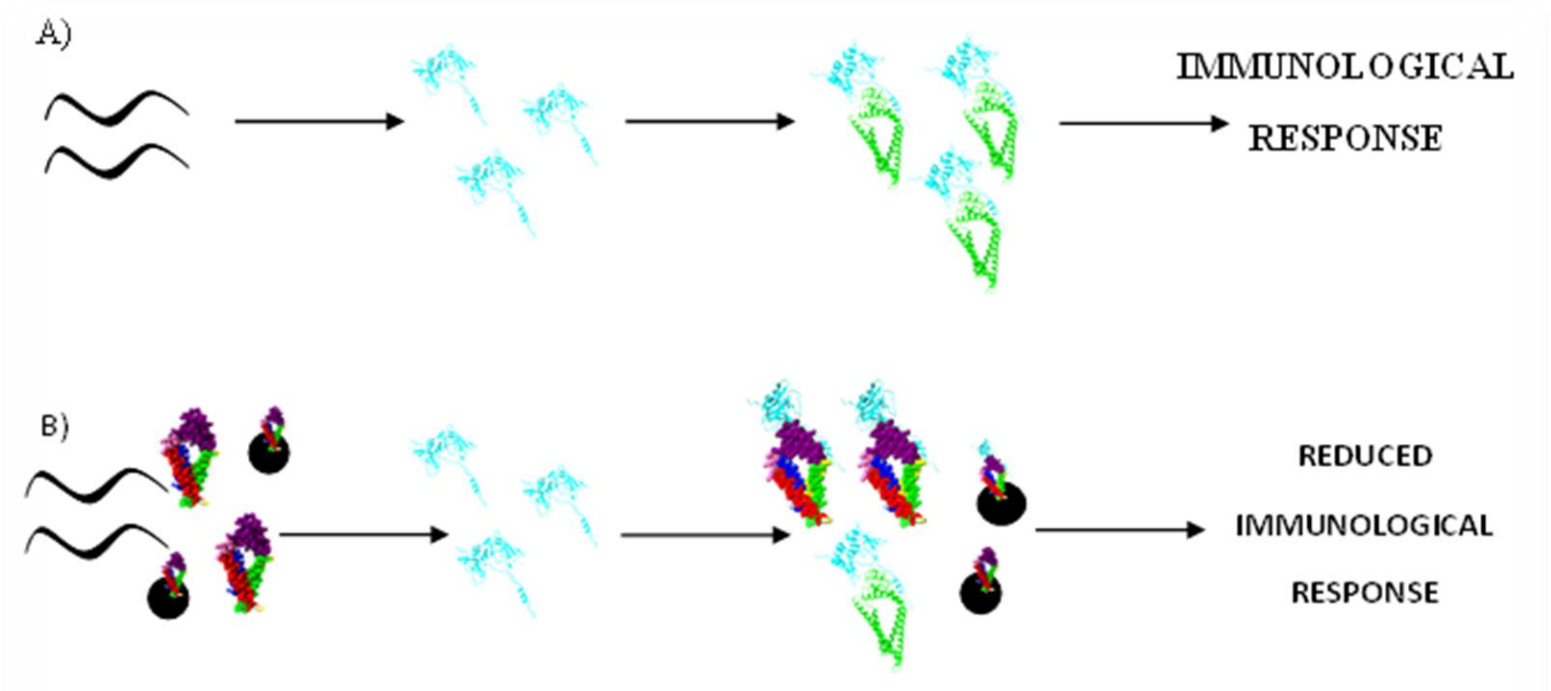

Figure 6.1. Image showing potential theory of parasitic nematodes modulating host immune response. A) In a normal infection, the detection of parasitic nematodes would induce elevated levels of TIMP-1. These active TIMP-1 molecules would bind to the CD63 receptor, TIMP-1 would display cytokine-like behaviour and drive the Th2 pathway. Leading to an appropriate immune response. B) Parasitic nematodes evade the host immune response, possibly by expression of CD63-like proteins released as excretory/secretory products e.g., exosomes, thus competing with CD63 and inhibiting binding to TIMP-1, preventing the appropriate immune response and modulating the Th1/Th2 and Treg levels, allowing chronic infection within the host.

One way the parasites could achieve this is through the excretory / secretory products released from the parasites, such as exosomes. To date, the gold standard for exosome isolation and purification is ultracentrifugation (Chen *et al.,* 2022). Future work would investigate using the specific antibody developed in this study, where *C. elegans* or other known parasitic nematodes do in fact secrete tsp-7 containing exosomes.

The large extracellular loop domain of the tetraspanin proteins contains the variable region, with CCG motifs embedded within the structure (Jancovičová *et al.,* 2020). The antibody produced to the tsp-7 peptide, could detect the wild- type strain and both mutant strains at a very low concentration in the ELISA assay. The western blot could only detect the wild type protein and not the mutant forms of tsp-7 which may indicate that the epitope for recognition may involve its tertiary structure. The protein sequences from the other nematode parasites identified in chapter 3, could be aligned with the LEL sequence of tsp-7. Thus, it would be interesting to investigate whether this antibody could also cross react with other nematodes as well. Identifying good immunoreactive parasitic antigens such as for the LEL domain of tsp-7 could prove beneficial in the future development of vaccines used to immunise against nematode / helminth infections, such as being developed for *S. mansoni* helminths by targeting its TSP-2 (Barbosa *et al*., 2021). The mutant tm5761, has a deletion of 96 amino acids (chapter 2.2.3). This means that the tsp-7 protein has lost transmembrane helices 2, 3 and part of the LEL domain. Figure 6.2 shows the theoretical structure of the mutant tm5761. The transmembrane helices 1 and small intracellular loop (SIL) may not be coded, the tsp-7 protein may be expressed in very low concentrations compared to N2 and mutant tm5046. This could explain the inability of the antibody

to detect mutant tm5761 in a western blot, and also the reason the concentration of tsp-7 was detected much lower in the ELISA assay.

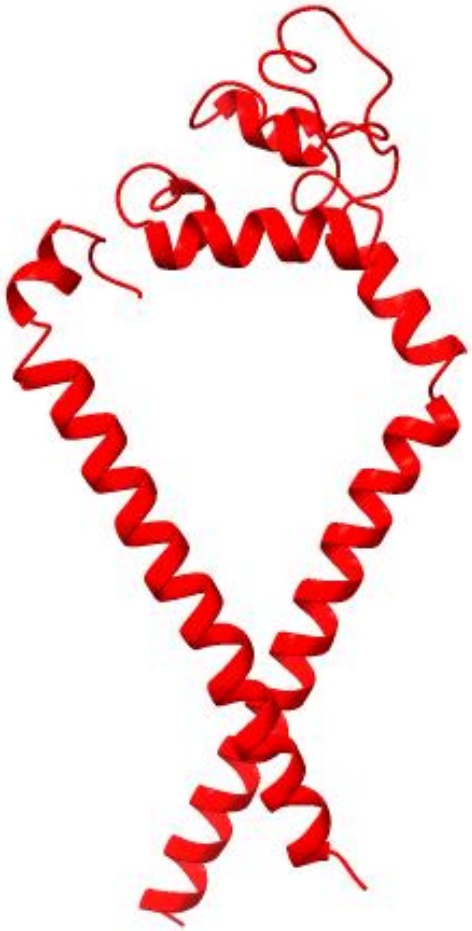

Figure 6.2 The mutant tm5761 has a 69 amino acid deletion. Transmembrane helices 2 and 3, as well as the small intracellular loop would not be expressed. The structure shows that the transmembrane helices 1 is not joined to the large extracellular loop or transmembrane helices 4. TM1-TM3, the SEL and the SIL are unlikely to be expressed, possibly leading to a non-functioning protein expressed at low levels within mutant tm5761.

When assessing the behavioural stress response, some studies create a concentration gradient across the agar, then use specialised computer software to determine the runs, omega turns and reversals automatically. The software is also able to determine to what degree the *C. elegans* turn along the gradient. A more robust future study would utilise this type of software (Jung *et al*., 2014)

Given the limitations of the visual assessments, in general, the results presented here showed that the mutant tm5046 *C. elegans* strain appears to be generally more tolerant to increased chemical stresses than the mutant tm5761 strain and more similar in its responses seen in the wild type The mutant tm5046 strain only has a deletion of four amino acids at the beginning of the LEL domain of tsp-7, whereas mutant tm5761 strain has the biggest amino acid deletion in which two of the four transmembrane helices are deleted from tsp-7.

An additional phenotype / physiological study that could be carried out on the wild type and tsp-7 mutant strains is to observe their stress responses to various concentrations of Ca^{2+}. It has previously been shown that an increase in Ca^{2+} results in an increase in exosomes (Messenger *et al*., 2018), the exosome concentration could then be measured. Once isolated the exosomes from the wild type and mutant strains could then be assessed, using a number of immunochemical approaches, to assess firstly, whether they contain tsp-7 and secondly, whether the wild type and tsp-7 mutant strains can bind human TIMP-1.

Figure 6.3 shows the pathway of tsp-7 protein in *C. elegans*, which plays a role in the immune system, in particular the degranulation of neutrophils. Tsp-7 also plays a role in the homeostasis and morphology of *C. elegans* (see chapter 3, Figure 3.8.1). The role TIMP-1 could have in regard to *C. elegans* tsp-7 protein and neutrophil degranulation is unknown.

In conclusion, the research presented in this thesis has proposed a 3D structure for nematode tsp-7 and theoretically identified that human TIMP-1 is able to bind to it. Expression of *C. elegans* tsp-7-GFP and immunofluorescence microscopy studies have supported this proposal. From these results it is hypothesised that the interaction of Human (host) TIMP-1 with the nematode (parasite) tsp-7 may play an important role in reducing the host's immune response to parasitic infection.

Finally, mutations of tsp-7 in *C. elegans* have shown significant alterations in both life span and responses to chemical and physical stress, which again indicates the many important roles that tsp-7 might have in the nematode, and this will require much more extensive investigations.

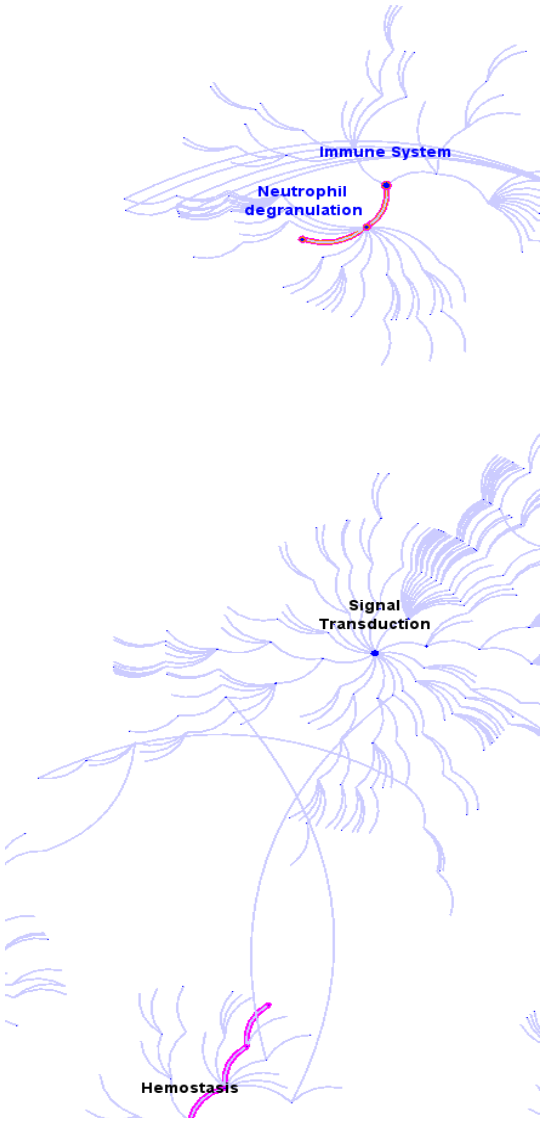

Figure 6.3. The tsp-7 protein from *C. elegans* is involved in the immune system, in particular the degranulation of neutrophils. As well as homeostasis and signal transduction pathways. This is achieved through the multiple protein complexes formed with the tsp-7 protein which can be found on the STRING database. Most of the proteins interactions for tsp-7 on the database are poorly annotated and are inferred from data mining, with very little experimental data available.

7. References

Adinarayanan, S., Critchley, J., Das, P. K., & Gelband, H. (2007). Diethylcarbamazine (DEC)-medicated salt for community-based control of lymphatic filariasis. *The Cochrane Database of Systematic Reviews, 2007*(1), CD003758. https://doi.org/10.1002/14651858.CD003758.pub2.

Afonso, A., Hunt, P., Cheesman, S., Alves, A. C., Cunha, C. V., do Rosário, V., & Cravo, P. (2006). Malaria parasites can develop stable resistance to artemisinin but lack mutations in candidate genes atp6 (encoding the sarcoplasmic and endoplasmic reticulum Ca2+ ATPase), tctp, mdr1, and cg10. *Antimicrobial Agents and Chemotherapy, 50*(2), 480–489. https://doi.org/10.1128/AAC.50.2.480-489.2006.

Ahmed N. H. (2014). Cultivation of parasites. *Tropical Parasitology, 4*(2), 80–89. https://doi.org/10.4103/2229-5070.138534.

Alberts B, Johnson A, Lewis J, et al. *Molecular Biology of the Cell* (4th ed.). Garland Science; 2002. T Cells and MHC Proteins. Available from: https://www.ncbi.nlm.nih.gov/books/NBK26926.

Al-Banna, L., & Gardner, S. L. (2022). The phylum nemata. *Reference Module in Life Sciences*. https://doi.org/10.1016/b978-0-12-822562-2.00028-1.

Albrecht, P. A., Fernandez-Hubeid, L. E., Deza-Ponzio, R., & Virgolini, M. B. (2022). The intertwining between lead and ethanol in the model organism *Caenorhabditis elegans*. *Frontiers in Toxicology, 4*, 991787. https://doi.org/10.3389/ftox.2022.991787.

Allen, J. E., Sutherland, T. E., & Rückerl, D. (2015). Il-17 and neutrophils: Unexpected players in the type 2 immune response. *Current Opinion in Immunology, 34*, 99–106. https://doi.org/10.1016/j.coi.2015.03.001.

Allen, J. E., & Sutherland, T. E. (2014). Host protective roles of type 2 immunity: parasite killing and tissue repair, flip sides of the same coin. *Seminars in Immunology*, *26*(4), 329–340. https://doi.org/10.1016/j.smim.2014.06.003.

Alspaugh J. A. (2015). Virulence mechanisms and *Cryptococcus neoformans* pathogenesis. *Fungal Genetics and Biology : FG & B*, *78*, 55–58. https://doi.org/10.1016/j.fgb.2014.09.004.

Alves, I., Fernandes, Â., Santos-Pereira, B., Azevedo, C. M., & Pinho, S. S. (2022). Glycans as a key factor in self and nonself discrimination: Impact on the breach of immune tolerance. *FEBS Letters*, *596(*12), 1485–1502. https://doi.org/10.1002/1873-3468.14347.

Ambrosetti, F., Jiménez-García, B., Roel-Touris, J., & Bonvin, A. M. J. J. (2020). Modeling Antibody-Antigen Complexes by Information-Driven Docking. *Structure*, *28*(1), 119–129.e2. https://doi.org/10.1016/j.str.2019.10.011.

Andreu, Z., & Yáñez-Mó, M. (2014). Tetraspanins in extracellular vesicle formation and function. *Frontiers in Immunology*, *5*, 442. https://doi.org/10.3389/fimmu.2014.00442.

Anthony, R. M., Rutitzky, L. I., Urban, J. F., Stadecker, M. J., & Gause, W. C. (2007). Protective immune mechanisms in helminth infection. *Nature Reviews Immunology, 7*(12), 975-987. doi:10.1038/nri2199.

Arpino, V., Brock, M., & Gill, S. E. (2015). The role of TIMPs in regulation of extracellular matrix proteolysis. *Matrix Biology : Journal of the International Society for Matrix Biology*, 44-46, 247–254. https://doi.org/10.1016/j.matbio.2015.03.005.

Artavanis-Tsakonas, K., Kasperkovitz, P. V., Papa, E., Cardenas, M. L., Khan, N. S., Van der Veen, A. G., Ploegh, H. L., & Vyas, J. M. (2011). The tetraspanin CD82 is specifically recruited to fungal and bacterial phagosomes prior to acidification. *Infection and Immunity*, *79*(3), 1098–1106. https://doi.org/10.1128/IAI.01135-10.

Audouze, K., & Taboureau, O. (2022). Emerging Bioinformatics Methods and Resources in Drug Toxicology. *Methods in Molecular Biology*, 2425, 133–146. https://doi.org/10.1007/978-1-0716-1960-5_6.

Bagrov, D. V., Senkovenko, A. M., Nikishin, I. I., Skryabin, G. O., Kopnin, P. B., & Tchevkina, E. M. (2021). Application of AFM, TEM, and NTA for characterization of exosomes produced by placenta-derived mesenchymal cells. *Journal of Physics: Conference Series, 1942*(1), 012013. https://doi.org/10.1088/1742-6596/1942/1/012013.

Bailly, C., & Thuru, X. (2023). Targeting of Tetraspanin CD81 with Monoclonal Antibodies and Small Molecules to Combat Cancers and Viral Diseases. *Cancers, 15*(7), 2186. https://doi.org/10.3390/cancers15072186.

Barbosa, M. M. F., Kanno, A. I., Barazzone, G. C., Rodriguez, D., Pancakova, V., Trentini, M., Faquim-Mauro, E. L., Freitas, A. P., Khouri, M. I., Lobo-Silva, J., Goncalves, V. M., Schenkman, R. P. F., Tanizaki, M. M., Boraschi, D., Malley, R., Farias, L. P., & Leite, L. C. C. (2021). Robust Immune Response Induced by *Schistosoma mansoni* TSP-2 Antigen Coupled to Bacterial Outer Membrane Vesicles. *International Journal of Nanomedicine, 16*, 7153–7168. https://doi.org/10.2147/IJN.S315786.

Barry, J. D., & McCulloch, R. (2001). Antigenic variation in trypanosomes: enhanced phenotypic variation in a eukaryotic parasite. *Advances in Parasitology,* 49, 1–70. https://doi.org/10.1016/s0065-308x(01)49037-3.

Becic, A., Leifeld, J., Shaukat, J., & Hollmann, M. (2022). Tetraspanins as Potential Modulators of Glutamatergic Synaptic Function. *Frontiers in Molecular Neuroscience*, 14, 801882. https://doi.org/10.3389/fnmol.2021.801882.

Bennouna, S., Bliss, S. K., Curiel, T. J., & Denkers, E. Y. (2003). Cross-talk in the innate immune system: neutrophils instruct recruitment and activation of dendritic cells during microbial infection. *Journal of Immunology 171*(11), 6052–6058. https://doi.org/10.4049/jimmunol.171.11.6052.

Berditchevski, F., & Odintsova, E. (2006). Tetraspanins as regulators of protein trafficking. *Traffic, 8*(2), 89–96. https://doi.org/10.1111/j.1600-0854.2006.00515.x.

Berger, A. (2000). Science commentary: Th1 and Th2 responses: What are they? *BMJ, 321*(7258), 424-424. doi:10.1136/bmj.321.7258.424.

Bhopale G. M. (2003). Pathogenesis of toxoplasmosis. *Comparative Immunology, Microbiology, and Infectious Diseases*, *26*(4), 213–222. https://doi.org/10.1016/S0147-9571(02)00058-9.

Boavida, L. C., Qin, P., Broz, M., Becker, J. D., & McCormick, S. (2013). Arabidopsis tetraspanins are confined to discrete expression domains and cell types in reproductive tissues and form homo- and heterodimers when expressed in yeast. *Plant Physiology*, *163*(2), 696–712. https://doi.org/10.1104/pp.113.216598.

Bogale, M., Baniya, A., & DiGennaro, P. (2020). Nematode Identification Techniques and Recent Advances. *Plants, 9*(10), 1260. https://doi.org/10.3390/plants9101260.

Bolte, S., & Cordelières, F. P. (2006). A guided tour into subcellular colocalization analysis in light microscopy. *Journal of Microscopy*, *224*(Pt 3), 213–232. https://doi.org/10.1111/j.1365-2818.2006.01706.x.

Borelli, V., Vita, F., Shankar, S., Soranzo, M., Banfi, E., & Scialino, G. et al. (2003). Human Eosinophil Peroxidase Induces Surface Alteration, Killing, and Lysis of Mycobacterium tuberculosis. *Infection and Immunity*, *71*(2), 605-613. doi: 10.1128/iai.71.2.605-613.2003.

Bredtmann, C. M., Krücken, J., Murugaiyan, J., Kuzmina, T., & von Samson-Himmelstjerna, G. (2017). Nematode Species Identification-Current Status, Challenges and Future Perspectives for Cyathostomins. *Frontiers in Cellular and Infection Microbiology, 7*, 283. https://doi.org/10.3389/fcimb.2017.00283.

Brenner S. (1974). The genetics of *Caenorhabditis elegans*. *Genetics, 77*(1), 71–94. https://doi.org/10.1093/genetics/77.1.71.

Brew, K., & Nagase, H. (2010). The tissue inhibitors of metalloproteinases (TIMPs): an ancient family with structural and functional diversity. *Biochimica et Biophysica Acta, 1803*(1), 55–71. https://doi.org/10.1016/j.bbamcr.2010.01.003.

Broekmans, O. D., Rodgers, J. B., Ryu, W. S., & Stephens, G. J. (2016). Resolving coiled shapes reveals new reorientation behaviors in *C. elegans. eLife, 5*, e17227. https://doi.org/10.7554/eLife.17227.

Bruschi, F., & Pinto, B. (2013). The significance of matrix metalloproteinases in parasitic infections involving the central nervous system. *Pathogens, 2*(1), 105–129. https://doi.org/10.3390/pathogens2010105.

Bubier, J. A., Sutphin, G. L., Reynolds, T. J., Korstanje, R., Fuksman-Kumpa, A., Baker, E. J., Langston, M. A., & Chesler, E. J. (2019). Integration of heterogeneous functional genomics data in gerontology research to find genes and pathway underlying aging across species. *PLOS ONE, 14*(4). https://doi.org/10.1371/journal.pone.0214523.

Burns, A.R. et al. (2020) 'Author correction: *Caenorhabditis elegans* is a useful model for anthelmintic discovery', *Nature Communications, 11*(1). doi:10.1038/s41467-020-17617-3.

Bystrom, J., Amin, K., & Bishop-Bailey, D. (2011). Analysing the eosinophil cationic protein--a clue to the function of the eosinophil granulocyte. *Respiratory Research, 12*, 10. https://doi.org/10.1186/1465-9921-12-10.

Caminati, M., Pham, D. L., Bagnasco, D., & Canonica, G. W. (2018). Type 2 immunity in asthma. *The World Allergy Organization Journal*, *11*(1), 13. https://doi.org/10.1186/s40413-018-0192-5.

Cantacessi, C., Hofmann, A., Pickering, D., Navarro, S., Mitreva, M., & Loukas, A. (2013). TIMPs of parasitic helminths - a large-scale analysis of high-throughput sequence datasets. *Parasites & Vectors, 6*, 156. https://doi.org/10.1186/1756-3305-6-156.

Canton, L., Lanusse, C., & Moreno, L. (2021). Rational Pharmacotherapy in Infectious Diseases: Issues Related to Drug Residues in Edible Animal Tissues. *Animals : An*

Open Access Journal from MDPI, 11(10), 2878. https://doi.org/10.3390/ani11102878.

Castelletto, M. L., Gang, S. S., & Hallem, E. A. (2020). Recent advances in functional genomics for parasitic nematodes of mammals. *The Journal of Experimental Biology*, *223*(Pt Suppl 1), jeb206482. https://doi.org/10.1242/jeb.206482.

CDC - Parasites - About Parasites. (2016, April 22). Retrieved April 2, 2020, from https://www.cdc.gov/parasites/about.html.

Chai, J.-Y. (2013). Praziquantel Treatment in Trematode and Cestode Infections: An Update. *Infection & Chemotherapy*, *45*(1), 32. doi: 10.3947/ic.2013.45.1.32.

Chang, N. C. (2020). Autophagy and stem cells: Self-eating for self-renewal. *Frontiers in Cell and Developmental Biology*, *8*. https://doi.org/10.3389/fcell.2020.00138.

Charlier, J. et al. (2020) "Initial assessment of the economic burden of major parasitic helminth infections to the ruminant livestock industry in Europe," *Preventive Veterinary Medicine*, *182*, p. 105103. https://doi.org/10.1016/j.prevetmed.2020.105103.

Charrin, S., Jouannet, S., Boucheix, C., & Rubinstein, E. (2014). Tetraspanins at a glance. *Journal of Cell Science*, *127*(17), 3641-3648. doi: 10.1242/jcs.154906.

Chen, J., Li, P., Zhang, T., Xu, Z., Huang, X., Wang, R., & Du, L. (2022). Review on Strategies and Technologies for Exosome Isolation and Purification. *Frontiers in Bioengineering and Biotechnology*, *9*, 811971. https://doi.org/10.3389/fbioe.2021.811971.

Chen, Y., Scarcelli, V., & Legouis, R. (2017). Approaches for Studying Autophagy in *Caenorhabditis elegans*. *Cells*, *6*(3), 27. https://doi.org/10.3390/cells6030027.

Cheng, G., Salerno, J. C., Cao, Z., Pagano, P. J., & Lambeth, J. D. (2008). Identification and characterization of VPO1, a new animal heme-containing peroxidase. *Free Radical Biology & Medicine*, *45*(12), 1682–1694. https://doi.org/10.1016/j.freeradbiomed.2008.09.009.

Choi, P., & Reiser, H. (1998). IL-4: role in disease and regulation of production. *Clinical and Experimental Immunology, 113*(3), 317–319. https://doi.org/10.1046/j.1365-2249.1998.00690.x.

Chulanetra, M., & Chaicumpa, W. (2021). Revisiting the Mechanisms of Immune Evasion Employed by Human Parasites. *Frontiers in Cellular and Infection Microbiology, 11*, 702125. https://doi.org/10.3389/fcimb.2021.702125.

Clark, I. C., Mudvari, P., Thaploo, S., Smith, S., Abu-Laban, M., Hamouda, M., Theberge, M., Shah, S., Ko, S. H., Pérez, L., Bunis, D. G., Lee, J. S., Kilam, D., Zakaria, S., Choi, S., Darko, S., Henry, A. R., Wheeler, M. A., Hoh, R., … Boritz, E. A. (2023). HIV silencing and cell survival signatures in infected T cell reservoirs. *Nature, 614*(7947), 318–325. https://doi.org/10.1038/s41586-022-05556-6.

Coakley, G., Buck, A., & Maizels, R. (2016). Host parasite communications—Messages from helminths for the immune system. *Molecular and Biochemical Parasitology, 208*(1), 33-40. doi: 10.1016/j.molbiopara.2016.06.003.

Codd, A., Teuscher, F., Kyle, D. E., Cheng, Q., & Gatton, M. L. (2011). Artemisinin-induced parasite dormancy: a plausible mechanism for treatment failure. *Malaria Journal*, *10*(1), 56. doi: 10.1186/1475-2875-10-56.

Cohen, F. E., & Sternberg, M. J. E. (1980). On the prediction of protein structure: The significance of the root-mean-square deviation. *Journal of Molecular Biology, 138*(2), 321–333. https://doi.org/10.1016/0022-2836(80)90289-2.

Colombo, M., Raposo, G., & Théry, C. (2014). Biogenesis, secretion, and intercellular interactions of exosomes and other extracellular vesicles. *Annual Review of Cell and Developmental Biology, 30*, 255–289. https://doi.org/10.1146/annurev-cellbio-101512-122326.

Colombo, M., Moita, C., van Niel, G., Kowal, J., Vigneron, J., Benaroch, P., Manel, N., Moita, L. F., Théry, C., & Raposo, G. (2013). Analysis of ESCRT functions in exosome biogenesis, composition and secretion highlights the heterogeneity of extracellular vesicles. *Journal of Cell Science*, *126*(Pt 24), 5553–5565. https://doi.org/10.1242/jcs.128868.

Cooper, P. (2009). Interactions between helminth parasites and allergy. *Current Opinion in Allergy and Clinical Immunology, 9*(1), 29-37. doi: 10.1097/ACI.0b013e32831f44a6.

Corthay, A. (2009). How do Regulatory T Cells Work? *Scandinavian Journal of Immunology, 70*(4), 326-336. doi:10.1111/j.1365-3083.2009.02308.x.

Costa, S., Ragusa, M. A., Lo Buglio, G., Scilabra, S. D., & Nicosia, A. (2022). The repertoire of tissue inhibitors of metalloproteases: Evolution, regulation of extracellular matrix proteolysis, engineering and therapeutic challenges. *Life, 12*(8), 1145. https://doi.org/10.3390/life12081145.

Croll, N. A., Smith, J. M., & Zuckerman, B. M. (1977). The aging process of the nematode *Caenorhabditis elegans* in bacterial and axenic culture. *Experimental Aging Research, 3*(3), 175–189. https://doi.org/10.1080/03610737708257101.

Dang, Z., Feng, J., Yagi, K., Sugimoto, C., Li, W., & Oku, Y. (2012). Mucosal Adjuvanticity of Fibronectin-Binding Peptide (FBP) Fused with *Echinococcus multilocularis* Tetraspanin 3: Systemic and Local Antibody Responses. *PLOS Neglected Tropical Diseases, 6*(9). doi:10.1371/journal.pntd.0001842.

Das, G., Shravage, B. V., & Baehrecke, E. H. (2012). Regulation and function of autophagy during cell survival and cell death. *Cold Spring Harbor Perspectives in Biology, 4*(6), a008813. https://doi.org/10.1101/cshperspect.a008813.

Dauros-Singorenko, P., Blenkiron, C., Phillips, A., & Swift, S. (2018). The functional RNA cargo of bacterial membrane vesicles. *FEMS Microbiology Letters, 365*(5). doi: 10.1093/femsle/fny023.

Davies, A. G., & McIntire, S. L. (2004). Using *C. elegans* to screen for targets of ethanol and behavior-altering drugs. *Biological Procedures Online, 6*, 113–119. https://doi.org/10.1251/bpo79.

Deleyto-Seldas, N., & Efeyan, A. (2021). The mtor–autophagy axis and the control of metabolism. *Frontiers in Cell and Developmental Biology, 9*. https://doi.org/10.3389/fcell.2021.655731.

Deo, S., Mistry, K., Kakade, A., & Niphadkar, P. (2010). Role played by Th2 type cytokines in IgE mediated allergy and asthma. *Lung India, 27*(2), 66. doi:10.4103/0970-2113.63609.

De la Parra-Guerra, A., & Olivero-Verbel, J. (2020). Toxicity of nonylphenol and nonylphenol ethoxylate on *Caenorhabditis elegans*. *Ecotoxicology and Environmental Safety, 187*, 109709. https://doi.org/10.1016/j.ecoenv.2019.109709.

Ding, X., Cao, Y., Xing, Y., Ge, S., Lin, M., & Li, J. (2019). TIMP-1 mediates inflammatory and immune response to IL-6 in adult orbital xanthogranulomatous disease. *Ocular Immunology and Inflammation, 28*(2), 288–297. https://doi.org/10.1080/09273948.2019.1581227.

Dong, C., & Flavell, R.A. (2000). Cell fate decision: T-helper 1 and 2 subsets in immune responses. *Arthritis Research and Therapy 2*, 179 . https://doi.org/10.1186/ar85.

Donskow-Łysoniewska, K., Maruszewska-Cheruiyot, M., & Stear, M. (2021). The interaction of host and nematode galectins influences the outcome of gastrointestinal nematode infections. *Parasitology, 148*(6), 648–654. https://doi.org/10.1017/s003118202100007x.

Doyle, E., Ridger, V., Ferraro, F., Turmaine, M., Saftig, P., & Cutler, D. (2011). CD63 is an essential cofactor to leukocyte recruitment by endothelial P-selectin. *Blood, 118*(15), 4265-4273. doi: 10.1182/blood-2010-11-321489.

Doyle, L. M., & Wang, M. Z. (2019). Overview of Extracellular Vesicles, Their Origin, Composition, Purpose, and Methods for Exosome Isolation and Analysis. *Cells, 8*(7), 727. https://doi.org/10.3390/cells8070727.

Drurey, C., & Maizels, R. M. (2021). Helminth extracellular vesicles: Interactions with the host immune system. *Molecular Immunology, 137*, 124–133. https://doi.org/10.1016/j.molimm.2021.06.017.

Dunlock V. E. (2020). Tetraspanin CD53: an overlooked regulator of immune cell function. *Medical Microbiology and Immunology, 209*(4), 545–552. https://doi.org/10.1007/s00430-020-00677-z.

Eberle, J. U., & Voehringer, D. (2016). Role of basophils in protective immunity to parasitic infections. *Seminars in Immunopathology, 38*(5), 605–613. https://doi.org/10.1007/s00281-016-0563-3.

Edgar, J. R., Eden, E. R., & Futter, C. E. (2014). Hrs- and CD63-dependent competing mechanisms make different sized endosomal intraluminal vesicles. *Traffic, 15*(2), 197–211. https://doi.org/10.1111/tra.12139.

Edwards, D. R., Handsley, M. M., & Pennington, C. J. (2008). The ADAM metalloproteinases. *Molecular Aspects of Medicine, 29*(5), 258–289. https://doi.org/10.1016/j.mam.2008.08.001.

Egea, V., Zahler, S., Rieth, N., Neth, P., Popp, T., Kehe, K., Jochum, M., & Ries, C. (2012). Tissue inhibitor of metalloproteinase-1 (TIMP-1) regulates mesenchymal stem cells through let-7f microrna and Wnt/β-catenin signaling. *Proceedings of the National Academy of Sciences, 109*(6). https://doi.org/10.1073/pnas.1115083109.

Ehrens, A., Lenz, B., Neumann, A.-L., Giarrizzo, S., Reichwald, J. J., Frohberger, S. J., Stamminger, W., Buerfent, B. C., Fercoq, F., Martin, C., Kulke, D., Hoerauf, A., & Hübner, M. P. (2021). Microfilariae trigger eosinophil extracellular DNA traps in a dectin-1-dependent manner. *Cell Reports, 34*(2), 108621. https://doi.org/10.1016/j.celrep.2020.108621.

Elfawal, M. A., Savinov, S. N., & Aroian, R. V. (2019). Drug screening for discovery of broad-spectrum agents for soil-transmitted nematodes. *Scientific Reports, 9*(1). https://doi.org/10.1038/s41598-019-48720-1.

Engel, P., Boumsell, L., Balderas, R., Bensussan, A., Gattei, V., Horejsi, V., Jin, B. Q., Malavasi, F., Mortari, F., Schwartz-Albiez, R., Stockinger, H., van Zelm, M. C., Zola, H., & Clark, G. (2015). CD Nomenclature 2015: Human Leukocyte Differentiation Antigen Workshops as a Driving Force in Immunology. *Journal of Immunology, 195*(10), 4555–4563. https://doi.org/10.4049/jimmunol.1502033.

Enokihara, H., & Koike, T. (1993). Biochemistry and biological activities of eosinophil granule proteins. Nihon rinsho. *Japanese Journal of Clinical Medicine, 51*(3), 605–612.

Erdmann, S. M., Heussen, N., Moll-Slodowy, S., Merk, H. F., & Sachs, B. (2003). CD63 expression on basophils as a tool for the diagnosis of pollen-associated food allergy: sensitivity and specificity. *Clinical and Experimental Allergy : Journal of the British Society for Allergy and Clinical Immunology*, *33*(5), 607–614. https://doi.org/10.1046/j.1365-2222.2003.01660.x.

Farquhar, M. J., Hu, K., Harris, H. J., Davis, C., Brimacombe, C. L., Fletcher, S. J., Baumert, T. F., Rappoport, J. Z., Balfe, P., & McKeating, J. A. (2012). Hepatitis C virus induces CD81 and claudin-1 endocytosis. *Journal of Virology*, *86*(8), 4305–4316. https://doi.org/10.1128/JVI.06996-11.

Fénéant, L., Levy, S., & Cocquerel, L. (2014). CD81 and hepatitis C virus (HCV) infection. *Viruses*, *6(*2), 535–572. https://doi.org/10.3390/v6020535.

Fitzsimmons, C. M., Falcone, F. H., & Dunne, D. W. (2014). Helminth Allergens, Parasite-Specific IgE, and Its Protective Role in Human Immunity. *Frontiers in Immunology*, *5*, 61. https://doi.org/10.3389/fimmu.2014.00061.

Florin, L., & Lang, T. (2018). Tetraspanin Assemblies in Virus Infection. *Frontiers in Immunology*, *9*, 1140. https://doi.org/10.3389/fimmu.2018.01140.

Forte, D., Salvestrini, V., Corradi, G., Rossi, L., Catani, L., Lemoli, R. M., Cavo, M., & Curti, A. (2017). The tissue inhibitor of metalloproteinases-1 (TIMP-1) promotes survival and migration of acute myeloid leukaemia cells through CD63/PI3K/Akt/p21 signalling. *Oncotarget*, *8*(2), 2261–2274. https://doi.org/10.18632/oncotarget.13664.

Fröhlich, E., & Wahl, R. (2017). Thyroid Autoimmunity: Role of Anti-thyroid Antibodies in Thyroid and Extra-Thyroidal Diseases. *Frontiers in Immunology*, *8*, 521. https://doi.org/10.3389/fimmu.2017.00521.

Furtado, L. F. V., Ana Cristina Passos De Paiva Bello, & Rabelo, É. M. L. (2016). Benzimidazole resistance in helminths: From problem to diagnosis. *Acta Tropica*, *162*, 95–102. doi: 10.1016/j.actatropica.2016.06.021.

Fu, E., Pan, L., Xie, Y., Mu, D., Liu, W., Jin, F., & Bai, X. (2015). Tetraspanin CD63 is a regulator of HIV-1 replication. *International Journal of Clinical and Experimental Pathology, 8*(2), 1184–1198.

Galli, S. J., & Tsai, M. (2012). IgE and mast cells in allergic disease. *Nature Medicine, 18*(5), 693–704. https://doi.org/10.1038/nm.2755.

Gang, S. S., & Hallem, E. A. (2016). Mechanisms of host seeking by parasitic nematodes. *Molecular and Biochemical Parasitology, 208*(1), 23–32. https://doi.org/10.1016/j.molbiopara.2016.05.007.

Grande, F., Occhiuzzi, M. A., Rizzuti, B., Ioele, G., De Luca, M., Tucci, P., Svicher, V., Aquaro, S., & Garofalo, A. (2019). CCR5/CXCR4 Dual Antagonism for the Improvement of HIV Infection Therapy. *Molecules, 24*(3), 550. https://doi.org/10.3390/molecules24030550.

Green, L., Monk, P., Partridge, L., Morris, P., Gorringe, A., & Read, R. (2011). Cooperative Role for Tetraspanins in Adhesin-Mediated Attachment of Bacterial Species to Human Epithelial Cells. *Infection and Immunity, 79*(6), 2241-2249. doi: 10.1128/iai.01354-10.

Gurung, S., Perocheau, D., Touramanidou, L., & Baruteau, J. (2021). The exosome journey: from biogenesis to uptake and intracellular signalling. *Cell Communication and Signaling : CCS, 19*(1), 47. https://doi.org/10.1186/s12964-021-00730-1.

Hahnel, S. R., Dilks, C. M., Heisler, I., Andersen, E. C., & Kulke, D. (2020). *Caenorhabditis elegans* in anthelmintic research - Old model, new perspectives. *International Journal for Parasitology- Drugs and Drug Resistance, 14*, 237–248. https://doi.org/10.1016/j.ijpddr.2020.09.005.

Han SK, Lee D, Lee H, Kim D, et al. 2016 OASIS 2: online application for survival analysis 2 with features for the analysis of maximal lifespan and health span in aging research. *Oncotarget* 11269.

Hawrylowicz C. M. (2005). Regulatory T cells and IL-10 in allergic inflammation. *The Journal of Experimental Medicine, 202*(11), 1459–1463. https://doi.org/10.1084/jem.20052211.

Heissig, B., Nishida, C., Tashiro, Y., Sato, Y., Ishihara, M., Ohki, M., Gritli, I., Rosenkvist, J., & Hattori, K. (2010). Role of neutrophil-derived matrix metalloproteinase-9 in tissue regeneration. *Histology and Histopathology, 25*(6), 765–770. https://doi.org/10.14670/HH-25.765.

Heshof, R., Visscher, B., Prömel, S., & Hughes, S. (2019). Large-scale cultivation of *Caenorhabditis elegans* in a bioreactor using a labor-friendly fed-batch approach. *BioTechniques*, *67*(1), 33–39. https://doi.org/10.2144/btn-2019-0008.

Hillier, L. D. W., Coulson, A., Murray, J. I., Bao, Z., Sulston, J. E., & Waterston, R. H. (2005). Genomics in *C. elegans*: So many genes, such a little worm: Table 1. *Genome Research, 15*(12), 1651–1660. https://doi.org/10.1101/gr.3729105.

Hotaling, S., Kelley, J. L., & Frandsen, P. B. (2021). Towards a genome sequence for every animal: Where are we now? https://doi.org/10.1101/2021.08.04.455150.

Hu, D., Song, X., Xie, Y., Zhong, X., Wang, N., Zheng, Y……. Yang, G. (2015). Molecular insights into a tetraspanin in the hydatid tapeworm *Echinococcus granulosus*. *Parasites & Vectors, 8*(1). doi: 10.1186/s13071-015-0926-y.

Huang, C., Hays, F. A., Tomasek, J. J., Benyajati, S., & Zhang, X. A. (2019). Tetraspanin CD82 interaction with cholesterol promotes extracellular vesicle-mediated release of ezrin to inhibit tumour cell movement. *Journal of extracellular vesicles*, *9*(1), 1692417. https://doi.org/10.1080/20013078.2019.1692417.

Hurwitz, S. N., Cheerathodi, M. R., Nkosi, D., York, S. B., & Meckes, D. G., Jr (2018). Tetraspanin CD63 Bridges Autophagic and Endosomal Processes To Regulate Exosomal Secretion and Intracellular Signaling of Epstein-Barr Virus LMP1. *Journal of Virology*, *92*(5), e01969-17. https://doi.org/10.1128/JVI.01969-17.

Huynh, K. K., Eskelinen, E. L., Scott, C. C., Malevanets, A., Saftig, P., & Grinstein, S. (2007). LAMP proteins are required for fusion of lysosomes with phagosomes. *The EMBO Journal, 26*(2), 313–324. https://doi.org/10.1038/sj.emboj.7601511.

Hwang, A. B., Ryu, E. A., Artan, M., Chang, H. W., Kabir, M. H., Nam, H. J., Lee, D., Yang, J. S., Kim, S., Mair, W. B., Lee, C., Lee, S. S., & Lee, S. J. (2014). Feedback regulation via AMPK and HIF-1 mediates ROS-dependent longevity in *Caenorhabditis elegans*. *Proceedings of the National Academy of Sciences of the United States of America, 111*(42), E4458–E4467. https://doi.org/10.1073/pnas.1411199111.

Iliff, A. J., & Xu, X. Z. S. (2020). *C. elegans*: a sensible model for sensory biology. *Journal of Neurogenetics, 34*(3-4), 347–350. https://doi.org/10.1080/01677063.2020.1823386

Inclan-Rico, J. M., & Siracusa, M. C. (2018). First Responders: Innate Immunity to Helminths. *Trends in Parasitology, 34*(10), 861–880. https://doi.org/10.1016/j.pt.2018.08.007.

Israels, S. J., McMillan-Ward, E. M., Easton, J., Robertson, C., & McNicol, A. (2001). CD63 associates with the alphaIIb beta3 integrin-CD9 complex on the surface of activated platelets. *Thrombosis and Haemostasis, 85*(1), 134–141.

Iyer, S. S., & Cheng, G. (2012). Role of interleukin 10 transcriptional regulation in inflammation and autoimmune disease. *Critical Reviews in Immunology, 32*(1), 23–63. https://doi.org/10.1615/critrevimmunol.v32.i1.30.

Jaiswal, J. K., Andrews, N. W., & Simon, S. M. (2002). Membrane proximal lysosomes are the major vesicles responsible for calcium-dependent exocytosis in nonsecretory cells. *The Journal of Cell Biology, 159*(4), 625–635. https://doi.org/10.1083/jcb.200208154.

Jankovic, D., & Feng, C. G. (2015). CD4(+) T Cell Differentiation in Infection: Amendments to the Th1/Th2 Axiom. *Frontiers in Immunology, 6*, 198. https://doi.org/10.3389/fimmu.2015.00198.

Jankovičová, J., Sečová, P., Michalková, K., & Antalíková, J. (2020). Tetraspanins, More than Markers of Extracellular Vesicles in Reproduction. *International Journal of Molecular Sciences, 21*(20), 7568. https://doi.org/10.3390/ijms21207568.

Jégou, A., Ziyyat, A., Barraud-Lange, V., Perez, E., Wolf, J. P., Pincet, F., & Gourier, C. (2011). CD9 tetraspanin generates fusion competent sites on the egg membrane for mammalian fertilization. *Proceedings of the National Academy of Sciences of the United States of America, 108*(27), 10946–10951. https://doi.org/10.1073/pnas.1017400108.

Jiang, X., Zhang, J., & Huang, Y. (2015). Tetraspanins in cell migration. *Cell Adhesion & Migration, 9*(5), 406–415. doi:10.1080/19336918.2015.1005465.

Jones, D. T., Taylor, W. R., & Thornton, J. M. (1992). The rapid generation of mutation data matrices from protein sequences. *Computer Applications in the Biosciences : CABIOS, 8*(3), 275–282. https://doi.org/10.1093/bioinformatics/8.3.275.

Jouvenet, N., Zhadina, M., Bieniasz, P. D., & Simon, S. M. (2011). Dynamics of ESCRT protein recruitment during retroviral assembly. *Nature Cell Biology, 13*(4), 394–401. https://doi.org/10.1038/ncb2207.

Jovic, K., Sterken, M. G., Grilli, J., Bevers, R. P. J., Rodriguez, M., Riksen, J. A. G., Allesina, S., Kammenga, J. E., & Snoek, L. B. (2017). Temporal dynamics of gene expression in heat-stressed *Caenorhabditis elegans*. *PLOS ONE, 12*(12), e0189445. https://doi.org/10.1371/journal.pone.0189445.

Jumper, J et al. Highly accurate protein structure prediction with AlphaFold. *Nature* (2021).

Jung, K. K., Liu, X. W., Chirco, R., Fridman, R., & Kim, H. R. (2006). Identification of CD63 as a tissue inhibitor of metalloproteinase-1 interacting cell surface protein. *The EMBO Journal, 25*(17), 3934–3942. https://doi.org/10.1038/sj.emboj.7601281.

Jung, S. K., Aleman-Meza, B., Riepe, C., & Zhong, W. (2014). QuantWorm: a comprehensive software package for *Caenorhabditis elegans* phenotypic assays. *PLOS ONE, 9*(1), e84830. https://doi.org/10.1371/journal.pone.0084830.

Justo, B. L., & Jasiulionis, M. G. (2021). Characteristics of TIMP1, CD63, and β1-Integrin and the Functional Impact of Their Interaction in Cancer. *International Journal of Molecular Sciences, 22*(17), 9319. https://doi.org/10.3390/ijms22179319.

Källquist, L., Hansson, M., Persson, A. M., Janssen, H., Calafat, J., Tapper, H., & Olsson, I. (2008). The tetraspanin CD63 is involved in granule targeting of neutrophil elastase. *Blood, 112*(8), 3444–3454. https://doi.org/10.1182/blood-2007-10-116285.

Kaminsky, R., Ducray, P., Jung, M., Clover, R., Rufener, L., Bouvier, J., Weber, S. S., Wenger, A., Wieland-Berghausen, S., Goebel, T., Gauvry, N., Pautrat, F., Skripsky, T., Froelich, O., Komoin-Oka, C., Westlund, B., Sluder, A., & Mäser, P. (2008). A new class of anthelmintics effective against drug-resistant nematodes. *Nature, 452*(7184), 176–180. https://doi.org/10.1038/nature06722.

Kanhere, A., Hertweck, A., Bhatia, U., Gökmen, M., Perucha, E., & Jackson, I. et al. (2012). T-bet and GATA3 orchestrate Th1 and Th2 differentiation through lineage-specific targeting of distal regulatory elements. *Nature Communications, 3*(1). doi: 10.1038/ncomms2260.

Kaul, Z., Mookherjee, D., Das, S., Chatterjee, D., Chakrabarti, S., & Chakrabarti, O. (2020). Loss of tumor susceptibility gene 101 (TSG101) perturbs endoplasmic reticulum structure and function. *Biochimica et Biophysica Acta (BBA) - Molecular Cell Research, 1867*(9), 118741. https://doi.org/10.1016/j.bbamcr.2020.118741.

Khantakova, J. N., Bulygin, A. S., & Sennikov, S. V. (2022). The Regulatory-T-Cell Memory Phenotype: What We Know. *Cells, 11*(10), 1687. https://doi.org/10.3390/cells11101687.

Khushman, M., Bhardwaj, A., Patel, G. K., Laurini, J. A., Roveda, K., Tan, M. C., Patton, M. C., Singh, S., Taylor, W., & Singh, A. P. (2017). Exosomal Markers (CD63 and CD9) Expression Pattern Using Immunohistochemistry in Resected Malignant and Nonmalignant Pancreatic Specimens. *Pancreas, 46*(6), 782–788. https://doi.org/10.1097/MPA.0000000000000847.

Kidd, P. (2003). Th1/Th2 Balance: The Hypothesis, its Limitations, and Implications for Health and Disease. *Alternative medicine Review : A Journal of Clinical Therapeutic, 8.* 223-46.

Kirienko, N. V., Kirienko, D. R., Larkins-Ford, J., Wählby, C., Ruvkun, G., & Ausubel, F. M. (2013). Pseudomonas aeruginosa disrupts *Caenorhabditis elegans* iron homeostasis, causing a hypoxic response and death. *Cell Host & Microbe, 13*(4), 406–416. https://doi.org/10.1016/j.chom.2013.03.003.

Kitadokoro, K., Bordo, D., Galli, G., Petracca, R., Falugi, F., Abrignani, S., … Bolognesi, M. (2001). CD81 extracellular domain 3D structure: insight into the tetraspanin superfamily structural motifs. *The EMBO Journal, 20*(1-2), 12–18. doi:10.1093/emboj/20.1.12.

Kobuch, J., Cui, H., Grünwald, B., Saftig, P., Knolle, P. A., & Krüger, A. (2015). TIMP-1 signaling via CD63 triggers granulopoiesis and neutrophilia in mice. *Haematologica, 100*(8), 1005–1013. https://doi.org/10.3324/haematol.2014.121590.

Kozak, F., & Kurzbach, D. (2021). How to assess the structural dynamics of transcription factors by integrating sparse NMR and EPR constraints with molecular dynamics simulations. *Computational and Structural Biotechnology Journal, 19*, 2097–2105. https://doi.org/10.1016/j.csbj.2021.04.020.

Kraft, S., Jouvin, M. H., Kulkarni, N., Kissing, S., Morgan, E. S., Dvorak, A. M., Schröder, B., Saftig, P., & Kinet, J. P. (2013). The tetraspanin CD63 is required for efficient IgE-mediated mast cell degranulation and anaphylaxis. *Journal of Immunology, 191*(6), 2871–2878. https://doi.org/10.4049/jimmunol.1202323.

Kraft, S., Fleming, T., Billingsley, J. M., Lin, S. Y., Jouvin, M. H., Storz, P., & Kinet, J. P. (2005). Anti-CD63 antibodies suppress IgE-dependent allergic reactions in vitro and in vivo. *The Journal of Experimental Medicine, 201*(3), 385–396. https://doi.org/10.1084/jem.20042085.

Krammer, S., Sicorschi Gutu, C., Grund, J. C., Chiriac, M. T., Zirlik, S., & Finotto, S. (2021). Regulation and function of Interferon-lambda (ifnλ) and its receptor in asthma. *Frontiers in Immunology, 12*. https://doi.org/10.3389/fimmu.2021.731807.

Krystel-Whittemore, M., Dileepan, K. N., & Wood, J. G. (2016). Mast Cell: A Multi-Functional Master Cell. *Frontiers in Immunology, 6*, 620. https://doi.org/10.3389/fimmu.2015.00620.

Kumari, S., & Kumar, P. (2023). Design and computational analysis of an MMP9 inhibitor in hypoxia-induced glioblastoma multiforme. *ACS Omega, 8*(11), 10565–10590. https://doi.org/10.1021/acsomega.3c00441.

Kummer, D., Steinbacher, T., Schwietzer, M. F., Thölmann, S., & Ebnet, K. (2020). Tetraspanins: integrating cell surface receptors to functional microdomains in homeostasis and disease. *Medical Microbiology and Immunology, 209*(4), 397–405. https://doi.org/10.1007/s00430-020-00673-3.

Kumsta, C., Chang, J. T., Schmalz, J., & Hansen, M. (2017). Hormetic heat stress and HSF-1 induce autophagy to improve survival and proteostasis in *C. elegans*. *Nature Communications, 8*, 14337. https://doi.org/10.1038/ncomms14337.

Lacy P. (2006). Mechanisms of degranulation in neutrophils. *Allergy, Asthma, and Clinical Immunology : Official Journal of the Canadian Society of Allergy and Clinical Immunology*, *2*(3), 98–108. https://doi.org/10.1186/1710-1492-2-3-98.

Lai, C. H., Chou, C. Y., Ch'ang, L. Y., Liu, C. S., & Lin, W. (2000). Identification of novel human genes evolutionarily conserved in *Caenorhabditis elegans* by comparative proteomics. *Genome Research, 10*(5), 703–713. https://doi.org/10.1101/gr.10.5.703.

Lamitina, S. T., Morrison, R., Moeckel, G. W., & Strange, K. (2004). Adaptation of the nematode *Caenorhabditis elegans* to extreme osmotic stress. *American Journal of Physiology -Cell Physiology*, *286*(4), C785–C791. https://doi.org/10.1152/ajpcell.00381.2003.

Larson, D., Hübner, M. P., Torrero, M. N., Morris, C. P., Brankin, A., Swierczewski, B. E., Davies, S. J., Vonakis, B. M., & Mitre, E. (2012). Chronic helminth infection reduces basophil responsiveness in an IL-10-dependent manner. *Journal of Immunology, 188*(9), 4188–4199. https://doi.org/10.4049/jimmunol.1101859.

Lasswitz, L., Zapatero-Belinchón, F. J., Moeller, R., Hülskötter, K., Laurent, T., Carlson, L. A., Goffinet, C., Simmons, G., Baumgärtner, W., & Gerold, G. (2022). The Tetraspanin CD81 Is a Host Factor for Chikungunya Virus Replication. *mBio, 13*(3), e0073122. https://doi.org/10.1128/mbio.00731-22.

Lawrence, S. M., Corriden, R., & Nizet, V. (2018). The Ontogeny of a Neutrophil: Mechanisms of Granulopoiesis and Homeostasis. *Microbiology and Molecular Biology Reviews* : *MMBR, 82*(1), e00057-17. https://doi.org/10.1128/MMBR.00057-17.

Lee, J., Jee, C., & McIntire, S. L. (2009). Ethanol preference in *C. elegans*. *Genes, Brain, and Behaviour, 8*(6), 578–585. https://doi.org/10.1111/j.1601-183X.2009.00513.x.

Lee, W., Lee, T. H., Park, B.-J., Chang, J.-W., Yu, J.-R., Koo, H.-S., Park, H., Yoo, Y. J., & Ahnn, J. (2005). *Caenorhabditis elegans* calnexin is n-glycosylated and required for stress response. *Biochemical and Biophysical Research Communications, 338*(2), 1018–1030. https://doi.org/10.1016/j.bbrc.2005.10.041.

Lee, W. C., Russell, B., & Rénia, L. (2022). Evolving perspectives on rosetting in malaria. *Trends in Parasitology, 38*(10), 882–889. https://doi.org/10.1016/j.pt.2022.08.001.

León, B., & Ballesteros-Tato, A. (2021). Modulating th2 cell immunity for the treatment of asthma. *Frontiers in Immunology, 12*. https://doi.org/10.3389/fimmu.2021.637948.

Li, P., Kaslan, M., Lee, S. H., Yao, J., & Gao, Z. (2017). Progress in Exosome Isolation Techniques. *Theranostics, 7*(3), 789–804. https://doi.org/10.7150/thno.18133.

Li, Y.-L., Langley, C. A., Azumaya, C. M., Echeverria, I., Chesarino, N. M., Emerman, M., Cheng, Y., & Gross, J. D. (2023). The structural basis for HIV-1 VIF antagonism of human APOBEC3G. *Nature*. https://doi.org/10.1038/s41586-023-05779-1.

Lighvani, A. A., Frucht, D. M., Jankovic, D., Yamane, H., Aliberti, J., Hissong, B. D., Nguyen, B. V., Gadina, M., Sher, A., Paul, W. E., & O'Shea, J. J. (2001). T-bet is rapidly induced by interferon-gamma in lymphoid and myeloid cells. *Proceedings of the National Academy of Sciences of the United States of America, 98*(26), 15137–15142. https://doi.org/10.1073/pnas.261570598.

Lipper, C. H., Gabriel, K. H., Seegar, T. C. M., Dürr, K. L., Tomlinson, M. G., & Blacklow, S. C. (2022). Crystal structure of the Tspan15 LEL domain reveals a conserved ADAM10 binding site. *Structure, 30*(2), 206–214.e4. https://doi.org/10.1016/j.str.2021.10.007.

Liu Z, Shi H, Liu J (2022) The C. elegans TspanC8 tetraspanin TSP-14 exhibits isoformspecific localization and function. *PLOS Genetics 18*(1): e1009936. https://doi.org/10.1371/journal.pgen.1009936.

Lu, M. R., Lai, C. K., Liao, B. Y., & Tsai, I. J. (2020). Comparative Transcriptomics across Nematode Life Cycles Reveal Gene Expression Conservation and Correlated Evolution in Adjacent Developmental Stages. *Genome Biology and Evolution, 12*(7), 1019–1030. https://doi.org/10.1093/gbe/evaa110.

Ma, Y., Iyer, R. P., de Castro Brás, L. E., Toba, H., Yabluchanskiy, A., Deleon-Pennell, K. Y., Hall, M. E., Lange, R. A., & Lindsey, M. L. (2015). Cross talk between inflammation and extracellular matrix following myocardial infarction. *Inflammation in Heart Failure*, 67–79. https://doi.org/10.1016/b978-0-12-800039-7.00004-9.

Maizels, R., Bundy, D., Selkirk, M., Smith, D., & Anderson, R. (1993). Immunological modulation and evasion by helminth parasites in human populations. *Nature, 365*(6449), 797-805. doi: 10.1038/365797a0.

Maizels, R, & McSorley, H. (2016). Regulation of the host immune system by helminth parasites. *Journal of Allergy and Clinical Immunology, 138*(3), 666-675. doi: 10.1016/j.jaci.2016.07.007.

Majewska, A. A., Huang, T., Han, B., & Drake, J. M. (2021). Predictors of zoonotic potential in helminths. *Philosophical Transactions of the Royal Society of London. Series B, Biological Sciences, 376*(1837), 20200356. https://doi.org/10.1098/rstb.2020.0356.

Makhijani, P., Basso, P. J., Chan, Y. T., Chen, N., Baechle, J., Khan, S., Furman, D., Tsai, S., & Winer, D. A. (2023). Regulation of the immune system by the insulin receptor

in health and disease. *Frontiers in Endocrinology, 14*. https://doi.org/10.3389/fendo.2023.1128622.

Marcilla, A., Martin-Jaular, L., Trelis, M., de Menezes-Neto, A., Osuna, A., Bernal, D., Fernandez-Becerra, C., Almeida, I. C., & Del Portillo, H. A. (2014). Extracellular vesicles in parasitic diseases. *Journal of Extracellular Vesicles, 3*, 25040. https://doi.org/10.3402/jev.v3.25040.

Masciopinto, F., Campagnoli, S., Abrignani, S., Uematsu, Y., & Pileri, P. (2001). The small extracellular loop of CD81 is necessary for optimal surface expression of the large loop, a putative HCV receptor. *Virus Research, 80*(1-2), 1–10. https://doi.org/10.1016/s0168-1702(01)00245-3.

Masucci, M. T., Minopoli, M., Del Vecchio, S., & Carriero, M. V. (2020). The emerging role of neutrophil extracellular traps (nets) in tumor progression and metastasis. *Frontiers in Immunology, 11*. https://doi.org/10.3389/fimmu.2020.01749.

Mathivanan, S., Ji, H., & Simpson, R. J. (2010). Exosomes: extracellular organelles important in intercellular communication. *Journal of Proteomics, 73*(10), 1907–1920. https://doi.org/10.1016/j.jprot.2010.06.006.

Matuszewski, M. A., Tupikowski, K., Dołowy, Ł., Szymańska, B., Dembowski, J., & Zdrojowy, R. (2016). Uroplakins and their potential applications in urology. *Central European Journal of Urology, 69*(3), 252–257. https://doi.org/10.5173/ceju.2016.638.

McSorley, H. J., Chayé, M. A. M., & Smits, H. H. (2019). Worms: Pernicious parasites or allies against allergies?. *Parasite Immunology, 41*(6), e12574. https://doi.org/10.1111/pim.12574.

Messenger, S. W., Woo, S. S., Sun, Z., & Martin, T. F. J. (2018). A Ca^{2+}-stimulated exosome release pathway in cancer cells is regulated by Munc13-4. *The Journal of Cell Biology*, *217*(8), 2877–2890. https://doi.org/10.1083/jcb.201710132.

Miller, C. M., Smith, N. C., Ikin, R. J., Boulter, N. R., Dalton, J. P., & Donnelly, S. (2009). Immunological Interactions between 2 Common Pathogens, Th1-Inducing Protozoan

Toxoplasma gondii and the Th2-Inducing Helminth *Fasciola hepatica*. *PLOS ONE, 4*(5). doi:10.1371/journal.pone.0005692.

Min, B., Brown, M. A., & Legros, G. (2012). Understanding the roles of basophils: breaking dawn. *Immunology, 135*(3), 192–197. https://doi.org/10.1111/j.1365-2567.2011.03530.x.

Min, G., Wang, H., Sun, T. T., & Kong, X. P. (2006). Structural basis for tetraspanin functions as revealed by the cryo-EM structure of uroplakin complexes at 6-A resolution. *The Journal of Cell Biology, 173*(6), 975–983. doi:10.1083/jcb.200602086.

Mkandawire, T. T., Grencis, R. K., Berriman, M., & Duque-Correa, M. A. (2022). Hatching of parasitic nematode eggs: a crucial step determining infection. *Trends in Parasitology, 38*(2), 174–187. https://doi.org/10.1016/j.pt.2021.08.008

Mkupasi, E. M., Sikasunge, C. S., Ngowi, H. A., & Johansen, M. V. (2013). Efficacy and Safety of Anthelmintics Tested against Taenia solium Cysticercosis in Pigs. *PLOS Neglected Tropical Diseases, 7*(7). doi: 10.1371/journal.pntd.0002200.

Mohd-Shaharuddin, N., Lim, Y. A., Ngui, R., & Nathan, S. (2021). Expression of ascaris lumbricoides putative virulence-associated genes when infecting a human host. *Parasites & Vectors, 14*(1). https://doi.org/10.1186/s13071-021-04680-y.

Moreau, E., & Chauvin, A. (2010). Immunity against helminths: interactions with the host and the intercurrent infections. *Journal of Biomedicine & Biotechnology*, 2010, 428593. https://doi.org/10.1155/2010/428593.

Motran, C. C., Silvane, L., Chiapello, L. S., Theumer, M. G., Ambrosio, L. F., Volpini, X., Celias, D. P., & Cervi, L. (2018). Helminth Infections: Recognition and Modulation of the Immune Response by Innate Immune Cells. *Frontiers in Immunology, 9*, 664. https://doi.org/10.3389/fimmu.2018.00664.

Muinao, T., Pal, M., & Boruah, H. P. D. (2018). Cytosolic and Transmembrane Protein Extraction Methods of Breast and Ovarian Cancer Cells: A Comparative Study.

Journal of Biomolecular Techniques : JBT, 29(3), 71–78. https://doi.org/10.7171/jbt.18-2903-002.

Mukai, K., Tsai, M., Starkl, P., Marichal, T., & Galli, S. J. (2016). IgE and mast cells in host defense against parasites and venoms. *Seminars in Immunopathology, 38*(5), 581–603. https://doi.org/10.1007/s00281-016-0565-1.

Müller, M., Saunders, C., Senftleben, A., Heidbuechel, J. P. W., Halwachs, B., Bolik, J., Hedemann, N., Röder, C., Bauerschlag, D., Rose-John, S., & Schmidt-Arras, D. (2022). Tetraspanin 8 Subfamily Members Regulate Substrate-Specificity of a Disintegrin and Metalloprotease 17. *Cells*, *11*(17), 2683. https://doi.org/10.3390/cells11172683.

Murakami, T., & Yamamoto, N. (2010). Role of CXCR4 in HIV infection and its potential as a therapeutic target. *Future Microbiology, 5*(7), 1025–1039. https://doi.org/10.2217/fmb.10.67.

Murav'ev, R. A., Fomina, V. A., & Rogovin, V. V. (2003). Zhelatinaznye granuly neĭtrofil'nykh granulotsitov [Gelatinase granules of the neutrophil granulocytes]. *Izvestiia Akademii Nauk. Seriia Biologicheskaia, (4),* 389–394.

Murphy G. (2011). Tissue inhibitors of metalloproteinases. *Genome Biology*, *12*(11), 233. https://doi.org/10.1186/gb-2011-12-11-233.

Mwape, K. E., & Gabriël, S. (2014). The Parasitological, Immunological, and Molecular Diagnosis of Human Taeniasis with Special Emphasis on Taenia solium Taeniasis. *Current Tropical Medicine Reports, 1*(4), 173–180. doi: 10.1007/s40475-014-0028-5.

Nag, K., & Chaudhary, A. (2009). Mediators of Tyrosine Phosphorylation in Innate Immunity: From Host Defense to Inflammation onto Oncogenesis. *Current Signal Transduction Therapy, 4*(2), 76–81. https://doi.org/10.2174/15743620978816750.

Nag, S., Gupta, S., Sisodia, J., & Misra, R. (2019). Asymptomatic filariasis and leprosy co-morbidity in a patient with suspected Guillain-Barrè syndrome: the first case report

of an incidental finding in a slit-skin smear. *Access Microbiology, 1*(8), e000046. https://doi.org/10.1099/acmi.0.000046.

Navarro, S., Boix, E., Cuchillo, C. M., & Nogués, M. V. (2010). Eosinophil-induced neurotoxicity: The role of eosinophil cationic protein/rnase 3. *Journal of Neuroimmunology*, *227*(1–2), 60–70. https://doi.org/10.1016/j.jneuroim.2010.06.012.

Newell Stamper, B. L., Cypser, J. R., Kechris, K., Kitzenberg, D. A., Tedesco, P. M., & Johnson, T. E. (2018). Movement decline across lifespan of *Caenorhabditis elegans* mutants in the insulin/insulin-like signaling pathway. *Aging Cell*, *17*(1), e12704. https://doi.org/10.1111/acel.12704.

Noy, P. J., Gavin, R. L., Colombo, D., Haining, E. J., Reyat, J. S., Payne, H., Thielmann, I., Lokman, A. B., Neag, G., Yang, J., Lloyd, T., Harrison, N., Heath, V. L., Gardiner, C., Whitworth, K. M., Robinson, J., Koo, C. Z., Di Maio, A., Harrison, P., Lee, S. P., … Tomlinson, M. G. (2019). Tspan18 is a novel regulator of the Ca2+ channel Orai1 and von Willebrand factor release in endothelial cells. *Haematologica, 104*(9), 1892–1905. https://doi.org/10.3324/haematol.2018.194241.

Obata-Ninomiya, K., Domeier, P. P., & Ziegler, S. F. (2020). Basophils and eosinophils in nematode infections. *Frontiers in Immunology*, 11. https://doi.org/10.3389/fimmu.2020.583824.

Olaniyan, L. W. B., Okoh, O. O., Mkwetshana, N. T., & Okoh, A. I. (2020). Environmental Water Pollution, Endocrine Interference and Ecotoxicity of 4-tert-Octylphenol: A Review. *Reviews of Environmental Contamination and Toxicology*, *248*, 81–109. https://doi.org/10.1007/398_2018_20.

Ouweneel, A. B., Thomas, M. J., & Sorci-Thomas, M. G. (2020). The ins and outs of lipid rafts: functions in intracellular cholesterol homeostasis, microparticles, and cell membranes: Thematic Review Series: Biology of Lipid Rafts. *Journal of Lipid Research*, *61*(5), 676–686. https://doi.org/10.1194/jlr.TR119000383.

Ozawa, K., Shinkai, Y., Kako, K., Fukamizu, A., & Doi, M. (2022). The molecular and neural regulation of ultraviolet light phototaxis and its food-associated learning

behavioral plasticity in *C. elegans*. *Neuroscience Letters*, *770*, 136384. https://doi.org/10.1016/j.neulet.2021.136384 .

Palmer, T. D., & Zijlstra, A. (2011). CD151: Basis Sequence: Mouse. *The AFCS-Nature Molecule Pages*, 2011, 10.1038/mp.a004123.01. doi:10.1038/mp.a004123.01.

Park, H. H., Jung, Y., & Lee, S. V. (2017). Survival assays using *Caenorhabditis elegans*. *Molecules and Cells*, *40*(2), 90–99. https://doi.org/10.14348/molcells.2017.0017.

Parthasarathy, V., Martin, F., Higginbottom, A., Murray, H., Moseley, G. W., Read, R. C., … Partridge, L. J. (2009). Distinct roles for tetraspanins CD9, CD63 and CD81 in the formation of multinucleated giant cells. *Immunology*, *127*(2), 237–248. doi:10.1111/j.1365-2567.2008.02945.x.

Pastuhov, S. I., Shimizu, T., & Hisamoto, N. (2017). Heavy Metal Stress Assay of *Caenorhabditis elegans*. *Bio-Protocol*, *7*(11), e2312. https://doi.org/10.21769/BioProtoc.2312.

Pearson W. R. (2013). An introduction to sequence similarity ("homology") searching. *Current Protocols in Bioinformatics*, Chapter 3, Unit3.1. https://doi.org/10.1002/0471250953.bi0301s42.

Perera, D. J., & Ndao, M. (2021). Promising Technologies in the Field of Helminth Vaccines. *Frontiers in Immunology*, *12*, 711650. https://doi.org/10.3389/fimmu.2021.711650.

Pesce, J. T., Liu, Z., Hamed, H., Alem, F., Whitmire, J., Lin, H., Liu, Q., Urban, J. F., Jr, & Gause, W. C. (2008). Neutrophils clear bacteria associated with parasitic nematodes augmenting the development of an effective Th2-type response. *Journal of Immunology*, *180*(1), 464–474. https://doi.org/10.4049/jimmunol.180.1.464.

Petersen, S. H., Odintsova, E., Haigh, T. A., Rickinson, A. B., Taylor, G. S., & Berditchevski, F. (2011). The role of tetraspanin CD63 in antigen presentation via MHC class II. *European Journal of Immunology*, *41*(9), 2556–2561. https://doi.org/10.1002/eji.201141438.

Pfistershammer, K., Majdic, O., Stöckl, J., Zlabinger, G., Kirchberger, S., Steinberger, P., & Knapp, W. (2004). CD63 as an activation-linked T cell costimulatory element. *Journal of Immunology, 173*(10), 6000–6008. https://doi.org/10.4049/jimmunol.173.10.6000.

Pileri, P., Uematsu, Y., Campagnoli, S., Galli, G., Falugi, F., Petracca, R., Weiner, A. J., Houghton, M., Rosa, D., Grandi, G., & Abrignani, S. (1998). Binding of hepatitis C virus to CD81. *Science, 282*(5390), 938–941. https://doi.org/10.1126/science.282.5390.938.

Pinheiro, C., Ribeiro, A., Cardoso, F., Martins, V., Figueiredo, B., Assis, N…...Oliveira, S.(2014). A multivalent chimeric vaccine composed of *Schistosoma mansoni* SmTSP-2 and Sm29 was able to induce protection against infection in mice. *Parasite Immunology, 36*(7), 303-312. doi: 10.1111/pim.12118.

PLOS Neglected Tropical Diseases. (n.d.). Retrieved March 30, 2020, from https://journals.plos.org/plosntds/s/journal-information.

Prakash, P. S., Weber, M. H. W., van Hellemond, J. J., & Falcone, F. H. (2022). Are humanized IgE reporter systems potential game changers in serological diagnosis of human parasitic infection?. *Parasitology Research, 121*(4), 1137–1144. https://doi.org/10.1007/s00436-021-07352-z.

Queirós, L., Pereira, J. L., Gonçalves, F. J. M., Pacheco, M., Aschner, M., & Pereira, P. (2019). *Caenorhabditis elegans* as a tool for environmental risk assessment: emerging and promising applications for a "nobelized worm". *Critical Reviews in Toxicology, 49*(5), 411–429. https://doi.org/10.1080/10408444.2019.1626801.

Raposo, G., Nijman, H. W., Stoorvogel, W., Liejendekker, R., Harding, C. V., Melief, C. J., & Geuze, H. J. (1996). B lymphocytes secrete antigen-presenting vesicles. *The Journal of Experimental Medicine, 183*(3), 1161–1172. https://doi.org/10.1084/jem.183.3.1161.

Rathmes, G., Rumisha, S. F., Lucas, T. C. D., Twohig, K. A., Python, A., Nguyen, M., Nandi, A. K., Keddie, S. H., Collins, E. L., Rozier, J. A., Gibson, H. S., Chestnutt, E. G., Battle, K. E., Humphreys, G. S., Amratia, P., Arambepola, R., Bertozzi-Villa, A.,

Hancock, P., Millar, J. J., Symons, T. L., … Weiss, D. J. (2020). Global estimation of anti-malarial drug effectiveness for the treatment of uncomplicated *Plasmodium falciparum* malaria 1991-2019. *Malaria Journal, 19*(1), 374. https://doi.org/10.1186/s12936-020-03446-8.

Reddy, K. C., Andersen, E. C., Kruglyak, L., & Kim, D. H. (2009). A polymorphism in npr-1 is a behavioral determinant of pathogen susceptibility in *C. elegans*. *Science* 382–384. https://doi.org/10.1126/science.1166527.

Rehborg, E. G., Wheeler, N. J., & Zamanian, M. (2023). Mapping resistance-associated anthelmintic interactions in the model nematode *Caenorhabditis elegans*. *bioRxiv : the preprint Server for Biology*, 2023.04.26.538424. https://doi.org/10.1101/2023.04.26.538424.

Reppert, N., & Lang, T. (2022). A conserved sequence in the small intracellular loop of tetraspanins forms an M-shaped inter-helix turn. *Scientific Reports, 12*(1). https://doi.org/10.1038/s41598-022-07243-y.

Resh M. D. (1999). Fatty acylation of proteins: new insights into membrane targeting of myristoylated and palmitoylated proteins. *Biochimica et Biophysica Acta, 1451*(1), 1–16. https://doi.org/10.1016/s0167-4889(99)00075-0.

Ries C. (2014). Cytokine functions of TIMP-1. *Cellular and Molecular Life Sciences : CMLS, 71*(4), 659–672. https://doi.org/10.1007/s00018-013-1457-3.

Robinson, J. D., & Powell, J. R. (2016). Long-term recovery from acute cold shock in *Caenorhabditis elegans*. *BMC Cell Biology, 17*, 2. https://doi.org/10.1186/s12860-015-0079-z.

Rodriguez, M., Snoek, L. B., De Bono, M., & Kammenga, J. E. (2013). Worms under stress: *C. elegans* stress response and its relevance to complex human disease and aging. *Trends in Genetics : TIG, 29*(6), 367–374. https://doi.org/10.1016/j.tig.2013.01.010.

Roeber, F., Morrison, A., Casaert, S., Smith, L., Claerebout, E., & Skuce, P. (2017). Multiplexed-tandem PCR for the specific diagnosis of gastrointestinal nematode

infections in sheep: a European validation study. *Parasites & Vectors, 10*(1), 226. https://doi.org/10.1186/s13071-017-2165-x.

Romagnani S. (1991). Type 1 T helper and type 2 T helper cells: functions, regulation and role in protection and disease. *International Journal of Clinical & Laboratory Research, 21*(2), 152–158. https://doi.org/10.1007/BF02591635.

Romagnani, S. (2004). Immunologic influences on allergy and the TH1/TH2 balance. *Journal of Allergy and Clinical Immunology*, *113*(3), 395-400. doi:10.1016/j.jaci.2003.11.025.

Romano, M., Fanelli, G., Albany, C. J., Giganti, G., & Lombardi, G. (2019). Past, Present, and Future of Regulatory T Cell Therapy in Transplantation and Autoimmunity. *Frontiers in Immunology, 10*. doi:10.3389/fimmu.2019.00043.

Rosales C. (2018). Neutrophil: A Cell with Many Roles in Inflammation or Several Cell Types?. *Frontiers in Physiology, 9*, 113. https://doi.org/10.3389/fphys.2018.00113.

Rous, B. A., Reaves, B. J., Ihrke, G., Briggs, J. A., Gray, S. R., Stephens, D. J., Banting, G., & Luzio, J. P. (2002). Role of adaptor complex AP-3 in targeting wild-type and mutated CD63 to lysosomes. *Molecular Biology of the Cell, 13*(3), 1071–1082. https://doi.org/10.1091/mbc.01-08-0409.

Saito, T., Hattori, T., Okuya, K., Manzoor, R., Miyamoto, H., Kajihara, M., & Takada, A. (2022). Molecular Mechanisms Underlying the Cellular Entry and Host Range Restriction of Lujo Virus. *mBio, 13*(1), e0306021. Advance online publication. https://doi.org/10.1128/mbio.03060-21.

Sakashita, T., Takanami, T., Yanase, S., Hamada, N., Suzuki, M., Kimura, T., Kobayashi, Y., Ishii, N., & Higashitani, A. (2010). Radiation biology of *Caenorhabditis elegans*: germ cell response, aging and behavior. *Journal of Radiation Research, 51*(2), 107–121. https://doi.org/10.1269/jrr.09100.

Schoeps, B., Frädrich, J., & Krüger, A. (2022). Cut loose TIMP-1: an emerging cytokine in inflammation. *Trends in Cell Biology*, S0962-8924(22)00207-0. Advance online publication. https://doi.org/10.1016/j.tcb.2022.08.005.

Schmid-Hempel, P. (2009). Immune defence, parasite evasion strategies and their relevance for 'macroscopic phenomena' such as virulence. *Philosophical Transactions of the Royal Society B: Biological Sciences, 364*(1513), 85-98. doi: 10.1098/rstb.2008.0157.

Schmidt, O., & Teis, D. (2012). The ESCRT machinery. *Current Biology : CB, 22*(4), R116–R120. https://doi.org/10.1016/j.cub.2012.01.028.

Schramm, G., Falcone, F. H., Gronow, A., Haisch, K., Mamat, U., Doenhoff, M. J., Oliveira, G., Galle, J., Dahinden, C. A., & Haas, H. (2003). Molecular characterization of an interleukin-4-inducing factor from *Schistosoma mansoni* eggs. *The Journal of Biological Chemistry, 278*(20), 18384–18392. https://doi.org/10.1074/jbc.M300497200.

Sepulveda, J., Tremblay, J. M., DeGnore, J. P., Skelly, P. J., & Shoemaker, C. B. (2010). *Schistosoma mansoni* host-exposed surface antigens characterized by sera and recombinant antibodies from schistosomiasis-resistant rats. *International Journal for Parasitology, 40*(12), 1407–1417. https://doi.org/10.1016/j.ijpara.2010.04.019.

Sheshachalam, A., Srivastava, N., Mitchell, T., Lacy, P., & Eitzen, G. (2014). Granule Protein Processing and Regulated Secretion in Neutrophils. *Frontiers in Immunology, 5*. doi: 10.3389/fimmu.2014.00448.

Shi, W., Xu, N., Wang, X., Vallée, I., Liu, M., & Liu, X. (2022). Helminth therapy for immune-mediated inflammatory diseases: Current and future perspectives. *Journal of Inflammation Research*, Volume 15, 475–491. https://doi.org/10.2147/jir.s348079.

Shimada, T., Yasuda, S., Sugiura, H., & Yamagata, K. (2019). Syntenin: PDZ Protein Regulating Signaling Pathways and Cellular Functions. *International Journal of Molecular Sciences, 20*(17), 4171. https://doi.org/10.3390/ijms20174171.

Simons, K., & Toomre, D. (2000). Lipid rafts and signal transduction. *Nature Reviews. Molecular Cell Biology, 1*(1), 31–39. https://doi.org/10.1038/35036052.

Singh, B., & Bhaskar, S. (2019). Methods for Detection of Autophagy in Mammalian Cells. *Methods in Molecular Biology, 2045*, 245–258. https://doi.org/10.1007/7651_2018_190.

Silva Pereira, S., Jackson, A. P., & Figueiredo, L. M. (2022). Evolution of the variant surface glycoprotein family in African trypanosomes. *Trends in Parasitology, 38*(1), 23–36. https://doi.org/10.1016/j.pt.2021.07.012.

Sobocińska, J., Roszczenko-Jasińska, P., Ciesielska, A., & Kwiatkowska, K. (2018). Protein Palmitoylation and Its Role in Bacterial and Viral Infections. *Frontiers in Immunology, 8*, 2003. https://doi.org/10.3389/fimmu.2017.02003.

Sokol, C. L., & Medzhitov, R. (2010). Role of basophils in the initiation of Th2 responses. *Current Opinion in Immunology, 22*(1), 73–77. https://doi.org/10.1016/j.coi.2010.01.012.

Sorci, G., Cornet, S., & Faivre, B. (2013). Immune Evasion, Immunopathology and the Regulation of the Immune System. *Pathogens, 2*(1), 71-91. doi: 10.3390/pathogens2010071.

Specht, S., Saeftel, M., Arndt, M., Endl, E., Dubben, B., Lee, N. A., Lee, J. J., & Hoerauf, A. (2006). Lack of eosinophil peroxidase or major basic protein impairs defense against murine filarial infection. *Infection and Immunity, 74*(9), 5236–5243. https://doi.org/10.1128/IAI.00329-06.

Spencer, L. A., Szela, C. T., Perez, S. A., Kirchhoffer, C. L., Neves, J. S., Radke, A. L., & Weller, P. F. (2009). Human eosinophils constitutively express multiple Th1, Th2, and immunoregulatory cytokines that are secreted rapidly and differentially. *Journal of Leukocyte Biology, 85*(1), 117–123. https://doi.org/10.1189/jlb.0108058.

Spencer, L. A., & Weller, P. F. (2010). Eosinophils and Th2 immunity: contemporary insights. *Immunology and Cell Biology, 88*(3), 250–256. https://doi.org/10.1038/icb.2009.115.

Stanley, P., & Okajima, T. (2010). Roles of glycosylation in Notch signaling. *Current Topics in Developmental Biology, 92*, 131–164. https://doi.org/10.1016/S0070-2153(10)92004-8.

Stear, M., Preston, S., Piedrafita, D., & Donskow-Łysoniewska, K. (2023). The immune response to nematode infection. *International Journal of Molecular Sciences*, *24*(3), 2283. https://doi.org/10.3390/ijms24032283.

Steinke, J. W., & Borish, L. (2001). Th2 cytokines and asthma. Interleukin-4: its role in the pathogenesis of asthma and targeting it for asthma treatment with interleukin-4 receptor antagonists. *Respiratory Research, 2*(2), 66–70. https://doi.org/10.1186/rr40.

Stepek, G., Buttle, D. J., Duce, I. R., & Behnke, J. M. (2006). Human gastrointestinal nematode infections: are new control methods required?. *International Journal of Experimental Pathology, 87*(5), 325–341. https://doi.org/10.1111/j.1365-2613.2006.00495.x.

Stephens, G. J., Bueno de Mesquita, M., Ryu, W. S., & Bialek, W. (2011). The emergence of long timescales and stereotyped behaviors in *C. elegans*. *BMC Neuroscience, 12*(S1). https://doi.org/10.1186/1471-2202-12-s1-p13.

Streetley, J., Fonseca, A.-V., Turner, J., Kiskin, N. I., Knipe, L., Rosenthal, P. B., & Carter, T. (2019). Stimulated release of intraluminal vesicles from Weibel-Palade Bodies. *Blood, 133*(25), 2707–2717. https://doi.org/10.1182/blood-2018-09-874552.

Takasaki, T., Yamada, T., Kinoshita, J., & Motomura, Y. (2020). Asymptomatic Colonic Anisakiasis: Is It So Rare?. *Case Reports in Gastroenterology, 14*(3), 593–597. https://doi.org/10.1159/000508822.

Tang, T. T., Lv, L. L., Lan, H. Y., & Liu, B. C. (2019). Extracellular Vesicles: Opportunities and Challenges for the Treatment of Renal Diseases. *Frontiers in Physiology, 10*, 226. https://doi.org/10.3389/fphys.2019.00226.

Taylor, M. J., Hoerauf, A., & Bockarie, M. (2010). Lymphatic filariasis and onchocerciasis. *Lancet, 376*(9747), 1175–1185. https://doi.org/10.1016/S0140-6736(10)60586-7

Tebbe, L., Kakakhel, M., Makia, M. S., Al-Ubaidi, M. R., & Naash, M. I. (2020). The Interplay between Peripherin 2 Complex Formation and Degenerative Retinal Diseases. *Cells, 9*(3), 784. https://doi.org/10.3390/cells9030784.

Termini, C. M., & Gillette, J. M. (2017). Tetraspanins Function as Regulators of Cellular Signalling. *Frontiers in Cell and Developmental Biology, 5*, 34. doi:10.3389/fcell.2017.00034.

Tippett, E., Cameron, P., Marsh, M., & Crowe, S. (2013). Characterization of tetraspanins CD9, CD53, CD63, and CD81 in monocytes and macrophages in HIV-1 infection. *Journal Of Leukocyte Biology*, *93*(6), 913-920. doi: 10.1189/jlb.0812391.

Toledo, A., Osorio, R., Matus, C., Martinez Lopez, Y., Ramirez Cruz, N., Sciutto, E., Fragoso, G., Arauz, A., Carrillo-Mezo, R., & Fleury, A. (2018). Human Extraparenchymal Neurocysticercosis: The Control of Inflammation Favors the Host…but Also the Parasite. *Frontiers in Immunology, 9*, 2652. https://doi.org/10.3389/fimmu.2018.02652.

Tomlinson M. G. (2017). Eye-Opening Potential for Tetraspanin Tspan12 as a Therapeutic Target for Diseases of the Retinal Vasculature. *Circulation, 136*(2), 196–199. https://doi.org/10.1161/CIRCULATIONAHA.117.028521.

Tsai, I. J., Zarowiecki, M., Holroyd, N., Garciarrubio, A., Sánchez-Flores, A., Brooks, K. L., Tracey, A., Bobes, R. J., Fragoso, G., Sciutto, E., Aslett, M., Beasley, H., Bennett, H. M., Cai, X., Camicia, F., Clark, R., Cucher, M., De Silva, N., Day, T. A., Deplazes, P., … Berriman, M. (2013). The genomes of four tapeworm species reveal adaptations to parasitism. *Nature, 496*(7443), 57–63. https://doi.org/10.1038/nature12031.

Tsuda, S., & Miyasato, M. (1993). Nihon rinsho. *Japanese Journal of Clinical Medicine, 51*(3), 613–619.

Tyagi, R. K., Gleeson, P. J., Arnold, L., Tahar, R., Prieur, E., Decosterd, L., … Druilhe, P. (2018). High-level artemisinin-resistance with quinine co-resistance emerges in P. falciparum malaria under in vivo artesunate pressure. *BMC Medicine, 16*(1). doi: 10.1186/s12916-018-1156-x.

Umeda, R., Satouh, Y., Takemoto, M., Nakada-Nakura, Y., Liu, K., Yokoyama, T., Shirouzu, M., Iwata, S., Nomura, N., Sato, K., Ikawa, M., Nishizawa, T., & Nureki, O. (2020). Structural insights into Tetraspanin CD9 function. *Nature Communications, 11*(1). https://doi.org/10.1038/s41467-020-15459-7.

Van Goor, J., Shakes, D. C., & Haag, E. S. (2021). Fisher vs. the worms: Extraordinary sex ratios in nematodes and the mechanisms that produce them. *Cells, 10*(7), 1793. https://doi.org/10.3390/cells10071793.

van Niel, G., Charrin, S., Simoes, S., Romao, M., Rochin, L., Saftig, P., Marks, M. S., Rubinstein, E., & Raposo, G. (2011). The tetraspanin CD63 regulates ESCRT-independent and -dependent endosomal sorting during melanogenesis. *Developmental Cell, 21*(4), 708–721. https://doi.org/10.1016/j.devcel.2011.08.019.

Vande Velde, F., Charlier, J., & Claerebout, E. (2018). Farmer Behavior and Gastrointestinal Nematodes in Ruminant Livestock-Uptake of Sustainable Control Approaches. *Frontiers in Veterinary Science, 5*, 255. https://doi.org/10.3389/fvets.2018.00255.

Varadi, M et al. AlphaFold Protein Structure Database: massively expanding the structural coverage of protein-sequence space with high-accuracy models. *Nucleic Acids Research* (2021).

Vereertbrugghen, A. et al. (2023) An ocular th1 immune response promotes corneal nerve damage independently of the development of Corneal epitheliopathy [Preprint]. doi:10.21203/rs.3.rs-2508656/v1.

Verweij, F. J., van Eijndhoven, M. A., Hopmans, E. S., Vendrig, T., Wurdinger, T., Cahir-McFarland, E., Kieff, E., Geerts, D., van der Kant, R., Neefjes, J., Middeldorp, J. M., & Pegtel, D. M. (2011). LMP1 association with CD63 in endosomes and secretion via exosomes limits constitutive NF-κB activation. *The EMBO Journal, 30*(11), 2115–2129. https://doi.org/10.1038/emboj.2011.123.

Vischer, U. M., Wagner, D. D. (1993). CD63 is a component of Weibel-Palade bodies of human endothelial cells. *Blood. 82*(4), 1184-91. https://www.ncbi.nlm.nih.gov/pubmed/8353283.

Voehringer, D. (2013). Protective and pathological roles of mast cells and basophils. Nature *Reviews Immunology, 13*(5), 362-375. doi: 10.1038/nri3427.

Weltje, L., vom Saal, F. S., & Oehlmann, J. (2005). Reproductive stimulation by low doses of xenoestrogens contrasts with the view of hormesis as an adaptive response. *Human & Experimental Toxicology, 24*(9), 431–437. https://doi.org/10.1191/0960327105ht551oa.

Willms, E., Cabañas, C., Mäger, I., Wood, M., & Vader, P. (2018). Extracellular Vesicle Heterogeneity: Subpopulations, Isolation Techniques, and Diverse Functions in Cancer Progression. *Frontiers in Immunology, 9*, 738. doi:10.3389/fimmu.2018.00738.

Wilson, R., Wright, J., de Castro-Borges, W., Parker-Manuel, S., Dowle, A., & Ashton,P .....Spithill, T. (2011). Exploring the Fasciola hepatica tegument proteome. *International Journal For Parasitology, 41*(13-14), 1347-1359. doi: 10.1016/j.ijpara.2011.08.003.

Winkelmann, F., Salazar, M. G., Hentschker, C., Michalik, S., Macháček, T., Scharf, C., Reisinger, E. C., Völker, U., & Sombetzki, M. (2022). Comparative Proteome Analysis of the tegument of male and female adult *Schistosoma mansoni*. *Scientific Reports 12*: 7569. https://doi.org/10.21203/rs.3.rs-1291198/v1.

Wirth, D., Özdemir, E., King, C., Ahlswede, L., Schneider, D., & Hristova, K. (2021). Quantitative characterization of tetraspanin 8 homointeractions in the plasma membrane. *The Biochemical Journal, 478*(19), 3643–3654. https://doi.org/10.1042/BCJ20210459.

Witter, A. R., Okunnu, B. M., & Berg, R. E. (2016). The Essential Role of Neutrophils during Infection with the Intracellular Bacterial Pathogen Listeria monocytogenes. *Journal of Immunology, 197*(5), 1557–1565. https://doi.org/10.4049/jimmunol.1600599.

Wolfert, M. A., & Boons, G. J. (2013). Adaptive immune activation: glycosylation does matter. *Nature Chemical Biology, 9*(12), 776–784. https://doi.org/10.1038/nchembio.1403.

Wu, T., Xu, H., Liang, X., & Tang, M. (2019). *Caenorhabditis elegans* as a complete model organism for biosafety assessments of nanoparticles. *Chemosphere, 221*, 708–726. https://doi.org/10.1016/j.chemosphere.2019.01.021.

Wubbolts, R., Leckie, R. S., Veenhuizen, P. T., Schwarzmann, G., Möbius, W., Hoernschemeyer, J., Slot, J. W., Geuze, H. J., & Stoorvogel, W. (2003). Proteomic and biochemical analyses of human B cell-derived exosomes. Potential implications for their function and multivesicular body formation. *The Journal of Biological Chemistry, 278*(13), 10963–10972. https://doi.org/10.1074/jbc.M207550200.

Yabluchanskiy, A., Ma, Y., Iyer, R. P., Hall, M. E., & Lindsey, M. L. (2013). Matrix metalloproteinase-9: Many shades of function in cardiovascular disease. *Physiology, 28(*6), 391–403. https://doi.org/10.1152/physiol.00029.2013.

Yamamoto-Imoto, H., Hara, E., Nakamura, S., & Yoshimori, T. (2022). Measurement of autophagy via LC3 western blotting following DNA-damage-induced senescence. *STAR Protocols, 3*(3), 101539. https://doi.org/10.1016/j.xpro.2022.101539.

Yang, D., Chen, Q., Su, S. B., Zhang, P., Kurosaka, K., Caspi, R. R., Michalek, S. M., Rosenberg, H. F., Zhang, N., & Oppenheim, J. J. (2008). Eosinophil-derived neurotoxin acts as an alarmin to activate the TLR2-MyD88 signal pathway in dendritic cells and enhances Th2 immune responses. *The Journal of Experimental Medicine, 205*(1), 79–90. https://doi.org/10.1084/jem.20062027.

Yang, X., Claas, C., Kraeft, S. K., Chen, L. B., Wang, Z., Kreidberg, J. A., & Hemler, M. E. (2002). Palmitoylation of tetraspanin proteins: modulation of CD151 lateral interactions, subcellular distribution, and integrin-dependent cell morphology. *Molecular Biology of the Cell, 13*(3), 767–781. https://doi.org/10.1091/mbc.01-05-0275.

Yang, Y., Liu, X. R., Greenberg, Z. J., Zhou, F., He, P., Fan, L., Liu, S., Shen, G., Egawa, T., Gross, M. L., Schuettpelz, L. G., & Li, W. (2020). Open conformation of tetraspanins shapes interaction partner networks on cell membranes. *The EMBO Journal, 39*(18), e105246. https://doi.org/10.15252/embj.2020105246.

Yeung, L., Hickey, M. J., & Wright, M. D. (2018). The Many and Varied Roles of Tetraspanins in Immune Cell Recruitment and Migration. *Frontiers in Immunology, 9*, 1644. https://doi.org/10.3389/fimmu.2018.01644.

Yoshida, T., Kawano, Y., Sato, K., Ando, Y., Aoki, J., Miura, Y., Komano, J., Tanaka, Y., & Koyanagi, Y. (2008). A CD63 mutant inhibits T-cell tropic human immunodeficiency virus type 1 entry by disrupting CXCR4 trafficking to the plasma membrane. *Traffic, 9*(4), 540–558. https://doi.org/10.1111/j.1600-0854.2007.00700.x.

Zajíčková, M., Nguyen, L. T., Skálová, L., Raisová Stuchlíková, L., & Matoušková, P. (2020). Anthelmintics in the future: current trends in the discovery and development of new drugs against gastrointestinal nematodes. *Drug Discovery Today, 25*(2), 430–437. https://doi.org/10.1016/j.drudis.2019.12.007.

Zakeri, A., Hansen, E., Andersen, S., Williams, A., & Nejsum, P. (2018). Immunomodulation by Helminths: Intracellular Pathways and Extracellular Vesicles. *Frontiers in Immunology, 9*(2349). doi: 10.3389/fimmu.2018.02349.

Zambrano-Villa, S., Rosales-Borjas, D., Carrero, J. C., & Ortiz-Ortiz, L. (2002). How protozoan parasites evade the immune response. *Trends in Parasitology, 18*(6), 272–278. https://doi.org/10.1016/s1471-4922(02)02289-4.

Zeng, L., Huang, L., Zhao, M., Liu, S., He, Z., Feng, J., Qin, C., & Yuan, D. (2018). Acute toxicity of zinc sulfate heptahydrate (znso4*7H2O) and copper (II) sulfate pentahydrate (cuso4*5H2O) on freshwater fish, Percocypris Pingi. *Fisheries and Aquaculture Journal, 09*(01). https://doi.org/10.4172/2150-3508.1000240.

Zhang, J. M., & An, J. (2007). Cytokines, inflammation, and pain. *International Anesthesiology Clinics, 45*(2), 27–37. https://doi.org/10.1097/AIA.0b013e318034194e.

Zhang, H., Liu, L., Jiang, C., Pan, K., Deng, J., & Wan, C. (2020). MMP9 protects against LPS-induced inflammation in osteoblasts. *Innate Immunity, 26*(4), 259–269. https://doi.org/10.1177/1753425919887236.

Zhang, S., Li, F., Zhou, T., Wang, G., & Li, Z. (2020). *Caenorhabditis elegans* as a Useful Model for Studying Aging Mutations. *Frontiers in Endocrinology, 11*, 554994. https://doi.org/10.3389/fendo.2020.554994.

Zhou, M., & Ouyang, W. (2003). The function role of GATA-3 in Th1 and Th2 differentiation. *Immunologic Research*, *28*(1), 25–37. https://doi.org/10.1385/IR:28:1:25.

Zimmerman, B., Kelly, B., McMillan, B., Seegar, T., Dror, R., Kruse, A., & Blacklow, S. (2016). Crystal Structure of a Full-Length Human Tetraspanin Reveals a Cholesterol-Binding Pocket. *Cell, 167*(4), 1041-1051.e11. doi: 10.1016/j.cell.2016.09.056.

8: Appendix

Supplementary 1 (S1):

Complete list of BlastP search results against the tsp-7 LEL domain, using WormBase.

Genome	Length	Score	E-val	%ID
Ancylostoma ceylanicum (PRJNA231479 - HY135)	89	278	2.00E-30	55.1
Ancylostoma ceylanicum (PRJNA231479 - HY135)	31	79	0.0086	45.2
Ancylostoma ceylanicum (PRJNA231479 - HY135)	31	79	0.0086	45.2
Ancylostoma ceylanicum (PRJNA231479 - HY135)	21	79	0.0086	52.4
Ancylostoma ceylanicum (PRJNA72583)	21	79	0.0086	52.4
Ancylostoma ceylanicum (PRJNA72583)	31	79	0.0086	45.2
Ancylostoma ceylanicum (PRJNA72583)	89	278	2.00E-30	55.1
Ancylostoma duodenale (PRJNA72581 - Baltimore)	21	79	0.0086	52.4
Ancylostoma duodenale (PRJNA72581 - Baltimore)	24	73	0.058	50
Ancylostoma duodenale (PRJNA72581 - Baltimore)	31	79	0.0086	45.2
Angiostrongylus cantonensis (PRJEB493 - Republic of China)	57	178	1.50E-16	54.4
Angiostrongylus cantonensis (PRJNA350391 - Guangzhou)	89	265	1.30E-28	51.7
Angiostrongylus cantonensis (PRJNA350391 - Guangzhou)	31	73	0.058	45.2

Angiostrongylus costaricensis (PRJEB494 - Costa Rica)	77	226	3.30E-23	50.6
Angiostrongylus costaricensis (PRJEB494 - Costa Rica)	31	74	0.042	45.2
Anisakis simplex (PRJEB496)	48	122	9.10E-09	43.8
Ascaris lumbricoides (PRJEB4950 - Republic of Ecuador)	48	124	4.80E-09	43.8
Ascaris lumbricoides (PRJEB4950 - Republic of Ecuador)	41	86	0.00091	36.6
Ascaris suum (PRJNA62057 - AG01)	48	124	4.80E-09	43.8
Ascaris suum (PRJNA62057 - AG01)	41	86	0.00091	36.6
Ascaris suum (PRJNA62057 - AG01)	48	124	4.80E-09	43.8
Ascaris suum (PRJNA62057 - AG01)	41	86	0.00091	36.6
Ascaris suum (PRJNA80881 - A. suum Australian isolate)	48	124	4.80E-09	43.8
Ascaris suum (PRJNA80881 - A. suum Australian isolate)	41	86	0.00091	36.6
Brugia malayi (PRJNA10729 - FR3)	48	122	9.10E-09	43.8
Brugia malayi (PRJNA10729 - FR3)	41	92	0.00013	39
Brugia timori (PRJEB4663 - Flores island/ Indonesia)	48	122	9.10E-09	43.8
Brugia timori (PRJEB4663 - Flores island/ Indonesia)	41	92	0.00013	39
Dracunculus medinensis (PRJEB500)	47	117	4.50E-08	42.6
Dracunculus medinensis (PRJEB500)	33	76	0.022	39.4
Enterobius vermicularis (PRJEB503 - Spain/Canary Islands)	32	74	0.042	37.5
Enterobius vermicularis (PRJEB503 - Spain/Canary Islands)	47	75	0.031	29.8
Enterobius vermicularis (PRJEB503 - Spain/Canary Islands)	37	99	1.40E-05	43.2
Enterobius vermicularis (PRJEB503 - Spain/Canary Islands)	24	94	7.10E-05	62.5

Enterobius vermicularis (PRJEB503 - Spain/Canary Islands)	23	72	0.08	47.8
Loa loa (PRJNA246086 - CAT)	48	123	6.60E-09	43.8
Loa loa (PRJNA246086 - CAT)	45	93	9.70E-05	35.6
Loa loa (PRJNA37757 - L. loa Cameroon isolate)	48	123	6.60E-09	43.8
Loa loa (PRJNA37757 - L. loa Cameroon isolate)	45	93	9.70E-05	35.6
Necator americanus (PRJNA72135 - N. amaericanus Hunan isolate)	31	79	0.0086	45.2
Necator americanus (PRJNA72135 - N. amaericanus Hunan isolate)	21	79	0.0086	52.4
Necator americanus (PRJNA72135 - N. amaericanus Hunan isolate)	89	275	5.10E-30	55.1
Onchocerca volvulus (PRJEB513 - O. volvulus Cameroon isolate)	40	119	2.40E-08	50
Onchocerca volvulus (PRJEB513 - O. volvulus Cameroon isolate)	35	76	0.022	37.1
Strongyloides stercoralis (PRJEB528 - PV0001)	38	127	1.80E-09	57.9
Strongyloides stercoralis (PRJEB528 - PV0001)	28	72	0.08	35.7
Thelazia callipaeda (PRJEB1205 - Switzerland/Ticino)	33	76	0.022	36.4
Thelazia callipaeda (PRJEB1205 - Switzerland/Ticino)	46	108	8.00E-07	39.1
Thelazia callipaeda (PRJEB1205 - Switzerland/Ticino)	37	89	0.00035	40.5
Toxocara canis (PRJEB533 - Brazil/Equador)	48	124	4.80E-09	43.8
Toxocara canis (PRJNA248777 - PN_DK_2014)	48	124	4.80E-09	43.8
Toxocara canis (PRJNA248777 - PN_DK_2014)	39	88	0.00048	41
Trichuris trichiura (PRJEB535 - Republic of Ecuador)	26	82	0.0033	50

Wuchereria bancrofti (PRJEB536)	48	122	9.10E-09	43.8
Wuchereria bancrofti (PRJEB536)	39	88	0.00048	38.5
Wuchereria bancrofti (PRJNA275548 - pt0022)	48	122	9.10E-09	43.8
Wuchereria bancrofti (PRJNA275548 - pt0022)	39	88	0.00048	38.5

Supplementary 2 (S2):

The complete list of Hits returned from the NCBI database when comparing the whole tsp-7 protein against the 19 parasitic nematode species identified.

Scientific Name	Max Score	Total Score	E value	Per. ident	Acc. Len	Accession
Ancylostoma ceylanicum	344	344	1.00E-120	71.98	232	EYC12107.1
Ancylostoma ceylanicum	251	251	3.00E-84	66.67	204	EPB72344.1
Ancylostoma ceylanicum	101	101	1.00E-24	26.74	299	EYC09299.1
Ancylostoma ceylanicum	89.4	89.4	1.00E-20	27.27	230	EPB69423.1
Ancylostoma ceylanicum	80.9	80.9	3.00E-17	25.98	283	EYB88728.1
Ancylostoma ceylanicum	80.5	80.5	5.00E-17	25.98	307	EYB88727.1
Ancylostoma ceylanicum	58.2	58.2	3.00E-09	26.03	234	EYC24051.1
Ancylostoma ceylanicum	51.6	51.6	8.00E-07	25	301	EYC05172.1

Ancylostoma ceylanicum	48.9	48.9	4.00E-06	26.06	223	EYB86373.1
Ancylostoma ceylanicum	49.3	49.3	4.00E-06	26.06	272	EYB86376.1
Ancylostoma ceylanicum	48.9	48.9	8.00E-06	26.76	393	EPB67813.1
Ancylostoma ceylanicum	48.5	48.5	1.00E-05	26.06	549	EYB86375.1
Ancylostoma ceylanicum	47.4	47.4	2.00E-05	26.06	500	EYB86374.1
Ancylostoma ceylanicum	43.1	43.1	2.00E-04	30.53	159	EPB68299.1
Ancylostoma ceylanicum	42.4	42.4	0.001	26.92	403	EYC41987.1
Ancylostoma duodenale	148	148	8.00E-45	76	117	KIH54038.1
Ancylostoma duodenale	72.8	72.8	1.00E-14	26.34	218	KIH59661.1
Ancylostoma duodenale	57	57	7.00E-09	25.62	234	KIH49009.1
Ancylostoma duodenale	45.1	45.1	1.00E-04	27.83	273	KIH57664.1
Angiostrongylus cantonensis	300	300	2.00E-103	69.01	213	KAE9415431.1
Angiostrongylus cantonensis	70.1	70.1	2.00E-13	26.99	263	KAE9416228.1
Angiostrongylus cantonensis	51.2	51.2	9.00E-07	29.37	260	KAE9413026.1
Angiostrongylus costaricensis	247	247	3.00E-83	65.03	176	VDM63043.1
Angiostrongylus costaricensis	100	100	1.00E-24	26.15	280	VDM59075.1
Angiostrongylus costaricensis	56.6	56.6	8.00E-09	28.8	229	VDM53786.1
Angiostrongylus costaricensis	51.2	51.2	9.00E-07	29.37	278	VDM53811.1

Anisakis simplex	169	169	1.00E-51	56.32	222	VDK17292.1
Anisakis simplex	72.8	72.8	7.00E-14	23.11	507	VDK51836.1
Anisakis simplex	44.7	44.7	7.00E-05	27.55	181	VDK68047.1
Anisakis simplex	45.8	45.8	8.00E-05	22.64	669	VDK46351.1
Anisakis simplex	44.3	44.3	2.00E-04	31.52	383	VDK42123.1
Brugia malayi	286	286	8.00E-98	59.48	229	XP_042936187.1
Brugia malayi	81.6	81.6	3.00E-17	25.29	305	XP_001899219.2
Brugia malayi	65.5	65.5	1.00E-11	22.81	272	CRZ23823.1
Brugia malayi	65.5	65.5	1.00E-11	22.81	277	XP_042929690.1
Brugia malayi	61.2	61.2	2.00E-10	28.27	229	XP_042937528.1
Brugia malayi	58.5	58.5	3.00E-09	25.47	276	XP_042931352.1
Brugia malayi	55.1	55.1	6.00E-08	23.65	354	CRZ23824.1
Brugia malayi	54.7	54.7	7.00E-08	23.65	359	XP_042929691.1
Brugia malayi	53.1	53.1	9.00E-08	22.17	201	XP_042929693.1
Brugia malayi	51.6	51.6	1.00E-06	25.95	393	XP_042929689.1
Brugia malayi	51.2	51.2	1.00E-06	25.95	388	CRZ23822.1
Brugia malayi	42.4	42.4	8.00E-04	23.08	283	XP_042929694.1
Brugia timori	259	259	1.00E-86	58.22	243	VDO39099.1
Brugia timori	78.2	78.2	4.00E-16	24.53	313	VDO07012.1
Brugia timori	46.6	46.6	4.00E-05	26.67	327	VDO37498.1
Dracunculus medinensis	229	229	3.00E-75	58.33	217	VDN58028.1
Dracunculus medinensis	78.6	78.6	3.00E-16	23.7	289	VDN56285.1
Dracunculus medinensis	65.5	65.5	8.00E-12	24.67	255	VDN56354.1
Dracunculus medinensis	59.3	59.3	1.00E-09	26.84	277	VDN60468.1
Dracunculus medinensis	56.6	56.6	8.00E-09	25.1	230	VDN53598.1

Dracunculus medinensis	53.1	53.1	3.00E-07	27.56	454	VDN59774.1
Enterobius vermicularis	234	234	2.00E-77	52.75	226	VDD87385.1
Enterobius vermicularis	73.2	73.2	1.00E-14	23.27	259	VDD86246.1
Enterobius vermicularis	60.8	60.8	2.00E-10	29.77	206	VDD97097.1
Enterobius vermicularis	48.1	48.1	1.00E-05	21.9	385	VDD84947.1
Loa loa	291	291	1.00E-99	59.05	229	XP_003143510.1
Loa loa	85.1	85.1	1.00E-18	25.58	305	XP_003135737.1
Loa loa	58.9	58.9	2.00E-09	24.89	280	XP_020303291.1
Loa loa	52	52	8.00E-08	30.25	129	XP_003150618.1
Loa loa	50.8	50.8	2.00E-06	27.1	485	XP_020303647.1
Loa loa	49.3	49.3	3.00E-06	26.4	230	XP_003136177.1
Loa loa	49.7	49.7	3.00E-06	24.45	258	XP_003139527.2
Necator americanus	254	254	3.00E-85	60.09	215	XP_013301032.1
Necator americanus	79.3	79.3	1.00E-16	26.43	282	XP_013299545.1
Necator americanus	58.5	58.5	2.00E-09	25.21	234	XP_013300931.1
Thelazia callipaeda	244	244	2.00E-81	57.82	214	VDM98125.1
Thelazia callipaeda	67.8	67.8	3.00E-12	25.58	429	VDN02853.1
Thelazia callipaeda	61.2	61.2	3.00E-10	23.21	279	VDN05153.1
Thelazia callipaeda	51.6	51.6	7.00E-07	25.58	283	VDN04793.1
Thelazia callipaeda	48.1	48.1	1.00E-05	25.17	387	VDN01923.1
Toxocara canis	243	243	5.00E-81	61.61	209	KHN76951.1

Toxocara canis	170	170	1.00E-52	58.54	190	VDM37215.1
Toxocara canis	79.3	79.3	1.00E-16	25.1	278	VDM44411.1
Toxocara canis	73.9	73.9	1.00E-14	26.88	271	KHN70970.1
Toxocara canis	63.9	63.9	4.00E-11	26.39	305	KHN80521.1
Toxocara canis	61.6	61.6	1.00E-10	25.81	223	VDM40706.1
Toxocara canis	61.6	61.6	2.00E-10	25.81	258	KHN86996.1
Toxocara canis	57.8	57.8	2.00E-09	31.07	170	KHN88039.1
Toxocara canis	52	52	4.00E-07	27.33	226	KHN78769.1
Toxocara canis	51.2	51.2	1.00E-06	19.31	357	KHN88055.1
Toxocara canis	48.5	48.5	5.00E-06	25.16	240	VDM50774.1
Toxocara canis	49.3	49.3	7.00E-06	25.38	606	KHN75172.1
Toxocara canis	47.4	47.4	2.00E-05	26.29	273	KHN70824.1
Toxocara canis	44.3	44.3	2.00E-04	23.78	244	VDM42670.1
Toxocara canis	43.9	43.9	3.00E-04	25.16	587	KHN84244.1
Trichuris trichiura	167	167	1.00E-50	41.46	251	CDW55483.1
Trichuris trichiura	76.3	76.3	3.00E-15	24.79	319	CDW52232.1
Trichuris trichiura	68.6	68.6	8.00E-13	24.15	263	CDW59630.1
Trichuris trichiura	67	67	2.00E-12	30.05	241	CDW54882.1
Trichuris trichiura	65.1	65.1	2.00E-11	25.99	290	CDW56958.1
Trichuris trichiura	65.1	65.1	2.00E-11	24.35	360	CDW57534.1
Trichuris trichiura	42.7	42.7	5.00E-04	23.87	233	CDW55054.1
Wuchereria bancrofti	255	255	9.00E-86	57.82	215	EJW84669.1
Wuchereria bancrofti	82	82	1.00E-17	25.29	274	EJW82622.1
Wuchereria bancrofti	81.6	81.6	4.00E-17	25.29	355	VDM09443.1
Wuchereria bancrofti	62	62	1.00E-10	26.69	229	EJW79305.1

Wuchereria bancrofti	48.5	48.5	6.00E-06	26.18	233	EJW79140.1
Wuchereria bancrofti	47.4	47.4	2.00E-05	27.5	263	EJW82663.1
Wuchereria bancrofti	46.6	46.6	3.00E-05	29.63	260	VDM15225.1

Supplementary 3 (S3):

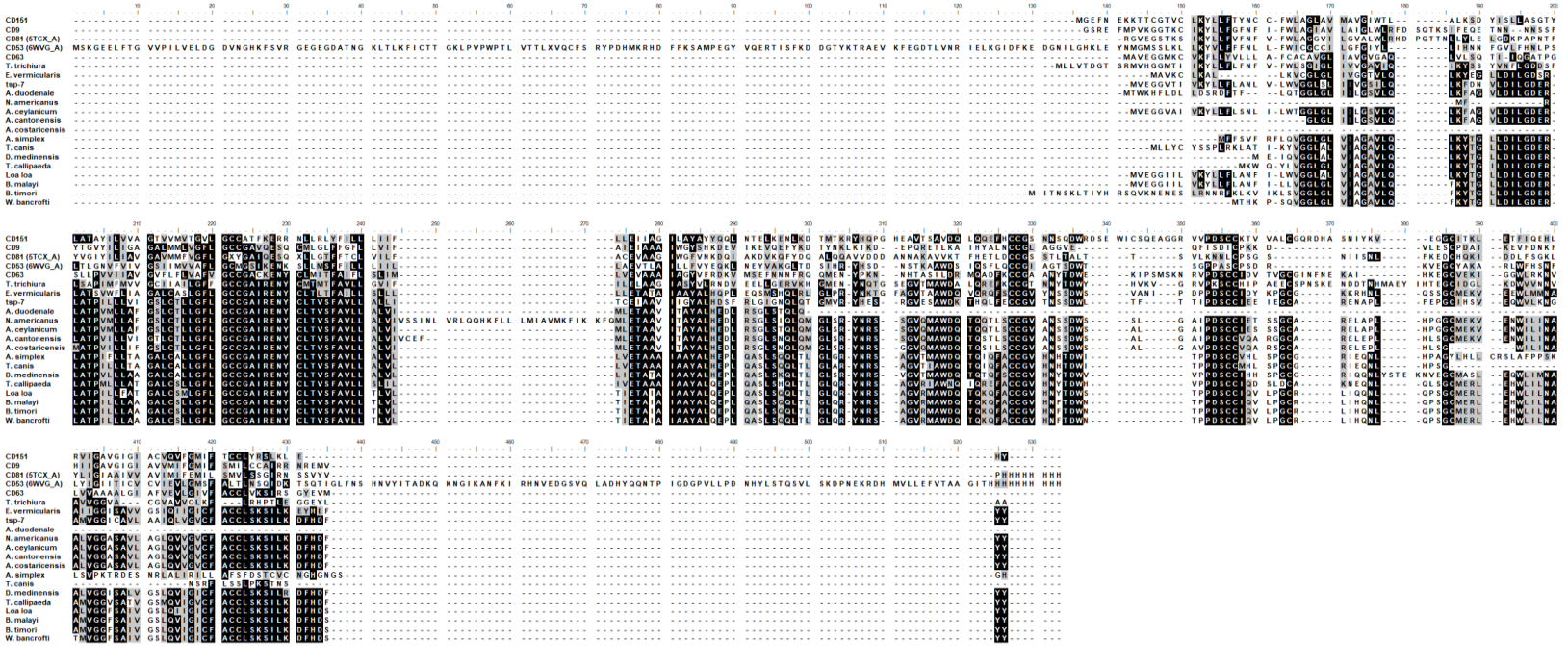

sequence alignment of tsp-7 against human tetraspanin proteins, and parasitic nematode proteins

Supplementary 4 (S4):

LEL domain comparison between C. elegans tsp-7 and human tetraspanin proteins. The complete LELE domain in tsp-7 contains 96 amino acids.

LEL Percentage Identity		
Tsp-7	CD63	23.3 (43 Amino Acids)
	CD151	33.3 (63 Amino Acids)
	CD81	26.9 (26 Amino Acids)
	CD53	31.7 (60 Amino Acids)
	CD9	23.3 (43 Amino Acids)

Supplementary 5 (S5):

The figure shows the tsp-7 protein modelled from SWISS-MODEL with the CD53 backbone (green structure) merged with the tsp-7 protein model from AlphaFold (yellow structure).

The LEL of both tsp-7 from SWISS-MODEL and tsp-7 from AlphaFold. The LEL is the least within the protein structure but is the main domain essential for protein-protein interactions.

Supplementary 6 (S6):

Independent T- test for each strain and observable stress response across different NaCl concentrations.

NaCl Coiling			
Strain	Concentration		Significance
N2	0.05	0.75	P=NS (P>0.05)
	0.05	2	P=NS (P>0.05)
	0.75	2	P=NS (P>0.05)
TM5046	0.05	0.75	P=NS (P>0.05)
	0.05	2	P=NS (P>0.05)
	0.75	2	P=NS (P>0.05)
TM5761	0.05	0.75	P<0.05
	0.05	2	P<0.01
	0.75	2	P=NS (P>0.05)
NaCl Sinusoidal			
N2	0.05	0.75	P=NS (P>0.05)
	0.05	2	P=NS (P>0.05)
	0.75	2	P=NS (P>0.05)
TM5046	0.05	0.75	P<0.05

	0.05	2	P=NS (P>0.05)
	0.75	2	P=NS (P>0.05)
TM5761	0.05	0.75	P=NS (P>0.05)
	0.05	2	P=NS (P>0.05)
	0.75	2	P<0.05
NaCl Reversal			
N2	0.05	0.75	P=NS (P>0.05)
	0.05	2	P<0.05
	0.75	2	P=NS (P>0.05)
TM5046	0.05	0.75	P=NS (P>0.05)
	0.05	2	P=NS (P>0.05)
	0.75	2	P=NS (P>0.05)
TM5761	0.05	0.75	P=0.064
	0.05	2	P<0.05
	0.75	2	P=NS (P>0.05)

Supplementary 7 (S7):

Independent T- test of each strain across different concentrations of $ZnSO_4$ from all three observable stress responses.

$ZnSO_4$ Coiling			
Strain	Concentration		Significance
N2	0	0.5	P=NS (P>0.05)
	0	1	P=NS (P>0.05)
	0.5	1	P=NS (P>0.05)
TM5046	0	0.5	P=NS (P>0.05)
	0	1	P=NS (P>0.05)
	0.5	1	P=NS (P>0.05)
TM5761	0	0.5	P=NS (P>0.05)
	0	1	P=NS (P>0.05)
	0.5	1	P=NS (P>0.05)
$ZnSO_4$ Sinusoidal			
N2	0	0.5	P<0.01
	0	1	P=NS (P>0.05)
	0.5	1	P<0.01
TM5046	0	0.5	P<0.05

	0	1	P=NS (P>0.05)
	0.5	1	P<0.05
TM5761	0	0.5	P=0.05
	0	1	P=0.05
	0.5	1	P=NS (P>0.05)
$ZnSO_4$ Reversal			
N2	0	0.5	P=NS (P>0.05)
	0	1	P=NS (P>0.05)
	0.5	1	P=NS (P>0.05)
TM5046	0	0.5	P=NS (P>0.05)
	0	1	P=NS (P>0.05)
	0.5	1	P=0.01
TM5761	0	0.5	P=NS (P>0.05)
	0	1	P=NS (P>0.05)
	0.5	1	P<0.05

Supplementary 8 (S8):

Independent T-test for each strain comparing the standard to the addition of 4-Octylphenol for each of the observable stress responses.

4-Octylphenol Coiling			
Strain	Concentration		Significance
N2	0	5mM	P=NS (P>0.05)
TM5046	0	5mM	P=NS (P>0.05)
TM5761	0	5mM	P=NS (P>0.05)
4-Octylphenol Sinusoidal			
N2	0	5mM	P=NS (P>0.05)
TM5046	0	5mM	P=NS (P>0.05)
TM5761	0	5mM	P=NS (P>0.05)
4-Octylphenol Reversal			
N2	0	5mM	P=0.071
TM5046	0	5mM	P=NS (P>0.05)
TM5761	0	5mM	P=NS (P>0.05)

Supplementary 9 (S9):

Independent T-test for each strain with the addition of absolute Ethanol across all observable stress responses.

Ethanol Coiling			
Strain	Concentration		Significance
N2	0	100	P=NS (P>0.05)
TM5046	0	100	P=NS (P>0.05)
TM5761	0	100	P=NS (P>0.05)
Ethanol Sinusoidal			
N2	0	100	P=0.01
TM5046	0	100	P<0.05
TM5761	0	100	P=NS (P>0.05)
Ethanol Reversal			
N2	0	100	P=NS (P>0.05)
TM5046	0	100	P=NS (P>0.05)
TM5761	0	100	P<0.05

Supplementary 10 (S10):

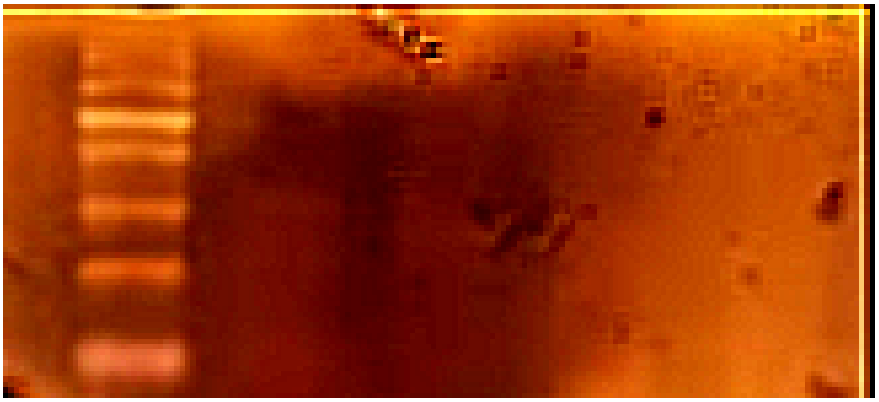

The SDS gel was stained with Page-blue. The image is quite poor and therefore has been inverted. It is difficult to determine any bands present. Each lane from left to right: tm5046, tm5761 and two lanes of N2 wild type lysate.

Supplementary 11 (S11):

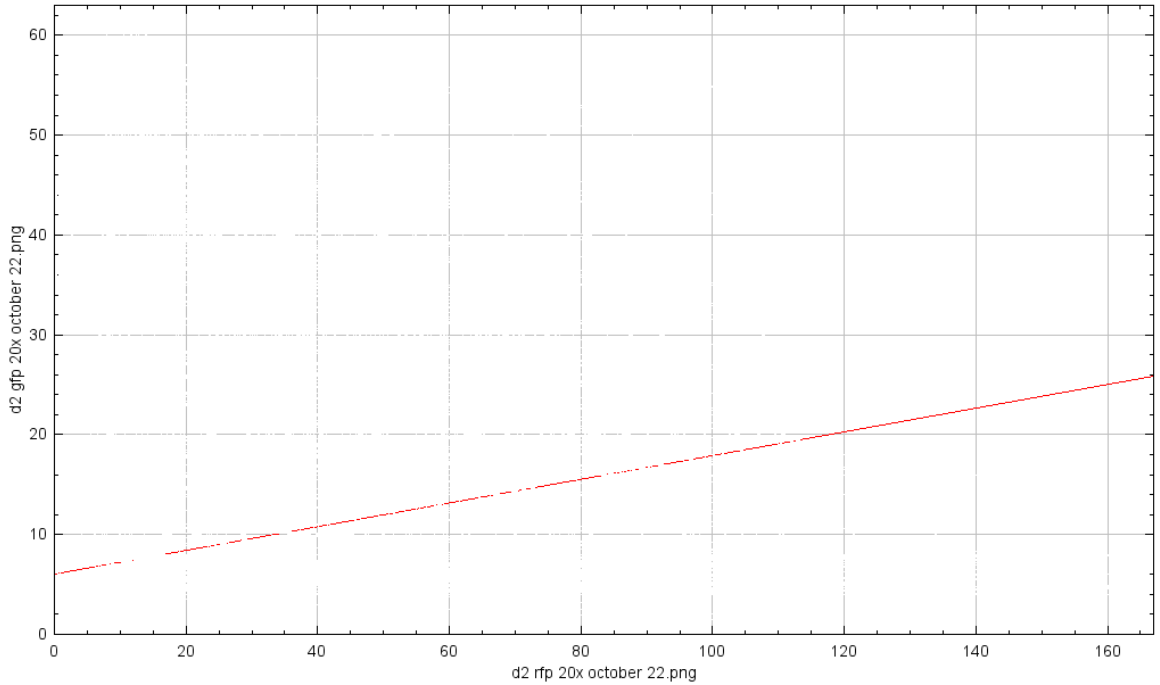

Scatter plot for figure 5.8.2 using the JACoP plugin on ImageJ. R= 0.12

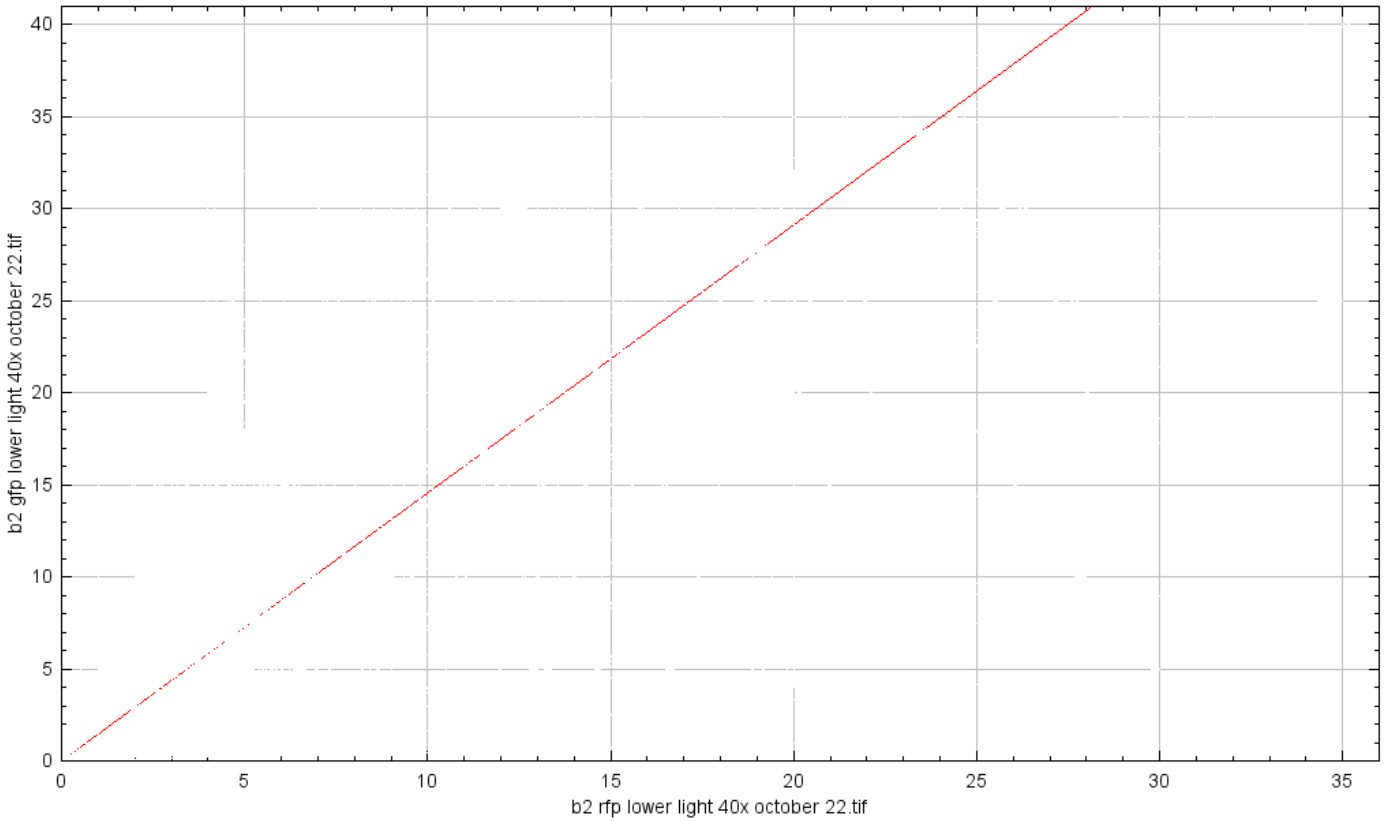

Scatter plot for figure 5.8.2 using the JACoP plugin on ImageJ. R= 0.862

Supplementary 12 (S12):

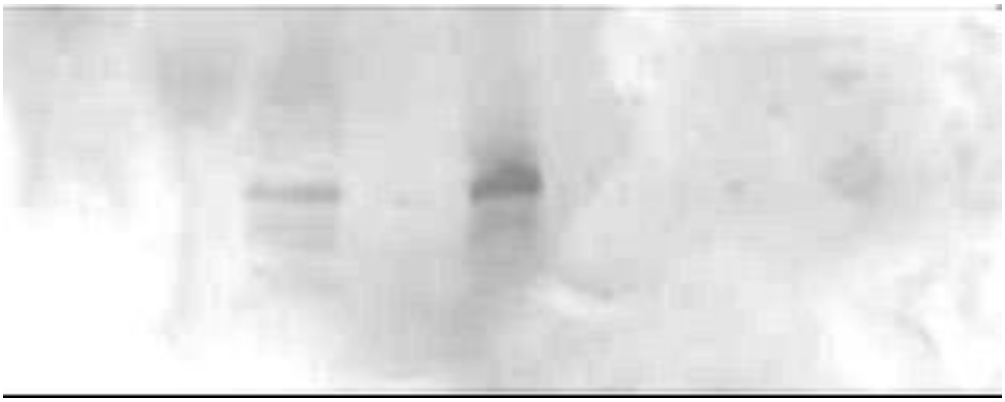

Western blot used to detect GAPDH in HEK and HRT cancer cell lysates. The western blot acted as a control to demonstrate the correct methodology was used throughout the study for detection of tsp-7 in *C. elegans*.